

UNIVERSIDAD AUTÓNOMA DE MADRID



FACULTAD DE MEDICINA

TRABAJO DE TESIS DOCTORAL

***“PATRONES DE EXPRESIÓN GÉNICA Y METILACIÓN EN EL
SCHWANNOMA VESTIBULAR”***

MIGUEL TORRES MARTÍN

MADRID 2014

D. JUAN ANTONIO REY, con DNI. 50410407-L, Doctor en Ciencias Biológicas, Investigador de la Unidad de Investigación del Hospital Universitario La Paz, Madrid; y D. LUIS LASSALETTA ATIENZA, con DNI. 2631770H, Jefe de sección del Hospital Universitario La Paz y Profesor Asociado Departamento de Cirugía de la Universidad Autónoma de Madrid,

CERTIFICAN QUE:

MIGUEL TORRES MARTÍN, con DNI. 02671174-T, Licenciado en Biología por la Universidad Autónoma de Madrid, ha realizado bajo su dirección el trabajo titulado “Patrones de Expresión Génica y Metilación en el Schwannoma Vestibular”, y que dicho trabajo reúne los requisitos necesarios para su exposición y defensa como tesis doctoral.

Madrid, junio de 2014

Fdo. Los directores de tesis

D. JUAN ANTONIO REY

D. LUIS LASSALETTA

Agradecimientos

Habitado a relatar listas de genes y funciones moleculares en mis artículos, intentaré que la presente dedicatoria a aquellas personas que han hecho posible esta tesis, no se transforme en eso.

Con la bata de científico puesta, agradezco, en primer y destacado lugar, al Dr. Juan Rey por aceptarme en su laboratorio, el primero que pisé, así como por su esfuerzo para formarme como científico. Después, al Dr. Luis Lassaletta, que a pesar de su apretadísima agenda, siempre ha tenido tiempo para el laboratorio en general, y para mí en particular.

El tiempo que he dedicado a aprender a analizar microarrays, no habría sido ni la mitad de no ser por la técnico Carolina Peña, que de forma prácticamente altruista, me ha ayudado con su trabajo en la poyata.

Al Dr. Fresno y Ángel, por su ayuda en la cuantitativa en particular y en otras tantas cosas en general.

Y al resto de compañeros que, a lo largo de estos años me habéis ayudado, en el trabajo o en la vida, a que el día a día fuera como ha sido.

Ya sin la bata, tengo que agradecer a mi familia su paciencia conmigo, especialmente a Mila por estar siempre ahí, y al pequeño Nikolay por alegrarme ambos cada día, con su simple presencia. Y a mi hermana, que me ha facilitado tanto las cosas acudiendo en cada llamada.

Y a mis padres, que con su esfuerzo y sacrificio en todos los aspectos, me han permitido ser lo que he querido ser.

Como en las redes genéticas, por mucho que haga un gen, no sería nada, ni remotamente nada, sin los demás. Así, este trabajo, bueno o malo, mejor o peor, relevante o no, solo ha sido posible con el apoyo de todos vosotros.

ÍNDICE

1. INTRODUCCIÓN.....	8
1.1 SCHWANNOMAS VESTIBULARES.....	9
1.1.1 Lugar de origen e histología del schwannoma vestibular.....	9
1.1.2 Incidencia.....	10
1.1.3 Neurofibromatosis tipo 2.....	11
1.1.4 Sintomatología y tratamiento de los schwannomas vestibulares.....	12
1.1.5 Complicaciones post-tratamiento.....	14
1.1.6 Ensayos clínicos en los schwannomas vestibulares.....	16
1.2 ALTERACIONES MOLECULARES DE LOS SCHWANNOMAS VESTIBULARES.....	17
1.2.1 Gen <i>NF2</i>	17
1.2.2 Características del producto proteico de <i>NF2</i> : Merlin.....	18
1.2.3 Funciones biológicas de merlin.....	19
1.2.4 <i>NF2</i> en otros tumores.....	22
1.2.5 Otras alteraciones moleculares en los schwannomas vestibulares.....	23
1.2.6 Alteraciones cromosómicas.....	23
1.2.7 Alteraciones genéticas.....	23
1.2.8 MicroRNAs en los schwannomas vestibulares.....	25
1.2.9 Metilación.....	25
1.3 MICROARRAYS.....	27
1.3.1 Microarrays de expresión.....	27
1.3.2 Microarrays de metilación.....	29
1.3.3 Aplicaciones de los microarrays.....	29
1.3.4 Limitaciones de los microarrays.....	31
1.3.5 Disponibilidad de los datos y su presentación en publicaciones.....	35
1.3.6 Análisis de enriquecimiento.....	35
1.3.7 Microarrays en schwannomas.....	36
2. OBJETIVOS.....	39
3. PUBLICACIONES.....	41
3.1 ARTÍCULO 1: "NF2 genetic alterations in sporadic vestibular schwannomas: clinical implications".....	43
3.2 ARTÍCULO 2: "DNA copy gains of tumor-related genes in vestibular schwannoma".....	52
3.3 ARTÍCULO 3: "Microarray analysis of gene expression in vestibular schwannomas reveals SPP1/MET signaling pathway and androgen receptor deregulation".....	60

3.4 ARTÍCULO 4: "Global profiling in vestibular schwannomas shows critical deregulation of microRNAs and upregulation in those included in chromosomal region 14q32"	78
3.5 ARTÍCULO 5: "Genome-wide methylation analysis in vestibular schwannomas shows putative mechanisms of gene expression modulation and global hypomethylation at the HOX gene cluster"	89
3.6 ARTÍCULO 6: "Global expression profile in low grade meningiomas and schwannomas shows up-regulation of PDGFD, CDH1 and SLIT2 in both tumors with respect to their healthy tissue"	113
4. RESULTADOS GLOBALES.....	129
4.1 ANÁLISIS MUTACIONAL DE <i>NF2</i>	130
4.2 PATRONES GENERALES DE LOS MICROARRAYS.....	132
4.3 AGRUPACIÓN DE LAS MUESTRAS.....	134
4.4 VALIDACIÓN DE LOS ANÁLISIS DE EXPRESIÓN.....	136
4.5 GENES INVOLUCRADOS EN MIELINIZACIÓN.....	138
4.6 METILACIÓN Y EXPRESIÓN DEL GEN <i>NF2</i>	142
4.7 ALTERACIONES EN RECEPTORES TIROSINA QUINASA.....	142
4.8 ADHESIÓN EN SCHWANNOMAS VESTIBULARES.....	143
4.9 DESREGULACIONES POR CROMOSOMAS.....	144
4.10 ANÁLISIS DE ENRIQUECIMIENTO.....	146
4.11 CARACTERÍSTICAS CLÍNICAS Y MICROARRAYS.....	148
4.12 SCHWANNOMAS Y MENINGIOMAS.....	150
5. DISCUSIÓN GENERAL.....	151
5.1 NEUREGULINA 1 Y LOS RECEPTORES ERBB2 Y ERBB3.....	158
5.2 RUTA DE LA AKT Y SU RELACIÓN CON MERLIN.....	160
5.3 OSTEOPONTINA.....	162
5.4 FACTORES DE CRECIMIENTO DERIVADOS DE PLAQUETAS (PDGF).....	163
5.5 RUTA DEL RECEPTOR TIROSINA QUINASA C-MET.....	166
5.6 EGFR.....	169
5.7 RUTA DE LAS CAVEOLINAS.....	170
5.8 RECEPTOR DE ANDRÓGENOS.....	172
5.9 HOMOGENEIDAD EN LOS SCHWANNOMAS VESTIBULARES.....	173
5.10 SCHWANNOMAS Y MENINGIOMAS.....	173
6. CONCLUSIONES.....	176
7. REFERENCIAS.....	179

RESUMEN

Los schwannomas vestibulares son tumores de bajo grado que se desarrollan a partir de las células de Schwann del VIII nervio craneal. Estos tumores pueden aparecer de forma esporádica y unilateral, o bilaterales asociados a la Neurofibromatosis tipo 2.

Molecularmente, la única característica que se da de manera frecuente en los schwannomas vestibulares es la mutación del gen *NF2*, así como la pérdida de heterocigosidad de este gen, alojado en 22q12.2.

En las publicaciones presentadas, utilizamos una serie de schwannomas vestibulares en microarrays -técnicas de alto rendimiento que permiten testar miles de variables en un solo experimento-, de expresión génica global, expresión de microRNAs y del estado de metilación de dinucleótidos de CpG. Como control, se utilizaron nervios no tumorales. Además, realizamos análisis para buscar alteraciones del gen *NF2* mediante PCR/dHPLC, MLPA y LOH del cromosoma 22q por microsatélites.

En los microarrays de expresión génica de los schwannomas, encontramos sobreexpresión en los tumores del oncogen *MET* y varios genes asociados –como *ERBB2*, *ERBB3*, *SEMA5A* o *PLXNB3*- infraexpresión del receptor de andrógenos, así como sobreexpresión del gen de la osteopontina, implicada en la degradación de merlin en cáncer de mama.

En los microarrays de expresión de microRNAs, identificamos sobreexpresión en los schwannomas del mayor clúster del genoma de estas moléculas no codificantes en la región cromosómica 14q32. Además, microRNAs implicados en el silenciamiento del gen *MET* –myomiRs- fueron hallados infraexpresados.

En los microarrays de metilación, hallamos procesos epigenéticos compatibles con los niveles de expresión de *MET*, *PMEPA*, el miR-21 o el miRNA-199a1. Así mismo, identificamos hipometilación de los genes *HOX* en los schwannomas vestibulares.

Para finalizar, comparamos el patrón de expresión de los schwannomas con meningiomas, otros tumores que aparecen frecuentemente en la neurofibromatosis tipo 2.

En conclusión, nuestros estudios de microarrays muestran potenciales dianas terapéuticas para los schwannomas vestibulares, así como ayudan a aumentar el conocimiento biológico de este tumor del sistema nervioso.

ABSTRACT

Vestibular schwannomas are low grade tumors that develop from Schwann cells in the VIIIth cranial nerve. These tumors may arise sporadically and unilaterally or bilaterally; they are associated to Neurofibromatosis type 2.

The only molecular characteristic that shares most of vestibular schwannomas is the mutation of NF2 gene and the loss of heterozygosity of 22q12.2, where this gene is harbored.

In the publications presented in this work, we use a vestibular schwannoma series in microarrays – high throughput technology which allows testing thousands of variables in a single experiment – of global gene expression, microRNA expression and the methylation status of CpG dinucleotides. As control, we used non-tumoral peripheral nerves. Furthermore, we performed mutational analysis of NF2 gene by PCR/dHPLC, MLPA and we tested LOH of chromosome 22.

In whole expression assays, we found overexpression of MET and associated genes –including *ERBB2*, *ERBB3*, *SEMA5A* or *PLXNB3*– and androgen receptor underexpression. Furthermore, we identified osteopontin gene overexpression, which protein is involved in merlin degradation in breast cancer.

By microarray analysis, we detected global upregulation in vestibular schwannomas of those microRNAs included in 14q32 region, which corresponds to the biggest cluster of non-coding RNA in the human genome. Additionally, several microRNAs implicated in MET gene silencing –named myomiRs– were found underexpressed.

DNA methylation microarrays displayed HOX genes hypomethylation in vestibular schwannomas. We also found epigenetic processes which could explain deregulation of several genes such as MET, PMEPA, miR-21 or miRNA-199a1.

Finally, we compared expression pattern of schwannomas with meningiomas, which are tumors that also arise in Neurofibromatosis type 2 patients.

In summary, our microarray studies show potential therapeutic targets in order to treat vestibular schwannomas, as well as increase biological knowledge about this nervous system tumor.

1. INTRODUCCIÓN

1. INTRODUCCIÓN

1.1 SCHWANNOMAS VESTIBULARES

Los schwannomas son tumores benignos que se originan a partir de las células de Schwann que recubren los axones de los nervios periféricos. También son llamados neurinomas, ya que antiguamente no resultaba posible determinar su origen celular exacto. Los schwannomas suelen estar encapsulados y permanecen anclados al nervio de origen (Wippold *et al*, 2007). Existen varias enfermedades genéticas que pueden dar lugar a la aparición de varios schwannomas en un mismo paciente. La más conocida corresponde a la neurofibromatosis tipo 2 (NF2), que se caracteriza por la aparición de schwannomas vestibulares bilaterales y espinales. Otra enfermedad genética que se caracteriza por la presencia de schwannomas es la schwannomatosis, que presenta la misma incidencia que la NF2 (MacCollin *et al*, 2005), como veremos más adelante. En este caso los schwannomas rara vez son vestibulares. Aunque los schwannomas pueden desarrollarse en cualquier nervio del sistema nervioso periférico, el lugar de aparición más habitual es en el nervio cocleovestibular -VIII nervio craneal-.

1.1.1 Lugar de origen e histología del schwannoma vestibular

Los schwannomas vestibulares son tumores de grado I, e histopatológicamente incluyen los subtipos celular, plexiforme y melanótico (Louis *et al*, 2007). La malignización de estos tumores es extremadamente rara. Históricamente, el lugar anatómico concreto de origen de los schwannomas vestibulares ha sido localizado en la transición entre las

células de Schwann y las células gliales del nervio cocleovestibular -también llamado zona de Obersteiner-Redlich- (Jia *et al*, 2008). Sin embargo, trabajos recientes han mostrado que la mayoría de estos tumores aparecen lateralmente a dicha zona de transición. Aunque los schwannomas vestibulares son más frecuentes en la parte vestibular del VIII nervio craneal, también pueden originarse en la coclear (Roosli *et al*, 2012). Al aumentar de tamaño, los schwannomas vestibulares desplazan las fibras nerviosas a la periferia en los tumores esporádicos, mientras que en los asociados a NF2 los axones quedan desorganizados en el tumor (Hoa & Slattery, 2012).

Desde el punto de vista histológico, los schwannomas vestibulares tienen dos áreas características fácilmente reconocibles, llamadas zonas A y B de Antoni (Antoni, 1920). La proporción es variable en diferentes tumores. El tipo A consiste en una masa muy celularizada, en la que destaca la presencia de Cuerpos de Verocay (Verocay, 1910). Estas formaciones, que recuerdan por su estructura a una empalizada, están formadas por células de Schwann y extracelularmente tienen un alto contenido en laminina (Baur *et al*, 1995). En el tipo B, las células son menos abundantes y no se organizan con un patrón concreto. Además, son frecuentes los agregados de otras células como linfocitos, mastocitos y vasos sanguíneos con paredes hialinizadas. Para algunos autores, las zonas B de Antoni son consideradas como una degeneración de las zonas A de Antoni (Sian & Ryan, 1981), formadas por el estrés oxidativo (Yokoo *et al*, 2007).

1.1.2 Incidencia

Los schwannomas vestibular comprenden el 10% de los tumores intracraneales. Una vez que los pacientes presentan sintomatología asociada a estos tumores, la incidencia varía entre 0,7 y 1,2 afectados por cada 100.000 habitantes (Tos & Thomsen,

1984; Babu *et al*, 2013). A menudo se detectan casos asintomáticos al realizar resonancias magnéticas por otros motivos, aumentando así la incidencia de estas lesiones (Anderson *et al*, 2000). Además, en autopsias de la población general, se detectaron tasas mayores al 1% (Schneider *et al*, 1983), aunque estos resultados no han podido ser confirmados por otros estudios (Karjalainen *et al*, 1984). Hasta el 95% de los schwannomas vestibulares aparecen de forma unilateral y esporádica, mientras que el 5% están asociados al genético de la NF2.

1.1.3 Neurofibromatosis tipo 2

La NF2 es una enfermedad autosómica dominante, causada por la mutación del gen *NF2* (Twist *et al*, 1994). La incidencia de la NF2 es aproximadamente de 1 entre 33.000 - 600.000 nacidos vivos, dependiendo de la población estudiada (Antinheimo *et al*, 2000b; Evans *et al*, 2010; Guerra-Jiménez *et al*, 2014). Su manifestación más frecuente es la aparición de schwannomas vestibulares bilaterales, aunque los pacientes también pueden desarrollar otros tumores como schwannomas espinales, meningiomas, ependimomas y menos frecuentemente gliomas (Gutmann *et al*, 1997a). Además, los pacientes de NF2 presentan polineuropatías periféricas -que provoca un mal funcionamiento de los nervios-, así como opacidad presenil del cristalino. Las lesiones cutáneas, también frecuentes en pacientes de NF2, provocaban su confusión con otra enfermedad genética, la neurofibromatosis tipo I.

Dentro de estos pacientes la penetrancia de la enfermedad es variable, apareciendo en algunos de ellos pequeños schwannomas a una avanzada edad mientras que en otros se producen varios tipos tumorales durante la infancia o la adolescencia. En cualquier caso, las manifestaciones clínicas suelen ser similares dentro de individuos de la misma

familia, lo que sugiere un fuerte componente genético en este fenómeno (Asthagiri *et al*, 2009). La mitad de los pacientes con NF2 heredan la mutación del gen *NF2* de sus progenitores, mientras que en la otra mitad, la alteración genética aparece *de novo* sin historia familiar previa. Además, un tercio de los casos presentan mosaicismo, lo que significa que no todas las células del individuo son portadores de la mutación del gen. La probabilidad de transmisión a la descendencia de esta enfermedad se reduce si la mutación de *NF2* no se detecta en sangre periférica (Moyhuddin *et al*, 2003; Evans *et al*, 2007). A pesar de que los pacientes con mosaicismo suelen presentar una sintomatología menos agresiva, los descendientes de estos individuos que hereden la mutación sufrirán síntomas más severos (Moyhuddin *et al*, 2003).

1.1.4 Sintomatología y tratamiento de los schwannomas vestibulares

La mayoría de los síntomas que provocan los schwannomas vestibulares están ligados a la afectación del VIII nervio craneal (Tabla 1). El deterioro de este nervio se produce bien por daño directo debido a la compresión de los axones, o bien por alteración en la vascularización de la zona. Los síntomas son muy variables (Selesnick *et al*, 1993), pero entre los más comunes se encuentran la pérdida de audición, el acúfeno, y la pérdida de equilibrio o vértigo. Además, debido a la proximidad del VII nervio craneal, la movilidad hemifacial de algunos pacientes puede verse alterada, si bien se trata de un signo poco frecuente a la hora de sospechar la presencia de un schwannoma vestibular. Debido a la detección relativamente temprana de estos tumores en cuanto al crecimiento del mismo dentro de la cavidad craneal, actualmente son infrecuentes otros síntomas asociados a un elevado tamaño tumoral como pérdida visual, diplopía o alteraciones de los nervios craneales bajos (Selesnick *et al*, 1993). En cualquier caso, el diagnóstico

definitivo se realiza mediante resonancia magnética con contraste de gadolinio, técnica que proporciona una gran fiabilidad (Jackler *et al*, 1990).

Tabla 1. Etapas clínicas del schwannoma vestibular.

Etapas	Síntomas
1. Intracanalicular	Pérdida de audición Tinnitus Vértigo
2. Invasión de la cisterna	Mayor pérdida de audición Dolor de cabeza Desequilibrio Mejora del vértigo por la compensación central
3. Compresión del tronco cerebral	Mayor pérdida de audición Aumento de desequilibrio Posible síntomas de nervios trigeminales
4. Hidrocefálica	Empeoramiento de los síntomas anteriores Hidrocefalia Dolor de cabeza Debilidad facial Pérdida de visión Diplopía Herniación tonsilar (muerte)

Clasificación basada en la localización del tumor tras su crecimiento desde el VIII nervio craneal en la zona intracanalicular. Se incluyen los síntomas más comunes de cada una de ellas.

Existen tres modalidades principales, aunque no únicas, de tratamiento para los schwannomas vestibulares (Tabla 2). Cuando el tumor se da en pacientes con edad avanzada, el tamaño es pequeño y la sintomatología escasa, se aplica la estrategia de "ver y escanear", que consiste en realizar resonancias magnéticas periódicas y no hacer intervenciones invasivas salvo que se produzca un crecimiento tumoral rápido o sintomático. La radiocirugía (radioterapia estereotáxica), cada vez más utilizada, está indicada en aquellos pacientes con tumores de pequeño tamaño, o en aquellos que por razones médicas o preferencias personales descarten la cirugía. El objetivo de esta técnica es controlar el crecimiento tumoral, no su erradicación. En el caso de la microcirugía, ésta se puede aplicar en la mayor parte de los casos, siempre que el paciente esté en condiciones físicas adecuadas para someterse a una intervención. A pesar de las elevadas

tasas de mortalidad que tenía asociada la cirugía en el pasado (Nikolopoulos & O'Donoghue, 2002), en la actualidad se trata de una intervención relativamente segura. Elegir el método óptimo del tratamiento es una tarea complicada, aunque la creciente disponibilidad de estudios al respecto está ayudando a afinar la selección de los distintos abordajes. En cualquier caso, la decisión última de qué tipo de tratamiento aplicar a cada paciente, corresponde al propio sujeto y al criterio y experiencia del médico.

1.1.5 Complicaciones post-tratamiento

Tanto en el caso de la microcirugía como en la radiocirugía, los tratamientos llevan asociados secuelas post-operatorias para los pacientes que varían en intensidad y frecuencia dependiendo del tamaño del tumor, el abordaje utilizado u otras causas intrínsecas de cada caso. La mayor parte de estas secuelas tienen su origen en el daño y el estrés vascular a los que están sometidos los nervios craneales VII y VIII durante la intervención. Una de las principales secuelas post-operatorias es la pérdida de audición, de grado variable, del lado afectado por el schwannoma vestibular. Casi de forma universal, tras el tratamiento la función vestibular está alterada, aunque afortunadamente ésta puede ser compensada por el sistema nervioso central. Una de las mayores preocupaciones a la hora de operar estos tumores -ya sea con microcirugía o con radiocirugía-, es intentar minimizar el daño que recibe el nervio facial, ya que se puede provocar parálisis facial postoperatoria del lado afectado. Los dos factores que más influyen en la conservación de la funcionalidad del nervio son el tamaño tumoral y la experiencia del cirujano (Myrseth *et al*, 2007).

Tabla 2. Principales tratamientos del schwannoma vestibular

Tratamiento	Descripción	Indicado para	Ventajas	Inconvenientes
Observación	Se realizan resonancias cada cierto tiempo para controlar el crecimiento tumoral, así como los síntomas del paciente	Schwannomas de pequeño tamaño en pacientes de edad avanzada, o bien aquellos sujetos que no deseen someterse a otro tratamiento	No es invasivo, por lo que no hay ninguna secuela más allá de las que cause el propio tumor	En ocasiones hay que acabar recurriendo a métodos invasivos, aunque demorar el tratamiento no suele suponer un problema para el paciente
Microcirugía	Resección del tumor total o parcial mediante intervención invasiva. Tres abordajes posibles:	Pacientes con un estado de salud tal que puedan soportar una cirugía invasiva	La recurrencia del tumor es muy baja, entre el 1%-3% según la serie	Riesgos derivados de una cirugía mayor, meningitis, hemorragias o infartos cerebrales. Dependiendo del abordaje, mayor o menor gravedad de los efectos secundarios
	Retrosigmoidea	Pacientes con audición	En caso de éxito, se puede conservar la audición	Riesgo de dañar el cerebelo y los senos venosos
	Fosa Media	Pacientes con pequeños tumores en los que se quiere salvar la audición	Mayor porcentaje de retención de audición	No hay inconvenientes específicos para este abordaje más allá de los quirúrgicos
	Tranlaberíntica	Tumores grandes en pacientes sin audición	Mejor exposición del tumor, menor riesgo de herniación cerebelar	Pérdida de audición segura
Radiocirugía estereotáxica	Control del crecimiento tumoral mediante una sola dosis de radiación	Schwannomas de pequeño tamaño en pacientes de edad avanzada, o aquellos que no soportarían la anestesia	No requiere someter al paciente a una intervención quirúrgica	Neuropatías de los nervios craneales adyacentes, pérdida de audición, vértigo, tinnitus, hidrocefalia y posibles tumores inducidos por la radiación han sido descritos
Radioterapia fraccionada estereotáxica	Control del crecimiento tumoral mediante varias dosis de radiación	Similares a la radiocirugía	Se pueden tratar tumores de mayor tamaño que con la radiocirugía	Similares a la radiocirugía

Otras complicaciones neurológicas más graves como meningitis, hemorragias o infartos cerebrales son también posibles tras el tratamiento del schwannoma vestibular, si bien las actuales técnicas microquirúrgicas han reducido su incidencia notablemente.

En el caso de los pacientes con NF2, se debe tener en cuenta que las consecuencias postoperatorias son más acentuadas debido a la aparición bilateral de los schwannomas vestibulares y a la mayor complejidad de estos tumores en relación con los nervios craneales. Además, la frecuente presencia de otros tumores como meningiomas y ependimomas obliga, en algunos casos, a realizar frecuentes operaciones a estos pacientes, lo que también condiciona de forma severa su calidad de vida.

1.1.6 Ensayos clínicos en schwannomas vestibulares

A día de hoy, se han realizado diversos ensayos farmacológicos para el tratamiento de los schwannomas vestibulares en pacientes afectados de NF2. Aunque no se ha logrado una gran eficacia, los resultados más prometedores se han obtenido con el anticuerpo monoclonal Bevacizumab, que inhibe de forma específica al factor de crecimiento del endotelio vascular *-VEGF-*. Este compuesto ha mostrado moderada eficacia para controlar el tamaño tumoral y mejorar la audición de los pacientes (Plotkin *et al*, 2009). En el caso de Erlotinib, que actúa como inhibidor del receptor del factor de crecimiento epidérmico humano tipo 1 *-EGFR-*, los pacientes no experimentaron ningún tipo de mejoría (Plotkin *et al*, 2010). Lapatinib, que además de actuar sobre EGFR, también lo hace sobre el receptor del factor de crecimiento epidérmico humano tipo 2 *-ERBB2-*, ha mostrado resultados más esperanzadores, mejorando ligeramente los niveles de audición y volumétricos del tumor (Karajannis *et al*, 2012). Everolimus, un fármaco inmunosupresor que inhibe el complejo de la diana de rapamicina en células de mamífero

-mTORC1-, no mostró ninguna respuesta clínica positiva en los pacientes sujetos al ensayo (Karajannis *et al*, 2014).

1.2 ALTERACIONES MOLECULARES DE LOS SCHWANNOMAS VESTIBULARES

Aunque existen numerosas vías de señalización alteradas en los schwannomas, la característica genética común a la mayoría de ellos es la pérdida de un ejemplar del cromosoma 22 (Rey *et al*, 1987; Bello *et al*, 1993), que a nivel molecular se identifica como pérdida de heterozigosidad -LOH- de *NF2*, lo que implica la pérdida de uno de los dos alelos del gen *NF2*. Además, en tumores asociados a la enfermedad genética de la schwannomatosis, la mutación del gen *SMARCB1*, localizado en el cromosoma 22 y cercano a *NF2*, es la alteración mayoritaria en estos schwannomas (Hulsebos *et al*, 2007; Boyd *et al*, 2008; Rousseau *et al*, 2011). En el caso de los schwannomas vestibulares, el único gen afectado por mutaciones en la mayoría de estos tumores -aunque no se da en todos-, es *NF2*.

1.2.1 Gen *NF2*

El gen *NF2* se localiza en la región 12 del brazo largo del cromosoma 22 (Rouleau *et al*, 1990; Wertelecki *et al*, 1988; Arai *et al*, 1992; Wolff *et al*, 1992). La región 22q12.2 aparece frecuentemente perdida en schwannomas vestibulares, con porcentajes que varían según las series del 30,4% (Martinez-Glez *et al*, 2009) al 57% (Hadfield *et al*, 2010). A pesar de la evidente relación entre la LOH de 22q y *NF2*, no siempre este gen está afectado por la delección o monosomía cromosómica, aunque suele ser lo habitual (Buckley *et al*, 2005). El gen *NF2* fue descrito en 1993 como el gen responsable de la NF2 por dos grupos independientes (Rouleau *et al*, 1993; Trofatter *et al*, 1993). El producto proteico de este gen

es conocido como merlin o schwannomina. El gen *NF2* cuenta con 17 exones, que mediante splicing alternativo da lugar a las dos principales isoformas de merlin. La isoforma 1 carece del exon 16, y genera una proteína merlin de 595 aminoácidos. En el caso de la isoforma 2, no se transcribe el exón 17 y la proteína resultante es de 590 aminoácidos. La isoforma 1 se relaciona con la función supresora de tumores de merlin, mientras que la isoforma 2 ha sido recientemente descrita como causante de la polineuropatía periférica que sufren los pacientes de *NF2* (Schulz *et al*, 2013).

1.2.2 Características del producto proteico de *NF2*: Merlin

Merlin pertenece a la familia de proteínas 4.1, cuya característica más representativa es el dominio Four point one, Ezrin, Radixin, Moesin –FERM- en el NH₂ terminal. Al igual que las otras proteínas ERM, merlin presenta, además del dominio FERM, una región de hélice alfa central; pero a diferencia de éstas, no tiene sitio de unión a la actina en el COOH terminal, sino en la región NH₂ (Sainio *et al*, 1997).

Merlin sufre numerosas modificaciones postraduccionales, relacionadas en algún grado todas ellas con su capacidad como proteína supresora de tumores. Merlin tiene dos conformaciones principales, que dependen de la fosforilación de la Serina en la posición 518. Esta fosforilación puede ser realizada mediante la "Protein Kinasa A" -PKA- o bien por la "V-akt murine thymoma viral oncogene homolog 1" -AKT1-, que provoca el paso de la forma cerrada -activa y supresora de tumores- a la forma abierta -inactiva-. Además, cuando AKT1 está activada, puede fosforilar a merlin en la Treonina 230 y en la Serina 315 (Tang *et al*, 2007); en estos dos casos se produce la degradación de merlin en el proteosoma. A diferencia de las quinasas, la myosin fosfatasa MYPT1-PP1δ defosforila merlin en la Serina 518 devolviéndolo a la conformación cerrada (Jin *et al*, 2006).

Recientemente, la sumoilación de merlin en la Lisina 76 de la proteína, se describió como fundamental para su actividad supresora de tumores (Qi *et al*, 2013). La sumoilación es una modificación postraducciona reversible de una proteína que afecta a las funciones de la misma. En merlin, el bloqueo de la sumoilación por mutación de *NF2* provoca la imposibilidad de entrar en el núcleo, alterando su función supresora de tumores.

1.2.3 Funciones biológicas de merlin

Merlin interacciona con numerosas proteínas en muy variadas rutas de señalización, ampliándose constantemente las proteínas a las que se asocia. En la Tabla 3 se muestran algunas de estas interacciones con otras proteínas. La distribución de merlin en la célula no es fija, sino que varía en función del contexto celular y fisiológico. En la células de Schwann, merlin colocaliza con la cadherina E -*CDH1*- en los paranodos y las incisuras de Schmidt-Lanterman (Yi *et al*, 2011), es decir, en las pequeñas porciones de citoplasma que quedan en las vainas de mielina.

Durante un largo periodo, las funciones de merlin se situaron principalmente asociadas al citoesqueleto y la membrana. En concreto, la inhibición de la proliferación celular por contacto entre células parece ser fundamental en su actividad supresora de tumores (McClatchey & Giovannini, 2005). Con relación a este punto, la asociación de merlin con la angiomotina, con la consecuente inhibición de Rac1 (Yi *et al*, 2011), parece desempeñar un papel imprescindible. Así mismo, la interacción de merlin con la proteína CD44 se ha asociado a este fenómeno (Morrison *et al*, 2001).

Tabla 3. Algunas de las proteínas y estructuras con asociación directa a merlin. Se han recogido las principales con sus correspondientes citaciones.

Molécula	Relación con merlín	Función	Citas
PAK	Fosforila merlin	Desactiva merlin	(Kaempchen <i>et al</i> , 2003; Kissil <i>et al</i> , 2003; Okada <i>et al</i> , 2005)
PKA	Fosforila merlin	Desactiva merlin	(Alfthan <i>et al</i> , 2004; Laulajainen <i>et al</i> , 2008)
AKT	Fosforila merlin	Provoca degradación de merlin	(Tang <i>et al</i> , 2007)
MYPT-PP1δ	Desfosforila merlin	Función supresora de tumores	(Jin <i>et al</i> , 2006)
NHERF1	Merlin se une a esta proteína	Provoca inhibición dependiente de contacto de EGFR	(Gonzalez-Agosti <i>et al</i> , 1999; Nguyen <i>et al</i> , 2001; Curto <i>et al</i> , 2007)
CD44	Merlin se une a su porción citoplasmática	Inhibición del crecimiento por contacto	(Morrison <i>et al</i> , 2001; Bai <i>et al</i> , 2007)
HGS	Unión a merlin	Reduce cantidad del receptor EGFR en membrana	(Scoles <i>et al</i> , 2002; Scoles <i>et al</i> , 2005)
CRL4^{DCAF1}	Merlin se une al complejo e impide ubiquitinación de otras proteínas	Función supresora de tumores	(Li <i>et al</i> , 2010; Li <i>et al</i> , 2014)
AMOT	Inhibida por merlin, boquea Rac	Función supresora de tumores	(Yi <i>et al</i> , 2011)
PIKE-L	Merlin se une a esta proteína	Bloqueo de PI3K	(Rong <i>et al</i> , 2004)
TARBP2	Interacción con merlin	Ubiquitinado y degradado por mediación de merlin	(Lee <i>et al</i> , 2004; Lee <i>et al</i> , 2006)
GTPBP4	Unión a merlin	Regula junto con merlin la expresión de ciclina D1	(Lee <i>et al</i> , 2007)
SPTBN2	La isoforma 2 de merlin se une a esta proteína	Organización del citoesqueleto	(Scoles <i>et al</i> , 1998)
Paxilina	Se une a merlin	Regula la localización de merlin	(Fernandez-Valle <i>et al</i> , 2002)
MPP1	Unión directa a merlin	Regulación de la polaridad celular	(Seo <i>et al</i> , 2009)
Microtúbulos	Merlin se une a los microtúbulos	Regulación del citoesqueleto	(Muranen <i>et al</i> , 2007)
Receptores tirosina quinasa	Merlin regula su acumulación en la membrana	Función supresora de tumores	(Lallemant <i>et al</i> , 2009)
Sintenina	La isoforma 1 de merlin se une a la sintenina	Desconocida	(Jannatipour <i>et al</i> , 2001)
MST 1/2	Activado por merlin	Activación de Yap, que regula el crecimiento celular	(Striedinger <i>et al</i> , 2008)
Erbin	Unión a merlin	Activación de PAK2 en contexto tejido-dependiente	(Wilkes <i>et al</i> , 2009)

Además, merlin regula la concentración de varios receptores tirosina quinasa en la membrana plasmática (Lallemant *et al*, 2009), disminuyendo la cantidad de éstos en

membrana cuando se produce contacto entre células para así evitar proliferación (Figura 1).

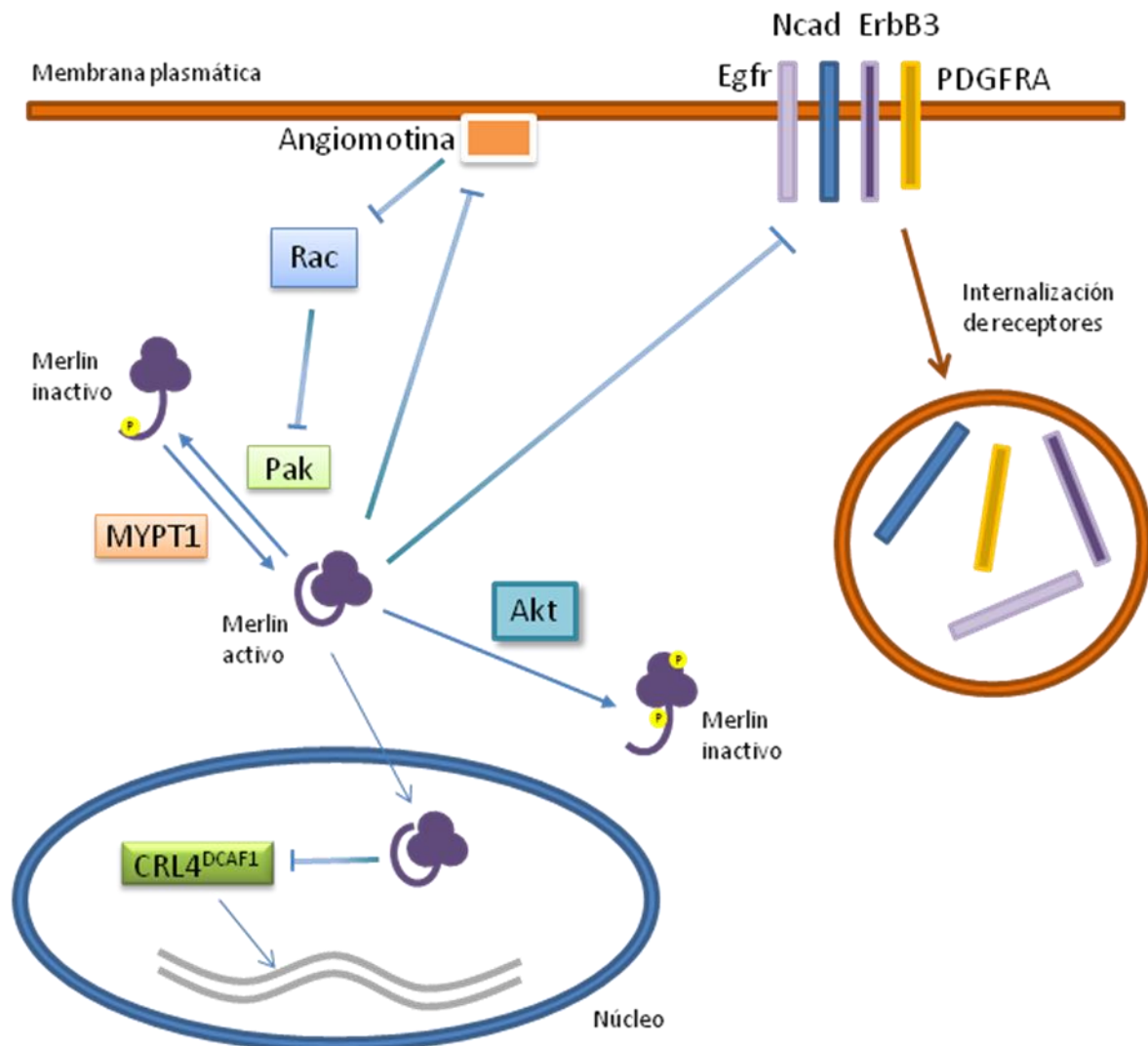


Figura 1. Esquema de las principales funciones de merlin. Cuando no está fosforilada, ejerce sus funciones supresoras de tumores en el núcleo.

Sin embargo, no todas las actividades de merlin están relacionadas con la membrana y el citoesqueleto. Li *et al*, (2010) describieron cómo merlin es capaz de internalizarse en el núcleo en su conformación cerrada y ejercer allí una nueva función supresora de tumores. El mecanismo consiste en que, una vez en el núcleo, merlin se une a la ubiquitina ligasa CRL4^{DCAF1} impidiendo que este complejo pueda ubiquitinar otros

sustratos. Como consecuencia de esta inhibición, se activa la transcripción de numerosos genes involucrados en funciones supresoras de tumores.

1.2.4 *NF2* en otros tumores

Aunque el schwannoma vestibular es el tumor con mayor frecuencia de alteraciones de este gen, *NF2* se encuentra también mutado en una amplia variedad de otros tipos tumorales. Meningiomas y ependimomas, que se originan de células aracnoideas y del epéndimo respectivamente, son tumores que presentan mutaciones de este gen con relativa frecuencia, detallada más abajo. En los meningiomas, la tasa de mutaciones de *NF2* depende del subtipo histológico, siendo los meningiomas fibroblásticos y transicionales, con tasas de hasta el 80%, los más afectados. En el caso de los meningiomas meningoteliales, el número baja considerablemente hasta el 25% (Wellenreuther *et al*, 1995). Asimismo, en el caso de los ependimomas, distintos subtipos también cuentan con diferentes niveles en la alteración de *NF2*. Entre un 29 y un 38% de los ependimomas espinales presentan pérdida de merlin (Gutmann *et al*, 1997b; Lamszus *et al*, 2001; Rajaram *et al*, 2005), siendo menos común en ependimomas de células claras (Fouladi *et al*, 2003) y en los craneales (Rajaram *et al*, 2005). Se ha descrito también una alta tasa de mutaciones de *NF2* en mesoteliomas (Bianchi *et al*, 1995), y en menor medida en gliomas, melanomas (Bianchi *et al*, 1994), cáncer de tiroides, carcinoma hepático, carcinoma de pulmón y leucemia aguda (Yoo *et al*, 2012). En tumores que presentan bajos niveles de merlin, se ha comprobado que un aumento del merlin funcional puede inhibir el crecimiento de gliomas (Lau *et al*, 2008) y melanomas (Murray *et al*, 2012).

1.2.5 Otras alteraciones moleculares en los schwannomas vestibulares

A pesar de que en los schwannomas vestibulares no se han hallado más mutaciones recurrentes que la del gen *NF2*, se han descrito diversas vías de señalización, así como aberraciones cromosómicas distintas a la LOH del 22q. Queda por comprobar si estas perturbaciones son preliminares a la pérdida de merlin o si bien son secundarias a su ausencia.

1.2.6 Alteraciones cromosómicas

Aunque en general la constitución alélica de los schwannomas se ha descrito como estable, se han encontrado pérdidas en 1p, 7p, 9p, 13p, 15p, 16p, 19p, 20q, 21q y Xq; y ganancias en 9q32, 11q, 17q, 19p y 19q (Antinheimo *et al*, 2000a; Warren *et al*, 2003; Koutsimpelas *et al*, 2011). Estas modificaciones suelen aparecer en bajos porcentajes de casos, como por ejemplo la ganancia de 9q32 detectada por Warren *et al*, (2003) que no pasa del 10% de los tumores analizados. Por ello, alteraciones concretas parecen ser algo esporádico de cada tumor, si bien hacen falta más estudios al respecto para poder confirmar esta hipótesis.

1.2.7 Alteraciones genéticas

De forma análoga a los tumores malignos de las vainas de los nervios periféricos -MPNST- (Frohnert *et al*, 2003), los schwannomas vestibulares producen de forma constitutiva el factor de crecimiento glial neuregulina 1 -*NRG1*-, así como sus receptores ErbB2 y ErbB3 (Hansen & Linthicum, 2004; Hansen *et al*, 2006; Doherty *et al*, 2008). El ligando NRG1 actúa uniéndose al receptor ErbB2, que se asociará al receptor ErbB3 provocando una cascada de señales que darán lugar a la supervivencia, proliferación y

diferenciación de las células de Schwann (Newbern & Birchmeier, 2010). Recientemente se ha demostrado que la proteína merlin producida en los axones, es capaz de regular esta vía reduciendo los niveles de ErbB2 (Schulz *et al*, 2014), lo que reafirma la importancia de estas moléculas en la formación de los schwannomas, además de sugerir un papel activo de los axones en el desarrollo de estos tumores.

Otro gen descrito con una expresión alterada, en este caso por infraexpresión, es la caveolina 1 -*CAV1*- (Aarhus *et al*, 2010). La proteína codificada por este gen es fundamental en la formación de caveolas, que son invaginaciones de la membrana plasmática ricas en colesterol y cuya ausencia se ha documentado en numerosos tumores incluyendo el carcinoma oral de células escamosas (Han *et al*, 2004). En otros tumores como el cáncer de pulmón, el cáncer de próstata o algunos subtipos de cáncer de mama, se produce sobreexpresión de caveolina 1 favoreciendo la progresión tumoral, por lo que parece que la función específica de este gen es propia de cada tejido.

En cultivos primarios derivados de schwannomas procedentes de pacientes con NF2, se ha demostrado la activación de las quinasas "P21 Protein (Cdc42/Rac)-Activated Kinase 1" -Pak1- (Yi *et al*, 2008). Una de las causas de esta activación es la deficiencia de merlin, que actúa como inhibidor (Kissil *et al*, 2003). Esta activación parece fundamental en los schwannomas, ya que si se silencian los genes que codifican Pak1-4 mediante la técnica de shRNA -integrándose un inserto en el genoma que posteriormente produce pequeños ARN de interferencia que bloquean el gen elegido-, se reduce la capacidad de las células tumorales para crecer. Más aún, las células acaban silenciando el inserto de PAK1-4 mediante metilación (Yi *et al*, 2008), aunque no está claro si este silenciamiento es por el reconocimiento de la célula de ADN extraño, o bien por otra causa.

1.2.8 MicroRNAs en los schwannomas vestibulares

Los microRNAs –miRNAs- son pequeñas moléculas de tamaño aproximado a 21-25 nucleótidos, que generalmente están implicados en la degradación de ARN mensajero mediante su unión a la zona 3'UTR de éste. Cada miRNA es teóricamente capaz de disminuir los niveles de miles de mensajeros diferentes, siendo los mensajeros diana específicos de tejido. En los últimos años, dos trabajos han mostrado alteraciones de miRNAs en schwannomas. En el primero, se encontró el miRNA-21 sobreexpresado, mientras que la “phosphatase and tensin homolog” -*PTEN*- fue descrito como posible diana del miRNA-21 al encontrarse infraexpresado (Cioffi *et al*, 2010). Por otra parte, se ha descrito infraexpresión de miRNA-7 por Saydam *et al*, (2011). Al aumentar los niveles de este miRNA en cultivos celulares y en xenotransplantes de schwannomas en ratones, se ha comprobado que el crecimiento de estos tumores se reduce drásticamente. Por lo tanto, basándonos tanto en estudios en schwannomas como en otros tumores donde han sido comprobadas sus capacidades tumorales, parece claro que los miRNA constituyen una prometedora diana terapéutica de igual forma que los genes codificantes de proteínas clásicos.

1.2.9 Metilación

La metilación de dinucleótidos de CpG en el ADN es probablemente la modificación epigenética -sin cambios en la secuencia de ADN- más estudiada. Generalmente, se considera que la metilación aberrante de promotores suele llevar asociada pérdida de expresión en un determinado gen, mientras que la pérdida de metilación en regiones promotoras tiene como consecuencia la expresión de dicho gen. Estos fenómenos de hiper e hipometilación han sido ampliamente descritos en procesos

neoplásicos, como por ejemplo la hipermetilación aberrante del gen *MGMT* y su asociación con la mejor respuesta a temozolamida en glioblastomas (Esteller *et al*, 2000).

El gen *NF2* ha sido objeto de estudio epigenético en schwannomas para verificar si este mecanismo de silenciamiento génico está asociado a la deficiencia de merlin funcional en estos tumores. El primer trabajo que testó la metilación de *NF2* fue llevado a cabo por Kino *et al*, (2001). En él, se sugirió la existencia de 3 sitios CpG en la región promotora del gen, que según su estado metilado o no metilado, influía en la expresión del mensajero de *NF2*, y que podrían ser causantes de silenciamiento en un 61% de casos. Gonzalez-Gomez *et al*, (2003), encontraron también un 18% de casos con metilación del promotor de *NF2*, además de otros genes como *THBS1* -36%-, *TP73* -27%-, *MGMT* -20%-, *TIMP3* -18%-, *RB1* -4.5%- y *p16^{INK4a}* -11%-. En un trabajo posterior, ampliando la serie a 88 schwannomas (Bello *et al*, 2007), se obtuvieron niveles similares en los genes *THBS1* -30%-, *TP73* -19%-, *MGMT* -16%- y *TIMP3* -17%-. Comparando el grado de metilación con características clínicas, se obtuvo una correlación inversa entre el grado de crecimiento tumoral en estos tumores y la metilación aberrante del gen *RASSF1A* (Lassaletta *et al*, 2007). Volviendo a la metilación del gen *NF2* en schwannomas, en trabajos posteriores se detectaron niveles muy bajos de metilación en este gen (Kullar *et al*, 2010; Koutsimpelas *et al*, 2012), o más recientemente ni siquiera encontrada (Lee *et al*, 2012). Por lo tanto, parece que la metilación del gen *NF2* en schwannomas no es un hecho frecuente que determine la expresión del gen, aunque tal vez la utilización de diferentes metodologías para el análisis de metilación podría justificar la divergencia de resultados. No obstante, otros genes sí podrían mostrar estas alteraciones epigenéticas, por lo que son necesarios estudios más profundos sobre el tema.

1.3 MICROARRAYS

Tradicionalmente, la búsqueda de diferencias biológicas entre distintos tejidos, individuos o especies se ha llevado a cabo mediante la experimentación individual de cada molécula testada. La tecnología de los microarrays ha supuesto un salto cuantitativo en la cantidad de datos obtenidos a partir de muestras biológicas, ya que posibilita la adquisición de decenas o centenares de miles de mediciones en el mismo experimento. A pesar de que a nivel cualitativo estos datos masivos no superan en fiabilidad a las mediciones individuales de técnicas clásicas -aunque la precisión de estas técnicas masivas, así como su análisis ha ido mejorando con el tiempo-, resultan obvias las ventajas de este tipo de experimentos. Actualmente, se puede obtener el perfil genético completo de una serie de muestras de forma rutinaria y con análisis estadísticos que no requieren complejo software o especialistas en programación, característica esta última importante, ya que amplía su uso a muchos centros de investigación.

Existen numerosas plataformas de microarrays, que no solo varían en el tipo de molécula a analizar -ADN, ARN, proteínas, etc- sino que además, dentro de cada una de ellas existen diferentes tecnologías.

1.3.1 Microarrays de expresión

Los más utilizados hasta ahora han sido aquellos destinados a cuantificar la expresión génica relativa de ARN mensajero. Existen dos tipos básicos de estos microarrays, los de ADNc (Schena *et al*, 1995) y los de oligonucleótidos (Lockhart *et al*, 1996). A día de hoy, tres compañías copan la mayoría de la producción de microarrays de

expresión, con diferentes tecnologías cada una de ellas. En la empresa Agilent, los oligonucleótidos se imprimen en el soporte mediante la tecnología de SurePrint, que permite diseñar oligonucleótidos de 60 bases. En el caso de Illumina, las sondas se unen a pequeñas bolas magnéticas que se distribuyen aleatoriamente a lo largo del microarray. Posteriormente, se escanea para buscar la localización de cada bola. Los nucleótidos tienen una longitud de 50 bases. Las sondas de Affymetrix son de 25 bases, y se imprimen en el soporte correspondiente mediante una combinación de química y fotolitografía. Los microarrays de expresión de esta empresa son sin duda los más extendidos en publicaciones científicas, contando con tres modelos. El primero de ellos, basado en la unión de las sondas a la zona 3' de cada mensajero, contiene sondas con complemento de secuencia bases perfecto y sin él para evitar inespecificidades. Con ello se consigue una medición individual de la expresión de cada gen. En el caso de los Gene arrays, solo contiene sondas que complementan de forma perfecta, pudiéndose unir éstas a lo largo de varias zonas del mensajero, que proporciona después un valor promedio que nos dirá el alcance de la expresión del gen. Por último, los Exon arrays, también con sondas complementan de forma perfecta con la secuencia de bases, están diseñados para ofrecer resolución de diferentes isoformas de cada gen, siendo por lo tanto los que más información proporcionan. A nivel de gen, los resultados de las tres plataformas de Affymetrix son similares, encontrándose pocas diferencias cuando son comparadas (Pradervand *et al*, 2008; Okoniewski *et al*, 2007; Robinson & Speed, 2007).

La expresión de los miRNAs también puede ser analizada mediante tecnología de microarrays. Debido a que el número de miRNAs aumenta constantemente, nuevas versiones de estos chips, independientemente de la compañía, aparecen en el mercado

cada poco tiempo. Las cuatro compañías con más presencia en este campo son Agilent, Affymetrix, Exiqon e Illumina. En el caso de Affymetrix, se usan 4 sondas por miRNA en hibridación perfecta. Estudios comparativos de las diferentes plataformas en las mismas muestras han encontrado que, aunque en general los datos son similares, existen diferencias entre los miRNAs que detecta cada plataforma (Callari *et al*, 2012; Del Vescovo *et al*, 2013).

1.3.2 Microarrays de metilación

Existen otros microarrays que nos ofrecen información epigenética sobre la probabilidad de que un dinucleótido de CpG determinado esté o no metilado. Los más extendidos en uso actualmente, y más recientes, son los Infinium HumanMethylation450 BeadChip, de la compañía Illumina. Hasta 485.577 sitios CpG pueden ser testados mediante esta plataforma. El funcionamiento de esta tecnología se basa en dos tipos de sondas. En las de tipo I, la señal de un sitio CpG como metilado y demetilado están en el mismo canal -rojo o verde-, pero usando distinto cebadores. En las de tipo II, el canal demetilado -rojo- y el metilado -verde- usan los mismos cebadores. Posteriormente, la comparación entre la señal emitida metilado/demetilado ofrecerá un valor beta, que es la probabilidad de que un sitio CpG concreto esté metilado -cercano a 1- o demetilado -cercano a 0-. El tratamiento de procesamiento y el estadístico posterior, varían de manera amplia según el tipo de estudio.

1.3.3 Aplicaciones de los microarrays

La principal aplicación de los microarrays en cáncer consiste en la comparación entre tejido sano -control- y tumoral, o bien la identificación de nuevos subgrupos entre

muestras neoplásicas de un mismo tipo histopatológico. Cuando se establecen previamente agrupaciones de muestras, se utilizan métodos supervisados que proporcionan diferencias estadísticas entre los grupos dados. Cuando no se conocen, o bien se quiere comprobar la relación de las muestras sin asignar características previas, se usan métodos no supervisados como el coeficiente de correlación de distancias de Pearson.

Existen numerosos estudios en la literatura de clasificaciones tumorales realizadas a partir de datos extraídos de microarrays, en muchos casos correlacionando los resultados moleculares con los parámetros clínicos. Uno de los primeros estudios en mostrar la capacidad de los microarrays de expresión para el descubrimiento y/o la predicción de clases -subtipos tumorales- fue descrita por Golub *et al*, (1999) entre leucemia mieloide y linfoblástica aguda. En cáncer de mama, Sørlie *et al*, (2001) establecieron, con el uso de microarrays de expresión de 427 genes, distintos subgrupos de tumores positivos al receptor de estrógenos con desigual pronóstico clínico. En glioblastomas, uno de los tumores más comunes y con peor pronóstico del sistema nervioso central, se identificaron cuatro grupos de expresión -proneural, neural, mesenquimal y clásico-, que se relacionaron además con numerosos parámetros moleculares descritos previamente como amplificación de *EGFR* -en el subtipo clásico y el neural-, la mutación de *TP53* -en el proneural- o de *NF1* -en el mesenquimal- (Verhaak *et al*, 2010).

Los patrones de expresión de miRNA en cáncer son claramente diferentes a los del tejido no tumoral (Iorio *et al*, 2005; Porkka *et al*, 2007) y al igual que los patrones de expresión génica, también han permitido la identificación de factores pronósticos, como

en carcinoma nasofaríngeo (Liu *et al*, 2012), en cáncer de colon (Zhang *et al*, 2013), en leucemia linfocítica crónica (Calin *et al*, 2005) o cáncer de páncreas (Roldo *et al*, 2006); así como la clasificación de tumores (Rosenfeld *et al*, 2008), incluso en muestras que no podían ser caracterizadas por ARN mensajero (Lu *et al*, 2005).

Los patrones obtenidos mediante microarrays de metilación, también han proporcionado información útil sobre la clasificación de diferentes tumores así como del pronóstico. En concreto, los llamados *CpG island methylator phenotype* -CIMP-, son subgrupos tumorales que presentan metilación de múltiples genes simultáneamente, lo que conlleva su silenciamiento. Dependiendo del tipo de cáncer, éste hecho se asocia con mejor o peor pronóstico. En neuroblastomas, el CIMP está asociado a mal pronóstico (Abe *et al*, 2005), mientras que en oligodendrogliomas se atribuye a una mejor respuesta del paciente al tratamiento quimioterapéutico (Mur *et al*, 2013).

1.3.4 Limitaciones de los microarrays

A pesar de la indudable aportación de los microarrays para el descubrimiento de nuevos subtipos tumorales, así como el establecimiento de otros ya existentes, esta tecnología presenta una serie de limitaciones que conviene poner de manifiesto para valorar de forma crítica los resultados de los diversos estudios. Las limitaciones dependen del tipo de microarray utilizado, ya que la problemática varía en función de la molécula necesaria para la hibridación -ADN, ARN, etc-, así como de la plataforma específica utilizada y el objetivo del estudio. Para el estudio del cáncer con microarrays de metilación y expresión, los principales obstáculos serían los siguientes:

- Muestra

En primer lugar, como siempre que se trabaje con tejidos tumorales, la muestra debería ser representativa del tumor a analizar y contener un porcentaje de células tumorales suficientemente alto para no diluir los resultados con otro material. En muchos casos, los tumores son heterogéneos, variando los patrones de expresión entre diferentes zonas de la misma masa tumoral. Esta heterogeneidad ha sido descrita en glioblastomas, detectando en un mismo tumor dos de los cuatro subtipos -proneural y mesenquimal- que han sido caracterizados en esta neoplasia (Sottoriva *et al*, 2013). Asimismo, en el caso de análisis que involucren ARN, especialmente el mensajero por su longitud, hay que tener precauciones que impidan su degradación, como por ejemplo la rápida congelación de la muestra mediante nitrógeno líquido tras su resección quirúrgica y su posterior conservación a -80 °C hasta que dicha muestra vaya a ser procesada. No obstante no pueden descartarse cambios en la expresión génica en el tumor desde el inicio de la intervención hasta su congelación.

- Controles

Para los estudios de expresión que requieran un control sano -no tumoral-, pueden existir limitaciones muy marcadas. Esto es especialmente relevante en aquellas neoplasias sin un origen celular claro o que están compuestas de varios tipos celulares, ya que el tejido sano de partida podría no ser representativo del tumor formado posteriormente. Este problema no se aplica a aquellos estudios en los que se comparan distintos tipos tumorales entre sí.

- Análisis de los datos

En el caso de los estudios que incluyen métodos supervisados de análisis, los umbrales sobre los que se considera si hay o no alteración de un determinado parámetro pueden dar lugar a una excesiva subjetividad. En el caso de la expresión diferencial para considerar un gen infra o sobreexpresado, el método está relativamente estandarizado, como proponen en el consorcio del control de calidad para microarrays (Shi *et al*, 2006). Concretamente, sugieren un p-valor no astringente, es decir, sin correcciones adicionales como la de Bonferroni; y definir la existencia de cambio en la expresión en base a una diferencia de al menos el doble entre grupos. En general este valor de corte suele ser adecuado para el estudio del cáncer, aunque en otro tipo de estudios puede resultar muy restrictivo, como por ejemplo en estudios en los que se compare la respuesta de cultivos a una infección vírica (Jang *et al*, 2011). Sin embargo, en los microarrays de metilación, tanto el procesamiento de los datos como los umbrales para considerar hiper o hipometilación, varían de forma muy pronunciada entre diferentes estudios.

- Efecto de lote

Existen además determinadas limitaciones técnicas, que si bien pueden ser minimizadas mediante una buena planificación del experimento, en otros casos habrá que realizar correcciones a posteriori. Un ejemplo es el efecto de proceso por lotes -o efecto batch-, que ocurre cuando todas las muestras del mismo estudio no pueden ser analizadas a la vez, sino que se procesan en diferentes tiempos. En este caso, habrá que asegurar que se eligen muestras de todos los tipos -por ejemplo tumores y controles- en cada lote, siempre y cuando se conozcan los grupos. Antes de aplicar medidas correctoras, conviene asegurarse de que el efecto existe, ya que en algunas plataformas puede ser más marcado

que en otras o incluso no existir. Una vez que se detectan los efectos de lote, habrá que aplicar las correcciones pertinentes, para lo que existen numerosos paquetes estadísticos (Chen *et al*, 2011). Uno de los métodos más fiables por su gran reproducibilidad, es el método bayesiano descrito por Johnson *et al*, (2007).

- Rango dinámico

Los datos ofrecidos por los microarrays, especialmente en el campo de la expresión, han de ser considerados como informativos. Indican hacia dónde varía una medición concreta, por ejemplo si un gen determinado está más o menos expresado en un tipo tumoral concreto, en lugar de ser interpretado únicamente como una medición cuantitativa del parámetro en cuestión. La expresión de un gen obtenida mediante microarrays tiende a ser distinta, generalmente menor, que la obtenida con PCR cuantitativa o las nuevas técnicas de secuenciación masiva como el RNA-seq. Ello es debido a la diferencia de rango dinámico entre una y otra técnica, fenómeno ampliamente descrito (Abruzzo *et al*, 2005; Dallas *et al*, 2005; Wang *et al*, 2009; Kogenaru *et al*, 2012; Zhao *et al*, 2014). A pesar de esto, en general, e independientemente de la plataforma utilizada, los datos de microarrays de expresión se correlacionan bien con los de PCR cuantitativa (Canales *et al*, 2006; Wang *et al*, 2006).

- Amplificaciones

En los microarrays de expresión, hay que destacar que desde que el ARN es purificado hasta que se hibrida en el propio microarray, existen varios pasos que pueden introducir un sesgo posterior en las mediciones. El más crítico es la amplificación, que se realiza con el objetivo de conseguir la cantidad necesaria de ARN, desde que la muestra se

procesa al inicio, para hibridarla posteriormente en el microarray. En algunos casos puede llegar a distorsionar los resultados (Diboun *et al*, 2006), aunque en general éstos son reproducibles independientemente del protocolo utilizado (Li *et al*, 2005; McClintick *et al*, 2003).

1.3.5 Disponibilidad de los datos y su presentación en publicaciones

A pesar de las limitaciones descritas para los microarrays, y el desarrollo de las nuevas tecnologías de secuenciación masiva, los microarrays continúan siendo empleados en muchos laboratorios, y siguen apareciendo numerosas aplicaciones de esta tecnología en la literatura científica. Por último, debemos destacar que en la mayoría de las publicaciones que usan microarrays, los datos sin procesar quedan disponibles para la comunidad científica, por lo que cualquier investigador interesado en ellos puede acceder y comprobar por sí mismo las conclusiones alcanzadas por los diferentes equipos de investigación, así como validar sus propios resultados o buscar nuevos hallazgos. Una de las plataformas más utilizadas es la *Gene Expression Omnibus* -GEO- database <http://www.ncbi.nlm.nih.gov/geo/>, siguiendo las indicaciones del *Minimum Information About a Microarray Experiment* -MIAME-, que son un conjunto de directrices para la correcta difusión de los datos (Brazma *et al*, 2001; Ball *et al*, 2004).

1.3.6 Análisis de enriquecimiento

Los resultados provenientes de microarrays pueden generar listas de cientos de miles de datos, lo que hace prácticamente imposible su análisis, al menos a nivel global, sin herramientas que lo faciliten. Para este trabajo, existen numerosas plataformas que traducen la ingente información que los investigadores proporcionan, devolviendo

resultados comprensibles como las rutas o vías moleculares de interés en nuestros datos. Uno de los análisis más extendidos es el de enriquecimiento, estando disponible de manera gratuita y libre en plataformas como DAVID (Huang *et al*, 2009a; Huang *et al*, 2009b) <http://david.abcc.ncifcrf.gov/>. El funcionamiento de este programa es relativamente sencillo, aunque tiene numerosas opciones para personalizar los resultados obtenidos que lo pueden complicar. Según la lista de genes introducida y el total de genes testados, el programa calcula el enriquecimiento relativo de las vías implicadas, proporcionando además un valor de la robustez del resultado.

1.3.7 Microarrays en schwannomas

En schwannomas vestibulares se han realizado diversos estudios con tecnología de microarrays, la mayoría en el campo de la expresión génica. En el primero de ellos, se usaron 4 filtros "Expressed sequence tags" -EST- (Adams *et al*, 1991) de 25.920 genes en 7 schwannomas vestibulares y un nervio sano como control (Welling *et al*, 2002). Se identificaron 42 genes sobreexpresados y 8 infraexpresados. En otro estudio, con 5 filtros EST de más de 25.000 genes en 8 schwannomas vestibulares y un nervio sano (Lasak *et al*, 2002), el gen *RB1* y varios genes codificadores de ciclinas fueron encontrados desregulados. Posteriormente, mediante microarrays Affymetrix HG-U133A en 16 tumores y 3 nervios sanos, se detectó la expresión aberrante de 78 genes (Cayé-Thomasen *et al*, 2010), 75 de los cuales presentaron sobreexpresión y 3 infraexpresión. De los 78 genes, 11 estaban implicados en diferenciación celular -como *CCND1*, *CHL1* o *ANXA1*- y 13 en adhesión -incluyendo *PTEN*, *LAMB2* o *L1CAM*-. Con los microarrays ABI 1700 en 25 schwannomas vestibulares y 3 controles, se obtuvo una amplia lista de genes alterados, entre los que figuraba la infraexpresión de la caveolina-1, que fue confirmada por

inmunohistoquímica (Aarhus *et al*, 2010). Recientemente, se compararon los patrones de expresión entre 6 schwannomas vestibulares sólidos y 11 quísticos, obteniéndose una serie de genes desregulados -*CNTF*, *COL4A3* o *COL4A4*- entre estos grupos (Zhang *et al*, 2014).

El patrón de expresión de schwannomas también ha sido comparado con el de meningiomas (Martinez-Glez *et al*, 2009). En este caso, utilizando microarrays de 96 genes, se establecieron dos grupos de expresión de schwannomas, uno de ellos mostrando un patrón similar al del tejido control -meninges-, mientras que el otro era más parecido a los meningiomas.

En cuanto a la expresión de miRNAs mediante microarrays, hay un solo estudio previo (Saydam *et al*, 2011). En este caso, se analizaron 10 tumores y 2 controles sanos, detectándose 19 miRNAs desregulados de los 407 testados. Hasta la fecha, no hay publicado ningún estudio de microarrays de metilación en schwannomas.

Si bien las funciones del producto proteico del gen *NF2*, merlin, son relativamente bien conocidas en comparación a lo publicado en la década anterior, siguen existiendo numerosas preguntas sin resolver respecto a su implicación en tumores de origen celular tan concreto. Así mismo, se han desentrañado varias vías moleculares alteradas en los schwannomas, que han posibilitado incluso diversos ensayos terapéuticos, aunque el alcance de éstos sea más bien limitado (Plotkin *et al*, 2009; Plotkin *et al*, 2010; Karajannis *et al*, 2012; Karajannis *et al*, 2014). Los métodos de datos masivos del presente trabajo, ayudarán sin duda a delimitar el perfil genético y epigenético de los schwannomas, siendo un primer paso hacia la búsqueda farmacológica de compuestos que ayuden a los pacientes que sufren esta enfermedad, y en el grado que sea posible, evitar los

tratamientos agresivos que en muchas ocasiones condiciona su calidad de vida. Además, con el objetivo de buscar dianas que sean especialmente válidas para pacientes con NF2, incluimos un estudio de la expresión comparada entre schwannomas y otros tumores comunes en esta enfermedad genética, los meningiomas.

2. OBJETIVOS

2. OBJETIVOS

- 1 – Establecer el estado mutacional del gen *NF2* y de la pérdida de heterocigosidad del brazo largo del cromosoma 22, a través de la búsqueda de alteraciones del gen de una serie de 51 schwannomas vestibulares esporádicos, así como de 6 con origen en pacientes de *NF2* y 4 schwannomas no-vestibulares.
- 2 – Testar la amplificación o ganancia de copias de varios genes relacionados con la génesis de schwannomas y tumores del sistema nervioso.
- 3 – Conocer el perfil genético, mediante microarrays de expresión del ARN mensajero y de miRNAs, en schwannomas vestibulares y una serie de controles no tumorales.
- 4 – Identificar alteraciones en la metilación de sitios CpGs en las mismas muestras testadas para los microarrays de expresión, con el fin de establecer posibles mecanismos de la desregulación génica.
- 5 – Con los datos obtenidos en los anteriores puntos, identificar marcadores moleculares con potencial diagnóstico, pronóstico y terapéutico.
- 6 – Para buscar marcadores especialmente útiles en pacientes con *NF2* testar, en una serie de meningiomas, genes desregulados en estos tumores y compararlos con el patrón obtenido en los schwannomas.

3. PUBLICACIONES

ARTÍCULOS PUBLICADOS PRESENTADOS

1 - NF2 genetic alterations in sporadic vestibular schwannomas: clinical implications. Luis Lassaletta, **Miguel Torres-Martín**, Carolina Peña-Granero, José María Roda, Santiago Santa-Cruz-Ruiz, Javier S. Castresana, Javier Gavilán y Juan A. Rey. *Otology & Neurotology*. Año: 2013 Volumen: 34 Páginas: 1355-1361.

2 - DNA copy gains of tumor-related genes in vestibular schwannoma. Luis Lassaletta, **Miguel Torres-Martín**, Jesús San-Román-Montero, Javier S. Castresana, Javier Gavilán y Juan A. Rey. *European Archives of Oto-Rhino-Laryngology*. Año: 2013 Volumen: 270 Páginas: 2433-2438.

3 - Microarray analysis of gene expression in vestibular schwannomas reveals SPP1/MET signaling pathway and androgen receptor deregulation. **Miguel Torres-Martín**, Luis Lassaletta, Jesús San-Román-Montero, José María de Campos, Alberto Isla, Javier Gavilán, Bárbara Melendez, Giovanni R. Pinto, Rommel R. Burbano, Javier S. Castresana y Juan A. Rey. *International Journal of Oncology*. Año: 2013 Volumen: 42 Páginas: 848-862.

4 - Global profiling in vestibular schwannomas shows critical deregulation of microRNAs and upregulation in those included in chromosomal region 14q32. **Miguel Torres-Martín**, Luis Lassaletta, de Campos JM, Alberto Isla, Javier Gavilán, Giovanni R. Pinto, Rommel R. Burbano, Farida Latif, Bárbara Melendez, Javier S. Castresana y Juan A. Rey. *PLoS One*. Año: 2013 Volumen: 8 Artículo: e65868.

ARTÍCULOS EN REVISIÓN PRESENTADOS

5 - Genome-wide methylation analysis in vestibular schwannomas shows putative mechanisms of gene expression modulation and global hypomethylation at the HOX gene cluster. **Miguel Torres-Martín**, Luis Lassaletta, José María de Campos, Alberto Isla, Giovanni R. Pinto, Rommel R. Burbano, Bárbara Melendez, Javier S. Castresana, y Juan A. Rey.

6 - Global expression profile in low grade meningiomas and schwannomas shows up-regulation of PDGFD, CDH1 and SLIT2 in both tumors with respect to their healthy tissue. **Miguel Torres-Martín**, Luis Lassaletta, Alberto Isla, Jose M de Campos, Giovanni R. Pinto, Rommel R. Burbano, Javier S. Castresana, Bárbara Meléndez y Juan A. Rey.

3.1 ARTÍCULO 1

TÍTULO: NF2 genetic alterations in sporadic vestibular schwannomas: clinical implications.

REVISTA: Otology & Neurotology. Año: 2013 Volumen: 34 Páginas: 1355-1361.

AUTORES: Luis Lassaletta, **Miguel Torres-Martín**, Carolina Peña-Granero, José María Roda, Santiago Santa-Cruz-Ruiz, Javier S. Castresana, Javier Gavilán y Juan A. Rey.

RESUMEN: En este trabajo se buscan si las alteraciones en el gen NF2 guardan relación clínica en pacientes con schwannoma vestibular esporádico. Se realizaron correlaciones entre las distintas alteraciones moleculares de *NF2* (mutación del gen y pérdida de heterocigosidad del cromosoma 22), y la información clínica de cada paciente. Se detectó cambio de secuencia de *NF2* en un 49% de los pacientes, LOH de 22q en el 57% y pérdida de al menos un exón mediante MLPA en el 13.7% de los casos. Se registró un solo evento mutacional en *NF2* en el 27% de los tumores, 2 en el 45%. No hubo asociación entre el tipo de mutación de *NF2* y parámetros clínicos. La presencia de mutaciones en *NF2* mediante la técnica de PCR/dHPLC (que detecta pequeñas mutaciones) se asoció a la ausencia de pérdida de audición en el momento de la detección de la lesión tumoral, así como a la no penetración del tumor en el canal auditivo interno. La inactivación del gen *NF2* mediante todas las técnicas empleadas fue más frecuente en pacientes fumadores que en no fumadores.

METODOLOGÍA:

- Se estudiaron 51 schwannomas vestibulares esporádicos y la correspondiente sangre periférica de los pacientes.
- La extracción del ADN genómico de tumor y sangre periférica se llevó a cabo utilizando Wizard® Genomic DNA Purification Kit de Promega.
- Para testar la pérdida de heterocigosidad en el brazo largo del cromosoma 22, se utilizaron 5 marcadores microsatélites de regiones altamente polimórfica -D22S275, D22S264, D22S929, D22S268 y D22S280-. Mediante esta técnica, al comparar el ADN de la muestra tumoral con el propio ADN de sangre periférica del paciente, se pueden identificar pérdidas alélicas en el tejido tumoral.
- El análisis mutacional de pequeñas delecciones, inserciones o cambios de secuencia, se realizó mediante la reacción en cadena de la polimeras/cromatografía líquida desnaturizante de alto rendimiento (PCR/dHPLC) como screening inicial. Tras la amplificación de un fragmento de ADN determinado mediante PCR, se desnaturaliza y renaturaliza el ADN para formar homoduplex y heteroduplex, que muestran un patrón diferente en el dHPLC. Posteriormente, se secuenciaron bidireccionalmente aquellas muestras con un cambio en el patrón de dHPLC.
- Para detectar grandes mutaciones como pérdida o duplicación de exones enteros, se empleó la amplificación múltiple dependiente de ligasa (MLPA). El kit usado fue la SALSA P044 NF2, que incluye los 17 exones de NF2 y dos regiones promotoras. Mediante el uso de muestras control, se puede determinar si el estado alélico de un fragmento analizado corresponde a: amplificación, ganancia de copias, constitución normal, pérdida de heterocigosidad o pérdida monosómica (de mayor a menor número de copias).

NF2 Genetic Alterations in Sporadic Vestibular Schwannomas: Clinical Implications

*Luis Lassaletta, †Miguel Torres-Martín, ‡Carolina Peña-Granero,
 ‡Jose Maria Roda, §Santiago Santa-Cruz-Ruiz, ||Javier S. Castresana,
 *Javier Gavilan, and †Juan A. Rey

*Department of Otolaryngology, †Unidad de Investigación, Molecular Neuro-Oncogenetics Laboratory,

‡Department of Neurosurgery, "La Paz" University Hospital, IdiPAZ, Madrid; §Department of
 Otolaryngology, Salamanca University Hospital, Salamanca; and ||Brain Tumor Biology Unit,
 University of Navarra School of Sciences, Pamplona, Spain

Hypothesis: NF2 gene alterations may have a clinical impact in non-NF2 vestibular schwannomas (VSs).

Background: It has been suggested that NF2 mutations might correlate with clinical expression of VS in NF2 patients. The aim of this study was to analyze the impact of genetic alterations in the NF2 gene on epidemiologic, clinical, and radiologic features of patients with sporadic VS. The association between cigarette consumption and the molecular genetic findings was also studied.

Methods: The study group consisted of 51 patients who underwent surgery for removal of vestibular schwannoma in our institution between January 2006 and December 2010. Five highly polymorphic microsatellite DNA markers were used to observe the frequency of loss of heterozygosity (LOH) in chromosome 22. The NF2 gene mutations were detected using polymerase chain reaction amplification and denaturing high-performance liquid chromatography analysis (PCR/dHPLC), and direct sequencing of NF2. Multiplex ligation-dependent probe amplification (MLPA) of the NF2 gene was also performed.

Results: An NF2 mutation was identified in 49%, 22q LOH in 57%, and MLPA alterations in 13.7% of the cases. One

mutational hit was present in 27%, and 2 hits were present in 45% of the tumors. No association was found between the type of NF2 mutation and relevant clinical parameters. The presence of NF2 mutations detected by PCR/dHPLC was associated with no complaint of hearing loss at the time of diagnosis ($p = 0.023$), with subjective aural fullness ($p = 0.022$) and with an absence of tumor involvement of the internal auditory canal ($p = 0.029$). Patients with NF2 mutations had lower mean corrected PTA thresholds compared with those with no NF2 mutation ($p = 0.037$). Inactivation of the NF2 gene by mutation, MLPA, or LOH was more frequent in smokers when compared with never smokers ($p = 0.048$).

Conclusion: NF2 mutations may play a role in the pathophysiology of hearing loss as well as in the pattern of growth of VS. Cigarette smoking in patients with VS seems to play a role in both the risk of developing the tumor and also in its genetic profile. More studies are needed to corroborate these results and, more broadly, to establish links between molecular and clinical data. **Key Words:** Clinical implications—Hearing loss—NF2 gene—NF2 mutation—Vestibular schwannoma.

Otol Neurotol 34:1355–1361, 2013.

Vestibular schwannomas (VSs) are benign tumors arising from the sheath of the cochleovestibular nerve. These tumors generally grow slowly, causing minimal symptoms at the time of diagnosis. Hearing loss and tinnitus are the main features of VS, whereas vertigo, facial paralysis, or other incapacitating symptoms are less common initial symptoms. The growth rate of VS is known to be extremely variable, with most tumors

growing slowly for many years. A peculiar aspect of these tumors is that their evolution in size and hearing level remains unpredictable. There is no correlation between tumor size and hearing loss (1).

Inactivation of Merlin, the product of the NF2 tumor suppressor gene, is responsible for VS development, in both sporadic and bilateral cases. To date, the loss of 22q harboring the NF2 gene has been the only constant genetic alteration reported in schwannomas (2). Inactivation of the NF2 gene occurs in more than 60% of schwannoma cases, either by mutation of both alleles or by loss of one allele and mutation of the other (3). However, as Merlin protein seems to be absent in most, if not all VS (4), other mechanisms may lead to inactivation of this protein.

Address correspondence and reprint requests to Luis Lassaletta, M.D., Department of Otolaryngology, IdiPAZ. Hospital La Paz, Paseo de la Castellana, 261, 28046 Madrid, Spain; E-mail: luikilassa@yahoo.com

Support for this work was provided by Grants 07/0577, 08/1849, and 10/1972 from Fondo de Investigación Sanitaria, Ministerio de Sanidad. The authors disclose no conflicts of interest.

Osteopontin has been described as responsible for Merlin degradation in breast cancer (5), and recently, this gene has also been reported to be upregulated in VS (6). Thus, osteopontin may inhibit Merlin in tumors with no *NF2* DNA alterations.

Cytogenetic and LOH (loss of heterozygosity) studies have shown monosomy or partial loss of the chromosome 22 in approximately 40% to 50% schwannomas (7–9). Other molecular alterations have been proposed to explain the molecular biology of VS. DNA copy number analysis has revealed recurrent chromosomal gains of 9q34 and 17q and losses of 1p and chromosome Y in a few cases (10,11). The DNA methylation process, which consists of the methylation of cytosine at position C5 in CpG dinucleotides, has been described in VS involving the *NF2* gene (12–15) and other tumor-related genes (16); nevertheless, controversial findings have been reported, as *NF2* frequencies of methylation in those reports ranged from 0% to 50%. Clinical implications of this feature have been analyzed in patients with VS (17). Recent studies on microarray gene expression profiling have provided data allowing the identification of gene expression patterns linked to differentially expressed genes and pathways that play key roles in schwannoma development (18–22). Cyclin D1 is a cell cycle regulatory protein for the mammalian G1-S phase transition and is implicated in cell proliferation and differentiation. Lassaletta et al. (23) found cyclin D1 immunohistochemical expression in 52% of cases of VS. Recently, immunogenic factors (24), cytokines, and growth factors (25) have also been proposed to play a role in the molecular pathophysiology of VS. Whereas a clear progression in mutation type distribution by severity has been described in *NF2* patients (26), the clinical significance of molecular alterations in sporadic VS is still unknown.

Little is known about the cause of VS. Risk factors including loud noise, mobile phone use, and some occupational hazards have been investigated with inconclusive results. Cigarette consumption has recently been suggested to have an effect on VS risk (27).

The aim of this study was to analyze the impact of genetic alterations of the *NF2* gene on epidemiologic, clinical, and radiologic features of patients with sporadic VS. A possible association between the smoking status of the patients and the genetic findings was also studied.

MATERIALS AND METHODS

Patients

The study group consisted of 51 patients who underwent surgery for removal of vestibular schwannoma in our institution between January 2006 and December 2010. Patients with a history of previous irradiation, previous VS surgery, known *NF2* disease, or origin different from the vestibular nerve were excluded. The study was approved by the hospital's ethics committee.

Epidemiologic, Clinical, and Radiologic Data

The population included 24 women and 27 men with a mean age at surgery of 48 years (range, 14–75 yr). The tumor was on

the left side in 23 cases (45%). The primary clinical complaint at the time of diagnosis was hearing loss (50%), tinnitus (20%), dizziness (11%), and vertigo (4%). Other symptoms accounted for 14% of cases. When specifically asked about particular complaints, the percentage of patients having each symptom was hearing loss (90%), tinnitus (72%), dizziness (47%), vertigo (20%), ear fullness (10%), and facial alterations (29%). Preoperative facial function was House-Brackmann Grade 1 in 96% and Grade 2 in 4% of patients. Mean pure-tone threshold for the tumor ear and the contralateral ear were 53 and 30 dB, respectively. To avoid the effect of presbycusis, the hearing loss of the contralateral ear was subtracted from the hearing loss of the affected ear (corrected threshold) as previously described (28). The mean corrected threshold was 30 dB. Mean speech reception threshold was 50 dB (range, 0–85 dB). Maximum speech discrimination score (SDS) ranged from 0% to 100%, with a mean of 58%. Tumor size measured as the largest diameter in the axial plane of MRI ranged from 5 to 52 mm (mean, 25 mm). In addition, the tumor volume was also measured using MRI, using the formula for an ellipsoid, as previously described (29). Mean tumor volume at presentation was 6.7 cm³, ranging from 0.16 to 37.483 cm³. Size was evaluated as Stage 1 (intracanalicular) in 2 cases (4%), Stage 2 (15 mm in its greatest diameter in the CPA) in 12 cases (23%), Stage 3 (16–30 mm in the CPA) in 29 cases (57%), and Stage 4 (>30 mm in the CPA) in 8 cases (16%). Tumor appearance was homogeneous (53%), heterogeneous (29%), and cystic (18%). Tumors in the CPA were centered in the internal auditory canal (IAC) in 82%, posterior in 12%, and anterior in 4% of the cases. Involvement of the fundus of the IAC was assessed on T2-weighted MRI as absence of the normal high cerebrospinal fluid signal intensity between the fundus and the distal end of the tumor. The fundus of the IAC was involved in 68% of the cases. Twenty-six patients (52%) were never smokers, whereas 14 (28%) were current smokers, and 10 (20%) were past smokers. Therefore, the number of never and ever smokers was 26 (52%) and 24 (48%), respectively.

Molecular Genetic Analysis

DNA Extraction

DNA was isolated from frozen vestibular schwannoma samples, using the Wizard Genomic DNA purification kit (Promega, Madison, WI, USA). DNA from the corresponding patients' peripheral blood was also extracted.

Loss of Heterozygosity Studies

The allelic status of 5 microsatellite markers at the D22S275, D22S264, D22S929, D22S268, and D22S280 loci (22q11-q12.3) was determined by labeling 5' primers with fluorescent markers (6-FAM/HEX and ROX as a size standard; Applied Biosystems, Foster City, CA, USA). Allelic ratios were defined according to previously described criteria: T2xN1/T1xN2 in which LOH < 0.6–1.67 > LOH (30).

PCR/dHPLC Analysis and Direct Sequencing of *NF2*

For *NF2* mutation screening, PCR/dHPLC analysis and direct sequencing of *NF2* were performed. Genomic DNA amplification was performed using standard PCR methods (total volume of 20 µl). A set of 15 primer pairs was used as described (31). Mutational screening was carried out using dHPLC following the manufacturer's protocols (Transgenomic WAVE dHPLC Systems). Samples with abnormal patterns were sequenced bidirectionally (ABI 3100 Avant; Applied Biosystems), using the

Big Dye sequencing kit (Applied Biosystems), to determine the position and nature of the alteration. For name mutations, sequence NM_000268.3 was used when the alteration appeared within mature mRNA, and NC_000022.10 when the mutation was inside of the intron sequence. Mutations were named according to den Dunnen and Antonarakis (32).

Multiplex Ligation-Dependent Probe Amplification of the NF2 Gene

We used a commercial MLPA kit for *NF2* gene analysis (SALSA P044 NF2). Information on the probe sequences and ligation sites can be found at <http://www.mlpa.com>. The MLPA protocol was performed as described by the manufacturers and according to the method we described previously (33), using 100 ng of DNA from control and tumor samples. The data analysis was performed with MRC-Coffalyser software (MRC-Holland) and Microsoft Excel. Values less than 0.1 were considered as background.

As MLPA and LOH by microsatellites give us overlapping information regarding 22q status, only microsatellite markers were taken into account for hits in *NF2*. MLPA was only considered for individual exon-probe deletion, in agreement with Hadfield et al. (9).

Statistical Analyses

Categorical variables were described by frequency (percentage) and continuous variables as mean (standard deviation). Groups of patients were compared using the Mann-Whitney test for continuous variables, and χ^2 and Fisher's exact tests for categorical values. Because of the limited sample size, only univariate (unadjusted) associations were generated. All analyses were performed using SPSS 13.0 for Windows. Differences were considered significant at a level of $p < 0.05$.

RESULTS

Table 1 shows the main genetic findings.

LOH Analysis

Using 5 microsatellites markers, LOH of 22q11-q12.3 occurred in 29 (57%) of 51 tumors.

Mutational Analysis by PCR/dHPLC

Mutational analysis by PCR/dHPLC showed 25 (49%) of 51 of the samples with at least 1 alteration at the *NF2* gene. Three of 25 altered tumors presented 2 mutations (Samples 35, 41, and 48), with a total of 28 mutations detected. By analyzing the changes in the nucleotide sequence, small deletions of 1 to 15 pairs of bases were the most common events with 13 cases (46%) followed by 12 point mutations (43%). Small insertions occurred in 2 cases. Seven mutations (25%) affected the intronic region. Patient 32 had both intron and exon affected regions. Nonsense mutation c.169C > T was the only one repeated in our series. Most changes of sequence occurred at exon 4 (8 cases) followed by exon 2 (4 cases). Exons 6 and 9 were not affected by any mutation. The first half of the *NF2* gene (exons 2–8) showed 71% of the total mutations. Two samples (11 and 48) presented the *NF2* gene mutated in both tumor DNA and peripheral blood.

These 2 cases had no features of *NF2* preoperatively or postoperatively, probably representing mosaic cases.

MLPA Analysis of the NF2 Gene

In agreement with LOH findings, MLPA analysis of the *NF2* gene (SALSA P044) showed results compatible with the total loss of an *NF2* allele in 19 cases (37%). Additionally, 7 (13.7%) of 51 cases displayed deletion of at least 1 exon. In 4 tumors with a MLPA deletion, no sequence alterations were found by PCR/dHPLC. However, 3 of these cases were concomitant with LOH of 22q. Multiple deletions were also present in 4 cases, that is, tumor 15, which showed a deletion from exons 14 to 17. By MLPA, exons 4 and 14 were the most commonly altered in the series with 3 cases each.

Summary of NF2 Analyses

Because of the biallelic gene constitution of the cell, at least 2 hits (by mutation, 22q LOH, etc) are theoretically needed to inactivate the tumor suppressor *NF2* gene (26). As shown in Table 1, two or more mutational hits were found in 23 (45%) tumors. Two were exclusively due to 2 mutations at the *NF2* sequence (Samples 41 and 48); 3 tumors had 2 hits because of a MLPA alteration adding LOH of 22q with no PCR/dHPLC alterations; the rest presented this pattern because of a combination of several LOH and sequence mutations found by MLPA and/or PCR/dHPLC. A single mutational event was established in 14 (27%) cases: 8 with LOH of 22q, 5 with a mutation detected by PCR/dHPLC, and 1 with a deletion found by MLPA. In 14 (27%) of 51 tumors, neither molecular alteration of the *NF2* gene nor 22q LOH / MLPA alteration were found.

Clinical Associations

In our study, the presence of *NF2* mutations by PCR/dHPLC was associated with no complaint of hearing loss at the time of diagnosis, subjective aural fullness, and no tumor involvement of the IAC (Table 2). *NF2* mutations detected by PCR/dHPLC were also associated with hearing level at the time of diagnosis. Patients with *NF2* mutations had lower mean corrected PTA thresholds compared with those with no *NF2* mutation (Table 2). No association was found between the mutation of the *NF2* gene and other epidemiologic, clinical, and radiologic relevant parameters.

An association was found between *NF2* gene status and smoking habits. Inactivation of the *NF2* gene by mutation, MLPA or LOH was more frequent in ever smokers when compared with never smokers (Table 3). No association was found between the status of the *NF2* gene and other relevant epidemiologic, clinical, and radiologic parameters.

DISCUSSION

VS arise from inactivation of the *NF2* tumor suppressor gene, which regulates Schwann cell growth. Mutations of the *NF2* gene have been found in both *NF2* and unilateral sporadic schwannoma patients (34). More than

TABLE 1. Mutational analysis of NF2 gene

Sample	LOH	MLPA	Tumor mutation NM_000268.3	Codon	Consequence	Blood status	Hits in NF2
1	N	-/-	-	-	-	-	0
2	N	-/-	c.359_360del2	p.Leu20Serfs*	Frame shift	-	1
3	+	-/+	-	-	-	-	1
4	N	-/-	-	-	-	-	0
5	+	-/+	NC_000022.10:g.71279A > C (IVS13-2A > C)	-	Splice acceptor	-	2
6	N	-/-	-	-	-	-	0
7	N	-/-	-	-	-	-	0
8	+	-/+	c.351T > A	p.Leu120Stop	Non-sense	-	2
9	+	-/+	-	-	-	-	1
10	+	-/-	c.459C > G	p.Tyr153Stop	Non-sense	-	2
11	+	-/+	c.431_432insAA	p.Tyr144Stop	Non-sense	Mutated	2
12	+	-/11	-	-	-	-	2
13	N	-/-	-	-	-	-	0
14	+	-/+	c.447G > A	p.=	Silent	-	2
15	+	+14-17	-	-	-	-	2
16	N	-/-	-	-	-	-	0
17	+	-/+	c.625A > T	p.Lys209Stop	Non-sense	-	2
18	N	-/-	-	-	-	-	0
19	+	-/+	NC_000022.10:g.54588_54622dup35 IVS6	-	Silent	-	2
20	+	-/+	c.1592delA	p.Lys531Argfs*	Frame shift	-	2
21	+	-/+	c.663C > G	p.Tyr221Stop	Non-sense	-	2
22	+	-/+	NC_000022.10:g.64892G > A (IVS10+1G > A)	-	Splice acceptor	-	2
23	+	+4,14	c.386_398del13	p.Glu129Alafs*	Frame shift	-	3
24	N	-/-	-	-	-	-	0
25	N	-/-	c.169C > T	p.Arg57Stop	Non-sense	-	1
26	+	-/+	c.737delC	p.Pro246Leufs*	Frame shift	-	2
27	+	-/+	-	-	-	-	1
28	+	+11,13	-	-	-	-	2
29	N	-/-	-	-	-	-	0
30	+	+4	c.401delC	p.Pro134Leufs*	Frame shift	-	3
31	+	-/+	NC_000022.10:g.38646G > A (IVS4-1 G > A)	-	Splice acceptor	-	2
32	+	-/+	NC_000022.10:g.71379_71405del	p.Thr480Serfs*	Frame shift	-	2
33	+	-/-	c.436_443del8	p.Val146Glnfs*	Frame shift	-	2
34	+	-/+	c.1076insT	p.R359MfsX*	Frame shift	-	2
35	+	+5,14	c.467G > A	p.Ser156Asn	Missense	-	4
			c.465_474del10	p.P155QfsX*	Frame shift	-	
36	N	-/-	-	-	-	-	0
37	N	-/-	-	-	-	-	0
38	+	-/-	-	-	-	-	1
39	N	-/4	-	-	-	-	1
40	+	-/+	-	-	-	-	1
41	N	-/-	c.169C > T	p.Arg57Stop	Non-sense	-	2
			NC_000022.10:g.74615_74636del(IVS14-26del)	-	Silent	-	
42	N	-/-	-	-	-	-	0
43	N	-/-	c.1230_1243del14	p.Gln410Hisfs*	Frame shift	-	1
44	N	-/-	-	-	-	-	0
45	+	-/+	-	-	-	-	1
46	N	-/-	c.206delA	p.Lys69Argfs*	Frame shift	-	1
47	N	-/-	-	-	-	-	0
48	N	-/-	c.414delT	p.Val139Cysfs*	Frame shift	-	2
			c.1600C > T	p.His534Tyr	Missense	Mutated	
49	+	-/+	-	-	-	-	1
50	+	-/-	-	-	-	-	1
51	N	-/-	NC_000022.10:g.38750delA (IVS4+20delA)	-	Silent	-	1

In chromosome 22q analysis, N is normal and + is positive for LOH. To name mutations, *del* corresponds to deletion, *ins* to insertion, > to change of a single nucleotide, and *dup* to duplication. When mutations occurred within introns, (IVS), the number of the affected is shown. Changes in codons and consequence of mutations in proteins are predicted from those changes obtained in DNA.

LOH indicates loss of heterozygosity; -/- indicates no losses; -/+ indicates complete deletion of one NF2 allele; -/"number" indicates partial deletion of the stated exons.

200 different mutations have been identified to date, including single-base substitutions, insertions, missense, and deletions (35). *NF2* gene inactivation is necessary for VS to grow. According to Knudsen's 2-hit hypothesis, in *NF2* patients, the germline *NF2* allele is inactivated and tumors occur when a wild-type allele is inactivated

by allelic loss, silencing, or mutation. On the other hand, sporadic unilateral VS formation is explained by somatic biallelic *NF2* inactivation as a result of the same molecular mechanisms (allelic loss, gene silencing, or mutation) (36).

In this study of 51 samples of unilateral VS, LOH alterations were found in 57% of cases, *NF2* mutations

TABLE 2. Association between NF2 mutation and clinical and radiologic variables

		No NF2 mutation	NF2 mutation	
Hearing loss	No	0 (0%)	5 (100%)	Fisher's exact test $p = 0.023$
	Yes	26 (56%)	20 (43%)	
Aural fullness	No	25 (57%)	19 (43%)	Fisher's exact test $p = 0.022$
	Yes	0 (0%)	5 (100%)	
Involvement of the IAC	No	5 (29%)	12 (71%)	Fisher's exact test $p = 0.029$
	Yes	21 (62%)	13 (38%)	
Corrected PTA threshold (500, 1,000, and 2,000 Hz)	Mean	36 dB (SD 15)	23 dB (SD 25)	Mann-Whitney test $p = 0.037$

were found in 49%, and MLPA alterations (other than those compatible with the total loss of chromosome 22) occurred in 13.7% of cases. Therefore, one mutational hit was present in 27%, and 2 hits were present in 45% of the tumors. High sensitivity in detection of DNA sequence variations is essential for mutation analysis in genetic diseases. In this study, we performed 3 different techniques to cover all the NF2 mutational screening: dHPLC for small sequence mutations, MLPA for large scale rearrangements, and LOH of 22q for detecting the absence of an entire copy of the gene. Even using these 3 methodologies, the possibility of missing a small subset of NF2 mutations cannot completely be discarded, that is, an insertion of a foreign gene (37). However, our results are similar to those reported by other authors, which suggests that the combination of DHPLC, MLPA, and LOH of 22q may be enough sensitive to detect most NF2 gene mutations in patients with VS. Martinez-Glez et al. (21) studied 23 frozen samples of schwannomas and found NF2 mutations in 34.8% and LOH alterations in 30.4% of the cases. Hadfield et al. (9) identified at least 1 point mutation in the NF2 gene in 65 (66%) of 98 sporadic VSs, with a higher incidence of frameshift (34%) than nonsense mutations (17%) in comparison with NF2-related tumors. In this study including 104 patients with unilateral sporadic VS, loss of heterozygosity (LOH) was found in 56% of the cases (9).

Previous studies have attempted to correlate the clinical expression of tumors with NF2 mutations, especially in NF2 patients (38); however, scarce information is available on this subject in terms of patients with sporadic VS. Deletion mutations that cause truncation of the NF2 protein have been reported to cause a more severe phenotype in NF2 patients, whereas missense mutations or small in-frame insertions have been reported to be associated with a mild phenotype (38). In the present study performed on 51 unilateral VS, no association was found between the type of NF2 mutation and relevant clinical parameters. However, a negative association was

found between mutation of the NF2 gene and hearing loss, as well as between mutation of the NF2 gene and involvement of the IAC fundus. Patients with NF2 mutations had better corrected hearing thresholds, less frequent involvement of the IAC fundus (which is usually associated with poorer hearing), and complained less frequently about hearing loss when compared with those without NF2 mutations.

Involvement of the IAC fundus is an important feature for the VS surgeon. Absence of fluid between the lateral end of the tumor and the IAC fundus on MRI seems to have a negative influence both on hearing outcome (39) and on facial function outcome (40) after VS surgery. The exact origin of VS in the VIIIth nerve remains uncertain. According to a recent study, VS may arise anywhere along the course of the axons of the cochleovestibular nerve, from the glial-Schwann cell junction up until terminations within the auditory and vestibular end organs (41). Moreover, its pattern of growth, spreading laterally toward the IAC fundus or medially from the IAC into the CPA angle is also unpredictable. The reason why tumors with NF2 mutations had less frequent involvement of the IAC fundus in our study may be related to these possible growth patterns and may be useful for predicting facial function or hearing outcome.

Hearing loss is the most common symptom in patients with VS. In the past, compressive mechanisms caused by the tumoral mass and its growth have been regarded as the most likely causes of hearing loss associated with VS. In recent years, molecular mechanisms have been proposed to explain this symptom (42). Lassaletta et al. (17) explored the methylation status of 16 tumor-related genes in 22 unilateral VS. DNA methylation values of 9% to 27% were found in 12 of the genes tested. A significant association was found between TP73 aberrant methylation and hearing loss. In another study using immunohistochemistry, cyclin D1 expression was observed in 52% of VS. Patients with negative cyclin D1 expression had a longer duration of deafness and higher 2,000-Hz hearing thresholds than cyclin-positive patients (23). Using microarray gene expression technology, tumor samples surgically removed from 11 patients with unilateral VSs were analyzed (43); the expression of platelet-derived growth factor A (PDGFA) was inversely correlated with hearing loss. In the present study, patients with NF2 mutation had better corrected hearing thresholds than those with no mutation. According to all these data, either NF2 mutation, other non-random genetic events, or

TABLE 3. Association between NF2 gene inactivation and smoking status

		NF2 normal or one mutational hit	NF2 inactivation (2 hits)	
Smoker	Never	19 (73%)	7 (27%)	Chi-squared test $p = 0.048$
	Ever	11 (46%)	13 (54%)	

deregulated expression of other genes also contribute to VS patients' hearing status.

In our study, inactivation of the *NF2* gene by mutation, MLPA or LOH was more frequent in smokers when compared with never smokers. To our knowledge, in contrast to several malignant tumors in which genetic alterations have been clearly related to cigarette smoking, no association between smoking and genetic alterations was previously reported in VS. The relationship between cigarette smoking and VS etiology has been studied in recent years. The results of a multicenter case-control study showed a significantly lower risk of VS in current smokers than in never smokers (44). Benson et al. (45) in a large prospective study confirmed a decreased incidence of VS in current smokers, and no clear association was found between smoking and the incidence of other tumors of the CNS, including glioma or meningiomas. Recently, Palmisano et al. (27) studied 451 VS cases and 710 controls. They confirmed that the risk of VS was greatly reduced in male current smokers and moderately reduced in female current smokers. The effect of cigarette smoking on hormonal status or the effects of hypoxia and reoxygenation on Schwann cells because of cigarette combustion products are possible mechanisms to explain the association between smoking and the risk of *NF2* inactivation. Furthermore, polyphenols present in tobacco may mimic the results obtained by Angelo et al. (46), whose experiments showed that, after applying curcumin (a polyphenol) to a schwannoma cell line, growth was inhibited in the tumor cells. Thus, smoking and VS may be related in 3 different ways. First, population studies show a lower rate of VS in smokers than in never-smokers; second, a component of tobacco (polyphenol) may exert growth inhibition in VS cells based on schwannoma cell lines studies (46); an third, our results seem to be contradictory with the previous points and show an increased *NF2* mutation rate in smokers with VS than nonsmokers with VS. Therefore, further studies are warranted to explain these phenomena. As new tobacco regulations are leading to a significant reduction in smoking in our country (47), it will be interesting to see if both the incidence of VS and the rate of *NF2* mutation in patients with VS is affected by this decrease.

In conclusion, there is growing evidence to explain hearing loss associated with VS patients using molecular data. *NF2* mutations may play a role in the pathophysiology of this symptom as well as in the growth pattern of these tumors. The role of cigarette smoking in patients with VS seems to play a role in both the risk of developing the tumor and also in its genetic profile. More studies are needed to corroborate these results and, more broadly, to establish links between the molecular and clinical data.

REFERENCES

- Forton GE, Cremers CW, Officiers EE. Acoustic neuroma ingrowth in the cochlear nerve: does it influence the clinical presentation? *Ann Otol Rhinol Laryngol* 2004;113:582-6.
- Mohyuddin A, Neary WJ, Wallace A, et al. Molecular genetic analysis of the *NF2* gene in young patients with unilateral vestibular schwannomas. *J Med Genet* 2002;39:315-22.
- Fong B, Barkhoudarian G, Pezeshkian P, et al. The molecular biology and novel treatments of vestibular schwannomas. *J Neurosurgery* 2011;115:906-14.
- Stemmer-Rachamimov AO, Xu L, Gonzalez-Agosti C, et al. Universal absence of merlin, but not other ERM family members, in schwannomas. *Am J Pathol* 1997;151:1649-54.
- Morrow KA, Das S, Metge BJ, et al. Loss of tumor suppressor Merlin in advanced breast cancer is due to post-translational regulation. *J Biol Chem* 2011;286:40376-85.
- Torres-Martin M, Lassaletta L, San-Roman-Montero J, et al. Microarray analysis of gene expression in vestibular schwannomas reveals SPPI/MET signaling pathway and androgen receptor deregulation. *Int J Oncol* 2013;42:848-62.
- Rey JA, Bello MJ, de Campos JM, Kusak ME, Moreno S. Cytogenetic analysis in human neurinomas. *Cancer Genet Cytogenet* 1987;28:187-8.
- Bello MJ, de Campos JM, Kusak ME, et al. Clonal chromosome aberrations in neurinomas. *Genes Chromosomes Cancer* 1993;6:206-11.
- Hadfield K, Smith M, Urquhart J, et al. Rates of loss of heterozygosity and mitotic recombination in *NF2* schwannomas, sporadic vestibular schwannomas and Schwannomatosis schwannomas. *Oncogene* 2010;29:6216-21.
- Leone PE, Bello MJ, Mendiola M, et al. Allelic status of 1p, 14q, and 22q and *NF2* gene mutations in sporadic schwannomas. *Int J Mol Med* 1998;1:889-92.
- Warren C, James LA, Ransdell RT, et al. Identification of recurrent regions of chromosome loss and gain in vestibular schwannoma using comparative genomic hybridisation. *J Med Genet* 2003;40:802-6.
- Kino T, Takeshima H, Nakao M, et al. Identification of the cis-acting region of *NF2* gene promoter as a potential target for mutation and methylation-dependent silencing in schwannomas. *Genes Cells* 2001;6:441-54.
- González-Gómez P, Bello J, Alonso E, et al. CpG island methylation in sporadic and neurofibromatosis type 2-associated schwannomas. *Clin Cancer Res* 2003;9:5601-6.
- Kullar PJ, Pearson DM, Malley DS, Collins VP, Ichimura K. CpG island hypermethylation of the neurofibromatosis type 2 (*NF2*) gene is rare in sporadic vestibular schwannomas. *Neuropathol Applied Neurobiol* 2010;36:505-14.
- Koutsimpleas D, Ruerup G, Mann WJ, Brieger J. Type 2 gene promoter methylation in sporadic vestibular schwannomas. *ORL J Otorhinolaryngol Head Neck Surg* 2012;74:33-7.
- Bello MJ, Martínez-Glez V, Franco-Hernández C, et al. DNA methylation pattern in 16 tumor-related genes in schwannomas. *Cancer Genet Cytogenet* 2007;172:84-6.
- Lassaletta L, Bello MJ, Del Río L, et al. DNA methylation of multiple genes in vestibular schwannoma: Relationship with clinical and radiological findings. *Otol Neurotol* 2006;27:1180-5.
- Welling DB, Lasak JM, Akhmetzheva E, Ghaheri B, Chang L-S. cDNA microarray analysis of vestibular schwannomas. *Otol Neurotol* 2002;23:736-48.
- Cayé-Thomase P, Borup R, Satangerup S-E, Thomsen J, Nielsen FC. Deregulated genes in sporadic vestibular schwannomas. *Otol Neurotol* 2010;31:256-66.
- Aarhus M, Bruland O, Saetran HA, et al. Global gene expression profiling and tissue microarray reveal novel candidate genes and down-regulation of the tumor suppressor gene *CAVI* in sporadic vestibular schwannomas. *Neurosurgery* 2010;67:998-1019.
- Martínez-Glez V, Franco-Hernández C, Álvarez L, et al. Meningiomas and schwannomas: Molecular subgroup classification found by expression arrays. *Int J Oncol* 2009;34:493-504.
- Torres-Martin M, Martínez-Glez V, Peña-Granero C, et al. Expression analysis of tumor-related genes involved in critical regulatory pathways in schwannomas. *Clin Transl Oncol* 2013;15:409-411.
- Lassaletta L, Patrón M, Del Río L, et al. Cyclin D1 expression and histopathologic features in vestibular schwannomas. *Otol Neurotol* 2007;28:939-41.

24. Archibald D, Neff B, Voss S, et al. B7-H1 expression in vestibular schwannomas. *Otol Neurotol* 2010;31:991–7.
25. Blair K, Kiang A, Wang-Rodriguez J, et al. EGF and bFGF promote invasion that is modulated by p13/Akt kinase and Erk in vestibular schwannoma. *Otol Neurotol* 2011;32:308–14.
26. Ahronowitz I, Xin W, Kiely R, et al. Mutational spectrum of the NF2 gene: a meta-analysis of 12 years of research and diagnostic laboratory findings. *Hum Mutat* 2007;28:1–12.
27. Palmisano S, Schwartzbaum J, Prochazka M, et al. Role of tobacco use in the etiology of acoustic neuroma. *Am J Epidemiol* 2012;175:1243–51.
28. Graamans K, Van Dijk JE, Janssen LW. Hearing deterioration in patients with a non-growing vestibular schwannoma. *Acta Otolaryngol* 2003;123:51–4.
29. Caye-Thomasen P, Werther K, Nalla A, et al. VEGF and VEGF receptor-1 concentration in vestibular schwannoma homogenates correlates to tumor growth rate. *Otol Neurotol* 2005;26:98–101.
30. Canzian F, Salovaara R, Hemminki A, et al. Automated assessment of loss of heterozygosity and replication error in tumors. *Cancer Res* 1996;56:3331–7.
31. Rouleau GA, Merel P, Lutchman M, et al. Alteration in a new gene encoding a putative membrane-organizing protein causes neurofibromatosis type 2. *Nature* 1993;363:515–21.
32. den Dunnen JT, Antonarakis SE. Mutation nomenclature extensions and suggestions to describe complex mutations: a discussion. *Hum Mutat* 2000;15:7–12.
33. Martinez-Glez V, Franco-Hernandez C, Lomas J, et al. Multiplex ligation-dependent probe amplification (MLPA) screening in meningioma. *Cancer Genet Cytogenet* 2007;173:170–2.
34. Lutchman M, Rouleau GA. Neurofibromatosis type 2: a new mechanism of tumor suppression. *Trends Neurosci* 1996;19:373–7.
35. Welling DB, Guida M, Goll F, et al. Mutational spectrums in the neurofibromatosis type 2 gene in sporadic and familial schwannomas. *Hum Genet* 1996;98:189–93.
36. Evans G. Neurofibromatosis type 2 (NF2) a clinical and molecular review. *Orphanet J Rare Dis* 2009;4:1–11.
37. Kluwe L, Nygren AO, Errami A, et al. Screening for large mutations of the NF2 gene. *Genes Chromosomes Cancer* 2005;42:384–91.
38. Neff BA, Welling DB, Akhrametyeva E, Chang LS. The molecular biology of vestibular schwannomas: dissecting the pathogenic process at the molecular level. *Otol Neurotol* 2006;27:197–208.
39. Kari E, Friedman RA. Hearing preservation: microsurgery. *Curr Opin Otolaryngol Head Neck Surg* 2012;20:358–66.
40. Rompaey VV, Dinther Jv, Zarowski A, Offeciers E, Somers T. Fundus obliteration and facial nerve outcome in vestibular schwannoma surgery. *Skull Base* 2011;21:99–102.
41. Roosli C, Linthicum FH Jr, Cureoglu S, Merchant SN. What is the site of origin of cochleovestibular schwannomas? *Audiol Neurotol* 2012;17:121–5.
42. Celis-Aguilar E, Lassaletta L, Torres-Martin M, et al. The molecular biology of vestibular schwannomas and its association with hearing loss: a review. *Genet Res Int* 2012;2012:856157.
43. Lassaletta L, Martinez-Glez V, Torres-Martin M, et al. cDNA microarray expression profile in vestibular schwannoma: correlation with clinical and radiological features. *Cancer Genet Cytogenet* 2009;194:125–7.
44. Schoemaker MJ, Swerdlow AJ, Auvinen A, et al. Medical history, cigarette smoking and risk of acoustic neuroma: an international case-control study. *Int J Cancer* 2007;120:103–10.
45. Benson VS, Green J, Pirie K, Beral V. Cigarette smoking and risk of acoustic neuromas and pituitary tumours in the Million Women Study. *Br J Cancer* 2010;102:1654–6.
46. Angelo LS, Wu JY, Meng F, et al. Combining curcumin (diferuloylmethane) and heat shock protein inhibition for neurofibromatosis 2 treatment: analysis of response and resistance pathways. *Mol Cancer Ther* 2011;10:2094–103.
47. Catalina Romero C, Sainz Gutiérrez JC, Quevedo Aguado L, et al. Prevalence of tobacco consumption among working population after the law 42/2010, Spain. *Salud Publica* 2012;86:177–88.

3.2 ARTÍCULO 2

TÍTULO: DNA copy gains of tumor-related genes in vestibular schwannoma.

REVISTA: European Archives of Oto-Rhino-Laryngology. Año: 2013 Volumen: 270

Páginas: 2433-2438.

AUTORES: Luis Lassaletta, **Miguel Torres-Martín**, Jesús San-Román-Montero,

Javier S. Castresana, Javier Gavilán y Juan A. Rey.

RESUMEN: La ganancia de copias es un mecanismo habitual de sobreexpresión génica en tumores. En este estudio, determinamos el nivel de dosis génica en 7 genes relacionados con schwannomas y otros tumores del sistema nervioso (*EGFR*, *ERBB2*, *ERBB3*, *ERBB4*, *MDM2*, *MDM4* y *NMYC*). Las ganancias génicas fueron correlacionadas con datos demográficos, clínicos y radiológicos. El 48% de las muestras presentaron al menos uno de los genes con ganancia de copias. No se detectó amplificación génica. Se encontró correlación clínica entre el tamaño tumoral y las ganancias de copias de *ERBB2*. Los pacientes con ganancia de copias en este gen, mostraron un mayor tamaño por diámetro y volumen. Las ganancias de copias detectadas en *EGFR*, *ERBB2*, *ERBB4* y *MDM4* se asociaron con la presencia de tinitus antes de la operación. Al contrario de lo que ocurre en el desarrollo de otros tumores del sistema nervioso, en los schwannomas vestibulares no parece que se den fenómenos de amplificación génica, al menos en los genes

estudiados. No obstante, pequeñas ganancias de copias podrían desempeñar alguna función en el comportamiento biológico de estos tumores. Estos resultados apoyan el papel de *ERBB2* en el desarrollo y crecimiento de los schwannomas vestibulares.

METODOLOGÍA:

- Se estudiaron 33 schwannomas vestibulares y sangre periférica de un individuo sano como control.
- La extracción del ADN genómico de tumor y sangre periférica se realizó mediante el Wizard® Genomic DNA Purification Kit de Promega.
- La PCR cuantitativa en tiempo real se realizó con el kit Quantimix Easy SYG de Biotools. El termociclador usado fue el modelo LightCycler de Roche. El gen elegido como control fue el ribosómico 18S, ya que su expresión es estable en diferentes tejidos y condiciones. La cantidad relativa de cada amplicón se determinó mediante el software LightCycler Relative Quantification de Roche. Tras normalizar los valores brutos con el gen control y la muestra control (no tumoral), se obtuvieron los valores procesados, donde 1 equivale a la constitución alélica no alterada. Valores comprendidos entre 2 y 5 son considerados como amplificación de bajo nivel (ganancia de copias), mientras que valores mayores de 5 habrían sido considerados amplificados.

DNA copy gains of tumor-related genes in vestibular schwannoma

Luis Lassaletta · Miguel Torres-Martín ·
Jesús San-Román-Montero · Javier S. Castresana ·
Javier Gavilán · Juan Antonio Rey

Received: 14 February 2012 / Accepted: 2 November 2012 / Published online: 21 November 2012
© Springer-Verlag Berlin Heidelberg 2012

Abstract DNA copy gains are a common event in tumor growth. This study determines the gene dosage/amplification of seven tumor-related genes in patients undergoing vestibular schwannoma (VS) surgery and analyzes its clinical implications. Thirty-three patients undergoing surgery for VS were studied. Seven genes (*EGFR*, *ERBB2*, *ERBB3*, *ERBB4*, *MDM2*, *MDM4*, and *NMYC*) were analyzed by Quantitative real-time PCR. Copy gains were correlated with demographic, clinical and radiological data. Of the 33 samples, 48 % were positive for copy gains in at least one gene. There were no positive samples for gene amplification. A clinical correlation between tumor size and copy gains of *ERBB2* was found. Patients with copy gains of this gene had larger tumors measured by diameter ($p = 0.027$) and volume ($p = 0.005$). Copy gains of *EGFR*, *ERBB2*, *ERBB4*, and *MDM4* were associated with preoperative tinnitus. Contrary to other tumors of the central nervous system, development of VS does not

appear to involve gene amplification. However, copy gains of certain tumor-related genes may play a role in the biological behavior of these neoplasms. Our findings support the role of *ERBB2* in VS development and growth

Keywords Acoustic neuroma · Vestibular schwannoma · Gene copies · DNA copy gains · Amplification · Tinnitus · Tumor size · Quantitative real-time PCR

Introduction

Amplifications are increases in the number of copies of a specific DNA fragment. They are common events in cancer, when an oncogene—in most of cases—is overexpressed prompted by the additional copies of the gene. A classical model of this mechanism is the amplification of v-erb-b2 erythroblastic leukemia viral oncogene homolog 2 (*ERBB2*), which is present in 30 % of breast carcinomas [1], clinical outcome being related to this feature [2]. While amplification represents tens or hundreds-fold the number of gene copies, it is possible to find minor alterations where the gene copies are increased but not enough to consider amplification itself. These low-level amplifications-copy gains-, have been described in association with cancer progression, from low-grade dermatofibrosarcoma protuberans to aggressive high-grade fibrosarcoma [3]; and they have also been described as a characteristic feature in certain groups of astrocytic gliomas and oligodendrogliomas [4–6].

Vestibular schwannomas (VSs) are common benign tumors accounting for 8–10 % of intracranial tumors and about 80 % of cerebellopontine tumors. The molecular changes involved in the pathogenesis of VS have been studied in the past years. Most studies have focused on the

L. Lassaletta (✉) · J. Gavilán
Department of Otolaryngology, Hospital La Paz/Autónoma
University School of Medicine, IdiPAZ, Pº de la Castellana, 261,
28046 Madrid, Spain
e-mail: luikilassa@yahoo.com

M. Torres-Martín · J. A. Rey
Unidad de Investigación, Laboratorio Oncogenética Molecular,
Hospital La Paz/Autónoma University School of Medicine,
IdiPAZ, Madrid, Spain

J. San-Román-Montero
Preventive Medicine and Public Health Teaching and Research
Unit, Department of Health Sciences, Universidad Rey Juan
Carlos, Madrid, Spain

J. S. Castresana
Brain Tumor Biology Unit-CIFA, University of Navarra School
of Sciences, Pamplona, Spain

molecular analysis of the Neurofibromatosis type 2 gene (*NF2*) [7, 8]. *NF2* encodes for a protein termed Merlin (Moesin-ezrin-radixin-like protein) or Schwannomin, which suppresses tumor progression by inhibiting the E3 ubiquitin ligase CRL4^{DCAF1} in the nucleus [9]; regulates the delivery of growth factor receptors to the plasma membrane in Schwann Cells [10]; inhibits the interaction of CD44-HA [11]; binds to ERBB2, regulating glial cell growth by controlling the phosphorylation of Src and its downstream effectors [12]; binds to PIKE-L, blocking its stimulatory effect on PI3K [13]; and plays a role in the regulation of epidermal growth factor receptor (EGFR) [14], β 1-integrin [15], and many other proteins [16]. In addition, Merlin has been found to cooperate with Expanded in *Drosophila* to activate the Hippo pathway [17]. Other molecular alterations studied in VS are the methylation of several genes [18, 19], some of them with clinical implication including *RASSF1A*, *CASP8*, *TP73* [20], and expression of cyclin D1 (*CCND1*) [21].

In VS, there is very limited information regarding gene amplification and copy gains or losses excepting loss at 22q, the region that contains Merlin and is usually affected by LOH [22]. Previous studies have analyzed gains or losses of different chromosomal regions or genes by comparative genomic hybridization (CGH) [23–26], by Multiplex Ligation-dependent Probe Amplification (MLPA) [27] and by Fluorescence in situ hybridization (FISH) [28].

In this study, we attempt to determine the gene dosage/amplification of seven tumor-related genes [*EGFR*, *ERBB2*, *ERBB3*, *ERBB4*, p53 binding proteins *MDM2* and *MDM4* and v-myc myelocytomatosis viral related oncogene (*NMYC*)], by quantitative real-time PCR in patients undergoing VS surgery and to analyze its clinical implications.

Materials and methods

Patient selection

The study group consisted of 33 patients who underwent surgery for removal of unilateral VS in our institution between November 2006 and November 2009. The study was approved by the ethical committee. Four patients had NF2 and the other 29 patients had no evidence of this disease. All tumors arose from the vestibular nerve.

Patients and DNA preparation

The population included 19 women and 14 men with a mean age at surgery of 43 years (range 21–65 years). The tumor was on the left side in 19 cases (57 %). Clinical complaints at the time of diagnosis were hearing loss (88 %), tinnitus (70 %), dizziness (45 %), and vertigo

(18 %). When specifically asked about particular complaints, the percentage of patients having each symptom was hearing loss (90 %), tinnitus (73 %), dizziness (47 %), vertigo (20 %), and facial alterations (29 %). Mean pure-tone threshold for the tumor ear and the contralateral ear was 59 and 24 dB, respectively. Maximum speech discrimination score ranged from 0 to 100 %, with a mean of 57 %. Tumor size measured as the largest diameter in the axial plane of MRI ranged from 5 to 42 mm (mean, 26 mm). In addition, the tumor volume was also measured from MRI, using the formula for an ellipsoid, as previously described [29]. For both tumor measures diameter and volume, the intrameatal part of the tumor was included. Mean tumor volume at presentation was 7.11 cm³, ranging from 0.078 to 37.483 cm³. Size was evaluated as stage 1 (intracanalicular) in two cases (6 %), as stage 2 (15 mm in its greatest diameter in the CPA) in six cases (18 %), as stage 3 (16–30 mm in the CPA) in 18 cases (54 %), and as stage 4 (>30 mm in the CPA) in seven cases (21 %). Tumor appearance was homogeneous (58 %), heterogeneous (27 %), and cystic (15 %). Tumor in the CPA was centered to the IAC in 77 %, posterior in 20 %, and anterior in 3 % of the cases. In 11 cases (33 %), a wait and scan policy was chosen, with at least two MRI previous to surgery. Tumor growth ranged from 1 to 10 mm in these cases.

DNA was prepared from frozen tissues in patients and blood in controls using standard methods using Genomic Wizard (Promega, Madison, USA) as previously described [30]. Genes studied and primers used are listed: *EGFR* exons 2, 17 and 25 corresponding to the intracellular, transmembrane and extracellular domain and located at 7p12 [4]; *ERBB2* at 17q11.2–q12 [5]; *ERBB3* at 12q13 and *ERBB4* at 2q33.3–q34 [31]; *MDM2* at 12q13–q14 and *MDM4* at 1q32 [32]; and *NMYC* at 2p24.3 [18]. Quantitative real-time PCR was performed using the Quantimix Easy SYG Kit (BIO-TOOLS, Madrid, Spain) and a LightCycler (Roche Molecular Biochemicals, Mannheim, Germany). The 18S gene was used as a control (2005). The relative amounts of every gene studied with respect to the control gene DNA, 18S, were determined using the LightCycler Relative Quantification Software provided by Roche Molecular Biochemicals. The final results were calculated as a ratio of each gene dosages normalized and reference gene values in every sample. A ratio between 2 and 5 was considered as a low amplification rate (copy gains), and values higher than 5.1 would have been considered positive for high amplification rates. Samples were analyzed in duplicate.

Statistical analyses

Categorical variables were described by frequency (percentage) and continuous variables as mean (standard deviation). Groups of patients were compared using the

t test for continuous symmetrically distributed variables, the Mann–Whitney test for continuous asymmetrically distributed variables, and Chi-square and Fisher exact tests for categorical values. Because of limited sample size, only univariate (unadjusted) associations were generated. All analyses were performed using SPSS 13.0 for Windows. Differences were considered significant at a level of $p < 0.05$. La Paz University Hospital institutional review board approval was obtained for this study.

Results

Copy gains

Of the 33 samples, 48 % were positive for copy gains in at least one gene (Table 1). 27 and 30 % of the samples showed copy gains in *EGFR* at intracellular and extracellular domains (exons 2 and 25), respectively, whereas 18 % showed copy gains in the membrane-domain (exon 17). Only one patient (3 %) displayed copy gains in *NMYC*. The percentage of samples with copy gains in *ERBB2*, *ERBB3* and *ERBB4* was 24, 21 and 15 %. Copy gains were present in 15 and 12 % of cases in *MDM2*, and *MDM4*, respectively. There were no positive samples for gene amplification in the present study.

Clinical associations

We studied the association between copy gains of the seven genes and clinical and radiological features. Copy gains of *ERBB2* were associated with tumor size. Mean tumor diameter was smaller in patients with no *ERBB2* gain copies (23.8 mm CI 95 % 19.9–27.7) when compared to those positive for gain copies (32.4 mm CI 95 % 26.3–38.5) ($p = 0.027$). The association was also significant using tumor volume (5.4 cm³ CI 95 % 2.9–7.8 vs 12.7 cm³ CI 95 % 6.7–18.8, $p = 0.005$). Copy gains of *EGFR*, *ERBB2*, *ERBB4*, *CCND1* and *MDM4* were associated with preoperative tinnitus (Table 2). No difference was found in terms of copy gains between NF2 and non-NF2 patients.

Discussion

We have analyzed 33 VS samples for gene amplification or copy gains in seven genes usually involved in the development of cancer of the nervous system. In our study, 48 % of the cases exhibited copy gains of at least one of the seven genes. All genes studied in this series had copy gains in at least one specimen, and no cases of amplification were found. Few previous studies about amplification or copy

gains have been performed in schwannomas, [24, 26–28]. The percentage of copy gains has ranged from 13 to 75 % using different techniques and studying several regions. In our study, we found copy gains of *EGFR* in 18–30 % of cases. Prayson et al. [28] studied the dosage of *EGFR* using FISH. As in our study, no cases of amplification were found, while copy numbers were increased in 30 % of the cases. Koutsimpelas et al. [26] reported the results of a CGH analysis performed in 20 sporadic VSs. They found losses on chromosomes 22q and 9p, whereas gains were observed on 17q, 19p and 19q. Warren et al. [24] studied 76 VS with CGH to identify chromosome regions that may harbor genes involved in tumorigenesis. Ten percent showed copy gains on chromosome 9q34, these tumors being larger than those without detectable gain in this region. Table 3 shows the results of main studies about copy gains in VS.

In the present study, the percentage of tumors with copy gains in *ERBB2*, *ERBB3* and *ERBB4* were 24, 21 and 15 %, respectively. We found a clinical correlation between the tumor size and copy gains of *ERBB2*. Patients with copy gains of this gene had larger tumors both using the maximum MRI diameter and tumor volume. Doherty et al. [33] reported *ERBB3* and *ERBB4* mRNA overexpression in 34 and 20 % of VS samples. They found several trends between ERBB signaling molecules and clinical parameters, including a positive correlation between *ERBB3* expression and tumor size in NF2-related VS but not in sporadic VS (data not shown in the study for the small number of patients in each category and, therefore, lack of statistical significance). The *ERBB2* gene has been implicated in VS development. It has been proposed to regulate glial cell growth via Merlin and Scr [12]. Moreover, its blockage with ERBB inhibitors trastuzumab and erlotinib has been shown to decrease growth of VS xenografts in nude mice [34]. Also, *ERBB2/ERBB3* receptors are a target for Neuregulin 1, a protein that is produced in an autocrine pathway in VS [35] and required for the proliferation of Schwann cells. All these findings support that *ERBB2/ERBB3* receptors play an essential role in sporadic VS development. The exact mechanism by which *ERBB2* copy gains induce a larger tumor size phenotype remains unclear.

In the present study, tinnitus was associated with the absence of copy gains in genes *EGFR*, *ERBB2*, *ERBB4* and *MDM4*. Being one of the most common symptoms in patients with VS, the pathogenesis of tinnitus in VS is not fully understood. Several potential mechanisms of tinnitus generation in VS have been suggested in the literature. Ephaptic coupling of cochlear nerve fibers by compression, cochlear dysfunction by ischemia or by biochemical degradation, efferent system dysfunction following compression of the efferent fibers in the inferior vestibular nerve,

Table 1 Gain status of each gene

Case/gene	EGFR 2	EGFR 17	EGFR 25	ERB-B2	ERB-B3	ERB-B4	MDM2	MDM4	N-MYC
1	+	–	+	+	–	–	–	–	–
2	–	–	–	–	–	–	–	–	–
3	–	–	–	–	–	–	–	–	–
4	+	+	+	+	+	–	–	+	–
5	–	–	–	–	–	–	–	–	–
6	+	+	+	+	+	+	+	+	–
7	–	–	–	+	–	–	+	–	–
8	–	–	–	–	–	–	–	–	–
9	–	–	–	–	–	–	–	–	–
10	–	–	–	–	–	–	–	–	–
11	–	–	–	–	–	–	–	–	–
12	–	–	–	–	–	–	–	–	–
13	–	–	–	–	–	–	–	–	–
14	–	+	+	–	–	–	–	–	–
15	+	–	–	–	+	+	–	–	–
16	–	–	–	–	–	–	+	–	–
17	–	–	–	–	–	–	–	–	–
18	–	–	+	+	–	–	–	–	–
19	–	–	–	–	+	–	–	–	–
20	–	–	–	–	–	–	–	–	–
21	–	–	–	–	–	–	–	–	–
22	–	–	–	–	+	–	+	–	–
23	–	–	–	–	–	–	–	–	–
24	–	–	–	–	–	–	–	–	–
25	–	–	–	–	–	–	–	–	–
26	–	–	–	–	–	–	–	–	–
27	+	–	+	–	–	–	–	–	–
28	–	–	–	–	–	–	–	–	–
29	+	–	+	–	–	–	–	–	–
30	+	+	+	+	+	+	+	+	+
31	+	+	+	+	+	+	–	+	–
32	–	–	–	–	–	–	–	–	–
33	+	+	+	+	–	+	–	–	–
Positive (%)	9 (27)	6 (18)	10 (30)	8 (24)	7 (21)	5 (15)	5 (15)	4 (12)	1 (3)

Positive in copy gains is showed as “+”, while normal status is indicated as “–”

Table 2 Tinnitus and copy gains of different genes

Gene with copy gains	Tinnitus absent (%)	<i>p</i> value
<i>EGFR</i> exon 17	100	<0.0001
<i>EGFR</i> exon 2	67	0.01
<i>EGFR</i> exon 25	70	0.002
<i>MDM4</i>	100	0.006
<i>ERBB2</i>	62	0.036
<i>ERBB4</i>	80	0.04

and cortical reorganization following hearing loss are among the most accepted theories [36]. In a recent study about different mutations in the *NF2* gene of NF2 patients, tinnitus was associated with nonsense/frameshift mutations, which were also associated with more severe NF2 symptoms when compared to large deletions [37]. Agrawal et al. [38] have recently reported an association between the presence of tinnitus at the time of diagnosis and VS growth.

Table 3 Main series about DNA copy gains on vestibular schwannoma

Author	Technique	Main/most frequent gains	N	Clinical implications
Antinheimo et al. [23]	CGH	Gain on 17 and 19 (8 %), but not consistent with FISH	25	No
Warren et al. [24]	CGH	Gain on 9q34- (10 %), gain on 10q26 (3 %)	76	Gain on 9q34 and tumor diameter
Ikeda et al. [25]	CGH	Gain on X, Y and 19	17 (13 VS)	No
Prayson et al. [28]	FISH on <i>EGFR</i>	Gains on six cases (30 %); not amplifications found	20	No
Martinez-Glez et al. [27]	MLPA	Duplications on 12q (34 %)	23	No
Koutsmpelas et al. [26]	CGH	Gain on 19p and 19q (35 %)	20	No
Present series	Quantitative real-time PCR	Gains on <i>ERBB2</i> (23 %) and <i>EGFR</i> (28 %)	33	Gain on <i>ERBB2</i> and tumor diameter and volume

CGH comparative genomic hybridization, FISH fluorescence in situ hybridization, MLPA multiplex ligation-dependent probe amplification

Conclusions

Contrary to other tumors of the central nervous system, development of VS does not appear to involve gene amplification. However, copy gains of certain tumor-related genes may play a role in the biological behavior of these tumors. Our findings support the role of *ERBB2* in VS development and growth. The relationship between *ERBB2* copy number and binding processes with *NF2* to regulate cell growth should be further studied to determine the potential role related to variations of *ERBB2* copy number.

Acknowledgments Support for this work was provided by grants 07/0577 and 10/1972 from FIS, Ministerio de Sanidad.

Conflict of interest The authors have no conflict of interest.

References

- Slamon DJ, Godolphin W, Jones LA et al (1989) Studies of the HER-2/neu proto-oncogene in human breast and ovarian cancer. *Science* 244:707–712
- Berchuck A, Kamel A, Whitaker R et al (1990) Overexpression of HER-2/neu is associated with poor survival in advanced epithelial ovarian cancer. *Cancer Res* 50:4087–4091
- Abbott JJ, Erickson-Johnson M, Wang X et al (2006) Gains of COL1A1-PDGFB genomic copies occur in fibrosarcomatous transformation of dermatofibrosarcoma protuberans. *Mod Pathol* 19:1512–1518
- Arjona D, Bello MJ, Alonso ME et al (2005) Molecular analysis of the EGFR gene in astrocytic gliomas: mRNA expression, quantitative-PCR analysis of non-homogeneous gene amplification and DNA sequence alterations. *Neuropathol Appl Neurobiol* 31:384–394
- Alonso ME, Bello MJ, Arjona D, Martinez V et al (2005) Real-time quantitative PCR analysis of gene dosages reveals gene amplification in low-grade oligodendrogliomas. *Am J Clin Pathol* 123:900–906
- Franco-Hernandez C, Martinez-Glez V, Arjona D et al (2007) EGFR sequence variations and real-time quantitative polymerase chain reaction analysis of gene dosage in brain metastases of solid tumors. *Cancer Genet Cytogenet* 173:63–67
- Twist EC, Rutledge MH, Rousseau M et al (1994) The neurofibromatosis type 2 gene is inactivated in schwannomas. *Hum Mol Genet* 3:147–151
- Mérel P, Hoang-Xuan K, Sanson M et al (1995) Predominant occurrence of somatic mutations of the NF2 gene in meningiomas and schwannomas. *Genes Chromosom Cancer* 13:211–216
- Li W, You L, Cooper J, Schiavon G et al (2010) Merlin/NF2 suppresses tumorigenesis by inhibiting the E3 ubiquitin ligase CRL4(DCAF1) in the nucleus. *Cell* 140:477–490
- Lallemant D, Manent J, Couvelard A et al (2009) Merlin regulates transmembrane receptor accumulation and signaling at the plasma membrane in primary mouse Schwann cells and in human schwannomas. *Oncogene* 28:854–865
- Bai Y, Liu YJ, Wang H et al (2007) Inhibition of the hyaluronan-CD44 interaction by merlin contributes to the tumor-suppressor activity of merlin. *Oncogene* 26:836–850
- Houshmandi SS, Emnett RJ, Giovannini M et al (2009) The neurofibromatosis 2 protein, merlin, regulates glial cell growth in an ErbB2- and Src-dependent manner. *Mol Cell Biol* 29:1472–1486
- Okada M, Wang Y, Jang SW et al (2009) Akt phosphorylation of merlin enhances its binding to phosphatidylinositols and inhibits the tumor-suppressive activities of merlin. *Cancer Res* 69:4043–4051
- Curto M, Cole BK, Lallemant D et al (2007) Contact-dependent inhibition of EGFR signaling by Nf2/Merlin. *J Cell Biol* 177:893–903
- Fernandez-Valle C, Tang Y, Ricard J et al (2002) Paxillin binds schwannomin and regulates its density-dependent localization and effect on cell morphology. *Nat Genet* 31:354–362
- Scoles DR (2008) The merlin interacting proteins reveal multiple targets for NF2 therapy. *Biochim Biophys Acta* 1785:32–54
- Hamaratoglu F, Willecke M, Kango-Singh M et al (2006) The tumour-suppressor genes NF2/Merlin and expanded act through Hippo signalling to regulate cell proliferation and apoptosis. *Nat Cell Biol* 8:27–36
- Gonzalez-Gomez P, Bello MJ, Alonso ME et al (2001) CpG island methylation in sporadic and neurofibromatosis type 2-associated schwannomas. *Clin Cancer Res* 9:5601–5606
- Bello MJ, Martinez-Glez V, Franco-Hernandez C et al (2007) DNA methylation pattern in 16 tumor-related genes in schwannomas. *Cancer Genet Cytogenet* 172:84–86
- Lassaletta L, Bello MJ, Del Río L et al (2006) DNA methylation of multiple genes in vestibular schwannoma: relationship with clinical and radiological findings. *Otol Neurotol* 27:1180–1185

21. Lassaletta L, Patrón M, Del Río L et al (2007) Cyclin D1 expression and histopathologic features in vestibular schwannomas. *Otol Neurotol* 28:939–941
22. Hadfield KD, Smith MJ, Urquhart JE et al (2010) Rates of loss of heterozygosity and mitotic recombination in NF2 schwannomas, sporadic vestibular schwannomas and schwannomatosis schwannomas. *Oncogene* 29:6216–6221
23. Antinheimo J, Sallinen SL, Sallinen P et al (2000) Genetic aberrations in sporadic and neurofibromatosis 2 (NF2)-associated schwannomas studied by comparative genomic hybridization (CGH). *Acta Neurochir (Wien)* 142:1099–1104
24. Warren C, James LA, Ramsden RT et al (2003) Identification of recurrent regions of chromosome loss and gain in vestibular schwannomas using comparative genomic hybridisation. *J Med Genet* 40:802–806
25. Ikeda T, Hashimoto S, Fukushima S et al (2005) Comparative genomic hybridization and mutation analyses of sporadic schwannomas. *J Neurooncol* 72:225–230
26. Koutsimpelas D, Felmeden U, Mann WJ et al (2011) Analysis of cytogenetic aberrations in sporadic vestibular schwannoma by comparative genomic hybridization. *J Neurooncol* 103:437–443
27. Martinez-Glez V, Franco-Hernandez C, Alvarez L et al (2009) Meningiomas and schwannomas: molecular subgroup classification found by expression arrays. *Int J Oncol* 34:493–504
28. Prayson RA, Yoder BJ, Barnett GH (2007) Epidermal growth factor receptor is not amplified in schwannomas. *Ann Diagn Pathol* 11:326–329
29. Cayé-Thomasen P, Werther K, Nalla A et al (2005) VEGF and VEGF receptor-1 concentration in vestibular schwannoma homogenates correlates to tumor growth rate. *Otol Neurotol* 26:98–101
30. Rey JA, Bello MJ, Jimenez-Lara AM et al (1992) Loss of heterozygosity for distal markers on 22q in human gliomas. *Int J Cancer* 51:703–706
31. Arjona D, Bello MJ, Alonso ME et al (2004) Molecular analysis of the erbB gene family calmodulin-binding and calmodulin-like domains in astrocytic gliomas. *Int J Oncol* 25:1489–1494
32. Riemenschneider MJ, Büschges R, Wolter M et al (1999) Amplification and overexpression of the MDM4 (MDMX) gene from 1q32 in a subset of malignant gliomas without TP53 mutation or MDM2 amplification. *Cancer Res* 59:6091–6096
33. Doherty JK, Ongkeko W, Crawley B, Andalibi A, Ryan AF (2008) ErbB and Nrg: potential molecular targets for vestibular schwannoma pharmacotherapy. *Otol Neurotol* 29:50–57
34. Clark JJ, Provenzano M, Diggelmann HR et al (2008) The ErbB inhibitors trastuzumab and erlotinib inhibit growth of vestibular schwannoma xenografts in nude mice: a preliminary study. *Otol Neurotol* 29:846–853
35. Hansen MR, Roehm PC, Chatterjee P et al (2006) Constitutive neuregulin-1/ErbB signaling contributes to human vestibular schwannoma proliferation. *Glia* 53:593–600
36. Baguley DM, Humphriss RL, Axon PR et al (2006) The clinical characteristics of tinnitus in patients with vestibular schwannoma. *Skull Base* 16:49–58
37. Selvanathan SK, Shenton A, Ferner R et al (2010) Further genotype–phenotype correlations in neurofibromatosis 2. *Clin Genet* 77:163–170
38. Agrawal Y, Clark JH, Limb CJ et al (2010) Predictors of vestibular schwannoma growth and clinical implications. *Otol Neurotol* 31:807–812

3.3 ARTÍCULO 3

TÍTULO: Microarray analysis of gene expression in vestibular schwannomas reveals SPP1/MET signaling pathway and androgen receptor deregulation.

REVISTA: International Journal of Oncology. Año: 2013 Volumen: 42 Páginas: 848-862.

AUTORES: **Miguel Torres-Martín**, Luis Lassaletta, Jesús San-Román-Montero, José María de Campos, Alberto Isla, Javier Gavilán, Bárbara Melendez, Giovanny R. Pinto, Rommel R. Burbano, Javier S. Castresana y Juan A. Rey.

RESUMEN: Mediante tecnología de microarrays, testamos las diferencias de expresión en genoma completo en una serie de schwannomas vestibulares y tejido sano. Encontramos 1.516 genes desregulados. Entre estos genes, destacamos el receptor *MET* y genes relacionados en su transactivación como las integrinas (*ITGA4*)/(*ITGAB6*), la plexina (*PLEXNB3*) y su ligando la semaforina A5 (*SEMA5*), así como la infraexpresión de caveolina-1 *CAV1*. Además, la infraexpresión del receptor de andrógenos (*AR*), podría indicar una causa o consecuencia hormonal en schwannomas vestibulares. Otro gen desregulado en nuestra serie de schwannomas, la osteopontina (*SPP1*), fue descrito previamente como responsable de la degradación de merlin a nivel de proteína, lo que podría ser un mecanismo análogo en aquellos schwannomas sin mutación de *NF2*. Por último, no encontramos grandes variaciones de expresión entre schwannomas con

distintas características clínicas o moleculares, aunque no son descartables variaciones en pequeños grupos de genes.

METODOLOGÍA:

- Se estudiaron 31 schwannomas vestibulares, 28 de ellos de origen esporádico y 3 de pacientes con NF2. Como control, se utilizaron 9 muestras; 8 de ellas nervios no tumorales y 1 proveniente de cultivo primario de células de Schwann.
- Para la extracción de ARN se utilizó el Rneasy® Mini Kit de Qiagen, que purifica los ARNs de más de 200 bases.
- El ARN fue hibridado en los microarrays de Affymetrix Human Gene 1.0 ST (capaz de testar 28.132 genes). La normalización y sumarización de los mismos se realizó mediante el algoritmo Robust Multichip Average (RMA). Al permitir estos microarrays hacer análisis a nivel de gen y a nivel de exones, ambos fueron usados. La corrección de lote se hizo mediante el paquete ComBat del programa estadístico R. Los análisis estadísticos se realizaron con el programa MultiExperiment Viewer. El umbral para considerar un gen desregulado fue del doble o la mitad de cambio entre los grupos analizados y un p-valor ≤ 0.05 (t-test).
- La extracción del ADN, el análisis molecular del gen *NF2* y la LOH del cromosoma 22 fueron determinados de la misma manera que en el Artículo 1.

- Los microarrays fueron validados en 48 genes mediante PCR en tiempo real con sondas TaqMan en un sistema de detección ABI PRISM 7900HT. Esta validación se realizó en todas las muestras (tumores y controles) por duplicado.

Microarray analysis of gene expression in vestibular schwannomas reveals SPP1/MET signaling pathway and androgen receptor deregulation

MIGUEL TORRES-MARTIN¹, LUIS LASSALETTA², JESUS SAN-ROMAN-MONTERO³, JOSE M. DE CAMPOS⁴, ALBERTO ISLA⁵, JAVIER GAVILAN², BARBARA MELENDEZ⁶, GIOVANNY R. PINTO⁷, ROMMEL R. BURBANO⁸, JAVIER S. CASTRESANA⁹ and JUAN A. REY¹

¹Research Unit, ²Department of Otolaryngology, La Paz University Hospital, Hospital La Paz Institute for Health Research (IdiPAZ); ³Teaching and Research Unit for Preventive Medicine and Public Health, Department of Health Sciences, Rey Juan Carlos University; ⁴Department of Neurosurgery, Jimenez Diaz Foundation; ⁵Department of Neurosurgery, La Paz University Hospital, IdiPAZ, Madrid; ⁶Molecular Pathology Research Unit, Virgen de la Salud Hospital, Toledo, Spain; ⁷Genetics and Molecular Biology Laboratory, Federal University of Piauí, Parnaíba; ⁸Human Cytogenetics Laboratory, Federal University of Pará, Belém, Brazil; ⁹Brain Tumor Biology Unit, University of Navarra School of Sciences, Pamplona, Spain

Received November 12, 2012; Accepted January 4, 2013

DOI: 10.3892/ijo.2013.1798

Abstract. Vestibular schwannomas are benign neoplasms that arise from the vestibular nerve. The hallmark of these tumors is the biallelic inactivation of neurofibromin 2 (*NF2*). Transcriptomic alterations, such as the neuregulin 1 (*NRG1*)/ErbB2 pathway, have been described in schwannomas. In this study, we performed a whole transcriptome analysis in 31 vestibular schwannomas and 9 control nerves in the Affymetrix Gene 1.0 ST platform, validated by quantitative real-time PCR (qRT-PCR) using TaqMan Low Density arrays. We performed a mutational analysis of *NF2* by PCR/denaturing high-performance liquid chromatography (dHPLC) and multiplex ligation-dependent probe amplification (MLPA), as well as a microsatellite marker analysis of the loss of heterozygosity (LOH) of chromosome 22q. The microarray analysis demonstrated that 1,516 genes were deregulated and 48 of the genes were validated by qRT-PCR. At least 2 genetic hits (allelic loss and/or gene mutation) in *NF2* were found in 16 tumors, seven cases showed 1 hit and 8 tumors showed no *NF2* alteration. *MET* and associated genes, such as integrin, alpha 4 (*ITGA4*)/*B6*, *PLEXNB3/SEMA5* and caveolin-1 (*CAVI*) showed a clear

deregulation in vestibular schwannomas. In addition, androgen receptor (*AR*) downregulation may denote a hormonal effect or cause in this tumor. Furthermore, the osteopontin gene (*SPPI*), which is involved in merlin protein degradation, was upregulated, which suggests that this mechanism may also exert a pivotal role in schwannoma merlin depletion. Finally, no major differences were observed among tumors of different size, histological type or *NF2* status, which suggests that, at the mRNA level, all schwannomas, regardless of their molecular and clinical characteristics, may share common features that can be used in their treatment.

Introduction

Schwannomas are benign tumors that arise from Schwann cells in the peripheral nerves. These tumors often originate from the vestibular nerve, although they can develop anywhere from the glial-Schwann junction up to the nerve terminations within the auditory and vestibular sensory organs (1). Although histologically benign, vestibular schwannomas may cause hearing loss, tinnitus, facial palsy and, when large enough, brain stem compression and even death. Vestibular schwannomas are usually sporadic and unilateral (95%) but may be bilateral when associated with neurofibromatosis type 2 (NF2) syndrome, which is caused by germline mutations of the neurofibromin 2 (*NF2*) gene. Moreover, patients with NF2 develop other tumors as well, such as meningiomas, ependymomas and gliomas (2).

The *NF2* gene, a tumor suppressor located at 22q12 that encodes a protein termed merlin or schwannomin (3), is mutated in up to 66% of sporadic schwannomas (4). The *NF2* gene is inactivated in most, if not all, schwannomas (5) and is frequently lost in conjunction with the loss of chromosome 22. Merlin is a member of the band 4.1 superfamily of proteins and exhibits sequence homology with the members

Correspondence to: Dr Miguel Torres-Martin or Dr Juan A. Rey, Research Unit, La Paz University Hospital, Hospital La Paz Institute for Health Research (IdiPAZ), Paseo de la Castellana 246, 28046 Madrid, Spain
E-mail: migtorres.martin@gmail.com
E-mail: jarey.hulp@salud.madrid.org

Key words: schwannoma, microarrays, androgen, MET, osteopontin SPP1, neurofibromin 2, *NF2*

of the ezrin/radixin/moesin (ERM) family, with 17 coding exons and 2 main isoforms, arising from alternative splicing of exons 16 and 17. In Schwann cells, merlin colocalizes with E-cadherin at the paranodes and Schmidt-Lanterman incisures in the myelinating peripheral nerve (6).

Merlin is involved in a variety of signaling pathways, such as mTORC1 regulation (7), activation of the Hippo pathway in *Drosophila* (8), membrane recruitment and activation of Rac/PAK (9) and, upon cell-to-cell contact, downregulation of the membrane levels of ErbB2, ErbB3 (10) and EGFR (11). Recently, merlin has been found to suppress tumorigenesis by entering the nucleus and binding to the E3 ubiquitin ligase CRL4^{DCAF1}, suppressing its activity (12). For translocation into the nucleus, merlin must be activated (closed state) by the dephosphorylation of myosin phosphatase target subunit 1 (*MYPT1*), although other mechanisms of activation should not be ruled out.

In addition to schwannomas, merlin alterations have been described in other tumor types, particularly meningiomas and ependymomas and, less commonly, in mesotheliomas, renal cell carcinomas, melanomas, colorectal cancers and glioblastomas (13). Furthermore, advanced breast cancer exhibits a loss of merlin expression via post-translational mechanisms (14). Other genetic changes that are rare in schwannomas, such as 1p losses and 9q34 and 17q gains, have been described in a few samples (15,16). Furthermore, epigenetic changes involving the *NF2* gene (17-21) and other tumor-related genes (22) have also been investigated in vestibular schwannomas.

There are only 3 studies available on the global gene expression profile in vestibular schwannomas. These studies used various microarray platforms: 4 EST filters from Research Genetics (Huntsville, AL, USA) (23), Affymetrix HG-U133A (24) and ABI 1700 (25). The first of these studies used 1 control nerve sample and 7 tumors, while the other two increased the controls to 3 and the tumors to 16 and 25, respectively. Due to the number of controls available, the statistical approach was different: the first approach was very restrictive and centered on specific probes, while the other two were less restrictive and even validated 7 genes by qRT-PCR. Apart from specific coincidences, these studies showed no common trends. With the less stringent method previously described (25), 1,650 genes appeared deregulated and the development of new tools for data analysis led to the conclusion that the ERK pathway was the core network. Our goal, with the help of new improved tools for data analysis, was to perform a more thorough analysis of the expression patterns of 31 schwannomas and 9 controls. Our results concur with earlier array analysis data on schwannomas, such as caveolin-1 (*CAV1*) downregulation (25), as well as with other studies conducted, using techniques such as qRT-PCR [i.e., neuregulin 1 (*NRG1*)-ErbB2-ErbB3 upregulation] and immunohistochemistry analysis (*CCND1* upregulation) (26).

In conclusion, the main finding of this study is the activation of the MET pathway due to changes in the expression of other modulators of this gene [integrin, alpha 4 (*ITGA4*)/*ITGB6* and *PLEXNB3/SEMA5*]. Furthermore, osteopontin (*SPPI*) upregulation, described in breast cancer as being responsible for merlin degradation (14), may explain the absence of merlin even in schwannomas with no DNA hits in *NF2* (5). Finally, we also performed correlation analyses with clinical and

molecular alterations, in order to identify markers with useful prognostic, diagnostic and therapeutic information.

Materials and methods

Sample and DNA/RNA preparation. The study group consisted of 31 patients who underwent vestibular schwannoma removal surgery at our institution. The study population included 17 females and 14 males. The local Ethics Review Board of La Paz University Hospital approved the study protocol according to the principles of the Declaration of Helsinki. All patients received detailed information of the study and provided their written informed consent prior to their inclusion. DNA was isolated from 31 frozen samples, corresponding to 28 sporadic and 3 *NF2*-associated vestibular schwannomas, using the Wizard Genomic DNA purification kit (Promega). DNA from the corresponding peripheral blood of the patients was also extracted. RNA was isolated using the RNeasy[®] Mini kit (Qiagen) in all tumoral and non-tumoral samples. The following non-tumoral samples were used as the controls: 2 auricular nerves, 2 cervical nerves, 1 facial nerve, 1 vestibular nerve and 1 nerve from the VIII cranial pair (all processed with the same protocol as schwannomas), as well as 1 commercial normal human adult Schwann cell (HSC) RNA, purchased from ScienCell (HSC total RNA, catalog number 1705).

Expression arrays. Affymetrix Human Gene 1.0 ST arrays were used to analyze gene expression levels. We processed 25 ng of total RNA as previously described by Gonzalez-Roca *et al* (27). In brief, library preparation and amplification were performed following the distributor's (Sigma-Aldrich) recommendations for whole transcriptome amplification (WTA2). Amplification was performed for 17 cycles and amplified cDNA was purified and quantified on a NanoDrop ND-1000 spectrophotometer (Thermo-Fischer). cDNA (8 µg) was subsequently fragmented by DNase I and biotinylated by terminal transferase obtained from a GeneChip Mapping 10Kv2 Assay kit (Affymetrix). Hybridization, washing, staining and scanning of Affymetrix Human Gene 1.0 ST arrays were performed following the manufacturer's recommendations. Scanned images (DAT files) were transformed into intensities (CEL files) by Affymetrix GeneChip Operating Software (GCOS). Arrays were processed at the IRB Barcelona Functional Genomics Core Facility. Data can be accessed at the Gene Expression Omnibus (GEO) database GSE39645.

Array normalization and summarization. Overall array intensity was normalized between arrays to correct for systematic bias in data and remove the impact of non-biological influences on biological data. Affymetrix arrays had multiple probes (probe set) directed to each gene. Following normalization, the probe intensity of all probes in a probe set was summarized to a single value. Normalization and summarization was performed using the Robust Multichip Average (RMA) algorithm (28).

Statistical array analysis. The 40 samples (31 tumors and 9 nerve controls) were processed in 2 batches, with controls and tumors in both batches. ComBat, an Empirical Bayes method (29), was subsequently used to remove the batch effect,

based on previous findings (30). In order to include genes for web tool analysis, those genes with at least a 2-fold change of expression and a $p < 0.05$ cut-off (t-test) were selected, as previously recommended (31). Bonferroni adjustment was used to obtain more restrictive results. For the analysis, we used probes from NM (messenger RNA) of RefSeq annotation and intron-free olfactory receptors were removed in order to avoid cross-hybridization (32). All statistical analyses were performed using MultiExperiment Viewer (MeV) (33,34). Principal component analysis (PCA) was performed by eigenvalue decomposition of the 3 principal components for tridimensional classification of the samples and an unsupervised hierarchical cluster by Pearson's correlation was selected to group the samples. The significance analysis of microarrays (SAM) statistical technique (with 1,000 permutations and a threshold fold change of 2) was also performed for descriptive and comparative purposes.

Array web tool analysis. To obtain a list of deregulated genes for use with web tool databases, a fold change ranking plus a non-stringent p-value cut-off ($p < 0.05$) was used. Three different open access databases were selected for the analysis:

DAVID (35,36). We used the RefSeq annotations selected for statistical array analysis as a background. A list of genes (upregulated, downregulated, or both) was then used to obtain enriched biological and/or molecular themes. Public genomic resources, such as Gene Ontology (GO), Swiss-Prot (SP) and Protein Information Resource (PIR), were selected for analysis.

Reactome (<http://www.reactome.org>). In this peer-reviewed and manually curated database, pathways can be easily analyzed by introducing a list of genes with the relative average expression of the groups (controls vs. tumors in our study).

WebGestalt (37). Similar to the DAVID database, this tool provides data that can also be checked with Transcription Factor Target analysis, WikiPathways and Cytogenetic band analysis. The configuration used for the analysis was the enrichment analysis at $p < 0.05$ using the hypergeometric test and BH adjustment.

Quantitative RT-PCR. To validate the expression pattern obtained by the microarrays, qRT-PCR amplifications were performed with TaqMan Gene Expression Assay products on an ABI PRISM 7900HT Sequence Detection system (Applied Biosystems, Foster City, CA, USA). The reactions were performed using TaqMan Low Density arrays (TLDA; Applied Biosystems) containing 50 ml TaqMan Universal PCR Master Mix (Applied Biosystems, Foster City, CA, USA) and 50 ml of a cDNA template corresponding to 100 ng total RNA per channel of the microfluidic card. A total of 48 genes studied in these assays were selected according to their deregulation and involvement in pathways of potential interest in the development of schwannomas as well as of other tumors: ANK2-Hs00153998_m1, ANK3-Hs00253210_m1, AR-Hs00171172_m1, ATF7IP2-Hs00228009_m1, CAV1-Hs00184697_m1, CCND1-Hs00765553_m1, CTNNA1-Hs00944794_m1, CXCL1-Hs00236937_m1, CXCL5-Hs00171085_m1, DSG2-Hs00170071_m1, EGFR-Hs01076086_m1, ERBB2-Hs01001586_m1, FABP4-Hs01086177_m1, FLOT1-Hs00195134_m1, GRB14-Hs00182949_m1, LICAM-Hs01109748_m1, LATS2-Hs00324396_m1, MCAM-Hs00174838_m1, MDM2-Hs9999

9008_m1, MET-Hs01565584_m1, NOV-Hs00159631_m1, NRG1-Hs00247625_m1, NRXN1-Hs00245125_m1, PAK2-Hs01127126_m1, PAK3-Hs00176828_m1, PAWR-Hs01088574_m1, PDGFA-Hs00964426_m1, PDGFB-Hs00966522_m1, PDGFC-Hs00211916_m1, PDGFD-Hs00228671_m1, PDGFRA-Hs00998026_m1, PIK3IP1-Hs00364629_m1, RASSF4-Hs00604698_m1, RENBP-Hs00234138_m1, SHOX2-Hs01059691_m1, TGFB3-Hs01086000_m1, VLDLR; FLJ35024-Hs00182461_m1, WWP1-Hs00366927_m1, CDH1-Hs01023894_m1, CXCL1-Hs00171086_m1, ERBB3-Hs00951455_m1, HEPACAM-Hs00404147_m1, IL8RA-Hs00174146_m1 and S100A9-Hs00610058_m1 (available upon request).

Calculation of gene expression was obtained as follows: average cycle threshold (Ct) values were obtained using SDS 2.2 software (Applied Biosystems). The maximum Ct value was set at 40. Ct values were normalized using 4 housekeeping genes (18S-Hs99999901_s1, ACTB-Hs99999903_m1, PPIA-Hs99999904_m1 and RPL18-Hs00965812_g1). The relative expression level of each target gene was expressed as $\Delta Ct = Ct_{ref} - Ct_{gene}$ (38). Reference-normalized expression measurements were adjusted by defining the lowest expression value as 0, with subsequent 1-unit increases reflecting an approximate doubling of the RNA. The non-parametric Mann-Whitney-Wilcoxon test was used to calculate the significance of differences between control samples and schwannomas.

Loss of heterozygosity (LOH) of 22q. In order to determine the 22q allelic constitution of schwannomas, the status of 5 microsatellite markers at the D22S275, D22S264, D22S929, D22S268 and D22S280 loci (22q11-q12.3) was verified by labeling 5' primers with fluorescent markers (6-FAM/HEX and ROX as a size standard) (Applied Biosystems). Allelic ratios were defined according to previously described criteria: $T2 \times N1/T1 \times N2$, in which the LOH was < 0.6 or > 1.67 (39).

PCR/denaturing high-performance liquid chromatography (dHPLC) analysis and direct sequencing of NF2. Genomic DNA amplification was performed using standard PCR methods (total volume of 20 μ l). A set of 15 primer pairs was used as previously described (3). Mutational screening was performed using dHPLC following the manufacturer's instructions (Transgenomic WAVE® dHPLC Systems). Samples with different patterns by dHPLC were sequenced bidirectionally (ABI 3100-Avant, Applied Biosystems), using the BigDye sequencing kit (Applied Biosystems), to determine the position and nature of the alteration. For the mutation description, sequence NM_000268.3 was used when the alteration appeared within mature mRNA and sequence NC_000022.10 was used when the mutation was located in other parts of the NF2 gene.

Multiplex ligation-dependent probe amplification (MLPA) analysis of NF2. To identify large NF2 deletions not detected by PCR/dHPLC, we used a commercial MLPA kit for analysis (SALSA P044 NF2; MRC-Holland, Amsterdam, The Netherlands). Information regarding the probe sequences and ligation sites can be found at <http://www.mlpa.com>. The MLPA protocol was performed as described by the manufacturer, using 100 ng of DNA from the control and tumor

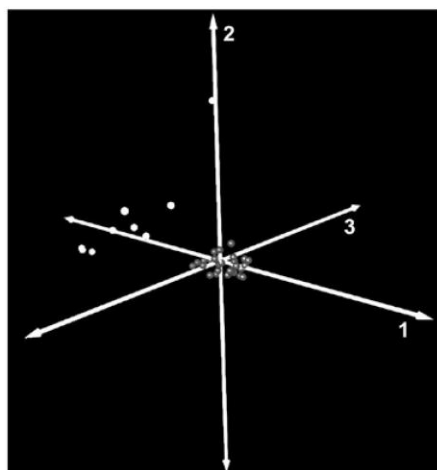


Figure 1. Three-dimensional representation of principal component analysis. Grey points represent 31 vestibular schwannomas, while the 9 controls are shown in white. The more remote control corresponds to human Schwann cell culture. Schwannomas appear tight together, contrary to the controls, which are less uniform.

samples. Data analysis was performed with MRC-Coffalyser software (MRC-Holland).

Clinical data. The tumors were located on the left side in 16 cases (52%). The mean age was 44.5 ± 14.3 years. Audiologic measurements included pre-operative and post-operative pure-tone average (PTA) and speech discrimination score (SDS). Hearing data were reported according to the recommendations of the American Academy of Otolaryngology-Head and Neck Surgery (AAO-HNS). Thus, class A was defined as PTA <30 dB and SDS >70%; class B, PTA 31-50 dB and SDS 50-100%; class C, PTA 51-100 dB and SDS 50-100%; and class D, any PTA and SDS <50%. Size was evaluated by the KOOS scale and characterized as stage 1 (intracanalicular) in 1 case (3%), stage 2 [15 mm in its greatest diameter in the cerebellopontine angle (CPA)] in 8 cases (26%), stage 3 (16-30 mm in the CPA) in 16 cases (52%) and stage 4 (>30 mm in the CPA) in 6 cases (19%). Tumor appearance was homogeneous (64%), heterogeneous (23%) and cystic (13%) as shown by MRI. The fundus of the internal auditory channel was affected in 65%

of cases. All tumor tissues obtained at surgery were fixed in 10% formalin and embedded in paraffin. Staining with hematoxylin and eosin was performed for routine microscopic diagnosis. Antoni type A regions consisted of interwoven bundles of long bipolar spindle cells, whereas Antoni type B regions exhibited a loose myxoid background containing more stellate tumor cells. The percentage of the different tissue types (A, B, or mixed) in each tumor sample was independently determined by 2 pathologists. The results were grouped in 2 types: type A, >70% of the tumor composed of type A tissue and type B, <70% of the tumor composed of type A tissue.

Results

Microarray analysis. PCA and hierarchical clustering depicted a clear distinction between control nerves and schwannomas (Fig. 1). The most distinct sample shown in the PCA corresponded to the control of cultured human Schwann cells, which was different from other controls due to additional material present at the non-tumoral nerves. Pearson's correlation grouped all 31 schwannomas into a large cluster, with small differences among the tumors (Fig. 2), whereas the control nerves exhibited greater differences. The hierarchical cluster analysis also recognized 2 schwannoma expression groups (1 and 2) that displayed only 16 differentially expressed genes. Likewise, tumors in group 2 were classified into subgroups 2-I and 2-II, that displayed 66 differentially deregulated genes, including *SEMA3D*, *MERTK*, *RELN* and *CD36*. No Bonferroni-adjusted genes were obtained in any of these groups.

An analysis of variance (ANOVA)/Welch's t-test ($p < 0.05$ and 2-fold changes) was performed to establish a list of 1,516 genes (Fig. 3), 1,105 of which were upregulated (available upon request) and 411 downregulated (available upon request) (89 were upregulated and 15 downregulated following a Bonferroni adjustment). Using more stringent methods, such as the significance analysis of microarrays (SAM) statistical technique, 922 deregulated genes were obtained vs. the 1,516 genes obtained by the t-test. A list of the 30 top fold change of upregulated (Table I) and downregulated (Table II) genes using the SAM method is shown.

The main results obtained using the database web tools are as follows:

DAVID. The clusters in DAVID were very similar when using a p-value cut-off <0.05 or <0.001, presenting variation primarily at the enrichment level. For the 1,065 upregulated

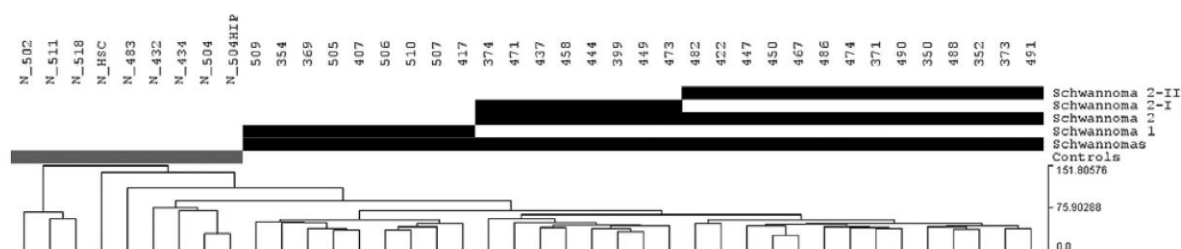


Figure 2. Cluster of samples. Hierarchical cluster of Euclidean distances of NM set of probes from RefSeq annotation. Controls and tumors are clearly grouped, whereas schwannomas show a similar pattern.

Table I. Top 30 upregulated genes by SAM method.

Gene symbol	RefSeq	Description	Location (chromosome)	Fold change
<i>C12orf69</i>	NM_001013698	Chromosome 12 open reading frame 69	12	11.72
<i>L1CAM</i>	NM_000425	L1 cell adhesion molecule	X	11.68
<i>GPR83</i>	NM_016540	G protein-coupled receptor 83	11	10.26
<i>GPR34</i>	NM_001097579	G protein-coupled receptor 34	X	9.71
<i>FCGBP</i>	NM_003890	Fc fragment of IgG binding protein	19	9.19
<i>SCN7A</i>	NM_002976	Sodium channel, voltage-gated, type VII, alpha	2	9.08
<i>ADAM23</i>	NM_003812	ADAM metalloproteinase domain 23	2	8.46
<i>GPR155</i>	NM_001033045	G protein-coupled receptor 155	2	7.90
<i>CDH19</i>	NM_021153	Cadherin 19, type 2	18	7.81
<i>MOXD1</i>	NM_015529	Monooxygenase, DBH-like 1	6	7.74
<i>ANKRD22</i>	NM_144590	Ankyrin repeat domain 22	10	7.66
<i>GRB14</i>	NM_004490	Growth factor receptor-bound protein 14	2	7.25
<i>GFRA3</i>	NM_001496	GDNF family receptor alpha 3	5	7.07
<i>RGS1</i>	NM_002922	Regulator of G protein signaling 1	1	6.85
<i>C10orf114</i>	NM_001010911	Chromosome 10 open reading frame 114	10	6.43
<i>SLC16A12</i>	NM_213606	Solute carrier family 16, member 12	10	6.35
<i>P2RY12</i>	NM_022788	Purinergic receptor P2Y, G-protein coupled, 12	3	6.29
<i>CHL1</i>	NM_006614	Cell adhesion molecule with homology to L1CAM	3	6.23
<i>FCGR3A</i>	NM_000569	Fc fragment of IgG, low affinity IIIa, receptor	1	5.89
<i>NLGN4X</i>	NM_020742	Neurologin 4, X-linked	X	5.81
<i>ARHGEF26</i>	NM_015595	Rho guanine nucleotide exchange factor	3	5.78
<i>ALDH1A1</i>	NM_000689	Aldehyde dehydrogenase 1 family, member A1	9	5.72
<i>NCAM2</i>	NM_004540	Neural cell adhesion molecule 2	21	5.69
<i>ARHGAP15</i>	NM_018460	Rho GTPase activating protein 15	2	5.58
<i>IFI44</i>	NM_006417	Interferon-induced protein 44	1	5.57
<i>RASSF4</i>	NM_032023	Ras association domain family member 4	10	5.52
<i>CX3CR1</i>	NM_001337	Chemokine C-X3-C motif receptor 1	3	5.50
<i>IFIT1</i>	NM_001548	Interferon-induced protein with tetratricopeptide repeats 1	10	5.48
<i>RSAD2</i>	NM_080657	Radical S-adenosyl methionine domain containing 2	2	5.47
<i>PDGFD</i>	NM_025208	Platelet-derived growth factor D	11	5.21

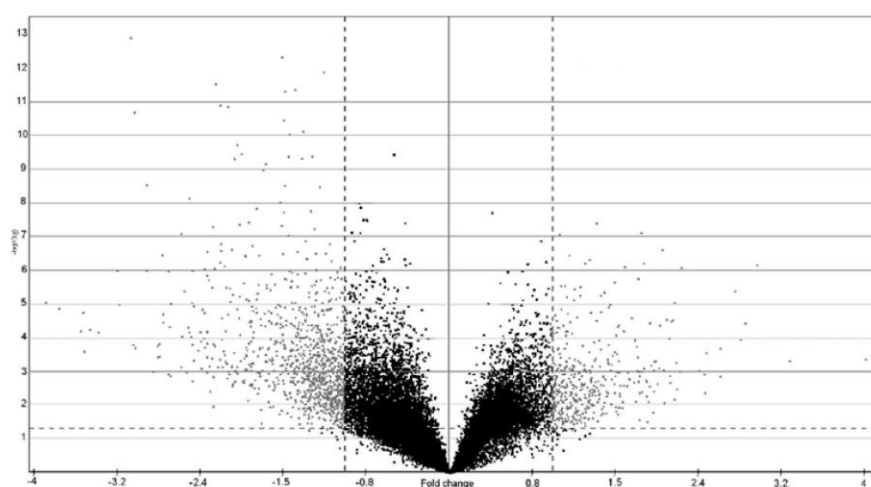
Figure 3. Volcano plot resulting from the comparison of schwannomas to controls. Dotted lines represent 2-fold (vertical) and $p < 0.05$ cut-off (horizontal). Only grey points matched these criteria.

Table II. Top 30 downregulated genes by SAM method.

Gene symbol	RefSeq	Description	Location (chromosome)	Fold change
<i>FABP4</i>	NM_001442	Fatty acid-binding protein 4	8	-28.98
<i>MFAP5</i>	NM_003480	Microfibrillar-associated protein 5	12	-13.40
<i>DPT</i>	NM_001937	Dermatopontin	1	-9.36
<i>PLA2G2A</i>	NM_000300	Phospholipase A2, group IIA	1	-9.00
<i>SFRP2</i>	NM_003013	Secreted frizzled-related protein 2	4	-8.69
<i>PRRX1</i>	NM_006902	Paired related homeobox 1	1	-8.39
<i>SLC22A3</i>	NM_021977	Solute carrier family 22 , member 3	6	-8.37
<i>GOS2</i>	NM_015714	G0/G1 switch 2	1	-7.93
<i>SLC14A1</i>	NM_001128588	Solute carrier family 14	18	-7.82
<i>PII6</i>	NM_153370	Peptidase inhibitor 16	6	-7.42
<i>SLPI</i>	NM_003064	Secretory leukocyte peptidase inhibitor	20	-6.87
<i>SELE</i>	NM_000450	Selectin E	1	-6.70
<i>CHI3L2</i>	NM_001025199	Chitinase 3-like 2	1	-6.35
<i>CCDC80</i>	NM_199511	Coiled-coil domain containing 80	3	-6.26
<i>ANPEP</i>	NM_001150	Alanyl aminopeptidase	15	-6.05
<i>S100A12</i>	NM_005621	S100 calcium binding protein A12	1	-6.02
<i>PDGFRL</i>	NM_006207	Platelet-derived growth factor receptor-like	8	-5.95
<i>CRABP2</i>	NM_001878	Cellular retinoic acid-binding protein 2	1	-5.80
<i>APLNR</i>	NM_005161	Apelin receptor	11	-5.76
<i>FAM171B</i>	NM_177454	Family with sequence similarity 171, B	2	-5.68
<i>AQP9</i>	NM_020980	Aquaporin 9	15	-5.48
<i>CXCR1</i>	NM_000634	Chemokine C-X-C receptor 1	2	-5.41
<i>ADCYAP1R1</i>	NM_001118	Adenylate cyclase activating polypeptide 1	7	-5.27
<i>IL1R2</i>	NM_004633	Interleukin 1 receptor, type II	2	-5.20
<i>DSG2</i>	NM_001943	Desmoglein 2	18	-5.11
<i>HSPB8</i>	NM_014365	Heat shock protein 8	12	-5.08
<i>HHIP</i>	NM_022475	Hedgehog interacting protein	4	-5.06
<i>THBS4</i>	NM_003248	Thrombospondin 4	5	-4.97
<i>PAK3</i>	NM_002578	p21 protein-activated kinase 3	X	-4.94
<i>CAV1</i>	NM_001753	Caveolin-1	7	-4.90

genes in the schwannomas, the main clusters of GO annotation were referred to as intrinsic to membrane, lysosomes, vacuoles, cell adhesion, axonogenesis and neuron development (Table III). For the 400 downregulated genes (Table IV), the clusters of GO annotation were extracellular region, cell adhesion, response to wounding, proteinaceous extracellular matrix and plasma membrane. The most significant deregulations were observed in the SP and PIR protein databases and the upregulated genes included glycoprotein, disulfide bond, membrane, lysosome and actin-binding. The downregulated genes were signal, secreted, cell adhesion, EGF-like domain, heparin-binding and chemotaxis. Comparisons between the schwannoma groups of the 16 differentially expressed genes between groups 1 and 2 showed no significant clusters. Otherwise, the differences observed between subgroups 2-I and 2-II included enriched extracellular regions and response to wounding.

Reactome. Using NM_ annotation, the average expression of control nerves and schwannomas for every deregulated gene was entered into this web tool. Upregulation of axon guidance (Table V) and signal transduction pathways (Table VI) were

the most significant events registered using this tool and deregulated genes included *ErbB2*, *NRG1*, *EGFR*, *LICAM*, *DCX* and *ERBB2IP*. Other deregulated signal pathways in our study included cytokine signaling in the immune system (available upon request) and cell metabolism (available upon request).

WebGestalt. The transcription factor target analysis showed significant enrichment of the forkhead box O4 (*FOXO4*), neurofibromin 1 (*NFI*) and lymphoid enhancer-binding factor 1 (*LEF1*) genes with the algorithm used in this program, when compared with the 1,465 deregulated genes. When the upregulated genes were analyzed individually, only *FOXO4* was significant, whereas the downregulated genes exhibited more than 20 significant transcription factor target sites, even after statistical adjustment. These downregulated genes included *NFI*, *FOXO4*, androgen receptor (*AR*) and zinc finger protein, subfamily 1A, 1 (*IKZF1*). By WikiPathways analysis and using the list of upregulated genes in schwannomas, focal adhesion and Toll-like receptor signaling were significantly affected. When only the downregulated genes were analyzed, the most significantly affected were adipogenesis, hedgehog signaling

Table III. DAVID clusters obtained with upregulated genes.

Cluster	Enrichment score	Category	Term	Fold enrichment	p-value
1	15.7	SP_PIR_KEYWORDS	Glycoprotein	1.56	5.74e-19
		UP_SEQ_FEATURE	Glycosylation site:N-linked (GlcNAc)	1.58	5.04e-18
		SP_PIR_KEYWORDS	Disulfide bond	1.60	1.48e-11
2	12.7	SP_PIR_KEYWORDS	Glycoprotein	1.56	5.74e-19
		UP_SEQ_FEATURE	Glycosylation site:N-linked (GlcNAc)	1.58	5.04e-18
		SP_PIR_KEYWORDS	Membrane	1.35	1.20e-12
3	9.8	GOTERM_BP_FAT	GO:0007155-cell adhesion	2.10	1.15e-07
		GOTERM_BP_FAT	GO:0022610-biological adhesion	2.10	1.25e-07
		SP_PIR_KEYWORDS	Cell adhesion	2.38	1.79e-06
4	9.3	SP_PIR_KEYWORDS	Lysosome	4.17	1.45e-10
		GOTERM_CC_FAT	GO:0000323-lytic vacuole	2.93	5.08e-07
		GOTERM_CC_FAT	GO:0005764-lysosome	2.93	5.08e-07
5	4.8	GOTERM_BP_FAT	GO:0009611-response to wounding	1.88	0.006957
		GOTERM_BP_FAT	GO:0006954-inflammatory response	2.02	0.106629
		GOTERM_BP_FAT	GO:0006952-defense response	1.70	0.116900
6	4.7	GOTERM_BP_FAT	GO:0048666-neuron development	2.14	0.007170
		GOTERM_BP_FAT	GO:0048812-neuron projection morphogenesis	2.46	0.011071
		GOTERM_BP_FAT	GO:0007409-axonogenesis	2.54	0.011999
7	4.5	GOTERM_CC_FAT	GO:0044459-plasma membrane part	1.36	6.55e-04
		GOTERM_CC_FAT	GO:0005887-integral to plasma membrane	1.42	0.054804
		GOTERM_CC_FAT	GO:0031226-intrinsic to plasma membrane	1.41	0.057849

Table IV. DAVID clusters obtained with downregulated genes.

Cluster	Enrichment score	Category	Term	Fold enrichment	p-value
1	19.0	SP_PIR_KEYWORDS	Signal	2.16	2.39e-19
		UP_SEQ_FEATURE	Signal peptide	2.16	8.97e-19
		UP_SEQ_FEATURE	Disulfide bond	2.39	2.56e-18
2	9.5	GOTERM_BP_FAT	GO:0009611-response to wounding	3.28	1.14e-07
		GOTERM_BP_FAT	GO:0006952-defense response	3.01	5.49e-07
		GOTERM_BP_FAT	GO:0006954-inflammatory response	3.80	5.78e-06
3	7.8	SP_PIR_KEYWORDS	Glycoprotein	1.95	2.13e-17
		UP_SEQ_FEATURE	Glycosylation site:N-linked (GlcNAc)	1.97	2.00e-16
		UP_SEQ_FEATURE	Topological domain:Extracellular	1.88	2.68e-06
4	7.4	GOTERM_CC_FAT	GO:0005578-proteinaceous extracellular matrix	3.55	5.92e-06
		GOTERM_CC_FAT	GO:0031012-extracellular matrix	3.40	7.90e-06
		SP_PIR_KEYWORDS	Extracellular matrix	4.14	3.77e-05
5	5.6	GOTERM_CC_FAT	GO:0005886-plasma membrane	1.53	9.68e-06
		GOTERM_CC_FAT	GO:0005887-integral to plasma membrane	1.91	6.95e-04
		GOTERM_CC_FAT	GO:0031226-intrinsic to plasma membrane	1.87	0.001409
6	4.7	SP_PIR_KEYWORDS	Cell adhesion	3.03	7.46e-04
		GOTERM_BP_FAT	GO:0007155-cell adhesion	2.13	0.111463
		GOTERM_BP_FAT	GO:0022610-biological adhesion	2.13	0.113672
7	4.5	SP_PIR_KEYWORDS	EGF-like domain	5.62	9.60e-10
		INTERPRO	IPR013032:EGF-like region, conserved site	4.10	3.54e-06
		INTERPRO	IPR000742:EGF-like, type 3	5.03	4.69e-06

Table V. Axon guidance in vestibular schwannomas.

Pathway	Description
Semaphorin interactions	The semaphorins 7A, 6D and 5A were overexpressed, as was the 5A receptor plexin-B3. In this pathway, Talin-1 (<i>TLN1</i>) also appeared to be overexpressed.
Neural cell adhesion molecule 1 (NCAM) signaling for neurite outgrowth	<i>NCAM1</i> gene, ribosomal protein S6 kinase, 90 kDa, polypeptide 5 (<i>RPS6KA5</i>) and son of sevenless homolog 1 (<i>SOS1</i>) were overexpressed, presumably upregulating MAP/kinases cascades according to this pathway.
Netrin-1 signaling	These genes play a vital role in axon guidance and neural migration during the development of the nervous system. The <i>NCK1</i> [which associates with the actin cytoskeleton mediated by <i>DCC</i> (deleted in colorectal cancer) and recruits Rac, Cdc42 and their effectors Pak and N-WASP in neurons] and the <i>NTN4</i> genes were overexpressed.
L1 cell adhesion molecule (<i>LICAM</i>) interactions	<i>LICAM</i> , activated leukocyte cell adhesion molecule (<i>ALCAM</i>), <i>NCAM1</i> and contactin 1 (<i>CNTN1</i>) were upregulated, while <i>EGFR</i> and doublecortin (<i>DCX</i>) were downregulated.
Robo receptor signaling	The slit homolog 2 (<i>SLIT2</i>) was upregulated in this pathway, while its receptor, <i>ROBO1</i> , appeared to be downregulated.

Table VI. Signal transduction in vestibular schwannomas.

Pathway	Description
G protein-coupled receptor (GPCR) signaling	There are more than 800 GPR genes in the genome. These receptors activate adenylyl cyclase to produce cAMP from ATP, or in the phosphatidylinositol pathway to produce a cell response, depending on the context. Sixteen of these receptors were deregulated in our tumor series (available upon request).
EGFR signaling	This receptor was markedly downregulated. In addition, <i>SOS1</i> (present in cytosol) was upregulated in this pathway.
ErbB2 signaling	The ligand NRG1 and its receptors ErbB2 and ErbB3 were upregulated. The ErbB2 interacting protein (<i>ERBB2IP</i>) was also upregulated. However, the ErbB4 signaling pathway was not deregulated.
Integrin cell surface interactions	Integrin α Ib β 3 signaling presented four upregulated elements. The amyloid β (A4) precursor protein-binding family B member 1-interacting protein (<i>APBB1IP</i>) and downstream effector Talin-1 (<i>TLN1</i>) were upregulated. This upregulation provoked the activation of integrin α Ib β 3 and the subsequent activation of tyrosine-protein kinase SYK (<i>SYK</i>), which was also upregulated, by Src.

and regulation of actin cytoskeleton. When both up- and down-regulated genes were analyzed, focal adhesion, α 6 β 4 integrin signaling and type II interferon signaling were significantly affected. With cytogenetic band analysis, we found chromosomal arm 4q and 1q31 band to be significantly enriched in the list of upregulated genes. Those on the downregulated list were enriched at the 12p12 band.

qRT-PCR validation. Validation of the expression pattern of 48 genes obtained by microarray analysis was performed by qRT-PCR (available upon request). In all cases, the trend observed in the microarrays (upregulation, downregulation or no deregulation) was confirmed by our experiments (Fig. 4). The fold change was usually larger in the qRT-PCR than in the

microarray analysis, a phenomenon that is well-established due to the wider dynamic range of the qRT-PCR technique (40 and available upon request).

NF2 mutational analysis by PCR/dHPLC, MLPA and LOH of the 22q status. A total of 17 tumors (55%) displayed *NF2* sequence variations by PCR/dHPLC, 3 of which had 2 mutations, with a total of 20 mutations detected. Ten small deletions between 1 and 15 bp were the most common alteration (50%), followed by 9 point mutations (45%) and 1 small insertion (3%). The most frequent mutation detected was the nonsense p.Arg57Stop (nucleotide change c.169C>T), which was present in 3 tumors at exon 2 of the *NF2* gene. Tumor 399, present in a patient with *NF2*, also showed the mutation in the peripheral

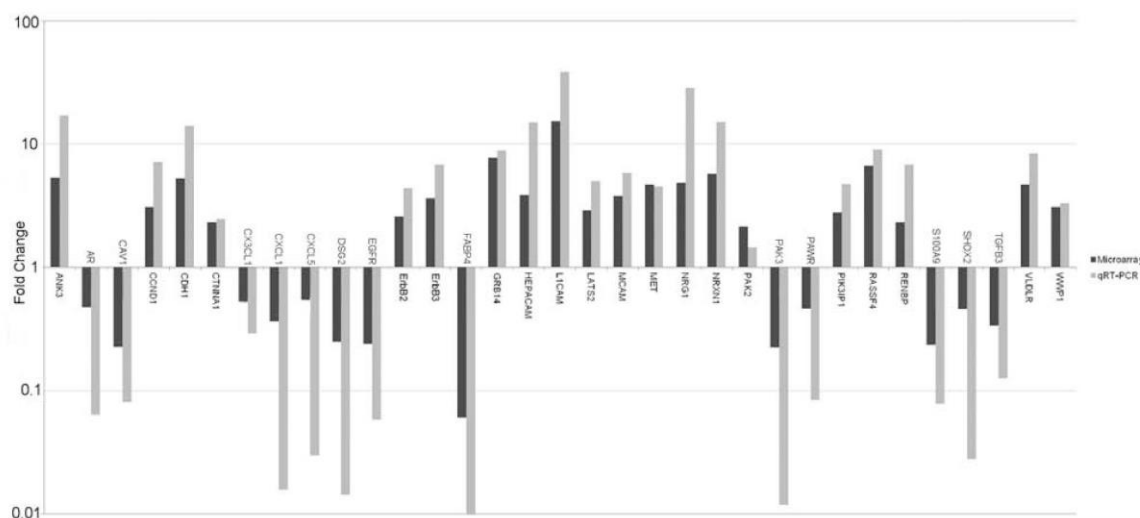


Figure 4. Microarray and qRT-PCR comparison. Fold change of 33 genes obtained by both microarray (black lines) and qRT-PCR analysis (grey lines). Values more than or equal to 1 represent upregulation and more than 1 downregulation in schwannomas. By the qRT-PCR method, gene deregulation was usually higher, due to the wider dynamic range of this technique compared to the microarray analysis.

blood sample. No other mutation was detected in more than one sample. Most sequence changes were at exon 4 (5 cases), followed by exon 2 (4 cases) and exon 5 (2 cases); exons 3, 6 and 9 were not affected by any mutation. The first half of the *NF2* gene (exons 2-8) accumulated 65% of the total mutations. Using 5 microsatellites markers, an LOH of 22q11-q12.3 occurred in 18 of the 31 (58%) tumors. In 13 cases, the LOH appeared along with a PCR/dHPLC alteration. In addition to the cases that were compatible with the total loss of an *NF2* allele, the MLPA for analysis of the *NF2* gene (SALSA P044), showed deletions of at least one exon in 6 tumors (19%). In 2 of these cases, the MLPA deletion corresponded to exon 2, which also displayed both sequence variations (at exon 2) and LOH of 22q, suggesting that this particular finding by MLPA could be considered an artifact. Alternatively, the presence of mosaicism in these tumors should not be discarded.

In conclusion, we found at least 2 inactivating hits in the *NF2* tumor suppressor gene in 16 (52%) specimens (Table VII). Two of these specimens were exclusively due to 2 mutations in the *NF2* sequence; 2 of the tumors had 2 hits due to an MLPA alteration (excluding the possible artifact) adding to the LOH of 22q. The remainder presented this pattern due to a combination of LOH of 22q and a sequence mutation found by MLPA and/or PCR/dHPLC. Seven cases (23%) displayed a single hit; 4 with LOH of 22q, 2 with a mutation detected by PCR/dHPLC and 1 with a deletion found by MLPA. Eight out of the 31 (26%) tumors in our series did not show any molecular alteration in the *NF2* gene.

Alternative splicing analysis. In addition to gene analysis, gene ST arrays offer the possibility of a limited analysis of alternative splicing in several genes. Therefore, we performed the analysis on individual gene probes. We found neurexin genes showing alternative splicing in tumors compared with the pattern shown by controls. All 3 neurexins presented a

long (α) and short (β) form coded by 2 different promoters, which may generate more than 1,000 isoforms through alternative splicing. In the neurexin-1 gene (*NRXN1*), transcript α (NM_004801) showed upregulation, while there was no variation in the expression of specific probes for transcript NM_138735. The neurexin-2 gene (*NRXN2*) showed downregulation of 3 out of the 23 probes of the α isoform (NM_015080) and no change in the β isoform (NM_138734). The neurexin-3 gene (*NRXN3*) showed upregulation of the β isoform NM_138970 and downregulation of the α isoform NM_004796-specific probes. Finally, the neuroligin-4X gene (*NLGN4X*) presented an overexpressed NM_181332 isoform and showed no changes in NM_020742.

Molecular and clinical correlation with arrays. The correlations between the molecular information of the tumor and the data from the microarray study were as follows: *NF2* mutated by dHPLC analysis vs. not mutated; *NF2* mutated by both dHPLC and MLPA P044 vs. not mutated; 22q LOH present vs. no 22q LOH; 2 or more hits in *NF2* vs. 1 or no hits. In each comparison, a group of 1 to 15 genes with significant p-values appeared to be deregulated (available upon request); however, none of the genes were deregulated when the p-value was Bonferroni-corrected.

The correlations with clinical features included the following: male vs. female; homogeneous vs. heterogeneous vs. cystic tumor; *NF2* syndrome-associated tumor vs. sporadic; smokers vs. non-smokers; high body mass index (BMI) vs. normal or low BMI; all variations in the 4 grades of the KOOS scale; involvement of the internal auditory canal or lack thereof; brainstem compression or lack thereof; pre-operative audiological class (in 4 groups); and left-side vs. right-side tumor. No significant Bonferroni-adjusted deregulated genes were found using these clinical outcomes, with the exception of Y-chromosome genes when males and females were

Table VII. Alterations detected in each tumor sample.

Sample	22q status ^a	Nucleotide	Codon	Peripheral blood status	MLPA ^b	<i>NF2</i> hits detected ^c
350	LOH	169C>T	p.Arg57Stop	-	-/del ex.2	2
352	LOH	447G>A	p.=	-	+/-	2
354	LOH	-/-	-	-	+/-del ex.14-17	2
369	N	-/-	-	-	-/-	0
371	LOH	1592delA		-	-/-	2
			p.Lys531Argfs*			
373	LOH	663C>G	p.Tyr221Stop	-	+/-	2
374	LOH	IVS10+1G>A	-	-	+/-	2
399	LOH	169C>T	p.Arg57Stop	Mutated	+/-del ex.2	2
407	N	-/-	-	-	-/-	0
417	N	-/-	-	-	-/-	0
422	LOH	737delC	p.Pro246Leufs*	-	+/-	2
437	LOH	401delC	p.Pro134Leufs*	-	+/-del ex.4	3
444	LOH	IVS4+1 G>A	-	-	+/-	2
447	LOH	1439_1446+19del27	p.Thr480Serfs*	-	+/-	2
449	LOH	436_443del8	p.Val146Glnfs*	-	-/-	2
450	LOH	1076insT	p.R359Mfs*	-	+/-	2
458	LOH	469G>A	p.Ser156Asn	-	+/-del ex.5.14	4
		467_476del10	p.P155Qfs*			
467	N	-/-	-	-	-/-	0
471	N	-/-	-	-	-/-	0
473	LOH	-/-	-	-	-/-	1
474	N	-/-	-	-	-/-del ex.4	1
482	LOH	-/-	-	-	+/-	1
486	N	169C>T	p.Arg57Stop	-	-/-	2
		IVS14-26del22	-			
488	N	-/-	-	-	-/-	0
490	N	1230_1243del14	p.Gln410Hisfs*	-	-/-	1
491	N	-/-	-	-	-/-	0
505	N	206delA	p.Lys69Argfs*	-	-/-	1
506	N	-/-	-	-	-/-	0
507	N	414delT	p.Val139Cysfs*	-	-/-	2
		1600C>T	p.His534Tyr	Mutated		
509	LOH	-/-	-	-	+/-	1
510	LOH	-/-	-	-	-/-	1

Consequences of mutations are predicted based on nucleotide change detected by PCR/dHPLC. *LOH, loss of heterozygosity; N, normal constitution. ^bA '-' suggest normal constitution, while a '+' supports the LOH by MLPA. ^c*NF2* hits are calculated adding each alteration. MLPA deletions, regardless of the number of exons, are considered as +1. When exon 2 showed deletion by MLPA in conjunction with mutation of this exon and LOH, it was not taken into account when counting the *NF2* hits.

compared. No exclusive clinicopathological similarities were found within schwannoma groups 1, 2-I and 2-II, even with the 3 *NF2*-associated samples distributed among all groups.

Discussion

We performed a microarray analysis and validation by qRT-PCR on 31 vestibular schwannomas and 9 control samples, in order to reveal targets and clues for the treatment of this

neoplasm. Describing a global mRNA status in a single article is an impossible goal. We therefore selected genes that were well-established as deregulated in these tumors to verify our results and then focused on deregulated genes in other tumors, as well as in our series, that had been insufficiently studied or not studied at all in schwannomas, such as *MET*, *AR* or *CAVI*.

NRG1 and *ErbB2-ErbB3* signaling pathway, a verification of deregulation. In 2003, malignant peripheral nerve sheath

tumors were found with constitutively activated NRG1/ErbB signaling (41). This pathway was later reported to be activated in schwannomas (42,43). Our results concur with those of previous studies regarding gene expression values compatible with overexpression (*NRG1*: 28.6-fold, $p=2.94e-5$; *ErbB2*: 4.38-fold, $p=2.94e-5$; *ErbB3*: 6.87-fold, $p=8.54e-5$). Ligand NRG1 binds to the ErbB2 receptor, which causes the ligand to bind with ErbB3 and downstream signaling leads to Schwann cell survival, migration, proliferation and differentiation (reviewed in 44). Merlin, which is presumably absent in all schwannomas, has been found to block ErbB2-Src signaling (45). We therefore validated the NRG1 and ErbB2-ErbB3 signaling pathway, which was previously reported and well-established as deregulated in schwannomas, using arrays and qRT-PCR, demonstrating that although we obtained control nerves from different regions (including the sensory and motor branches), our results are in agreement as regards this pathway.

TGF β and PAK signaling. A member of this pathway is the ErbB2 interacting protein (*ERBB2IP*), which was upregulated in our series (2.41-fold, $p=0.023$). This protein regulates signaling and myelination (46) and has been found to cooperate with merlin by blocking PAK2 activation induced by TGF β signaling (47). Our results demonstrated that *PAK2* was slightly upregulated (1.45-fold, $p=0.006805$) and *TGF β 3* was downregulated (-8-fold, $p=2.25e-5$). Moreover, *TGF β 1*, *TGF β R1* and *TGF β R2* were upregulated in schwannomas, in contrast with previous reports, where no evident changes were observed (48). In contrast to *PAK2* expression, *PAK3* was downregulated (-76-fold, $p=4.02e-7$) and *PAK1* was not affected. Thus, TGF β and PAK signaling may cooperate in schwannoma development and/or maintenance, although further research is required to elucidate the underlying mechanism.

EGFR downregulation, a controversial state. In contrast to *ErbB2* and *ErbB3*, *EGFR* (another receptor of this family) was downregulated in schwannomas (-17.3-fold, $p=2.26e-12$). Previous studies have suggested that this receptor is mediated for internalization and is retained in an insoluble membrane compartment by merlin via NHE-RF1 (*SLC9A3R1*) (11,49). The expression of *EGFR* seems to be restrained in schwannomas. However, its function as an activator of cell proliferation cannot be ruled out, since EGFR may still be signaling downstream in a merlin-absent context, despite the lack of proliferation of the human schwannoma cells following exposure to the ligand EGF (50), in contrast to non-tumoral vestibular cells (51). Previous studies have described no *EGFR* expression (52,53), whereas other studies have shown *EGFR* upregulation (54). Therefore, no firm conclusion was reached as regards the role of this receptor in schwannomas.

CAV1 downregulation: A broad spectrum of mechanisms. Another proposed pathway for the internalization of EGFR is CAV1-mediation followed by DNA damage (55). *CAV1* encodes for caveolin-1, a protein involved in caveolae formation. We demonstrated that this gene is downregulated in schwannomas (-12.4-fold, $p=2.27e-5$), in agreement with the results of Aarhus *et al* (25). *CAV1* loss accelerates proliferation and cooperates in oncogenic transformation (56). Furthermore, Brennan *et al* (57) proposed a model by which desmoglein 2

(*DSG2*) could be cleared from the plasma membrane and possibly activate mitogenic cell signaling through its interaction with CAV1. In a CAV1-loss context, these desmogleins could disrupt and affect cell-cell adhesion. Our results showed the downregulation of both *DSG2* (-70-fold, $p=2.94e-5$) and *CAV1* genes. Thus, the role of CAV1-DSG2 does not appear to be paramount in schwannomas, suggesting that expression changes in these genes must be related to other biological consequences. *CAV1* expression variants may participate in other pathways through different mechanisms, as explained below.

Heat shock protein deregulation; a consequence of the lack of caveolin-1? Recently, Ciocca *et al* (58) showed that breast tumor onset and reduced apoptosis driven by Her-2/neu expression were accelerated in mice lacking CAV1; the absence of CAV1 alters the expression of several stress-related proteins, such as heat shock proteins (HSPs). In our series, 5 HSPs were deregulated (*HSPA12A*: 3.31-fold, $p=4.34e-4$; *HSPA13*: 2.54-fold, $p=0.0035$; *HSPA4L*: 2.38-fold, $p=1.17e-4$; *HSPB6*: -2.19-fold, $p=5.76e-4$; *HSPB8*: -3.77-fold, $p=0.001$), suggesting that the CAV1/HSPs interaction may also play a role in schwannomas.

Immunoglobulin superfamily and L1 family proteins. The *HEPACAM* gene, which encodes a cell adhesion molecule of the immunoglobulin family, was upregulated (14.9-fold, $p=6.58e-4$), in contrast to malignant tumors such as hepatocellular carcinoma, in which it is usually downregulated (59). This protein interacts with the F-actin cytoskeleton and cell-extracellular matrix and is required to modulate cell motility (60). *CAV1* downregulates *HEPACAM* signal transduction in lipid rafts/caveolae (61), a common mechanism of action for this gene. Other members of the immunoglobulin superfamily, in particular L1 family proteins, were also upregulated in our experiments. These members included L1 (*LICAM*: 38.31-fold, $p=2.94e-5$), CHL1 (*CHL1*: 8.51-fold, $p=1.52e-4$) and NrCAM (*NRCAM*: 5.50-fold, $p=2.26e-4$). These results coincide with those previously reported (62). Neurofascin (*NFASC*), the last L1 family member, presented a normal expression level, while its associated protein doublecortin (*DCX*) was downregulated (-2.46-fold, $p=5.93e-4$). The L1 family has been shown to participate mainly in nervous system processes, such as neurite outgrowth (63), but has also been involved in non-neural roles, such as cancer progression (64). Therefore, *HEPACAM* gene overexpression concomitant with *CAV1* downregulation may participate in schwannoma development and/or maintenance and some members of the immunoglobulin superfamily appear deregulated in schwannomas.

Androgen receptor downregulation: A hormonal cause or consequence of schwannomas? Androgen receptor for dihydrotestosterone (AR), which was downregulated in our series (-15.7-fold, $p=2.94e-5$), is a steroid hormone nuclear receptor and is a target in prostate cancer treatment by androgen deprivation. This type of cancer frequently evolves into a resistant androgen-independent prostate cancer by mutations in AR (65). An androgen-dependent interaction has been established between the NH2 terminus region of CAV1 and the NH2 terminal domain and ligand-binding domain of AR (66). *CAV1* is also a co-activator of AR and may enhance AR

ligand-dependent transcriptional activation in the presence of androgen (67). Our results demonstrated that the mRNA levels of both transcripts were downregulated, suggesting that there may be a mechanism by which AR and CAV1 are related to the development and/or maintenance of schwannomas. There were no differences between males and females in terms of AR at the mRNA level. Dexamethasone, frequently used as post-operative treatment to decrease brainstem and cranial nerve inflammation, may downregulate AR levels. In the present series, none of the patients received this drug prior to surgery.

Apoptotic PAWR downregulation. In the absence of androgen signaling or AR silencing, the apoptotic pathway should be activated by prostate apoptosis response 4 (PAWR) through the transcription of c-FLIP, as previously reported (68). PAWR is also an activator of myosin phosphatase (69) and can dephosphorylate merlin in non-mutated tissues and recover its anti-tumor function. In our study, PAWR was found to be underexpressed (-11.9-fold, $p=2.94e-5$), as previously reported in other tumors, such as renal cell carcinoma (70) and neuroblastoma (71). Likewise, PAWR-null mice were shown to exhibit an increased rate of developing tumors, particularly in hormone-dependent tissues (72). Therefore, in schwannoma cells, apoptosis mediated by CAV1-AR-PAWR does not seem to occur due to the downregulation of PAWR mRNA in the tumor cells. There must, therefore, be another role for these downregulated molecules in schwannoma.

MET pathway, a core network in schwannomas. At the protein level, the AKT1 signaling pathway has been shown to restrain PAWR in the cytosol by phosphorylation, inhibiting its function as a proapoptotic factor in the nucleus (73). In schwannomas, the AKT pathway has been found to be activated (74) and it is well established that PI3K is an activator of AKT (75). Phosphoinositide-3-kinase interacting protein 1 (PIK3IP1) (76), an inhibitor of PI3K, was upregulated (4.76-fold, $p=2.94e-5$) as was the PI3K activator MET (4.5-fold, $p=2.94e-5$) and related genes. Therefore, PI3K activation of AKT seems possible via MET signaling based on the mRNA analysis, although PIK3IP1 is supposed to block PI3K. MET is a tyrosine kinase receptor involved in the activation of several cellular mechanisms, such as proliferation, motility, migration and invasion through different pathways, depending on the activating signal. MET is transactivated by several mechanisms, such as its ligand HGF, ErbB3 receptor, $\alpha\beta4$ integrins, CD44 and G-coupled proteins (reviewed in 77). In schwannomas, MET and its ligand HGF were expressed in all analyzed samples, as determined by qRT-PCR and immunohistochemistry (78), although no healthy tissue was used as the control; therefore, no alterations of expression were established. CAV1, which is downregulated in schwannomas, has been found to inhibit MET signaling in osteosarcoma transformation (79), which suggests that if this mechanism is analogous, CAV1 downregulation could trigger MET signaling in schwannomas. Moreover, the neural development molecules semaphorin 5A and plexin-B3 were overexpressed (SEMA5A: 3.14-fold, $p=3.64e-5$; PLXB3: 2.28-fold, $p=5.05e-5$) and able to trigger the intracellular signaling of MET (80). Finally, secreted phosphoprotein 1/osteopontin (SPPI), an enhancer of MET activator protein CD44, is upregulated (5.8-fold, $p=9.23e-4$). Due to its

involvement in several deregulated signals, the MET pathway seems to exert a pivotal role in schwannoma development and CAV1 may also exert its protumoral effect in this manner.

Absence of merlin may be due to more than just mutational mechanisms. We detected 22q LOH alterations in 58% of the samples, a finding that agrees with previous reports (4). Furthermore, 64.5% of the tumors had at least 1 hit in the sequence analysis by the combination of PCR/dHPLC and MLPA. This is also in agreement with previously reported data (4), although the percentage is lower in comparison to other studies (25). Despite the molecular analysis performed, 26% of the samples did not exhibit mutations and NF2 mRNA expression was not manifestly deregulated (available upon request), as in previous reports (25). Therefore, other mechanisms may cause the complete absence of merlin in schwannomas (5). The merlin protein is degraded by ubiquitination in advanced breast cancer due to osteopontin-initiated signaling via AKT (14). As PI3K/AKT activation occurs through ErbB3 and MET (77), which, as mentioned above, was upregulated in our series, we suggest that SPPI upregulation, in addition to the mutations of the NF2 gene and 22q LOH, may lead to the complete absence of the merlin protein in schwannomas, even in samples with no hits in the NF2 gene and taking into consideration that epigenetic inactivation of this gene seems to be a rare event in schwannomas (17-21).

Schwannoma cells are pre-myelinated cells. The development of myelinating and non-myelinating Schwann cell lineages includes 3 states: Neural crest cells that give rise to the Schwann cell precursors, which evolve into the immature Schwann cells (81). Our results using the database web tools demonstrate enriched axonogenesis and neuronal development, suggesting that schwannoma cells may be in a pre-differentiation state, as previously reported (62). In light of our results, the expression pattern obtained in schwannomas seems to be intermediate between the Schwann cell precursor and the neural crest cell. Both states, as well as schwannomas, exclusively overexpress $\alpha4$ -integrin (ITGA4, 1.8-fold, $p=0.003$), AP2a (TFAP2A, 1.41-fold, $p=0.009$) and Ncad (CDH2, 4.5-fold, $p=5.42e-4$). Cad19 (CDH19), which is only expressed in the Schwann cell precursor (82), is overexpressed in schwannomas (10.8-fold, $p=6.54e-5$). However, BFABP, DHH, P0, PMP22 and PLP are not overexpressed in schwannomas or neural crest cells, but only in Schwann cell precursors. Therefore, based on these findings, it is difficult to specify which state (between the neural crest and Schwann cell precursor) is most similar to that found in schwannomas; however, it seems clear that the gene expression pattern of these tumors corresponds to a previous state of myelinating Schwann cells.

Vestibular schwannoma grouping; fact or artifact? Similarly to previous reports (25,83), 2 mRNA expression groups in schwannoma were found in our study; however, although several genes were differentially expressed between groups of schwannomas, no major differences were observed between the groups. Furthermore, the absence of deregulated genes at the Bonferroni-adjusted level (except for males vs. females) between different tumor characteristics (e.g., homogeneous, heterogeneous or cystic; schwannomas from NF2 patients and sporadic; and different tumor sizes) indicate that, at least at the

mRNA expression level, there are no significant differences among vestibular schwannomas based on our experiments. Although 2 groups were identified, the homogeneity of the expression exhibited by several genes suggests that a potential therapeutic target could be suitable for all NF2 and sporadic vestibular schwannoma patients.

Gene NF1. *NF1* was faintly upregulated (1.88-fold, $p=0.012$). The transcription factor target analysis using the WebGestalt tool showed that this gene was enriched, suggesting that schwannomas may also be related to *NF1* deregulation.

Alternative splicing; a possible mechanism of tumorigenesis in schwannomas. Neurexins and neuroligins play essential roles in the development and function of the synapses in the nervous system, as well as in vessel tone and angiogenesis in the vascular system (84). Our results demonstrate a clear, distinct pattern in tumors compared with controls in the various isoforms available in the Gene 1.0 ST arrays. Thus, different isoforms of neurexins and neuroligins may appear in schwannomas compared with non-tumoral nerves. Further studies are warranted, with more specific arrays for alternative splicing, to identify other genes exhibiting this phenomenon.

Conclusions. In conclusion, based on our array expression pattern of 31 tumors and 9 controls and the validation of 48 genes by qRT-PCR, we discovered that the expression profile of vestibular schwannomas returns to a prior state which is similar to a Schwann precursor cell state rather than to mature myelinating Schwann cells. Our findings also demonstrate that the MET signaling pathway, which is possibly enhanced by the upstream signaling of *SPPI*, *ITGA4/B6*, *PLEXNB3/SEMA5A* and *CAVI*, appears to play a paramount role in the development and maintenance of vestibular schwannoma. A hormonal effect may also be involved in tumor formation, based on the deregulation of androgen receptor (AR). In addition, there were no expression differences between NF2-associated and sporadic tumors. Finally, osteopontin upregulation may contribute to merlin degradation in schwannomas with no apparent genetic (22q LOH and/or mutation) *NF2* inactivation.

Acknowledgements

The authors would like to thank Carolina Peña-Granero for her excellent technical assistance, Herbert Auer for his assistance with the array analysis and J.A. Fresno and A. Gamez for assistance with qRT-PCR. This study was supported by grants PI07/0577, PI08/1849 and PI10/1972 from Fondo de Investigaciones Sanitarias, Ministerio de Ciencia e Innovación, Spain and PI10-045, and from the Fundación Sociosanitaria de Castilla-La Mancha, Spain.

References

- Roosli C, Linthicum FH Jr, Cureoglu S and Merchant SN: What is the site of origin of cochleovestibular schwannomas? *Audiol Neurotol* 17: 121-125, 2012.
- Evans DG, Sainio M and Baser ME: Neurofibromatosis type 2. *J Med Genet* 37: 897-904, 2000.
- Rouleau GA, Merel P, Lutchman M, et al: Alteration in a new gene encoding a putative membrane-organizing protein causes neuro-fibromatosis type 2. *Nature* 363: 515-521, 1993.
- Hadfield KD, Smith MJ, Urquhart JE, et al: Rates of loss of heterozygosity and mitotic recombination in NF2 schwannomas, sporadic vestibular schwannomas and schwannomatosis schwannomas. *Oncogene* 29: 6216-6221, 2010.
- Stemmer-Rachamimov AO, Xu L, Gonzalez-Agosti C, et al: Universal absence of merlin, but not other ERM family members, in schwannomas. *Am J Pathol* 151: 1649-1654, 1997.
- Yi C, Troutman S, Fera D, Stemmer-Rachamimov A, et al: A tight junction-associated Merlin-angiomotin complex mediates Merlin's regulation of mitogenic signaling and tumor suppressive functions. *Cancer Cell* 19: 527-540, 2011.
- James MF, Han S, Polizzano C, et al: NF2/merlin is a novel negative regulator of mTOR complex 1, and activation of mTORC1 is associated with meningioma and schwannoma growth. *Mol Cell Biol* 29: 4250-4261, 2009.
- Hamaratoglu F, Willecke M, Kango-Singh M, et al: The tumour-suppressor genes NF2/Merlin and Expanded act through Hippo signalling to regulate cell proliferation and apoptosis. *Nat Cell Biol* 8: 27-36, 2006.
- Okada T, Lopez-Lago M and Giancotti FG: Merlin/NF-2 mediates contact inhibition of growth by suppressing recruitment of Rac to the plasma membrane. *J Cell Biol* 171: 361-371, 2005.
- Lallemant D, Manent J, Couvelard A, et al: Merlin regulates transmembrane receptor accumulation and signaling at the plasma membrane in primary mouse Schwann cells and in human schwannomas. *Oncogene* 28: 854-865, 2009.
- Curto M, Cole BK, Lallemant D, Liu CH and McClatchey AI: Contact-dependent inhibition of EGFR signaling by NF2/Merlin. *J Cell Biol* 177: 893-903, 2007.
- Li W, You L, Cooper J, et al: Merlin/NF2 suppresses tumorigenesis by inhibiting the E3 ubiquitin ligase CRL4(DCAF1) in the nucleus. *Cell* 140: 477-490, 2010.
- Li W, Cooper J, Karajannis MA and Giancotti FG: Merlin: a tumour suppressor with functions at the cell cortex and in the nucleus. *EMBO Rep* Feb 21, 2012 (Epub ahead of print). doi: 10.1038/sj.embor.2012.11.
- Morrow KA, Das S, Metge BJ, et al: Loss of tumor suppressor Merlin in advanced breast cancer is due to post-translational regulation. *J Biol Chem* 286: 40376-40385, 2011.
- Leone PE, Bello MJ, Mendiola M, et al: Allelic status of 1p, 14q, and 22q and NF2 gene mutations in sporadic schwannomas. *Int J Mol Med* 1: 889-892, 1998.
- Warren C, James LA, Ramsden RT, Wallace A, Baser ME, Varley JM and Evans DG: Identification of recurrent regions of chromosome loss and gain in vestibular schwannomas using comparative genomic hybridisation. *J Med Genet* 40: 802-806, 2003.
- Kino T, Takeshima H, Nakao M, et al: Identification of the cis-acting region in the NF2 gene promoter as a potential target for mutation and methylation-dependent silencing in schwannoma. *Genes Cells* 6: 441-454, 2001.
- Gonzalez-Gomez P, Bello MJ, Alonso ME, et al: CpG island methylation in sporadic and neurofibromatosis type 2-associated schwannomas. *Clin Cancer Res* 9: 5601-5606, 2003.
- Kullar PJ, Pearson DM, Malley DS, Collins VP and Ichimura K: CpG island hypermethylation of the neurofibromatosis type 2 (NF2) gene is rare in sporadic vestibular schwannomas. *Neuropathol Appl Neurobiol* 36: 505-514, 2010.
- Koutsimpelas D, Ruerup G, Mann WJ and Brieger J: Lack of neurofibromatosis type 2 gene promoter methylation in sporadic vestibular schwannomas. *ORL J Otorhinolaryngol Relat Spec* 74: 33-37, 2012.
- Lee JD, Kwon TJ, Kim UK and Lee WS: Genetic and epigenetic alterations of the NF2 gene in sporadic vestibular schwannomas. *PLoS One* 7: e30418, 2012.
- Bello MJ, Martinez-Glez V, Franco-Hernandez C, et al: DNA methylation pattern in 16 tumor-related genes in schwannomas. *Cancer Genet Cytogenet* 172: 84-86, 2007.
- Welling DB, Lasak JM, Akhmet'yeva E, Ghaehri B and Chang LS: cDNA microarray analysis of vestibular schwannomas. *Otol Neurotol* 23: 736-748, 2002.
- Cayé-Thomasen P, Borup R, Stangerup SE, Thomsen J and Nielsen FC: Deregulated genes in sporadic vestibular schwannomas. *Otol Neurotol* 31: 256-266, 2010.
- Aarhus M, Bruland O, Sætran HA, Mork SJ, Lund-Johansen M and Knappskog PM: Global gene expression profiling and tissue microarray reveal novel candidate genes and down-regulation of the tumor suppressor gene *CAVI* in sporadic vestibular schwannomas. *Neurosurgery* 67: 998-1019, 2010.

26. Lassaletta L, Patrón M, Del Río L, Alfonso C, Roda JM, Rey JA and Gavilan J: Cyclin D1 expression and histopathologic features in vestibular schwannomas. *Otol Neurotol* 28: 939-941, 2007.
27. Gonzalez-Roca E, Garcia-Albéniz X, Rodriguez-Mulero S, Gomis RR, Kornacker K and Auer H: Accurate expression profiling of very small cell populations. *PLoS One* 5: e14418, 2010.
28. Irizarry RA, Bolstad BM, Collin F, Cope LM, Hobbs B and Speed TP: Summaries of Affymetrix GeneChip probe level data. *Nucleic Acids Res* 31: e15, 2003.
29. Johnson WE, Li C and Rabinovic A: Adjusting batch effects in microarray expression data using empirical Bayes methods. *Biostatistics* 8: 118-127, 2007.
30. Chen C, Grennan K, Badner J, Zhang D, Gershon E, Jin L and Liu C: Removing batch effects in analysis of expression microarray data: an evaluation of six batch adjustment methods. *PLoS One* 6: e17238, 2011.
31. MAQC Consortium, Shi L, Reid LH, Jones WD, *et al*: The MicroArray Quality Control (MAQC) project shows inter- and intraplatform reproducibility of gene expression measurements. *Nat Biotechnol* 24: 1151-1161, 2006.
32. Zhang X, De la Cruz O, Pinto JM, Nicolae D, Firestein S and Gilad Y: Characterizing the expression of the human olfactory receptor gene family using a novel DNA microarray. *Genome Biol* 8: R86, 2007.
33. Saeed AI, Sharov V, White J, *et al*: TM4: a free, open-source system for microarray data management and analysis. *Biotechniques* 34: 374-378, 2003.
34. Saeed AI, Bhagabati NK, Braisted JC, *et al*: TM4 microarray software suite. *Meth Enzymol* 411: 134-193, 2006.
35. Huang da W, Sherman BT and Lempicki RA: Systematic and integrative analysis of large gene lists using DAVID bioinformatics resources. *Nat Protoc* 4: 44-57, 2009.
36. Huang da W, Sherman BT and Lempicki RA: Bioinformatics enrichment tools: paths toward the comprehensive functional analysis of large gene lists. *Nucleic Acids Res* 37: 1-13, 2009.
37. Duncan D, Prodduturi N and Zhang B: WebGestalt2: an updated and expanded version of the Web-based Gene Set Analysis Toolkit. *BMC Bioinformatics* 11: P10, 2010.
38. Livak KJ and Schmittgen TD: Analysis of relative gene expression data using real-time quantitative PCR and the 2(-Delta Delta C(T)) Method. *Methods* 25: 402-408, 2001.
39. Canzian F, Salovaara R, Hemminki A, Kristo P, Chadwick RB, Aaltonen LA and de la Chapelle A: Semiautomated assessment of loss of heterozygosity and replication error in tumors. *Cancer Res* 56: 3331-3337, 1996.
40. Abruzzo LV, Lee KY, Fuller A, Silverman A, Keating MJ, Medeiros LJ and Coombes KR: Validation of oligonucleotide microarray data using microfluidic low-density arrays: a new statistical method to normalize real-time RT-PCR data. *Biotechniques* 38: 785-792, 2005.
41. Frohnert PW, Stonecypher MS and Carroll SL: Constitutive activation of the neuregulin-1/ErbB receptor signaling pathway is essential for the proliferation of a neoplastic Schwann cell line. *Glia* 43: 104-118, 2003.
42. Stonecypher MS, Chaudhury AR, Byer SJ and Carroll SL: Neuregulin growth factors and their ErbB receptors form a potential signaling network for schwannoma tumorigenesis. *J Neuropathol Exp Neurol* 65: 162-175, 2006.
43. Hansen MR, Roehm PC, Chatterjee P and Green SH: Constitutive neuregulin-1/ErbB signaling contributes to human vestibular schwannoma proliferation. *Glia* 53: 593-600, 2006.
44. Newbern J and Birchmeier C: Nrg1/ErbB signaling networks in Schwann cell development and myelination. *Semin Cell Dev Biol* 21: 922-928, 2010.
45. Houshmandi SS, Emmett RJ, Giovannini M and Gutmann DH: The neurofibromatosis 2 protein, merlin, regulates glial cell growth in an ErbB2- and Src-dependent manner. *Mol Cell Biol* 29: 1472-1486, 2009.
46. Tao Y, Dai P, Liu Y, Marchetto S, Xiong WC, Borg JP and Mei L: Erbin regulates NRG1 signaling and myelination. *Proc Natl Acad Sci USA* 106: 9477-9482, 2009.
47. Wilkes MC, Repellin CE, Hong M, Bracamonte M, Penheiter SG, Borg JP and Leof EB: Erbin and the NF2 tumor suppressor Merlin cooperatively regulate cell-type-specific activation of PAK2 by TGF-beta. *Dev Cell* 16: 433-444, 2009.
48. Löttrich M, Mawrin C, Chamaon K, Kirches E, Dietzmann K and Freigang B: Expression of transforming growth factor-beta receptor type 1 and type 2 in human sporadic vestibular Schwannoma. *Pathol Res Pract* 203: 245-249, 2007.
49. Cole BK, Curto M, Chan AW and McClatchey AI: Localization to the cortical cytoskeleton is necessary for NF2/merlin-dependent epidermal growth factor receptor silencing. *Mol Cell Biol* 28: 1274-1284, 2008.
50. Ammoun S, Flaiz C, Ristic N, Schuldt J and Hanemann CO: Dissecting and targeting the growth factor-dependent and growth factor-independent extracellular signal-regulated kinase pathway in human schwannoma. *Cancer Res* 68: 5236-5245, 2008.
51. Bartolami S, Augé C, Travo C, Ventéo S, Knipper M and Sans A: Vestibular Schwann cells are a distinct subpopulation of peripheral glia with specific sensitivity to growth factors and extracellular matrix components. *J Neurobiol* 57: 270-290, 2003.
52. Prayson RA, Yoder BJ and Barnett GH: Epidermal growth factor receptor is not amplified in schwannomas. *Ann Diagn Pathol* 11: 326-329, 2007.
53. Wickremesekera A, Hovens CM and Kaye AH: Expression of ErbB-1 and 2 in vestibular schwannomas. *J Clin Neurosci* 14: 1199-1206, 2007.
54. Doherty JK, Ongkeko W, Crawley B, Andalibi A and Ryan AF: ErbB and Nrg: potential molecular targets for vestibular schwannoma pharmacotherapy. *Otol Neurotol* 29: 50-57, 2008.
55. Zhu H, Yue J, Pan Z, *et al*: Involvement of Caveolin-1 in repair of DNA damage through both homologous recombination and non-homologous end joining. *PLoS One* 5: e12055, 2010.
56. Cerezo A, Guadamillas MC, Goetz JG, Sánchez-Perales S, Klein E, Assoian RK and del Pozo MA: The absence of caveolin-1 increases proliferation and anchorage-independent growth by a Rac-dependent, Erk-independent mechanism. *Mol Cell Biol* 29: 5046-5059, 2009.
57. Brennan D, Peltonen S, Dowling A, *et al*: A role for caveolin-1 in desmoglein binding and desmosome dynamics. *Oncogene* 31: 1636-1648, 2012.
58. Ciocca DR, Cuello-Carrión FD, Natoli AL, Restall C and Anderson RL: Absence of caveolin-1 alters heat shock protein expression in spontaneous mammary tumors driven by Her-2/neu expression. *Histochem Cell Biol* 137: 187-194, 2012.
59. Chung Moh M, Hoon Lee L and Shen S: Cloning and characterization of hepaCAM, a novel Ig-like cell adhesion molecule suppressed in human hepatocellular carcinoma. *J Hepatol* 42: 833-841, 2005.
60. Moh MC, Tian Q, Zhang T, Lee LH and Shen S: The immunoglobulin-like cell adhesion molecule hepaCAM modulates cell adhesion and motility through direct interaction with the actin cytoskeleton. *J Cell Physiol* 219: 382-391, 2009.
61. Moh MC, Lee LH, Zhang T and Shen S: Interaction of the immunoglobulin-like cell adhesion molecule hepaCAM with caveolin-1. *Biochem Biophys Res Commun* 378: 755-760, 2009.
62. Hung G, Colton J, Fisher L, Oppenheimer M, Faudoa R, Slattery W and Linthicum F: Immunohistochemistry study of human vestibular nerve schwannoma differentiation. *Glia* 38: 363-370, 2002.
63. Hortsch M: The LI family of neural cell adhesion molecules: old proteins performing new tricks. *Neuron* 17: 587-593, 1996.
64. Fogel M, Gutwein P, Mechttersheimer S, *et al*: LI expression as a predictor of progression and survival in patients with uterine and ovarian carcinomas. *Lancet* 362: 869-875, 2003.
65. Tilley WD, Buchanan G, Hickey TE and Bentel JM: Mutations in the androgen receptor gene are associated with progression of human prostate cancer to androgen independence. *Clin Cancer Res* 2: 277-285, 1996.
66. Lu ML, Schneider MC, Zheng Y, Zhang X and Richie JP: Caveolin-1 interacts with androgen receptor. A positive modulator of androgen receptor mediated transactivation. *J Biol Chem* 276: 13442-13451, 2001.
67. Bryant KG, Camacho J, Jasmin JF, *et al*: Caveolin-1 overexpression enhances androgen-dependent growth and proliferation in the mouse prostate. *Int J Biochem Cell Biol* 43: 1318-1329, 2011.
68. Gao S, Wang H, Lee P, *et al*: Androgen receptor and prostate apoptosis response factor-4 target the c-FLIP gene to determine survival and apoptosis in the prostate gland. *J Mol Endocrinol* 36: 463-483, 2006.
69. Vetterkind S, Lee E, Sundberg E, Poythress RH, Tao TC, Preuss U and Morgan KG: Par-4: a new activator of myosin phosphatase. *Mol Biol Cell* 21: 1214-1224, 2010.
70. Cook J, Krishnan S, Ananth S, *et al*: Decreased expression of the pro-apoptotic protein Par-4 in renal cell carcinoma. *Oncogene* 18: 1205-1208, 1999.
71. Kögel D, Reimertz C, Mech P, *et al*: Dlk/ZIP kinase-induced apoptosis in human medulloblastoma cells: requirement of the mitochondrial apoptosis pathway. *Br J Cancer* 85: 1801-1808, 2001.

72. García-Cao I, Duran A, Collado M, *et al*: Tumour-suppression activity of the proapoptotic regulator Par4. *EMBO Rep* 6: 577-583, 2005.
73. Goswami A, Burikhanov R, de Thonel A, *et al*: Binding and phosphorylation of par-4 by akt is essential for cancer cell survival. *Mol Cell* 20: 33-44, 2005.
74. Jacob A, Lee TX, Neff BA, Miller S, Welling B and Chang LS: Phosphatidylinositol 3-kinase/AKT pathway activation in human vestibular schwannoma. *Otol Neurotol* 29: 58-68, 2008.
75. Krasilnikov MA: Phosphatidylinositol-3 kinase dependent pathways: the role in control of cell growth, survival, and malignant transformation. *Biochemistry (Mosc)* 65: 59-67, 2000.
76. Zhu Z, He X, Johnson C, *et al*: PI3K is negatively regulated by PIK3IP1, a novel p110 interacting protein. *Biochem Biophys Res Commun* 358: 66-72, 2007.
77. Organ SL and Tsao MS: An overview of the c-MET signaling pathway. *Ther Adv Med Oncol* 3 (Suppl 1): S7-S19, 2011.
78. Moriyama T, Kataoka H, Kawano H, *et al*: Comparative analysis of expression of hepatocyte growth factor and its receptor, c-met, in gliomas, meningiomas and schwannomas in humans. *Cancer Lett* 124: 149-155, 1998.
79. Cantiani L, Manara MC, Zucchini C, *et al*: Caveolin-1 reduces osteosarcoma metastases by inhibiting c-Src activity and met signaling. *Cancer Res* 67: 7675-7685, 2007.
80. Artigiani S, Conrotto P, Fazzari P, *et al*: Plexin-B3 is a functional receptor for semaphorin 5A. *EMBO Rep* 5: 710-714, 2004.
81. Mirsky R, Woodhoo A, Parkinson DB, Arthur-Farraj P, Bhaskaran A and Jessen KR: Novel signals controlling embryonic Schwann cell development, myelination and dedifferentiation. *J Peripher Nerv Syst* 13: 122-135, 2008.
82. Takahashi M and Osumi N: Identification of a novel type II classical cadherin: rat cadherin19 is expressed in the cranial ganglia and Schwann cell precursors during development. *Dev Dyn* 232: 200-208, 2005.
83. Martinez-Glez V, Franco-Hernandez C, Alvarez L, *et al*: Meningiomas and schwannomas: molecular subgroup classification found by expression arrays. *Int J Oncol* 34: 493-504, 2009.
84. Bottos A, Destro E, Rissone A, *et al*: The synaptic proteins neuroligins and neuroligins are widely expressed in the vascular system and contribute to its functions. *Proc Natl Acad Sci USA* 106: 20782-20787, 2009.

3.4 ARTÍCULO 4

TÍTULO: Global profiling in vestibular schwannomas shows critical deregulation of microRNAs and upregulation in those included in chromosomal region 14q32.

REVISTA: PLoS One. Año: 2013 Volumen: 8 Artículo: e65868.

AUTORES: **Miguel Torres-Martín**, Luis Lassaletta, de Campos JM, Alberto Isla, Javier Gavilán, Giovanni R. Pinto, Rommel R. Burbano, Farida Latif, Bárbara Melendez, Javier S. Castresana y Juan A. Rey.

RESUMEN: Los microRNAs son ARNs no codificantes de entre 21 y 25 nucleótidos que regulan la expresión génica a nivel post-transcripcional. Generalmente, el mecanismo es mediante la degradación del ARN mensajero. Se encontraron un total de 174 miRNAs desregulados en los schwannomas. Entre otros, se identificó la infraexpresión de miR-10b, miR-206, miR-183 y miR-204; así como la sobreexpresión de miR-431, miR-221 y miR-21. Además, se identificó la sobreexpresión de un clúster de miRNAs localizado en el cromosoma 14q32. Se validaron 10 miRNAs por PCR en tiempo real: 4 mostraban sobreexpresión, 4 infraexpresión y en 2 no había cambios. En todos los casos la tendencia de la desregulación se mantuvo entre los datos procedentes del análisis por microarrays y los datos obtenidos mediante PCR en tiempo real.

METODOLOGÍA:

- El ARN total, que incluye los miRNAs de las muestras, fue extraído con el kit mirVana miRNA Isolation de Ambion.
- El ARN de 16 schwannomas vestibulares y 3 controles -nervios sanos- se hibridó en el microarray GeneChip miRNA 1.0, de Affymetrix. Esta plataforma nos permite testar los niveles de expresión de los miRNAs presentes en la miRBase (<http://www.mirbase.org/>) de la versión 11.0 del 15 de abril de 2008. La corrección por lotes se realizó con el programa Partek Genomic Suite 6.6. El umbral para considerar un miRNA como desregulado entre dos grupos fue del doble o la mitad de cambio entre los grupos analizados y un p-valor ≤ 0.05 (t-test).
- La extracción del ADN, el análisis molecular del gen *NF2* y la LOH del cromosoma 22 fueron determinados de la misma manera que en el Artículo 1.
- La validación por PCR en tiempo real se llevo a cabo mediante miRCURY locked nucleic acid (LNA), Universal RT microRNA PCR protocol qRT-PCR de la compañía Exiqon. La síntesis de cDNA y las amplificaciones se realizaron de acuerdo a las recomendaciones del fabricante por duplicado.

Global Profiling in Vestibular Schwannomas Shows Critical Deregulation of MicroRNAs and Upregulation in Those Included in Chromosomal Region 14q32

Miguel Torres-Martin^{1*}, Luis Lassaletta², Jose M. de Campos³, Alberto Isla⁴, Javier Gavilan², Giovanni R. Pinto⁵, Rommel R. Burbano⁶, Farida Latif⁷, Barbara Melendez⁸, Javier S. Castresana⁹, Juan A. Rey¹

1 Neuro-Oncology Laboratory, Research Unit, La Paz University Hospital, IdiPAZ, Madrid, Spain, **2** Department of Otolaryngology, La Paz University Hospital, IdiPAZ, Madrid, Spain, **3** Neurosurgery Department, Fundacion Jimenez Diaz, Madrid, Spain, **4** Neurosurgery Department, La Paz University Hospital, IdiPAZ, Madrid, Spain, **5** Genetics and Molecular Biology Laboratory, Federal University of Piauí, Parnaíba, Brasil, **6** Human Cytogenetics Laboratory, Federal University of Pará, Belém, Brasil, **7** Centre for Rare Diseases and Personalised Medicine, School of Clinical and Experimental Medicine, University of Birmingham, Birmingham, United Kingdom, **8** Molecular Pathology Research Unit, Virgen de la Salud Hospital, Toledo, Spain, **9** Brain Tumor Biology Unit, University of Navarra School of Sciences, Pamplona, Spain

Abstract

Background: Vestibular schwannomas are benign tumors that arise from Schwann cells in the VIII cranial pair and usually present *NF2* gene mutations and/or loss of heterozygosity on chromosome 22q. Deregulation has also been found in several genes, such as *ERBB2* and *NRG1*. MicroRNAs are non-coding RNAs approximately 21 to 23 nucleotides in length that regulate mRNAs, usually by degradation at the post-transcriptional level.

Methods: We used microarray technology to test the deregulation of miRNAs and other non-coding RNAs present in GeneChip miRNA 1.0 (Affymetrix) over 16 vestibular schwannomas and 3 control-nerves, validating 10 of them by qRT-PCR.

Findings: Our results showed the deregulation of 174 miRNAs, including miR-10b, miR-206, miR-183 and miR-204, and the upregulation of miR-431, miR-221, miR-21 and miR-720, among others. The results also showed an aberrant expression of other non-coding RNAs. We also found a general upregulation of the miRNA cluster located at chromosome 14q32.

Conclusion: Our results suggest that several miRNAs are involved in tumor formation and/or maintenance and that global upregulation of the 14q32 chromosomal site contains miRNAs that may represent a therapeutic target for this neoplasm.

Citation: Torres-Martin M, Lassaletta L, de Campos JM, Isla A, Gavilan J, et al. (2013) Global Profiling in Vestibular Schwannomas Shows Critical Deregulation of MicroRNAs and Upregulation in Those Included in Chromosomal Region 14q32. PLoS ONE 8(6): e65868. doi:10.1371/journal.pone.0065868

Editor: Paul J. Galaray, Mayo Clinic, United States of America

Received: January 18, 2013; **Accepted:** April 29, 2013; **Published:** June 11, 2013

Copyright: © 2013 Torres-Martin et al. This is an open-access article distributed under the terms of the Creative Commons Attribution License, which permits unrestricted use, distribution, and reproduction in any medium, provided the original author and source are credited.

Funding: Supported by grants PI 07/0577 and 10/1972 from FIS, Ministerio de Sanidad, Servicios Sociales e Igualdad, Spain and grant PI10-045 from the Fundación Sociosanitaria de Castilla-La Mancha of the Consejería de Salud y Bienestar Social, Junta de Comunidades de Castilla-La Mancha, Spain. The funders had no role in study design, data collection and analysis, decision to publish, or preparation of the manuscript.

Competing Interests: The authors have declared that no competing interests exist.

* E-mail: migtorres.martin@gmail.com

Introduction

Schwannomas are benign tumors that arise from Schwann cells in the peripheral nerves. These tumors often originate from the vestibular nerve, and although they are histologically benign, vestibular schwannomas may cause hearing loss, tinnitus, facial palsy, and when large enough, brain stem compression and even death. Vestibular schwannomas may appear unilaterally but may also appear bilaterally when associated with neurofibromatosis type 2 syndrome (NF2). Patients with NF2 also develop other tumors such as meningiomas and gliomas [1]. The molecular hallmark of the disease is the biallelic inactivation of the tumor suppressor *NF2* gene by several mechanisms [2], such as mutation or loss of heterozygosity (LOH) of chromosome 22 where this gene is hosted (i.e., 22q12.2). Since the first description of monosomy 22 in schwannomas by cytogenetic analyses [3], other genetic alterations in these tumors have been identified, including

chromosomal gains of 9q34 and 17q and losses of 1p [4–6]. For an extensive review, see citation [7]. Contrary to non-head and neck schwannomas, sporadic vestibular schwannomas have shown no mutations on *BRAF*, *EGFR*, *PIK3CA* or *KRAS* [8]. Controversial findings on epigenetic aberrant methylation of *NF2* in schwannomas have been provided [9–12], and data on promoter methylation of tumor-related genes have also been described [13]. The *NF2* gene encodes for Merlin or Schwannomin [14,15], a protein that shares sequence homology with members of the ezrin/radixin/moesin (ERM) family. Merlin is involved in an array of signaling pathways, such as the suppression of tumorigenesis by its entering into the nucleus and binding to DCAF1 through the blocking of CRL4^{DCAF1} action [16], or downregulation of membrane levels of ErbB2, ErbB3 and EGFR upon cell-to-cell contact [17,18]. Using microarray technology in schwannomas, complete genome expression analysis is possible, and several regulatory pathways and specific genes, such as *CAVI*, have been

found to display an altered expression pattern [19–23]. MicroRNAs (miRNAs) are endogenous, non-coding RNAs 21 to 23 nucleotides in length that regulate gene expression at the post-transcriptional level by, among other mechanisms, binding and repressing target mRNAs [24]. Each miRNA is able to regulate thousands of mRNAs, and each miRNA acts in a tissue-specific manner [25]. Overexpression of miRNAs may involve tumor development by silencing certain tumor suppressor genes. On the other hand, underexpression of miRNAs may cause tumor progression by upregulating target oncogenes. Thus, miRNAs might be considered oncogenes or tumor suppressor genes in and of themselves. A wide variety of tumors have been found with altered miRNA expression, such as breast cancers [26], hepatocellular carcinomas [27], osteosarcomas [28] and many others [29]. Aberrant expression patterns in miRNAs have also been described in tumors that affect the nervous system, such as gliomas and meningiomas [30,31].

In schwannomas, the regulation of two miRNAs has been associated with tumorigenesis: miR-21 upregulation [32] and miR-7 downregulation [33], which suggests that deregulation of these small RNAs plays a role in the development of these tumors. In the light of these results, we performed a microarray analysis on 16 schwannomas and 3 control-nerves for non-coding RNAs, in order to identify new targets for the disease.

Materials and Methods

Patient Samples

The study group consisted of 16 patients who underwent surgery at our center for the removal of vestibular Schwannoma. Fifteen of these patients presented sporadic schwannomas and 1 sample (tumor S1) was from a patient diagnosed with NF2. The population included 7 women and 9 men. The mean age of the patients was 45.2 ± 14.9 years. The local ethics review board of the University Hospital La Paz approved the study protocol, which was based on the principles of the Declaration of Helsinki. All

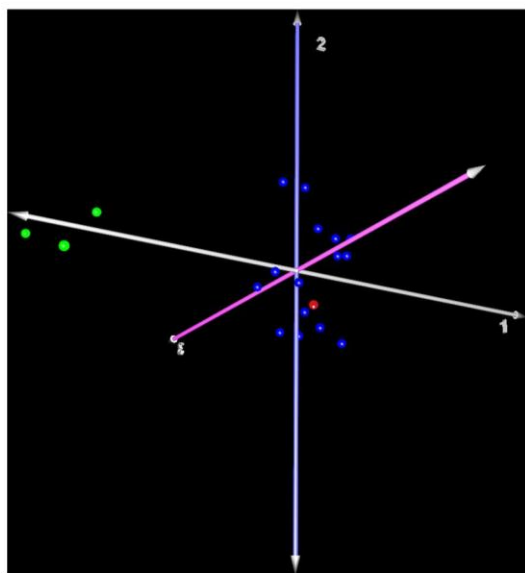


Figure 1. Three dimensional representation of the Principal Component Analysis of the 16 schwannomas (blue dots corresponding to sporadic and red dot to the NF2 patient) and the 3 control nerves (green dots).
doi:10.1371/journal.pone.0065868.g001

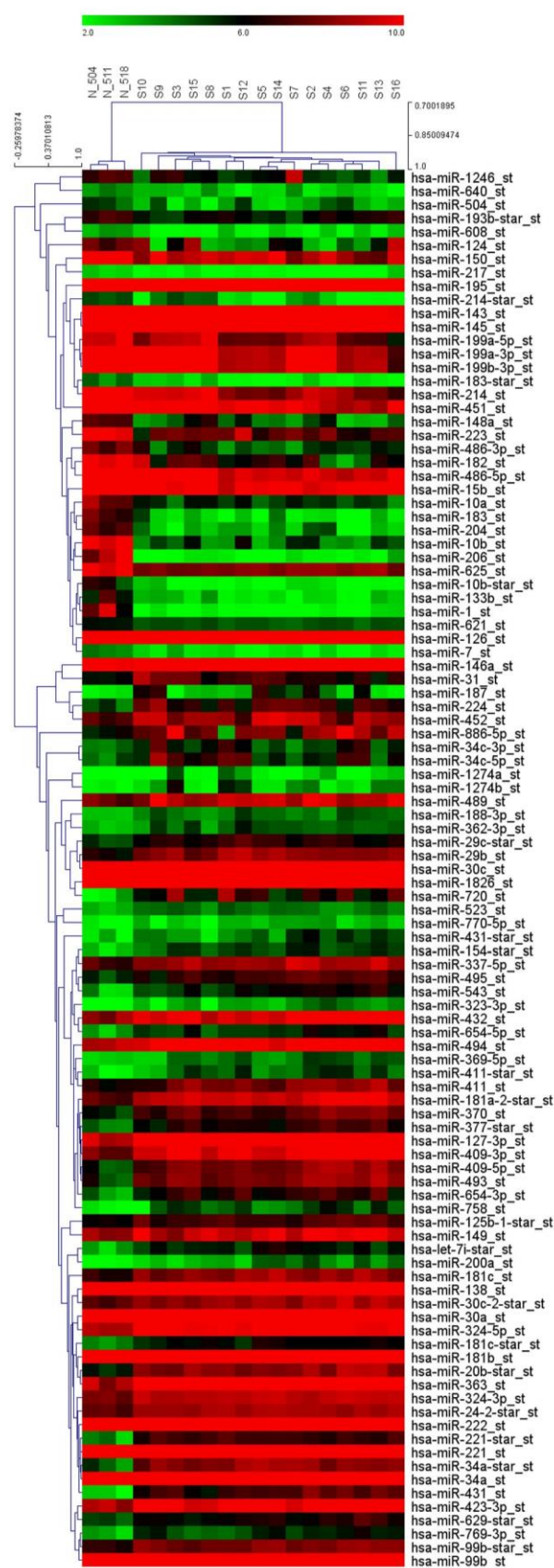


Figure 2. Hierarchical cluster by Pearson's correlation of all 19 samples (16 schwannomas and 3 control nerves) and miRNAs matching the criteria established as deregulated (2-fold change in expression and a $p < 0.05$ cutoff by one-way ANOVA).
doi:10.1371/journal.pone.0065868.g002

patients received detailed information on the study and provided their written informed consent prior to their inclusion in the study.

DNA/RNA Preparation

DNA was isolated using the Wizard Genomic DNA Purification Kit (Promega). DNA was also extracted from the corresponding patients' peripheral blood. Total RNA was extracted using the mirVana miRNA Isolation Kit (Ambion, CA, USA). A hypoglossal ansa cervicalis nerve and two auricular nerves from non-tumoral patients were used as control samples.

Table 1. The top 30 upregulated miRNAs obtained by microarray analysis, ordered by positive fold-change in schwannomas.

miRNA	p-value	Fold-Change
hsa-miR-431	5.47E-09	29.93
hsa-miR-720	4.96E-05	16.40
hsa-miR-34a*	2.73E-09	14.80
hsa-miR-221*	1.04E-09	9.96
hsa-miR-21	0.00116	9.71
hsa-miR-493	4.23E-07	8.48
hsa-miR-409-5p	9.25E-07	8.31
hsa-miR-363*	0.00010	8.09
hsa-miR-363	4.86E-09	8.05
hsa-miR-154	2.85E-05	7.53
hsa-miR-654-3p	0.00001	7.45
hsa-miR-20b*	3.33E-08	7.14
hsa-miR-543	3.29E-05	6.79
hsa-miR-377*	5.19E-06	5.63
hsa-miR-758	0.00057	5.63
hsa-miR-22*	5.70E-05	5.51
hsa-miR-127-3p	9.35E-07	5.42
hsa-miR-542-5p	0.00140	5.34
hsa-miR-200a	0.00028	5.31
hsa-miR-34a	4.27E-13	5.23
hsa-miR-224	0.00052	5.23
hsa-let-7i*	5.30E-06	5.17
hsa-miR-409-3p	9.77E-06	4.98
hsa-miR-221	1.23E-12	4.82
hsa-miR-184	0.01893	4.73
hsa-miR-181a-2*	2.89E-06	4.65
hsa-miR-493*	0.00094	4.65
hsa-miR-410	0.00096	4.47
hsa-miR-222	1.28E-10	4.47
hsa-miR-181c*	1.35E-07	4.30

doi:10.1371/journal.pone.0065868.t001

Mutational and MLPA Analysis of *NF2* and LOH of Chromosome 22q

We performed a mutational analysis of the *NF2* gene by dHPLC/PCR and a specific *NF2* SALSA of MLPA (MRC-Holland) and tested the LOH status of chromosome 22q. In brief, the LOH of chromosome 22q was tested using 5 microsatellite markers (D22S275, D22S264, D22S929, D22S268 and D22S280 located at 22q11-q12.3). For the PCR/dHPLC analysis of the *NF2* gene, a set of 15 primer pairs were selected using the standard PCR method and the dHPLC manufacturer's protocols. For the MLPA analysis, SALSA P044, which contains probes for all *NF2* exons, was used. Complete procedures were described previously [34].

miRNA Expression Array

We used the GeneChip miRNA 1.0 array (Affymetrix) with coverage of miRBase v.11. The array contains 4 [35] probe sets for mature miRNA and is able to detect the expression of 847 human mature miRNAs and 922 small nucleolar RNAs (snoRNAs) and small Cajal body-specific RNAs (scaRNAs). Hybridization targets were prepared from 500 ng of total RNA using the FlashTag Biotin HSR Kit (Genisphere). The labeled samples were hybridized to GeneChip miRNA arrays (Affymetrix). GeneChips were scanned in a GeneChip Scanner 3000 (Affymetrix). CEL files were generated from DAT files using AGCC software (Affymetrix). To generate the log2 expression estimates, the overall array intensity was normalized between the arrays, and the probe intensity for all probes in a probeset were summarized to a single value using the RMA (Robust Multichip Average) algorithm [36]. The arrays were processed at the IRB Barcelona Functional Genomics Core Facility. The microarray data was entered into the NCBI Gene Expression Omnibus database and are accessible through GEO Series accession number GSE43571.

Statistical Array Analysis

Given that the 19 samples were processed in two separate batches, with controls and tumors in both, the batch-removal tool of the Partek Genomic Suite 6.6 was used to remove the batch effect. We also used this software in order to include genes as deregulated, and we selected those genes with at least a 2-fold change in expression and a $p < 0.05$ cutoff in the one-way ANOVA test. The rest of statistical analyses were performed using MultiExperiment Viewer (MeV) [37]. Principal component analysis (PCA) was performed by eigenvalue decomposition of the 3 principal components for three-dimensional classification of the samples, and an unsupervised hierarchical cluster by Pearson's correlation was selected to group the samples and the deregulated miRNAs. We used the mirWalk (<http://www.umm.uni-heidelberg.de/apps/zmf/mirwalk/index.html>) and DAVID (<http://david.abcc.ncifcrf.gov/>) web tools in order to predict the biological meaning of the deregulated miRNAs [38,39]. As *NF2* vestibular schwannoma had the same way as the other tumors, we decided to include it in the statistical study.

Validation by qRT-PCR

For validation by miRCURY locked nucleic acid (LNA)TM Universal RT microRNA PCR protocol qRT-PCR (Exiqon), we used the 3 control nerves and 7 of the 16 Schwannoma chosen at random. A total of 10 miRNAs with aberrant expression were selected based on potential pathways of interest and/or chromosomal location (hsa-miR-1, hsa-miR-10b, hsa-miR-133b, hsa-miR-183, hsa-miR-206, hsa-miR-221, hsa-miR-370, hsa-miR-431, hsa-miR-493 and hsa-miR-720). The cDNA synthesis and

Table 2. The top 30 downregulated miRNAs obtained by microarray analysis, ordered by negative fold-change in schwannomas.

miRNA	p-value	Fold-Change
hsa-miR-206	2.17E-09	−222.68
hsa-miR-1	3.85E-09	−62.96
hsa-miR-10b	4.85E-08	−51.58
hsa-miR-183	1.01E-06	−25.33
hsa-miR-182	0.00019	−24.44
hsa-miR-204	3.57E-06	−17.68
hsa-miR-10b*	5.15E-08	−14.51
hsa-miR-133b	8.36E-08	−11.44
hsa-miR-214	2.59E-05	−11.13
hsa-miR-383	7.99E-06	−10.03
hsa-miR-223	0.000085	−7.73
hsa-miR-148a	0.000486	−7.61
hsa-miR-34b	0.005987	−7.36
hsa-miR-10a	0.000004	−7.31
hsa-miR-486-3p	0.000185	−6.58
hsa-miR-509-3p	1.14E-05	−6.57
hsa-miR-486-5p	9.88E-05	−6.27
hsa-miR-199a-3p	0.002156	−5.42
hsa-miR-199b-3p	0.002919	−5.33
hsa-miR-133a	4.49E-06	−5.18
hsa-miR-214*	0.015433	−4.01
hsa-miR-15b	2.10E-05	−3.87
hsa-miR-625	3.35E-07	−3.76
hsa-miR-143	0.000495	−3.74
hsa-miR-138-2*	0.000303	−3.59
hsa-miR-183*	2.30E-05	−3.55
hsa-miR-143*	0.01991	−3.29
hsa-miR-92a-1*	0.01092	−3.23
hsa-miR-595	8.73E-05	−3.17
hsa-miR-199a-5p	0.02445	−3.10

doi:10.1371/journal.pone.0065868.t002

real-time amplification were performed as recommended by the manufacturer. All tests were performed in duplicate.

The calculation of gene expression was conducted as follows: Average cycling threshold (Ct) values were obtained using SDS 2.2 software (Applied Biosystems). The maximum Ct value was set at 40. Ct values were normalized using two housekeeping non-coding RNAs extracted from data obtained in arrays (SNORD49A and hsa-miR-130). The relative expression level of each target gene was expressed as $\Delta Ct = C_{tref} - C_{tgene}$ [40]. Reference-normalized expression measurements were adjusted by defining the lowest expression value as 0, with subsequent 1-unit increases reflecting an approximate doubling of the RNA. The non-parametric Mann-Whitney-Wilcoxon test at $p < 0.05$ coupled with the Benjamini-Hochberg correction test was used to calculate the significance of differences between the control samples and the schwannomas.

Results

Allelic Status of 22q and Mutational Analysis of NF2

A total of 9 samples (56%) presented 22q LOH using microsatellite markers. Eight of the schwannomas (50%) had NF2 sequence mutations detected by PCR/dHPLC, and 10 of the schwannomas (62%) had NF2 sequence mutations detected by the combined MLPA and PCR/dHPLC analysis. In 7 cases, LOH was concomitant with either MLPA or PCR/dHPLC alteration. In 4 cases, no alterations were found. We found no mutations in the patients' peripheral blood, with the exception of the NF2 patient. The individual results are shown in Table S1.

Deregulation in miRNAs

When the control nerves and the schwannomas were compared using the one-way ANOVA at $p < 0.05$ and with at least a 2-fold change, we found 176 deregulated miRNAs from a total of 847 human miRNAs available in the array. Of these, 119 (14%) were found to be upregulated and 57 (6.7%) were downregulated. The top 30 of each group are shown in Tables 1 and 2, and the full results of the deregulation can be seen in Table S2. The PCA showed a clear distinction between the control nerves and the schwannomas, and the tumor from the NF2 patient grouped together with the other schwannomas (Figure 1). The hierarchical cluster of deregulated genes showed no major differences at the miRNA level between the schwannomas (included that tumor from a NF2 patient) but showed differences with respect to the controls (Figure 2).

The chromosomal location of the miRNA affected by deregulation is shown in Table 3. Chromosome 14 was the most affected, with 52% of all miRNAs located on this chromosome deregulated; all of these miRNAs were overexpressed, but one was downregulated. Chromosome X also presented a high degree of deregulation, with more than 27% of all miRNAs in this chromosome showing aberrant expression. Other chromosomes displaying significant rates of abnormally expressed miRNAs were chromosome 1 (28%), chromosome 7 (26%) and, although fewer miRNA probes were available in the array for this study, chromosome 6 (29%) and 18 (33%).

Deregulation in other Non-coding RNAs

Other non-coding RNAs appeared deregulated: 128 of all snoRNAs available in the array corresponded to HAC-Box, with one downregulated (U71c) and 25 upregulated. A total of 67 of the 274 CD-box snoRNAs were upregulated, and only 5 of the other 499 snoRNAs were upregulated. The scaRNAs were not deregulated, and the 5.8s rRNAs were upregulated in all 10 copies available at the probeset. The 30 most deregulated non-coding RNAs are shown in Table 4.

Web-tool Analysis

Using mirWalk, a web-tool that finds gene targets from a given list of miRNAs, we obtained a set of validated gene targets using our lists of upregulated and downregulated miRNAs. These lists of targets, with 1554 and 1597 genes respectively, were analyzed separately using the DAVID platform, which uses a set of functional annotation tools to find biological meaning from data using gene ontology terms, BioCarta, etc. Using these web tools, the main deregulated pathways identified were vasculature and nervous system development (Tables S3 and S4).

Table 3. Available miRNAs correspond to those miRNAs tested in the microarray.

Chromosome	Available miRNAs	Up-regulated	Down-regulated	Total	Percentage of deregulation (%)
1	61	14	3	17	27.9
2	23	2	3	5	21.7
3	35	2	2	4	11.4
4	31	0	2	2	6.5
5	30	2	4	6	20.0
6	17	3	2	5	29.4
7	42	4	7	11	26.2
8	27	1	3	4	14.8
9	30	1	4	5	16.7
10	23	1	2	3	13.0
11	38	3	2	5	13.2
12	42	2	0	2	4.8
13	25	0	2	2	8.0
14	81	40	2	42	51.9
15	27	4	1	5	18.5
16	17	4	2	6	35.3
17	48	6	4	10	20.8
18	9	0	3	3	33.3
19	102	9	4	13	12.7
20	19	0	0	0	0.0
21	7	1	0	1	14.3
22	19	0	1	1	5.3
X	89	20	4	24	27.0

Up or downregulation was obtained from those with at least a 2-fold change and $p > 0.05$ when schwannomas and control nerves were compared. Other non-coding RNAs were not considered in this table.
doi:10.1371/journal.pone.0065868.t003

Microarray Data Correlation versus *NF2* Alterations and 22q Allelic Status

We also tested the possibility that grouping schwannomas by their molecular characteristics such as the presence or not of *NF2* mutations or LOH 22q/normal 22q, would result in a statistically significant subset of over- or under-expressed miRNAs (using the one-way ANOVA at $p < 0.05$ and at least a 2-fold change). Fourteen miRNAs matched these criteria, and a number of the miRNAs displayed statistical significance in several comparisons (Table S5). These included the presence of 22q LOH vs. normal constitution (with significant upregulation of miR-195* in miRNAs with LOH), the presence of sequence alteration by all methods vs. normal miRNAs (4 miRNAs), sequence alteration exclusively by PCR/dHPLC vs. normal miRNAs (3 miRNAs), and one or more detected alterations vs. no detected alterations (9 miRNAs).

Validation by qRT-PCR

Validation of the expression patterns of 11 miRNAs and SNORD49A obtained through microarray analysis by performing qRT-PCR (Table 5). In all cases, the trend observed in the microarrays (upregulation, downregulation or no deregulation) was confirmed by this technique.

Discussion

In this study, we used 16 schwannomas and 3 control nerves to analyze the expression levels of miRNAs and other non-coding

RNAs in Affymetrix microarrays. As an alternative for control purposes, in vitro cultures of Schwann cells may be used. However, although it is possible to obtain up to 90% purity of Schwann cells [41], it has been reported that Schwann cells in cultures modify their native gene expression [42]. Thus, it appears that peripheral nerve may be a more reliable control in expression studies, as it has been proved by several reports [20,21,33]. Our findings showed deregulation in schwannomas of more than 150 miRNAs and a set of other non-coding miRNAs, with special upregulation of those miRNAs located in the chromosomal 14q region. Eleven of the miRNAs and 1 snoRNA were validated by qRT-PCR.

The most downregulated miRNAs in this study include the myomiRs, composed of three clusters: miR-1-1/miR-133a-2, miR-1-2/miR-133a-1, and miR-206/miR-133b. These miRNAs have been identified as typically downregulated in several types of cancer, such as colorectal cancer and hepatocellular carcinoma (reviewed in citation [43]). Other miRNAs with reduced expression in our series included miR-10b, which has also been associated with other cancers such as gliomas [44], metastatic breast carcinomas [45] and pancreatic carcinomas [46]; however, in all of these cases, miR-10b was upregulated [44]. Decreased expression of this miRNA has been reported to escape senescence by Argonaute 2 expression in stem cells [47]. The miRNA 183/182 cluster, which was downregulated in our series, has also been found to be deregulated in medulloblastoma [48] and prostate cancer [49], and the cluster has been shown to inhibit cell proliferation and migration by targeting *FGF9* and *NTM* in

Table 4. The top 30 deregulated non-miRNAs present in the arrays.

Transcript ID	Chr	Sequence	p-value	Fold-Change
HBII-99	20	CDBox	1.14E-07	5.97
14q(II-12)	14	CDBox	6.83E-07	5.41
U48	6	CDBox	7.30E-06	5.05
14q(II-4)	14	CDBox	8.33E-06	5.05
U107	X	HAcaBox	2.61E-09	4.95
HBII-180C	19	CDBox	7.09E-09	4.90
14q(II-14)	14	CDBox	2.52E-05	4.85
U43	22	CDBox	3.53E-07	4.46
U31	11	CDBox	3.73E-06	4.42
14q(II-3)	14	CDBox	8.57E-06	4.42
U43	22	CDBox	7.81E-07	4.31
ENSG00000200879	11	snoRNA	7.21E-11	4.24
14q(II-14)	14	CDBox	5.42E-05	4.20
ACA7	3	HAcaBox	3.00E-06	4.09
U46	1	CDBox	7.68E-08	4.06
U8	17	CDBox	1.82E-06	4.02
ACA48	17	HAcaBox	6.70E-07	3.98
ENSG00000202252	11	snoRNA	3.03E-05	3.91
U8	17	CDBox	3.32E-07	3.87
U46	1	CDBox	4.34E-07	3.78
14q(II-26)	14	CDBox	0.00128	3.76
ACA16	1	HAcaBox	7.13E-05	3.70
ENSG00000207118	11	snoRNA	0.00011	3.68
U103	1	CDBox	3.05E-08	3.68
ACA48	17	HAcaBox	1.64E-06	3.61
ACA16	1	HAcaBox	3.75E-06	3.54
HBII-85-8	15	CDBox	3.89E-07	3.49
U33	19	CDBox	4.22E-08	3.44
14q(II-12)	14	CDBox	3.84E-05	3.43
HBII-180A	19	CDBox	5.51E-08	3.43

doi:10.1371/journal.pone.0065868.t004

Schwann cells [50]. Furthermore, miR-183 has been found to be capable of regulating Ezrin protein (a member of the family with similarity to Merlin) in osteosarcoma and lung cancer [51,52]. The miRNA 183/182 cluster may therefore be involved in Schwannoma formation if it plays a similar role in these neoplasms. In malignant peripheral nerve sheath tumors (MPNSTs), miR-204 is downregulated [53], in a similar pattern as that found in the schwannomas in our arrays. As these tumors also developed from Schwann cells, there may be common features associated with this particular miRNA that appear to participate in the development of both neoplasms.

The upregulated miRNAs in our studies include miR-21, which targets PTEN in non-small cell lung cancer [54]; cluster miR-221/miR-222, which is activated in Schwann cell proliferation following sciatic nerve injury by targeting *LASS2* [55] and accelerates proliferation during liver regeneration [56]; and miR-370, which is capable of reducing *NFI* mRNA levels in acute myeloid leukemia [57] and is also overexpressed in prostate cancer [58]. Another miRNA with increased expression is miR-493, which is defined as a tumor suppressor in bladder cancer and

Table 5. The qRT-PCR showed all miRNAs significantly up or downregulated in schwannomas compared to control-nerves (at least a 2-fold change and $p > 0.05$), except in those two used as house-keeping (SNORD49A and miR-103).

miRNA	Location	Fold-change	P-value
miR-1	20q13.33	126.72	0.0251
miR-10b	2q31.1	269.19	0.0251
miR-133b	6p12.2	210.49	0.0251
miR-183	7q32.2	57.34	0.0251
miR-206	6p12.2	379.28	0.0251
miR-221	Xp11.3	-9.62	0.0251
miR-370	14q32.2	-3.13	0.0364
miR-431	14q32.2	-6.38	0.0251
miR-493	14q32.2	-7.99	0.0251
miR-720	3q26.1	-3.49	0.0364
SNORD49A	17p11.2	1.01	0.7324
miR-103	5q34	-1.01	0.7324

doi:10.1371/journal.pone.0065868.t005

is capable of downregulating FZD4 and RhoC protein expression [59]. Thus, several of these miRNAs may contribute to the benign proliferation observed in schwannomas, such as miR-221/miR-222, due to their demonstrated capacity to affect proliferation and regeneration in various tissues, including nerve tissue.

Web-tool analysis (performed using DAVID) provides us with the theoretical results of validated genes affected by miRNA deregulation (performed with mirWalk) and the pathways and related components that involve these genes. The DAVID results showed several processes related to carcinogenesis in the Kyoto Encyclopedia of Genes and Genomes (KEGG), including hsa05215:Prostate cancer, hsa05214:Glioma and the hsa04012:ErbB signaling pathway. However, when the up- or down-regulated miRNAs we had previously identified were considered, the findings showed similar deregulated GO-terms (e.g., GO:0010604 positive regulation of the macromolecule metabolic process; GO:0051960 regulation of nervous system development; GO:0051270 regulation of cell motion, etc.). Therefore, the data obtained from the analysis of our deregulated miRNAs with these web-tools must be viewed with caution, and no definitive conclusions should be drawn. This event might be related to the lack of tissue specificity when selecting deregulated miRNAs that were validated for target genes. Once more detailed data are available on this subject, a re-evaluation of the pathways affected by miRNA interaction may be performed. We previously analyzed the critical regulatory pathways that are abnormally expressed in schwannomas by studying the expression levels of 96 tumor-related genes [21]. Those genes coding for proteins related to apoptosis and angiogenesis and genes related to DNA damage repair were the most frequently altered.

When the chromosomal location of the abnormally expressed miRNAs was analyzed, we found a clear upregulation for those miRNAs located in the chromosomal 14q32 region. Only two miRNAs, miR-203 and miR-625, had reduced expression, while approximately 40 miRNAs showed overexpression, including miR-431, miR-370 and miR-493, as validated by qRT-PCR. This region involves a large miRNA cluster [60] [61] altered in several neoplasms such as gliomas (by downregulation) [62] and a subtype of acute myeloid leukemia (by upregulation) [63]. Consequently, this region also appears to play a pivotal role in

Schwannoma formation and/or maintenance. On chromosome 22, which usually suffers a loss of heterozygosity in Schwannoma, 5% of the miRNAs located in this region appeared deregulated. In fact, only miR-185 (at 22q11) displayed reduced expression levels. This finding suggests that, in schwannomas, losses involving 22q do not seem to affect the expression pattern of miRNA located there. However this particular miRNA (miR-185) may be affected as a result of other yet unknown regulatory molecular mechanisms.

Several deregulated miRNAs we identified concur with the data from previous reports in schwannomas [32,33]. In agreement with the data, miR-7, miR-638, miR-143* and miR-498 were downregulated, and miR-221, miR-21, miR-29, miR-30a and miR-138 were upregulated in our study. On the other hand, a few of the miRNAs, such as miR-34a, let-7d and miR-451, did not match the same trend of aberrant expression as that previously described. Establishing a reason for these divergences is a difficult task, because neither the number of samples nor the methodology used should influence the result. Therefore, our findings generally concur with the results of previous reports, although several miRNAs with a different expression pattern were identified.

We found alterations in other non-coding RNAs (snoRNAs and scaRNAs) using this type of array. These alterations have been associated with the development or progression of breast cancer and acute leukemia [64,65]. Our results showed that at least 98 of these non-coding RNAs were deregulated, almost all by increased expression, except for HACA-Box SNORA71C. A total of 14 SnoRNAs were also located in chromosome 14q32, highlighting the paramount role played by the miRNAs located in this genomic region in Schwannoma development.

Schwannomas with specific molecular characteristics, such as gene mutations of *NF2* and/or LOH of 22q region, may present a different miRNA expression pattern when compared to unaltered schwannomas. When comparing levels of miRNA expression obtained from arrays with other molecular studies performed on these tumors (*NF2* mutation detection or 22q allelic status determination), we found 14 miRNAs with aberrant expression. For example, abnormal overexpression of miR-155, which is associated with schwannomas with no alterations of any sort, displayed a statistical significance of $p < 0.001$; however, miR-125b-2* was found to be significantly downregulated in those tumors carrying a mutation ($p < 0.01$). Despite these differences, establishing a molecular reason for these particular alterations is difficult. Furthermore, the p -values were relatively high compared with those obtained when tumors and controls were studied, and outliers could not be ruled out as playing a role in these results. We therefore concluded that, at the miRNA level, a few miRNA

subsets may have relevance depending on the genetic status of the tumor (the presence of *NF2* mutation and/or LOH of 22q), although more research needs to be conducted on this particular aspect.

In conclusion, our results show that the non-coding RNA expression pattern is critically affected in schwannomas when compared to healthy tissue. Of these, miRNAs seems to be the most frequently affected, given that at least 20% appear deregulated, including several depicted in other tumors. These mRNAs include miR-10b and miR-204. Furthermore, a well-described cluster of non-coding RNAs in the chromosomal region 14q32 seems to present global upregulation, suggesting that miRNA deregulation in this region might play a significant role in the development and/or maintenance of these tumors. Finally, other non-coding RNAs, although less numerous when compared with miRNAs, also seem to be altered in schwannomas.

Supporting Information

Table S1 Mutations detected on vestibular schwannomas and LOH status of chromosome 22q.
(XLSX)

Table S2 Deregulation of all human probes in microarrays. Output obtained from Partek Genomic Suite 6.6 for one-way ANOVA.
(XLSX)

Table S3 Downregulated pathways obtained by DAVID.
(XLSX)

Table S4 Upregulated pathways obtained by DAVID.
(XLSX)

Table S5 Deregulation profile in miRNA based on molecular characteristics of schwannomas.
(XLSX)

Acknowledgments

We would like to thank Herbert Auer for his assistance in the array analysis and Angelo Gamez and Juan A. Fresno for their help with the qRT-PCR.

Author Contributions

Conceived and designed the experiments: MTM LLJR. Performed the experiments: MTM. Analyzed the data: MTM GP RB. Contributed reagents/materials/analysis tools: BM JC JdC AI LLJR FLJG. Wrote the paper: MTM LLJR.

References

- Evans DG, Sainio M, Baser ME (2000) Neurofibromatosis type 2. *J Med Genet* 37: 897–904.
- Hadfield KD, Smith MJ, Urquhart JE, Wallace AJ, Bowers NL, et al. (2010) Rates of loss of heterozygosity and mitotic recombination in NF2 schwannomas, sporadic vestibular schwannomas and schwannomatosis schwannomas. *Oncogene* 29: 6216–6221. doi:10.1038/nc.2010.363.
- Rey JA, Bello MJ, De Campos JM, Kusak ME, Moreno S (1987) Cytogenetic analysis in human neurinomas. *Cancer Genet Cytogenet* 28: 187–188.
- Leone PE, Bello MJ, Mendiola M, Kusak ME, De Campos JM, et al. (1998) Allelic status of 1p, 14q, and 22q and NF2 gene mutations in sporadic schwannomas. *Int J Mol Med* 1: 889–892.
- Warren C, James LA, Ramsden RT, Wallace A, Baser ME, et al. (2003) Identification of recurrent regions of chromosome loss and gain in vestibular schwannomas using comparative genomic hybridisation. *J Med Genet* 40: 802–806.
- Bello MJ, De Campos JM, Kusak ME, Vaquero J, Sarasa JL, et al. (1993) Clonal chromosome aberrations in neurinomas. *Genes Chromosomes Cancer* 6: 206–211.
- Sandberg AA, Stone JF (2008) *The Genetics and Molecular Biology of Neural Tumors*. Totawa: Humana Press.
- De Vries M, Bruijn IB, Cleton-Jansen A-M, Malessy MJA, Van der Mey AGL, et al. (2013) Mutations affecting BRAF, EGFR, PIK3CA, and KRAS are not associated with sporadic vestibular schwannomas. *Virchows Arch* 462: 211–217. doi:10.1007/s00428-012-1342-8.
- Kino T, Takeshima H, Nakao M, Nishi T, Yamamoto K, et al. (2001) Identification of the cis-acting region in the NF2 gene promoter as a potential target for mutation and methylation-dependent silencing in schwannoma. *Genes Cells* 6: 441–454.
- Gonzalez-Gomez P, Bello MJ, Alonso ME, Lomas J, Arjona D, et al. (2003) CpG island methylation in sporadic and neurofibromatosis type 2-associated schwannomas. *Clin Cancer Res* 9: 5601–5606.
- Kullar PJ, Pearson DM, Malley DS, Collins VP, Ichimura K (2010) CpG island hypermethylation of the neurofibromatosis type 2 (NF2) gene is rare in sporadic vestibular schwannomas. *Neuropathol Appl Neurobiol* 36: 505–514. doi:10.1111/j.1365-2990.2010.01090.x.

12. Koutsimpelas D, Ruerup G, Mann WJ, Brieger J (2012) Lack of neurofibromatosis type 2 gene promoter methylation in sporadic vestibular schwannomas. *ORL J Otorhinolaryngol Relat Spec* 74: 33–37. doi:10.1159/000334968.
13. Bello MJ, Martinez-Glez V, Franco-Hernandez C, Peña-Granero C, De Campos JM, et al. (2007) DNA methylation pattern in 16 tumor-related genes in schwannomas. *Cancer Genet Cytogenet* 172: 84–86. doi:10.1016/j.cancergen-cyto.2006.02.022.
14. Rouleau GA, Merel P, Lutchman M, Sanson M, Zucman J, et al. (1993) Alteration in a new gene encoding a putative membrane-organizing protein causes neuro-fibromatosis type 2. *Nature* 363: 515–521. doi:10.1038/363515a0.
15. Trofatter JA, MacCollin MM, Rutter JL, Murrell JR, Duyao MP, et al. (1993) A novel moesin-, ezrin-, radixin-like gene is a candidate for the neurofibromatosis 2 tumor suppressor. *Cell* 72: 791–800.
16. Li W, You L, Cooper J, Schiavon G, Pepe-Caprio A, et al. (2010) Merlin/NF2 suppresses tumorigenesis by inhibiting the E3 ubiquitin ligase CRL4(DCAF1) in the nucleus. *Cell* 140: 477–490. doi:10.1016/j.cell.2010.01.029.
17. Lallemand D, Manent J, Couvelard A, Watilliaux A, Siena M, et al. (2009) Merlin regulates transmembrane receptor accumulation and signaling at the plasma membrane in primary mouse Schwann cells and in human schwannomas. *Oncogene* 28: 854–865. doi:10.1038/ncr.2008.427.
18. Curto M, Cole BK, Lallemand D, Liu C-H, McClatchey AI (2007) Contact-dependent inhibition of EGFR signaling by NF2/Merlin. *J Cell Biol* 177: 893–903. doi:10.1083/jcb.200703010.
19. Welling DB, Lasak JM, Akhmanetyeva E, Ghaehri B, Chang L-S (2002) cDNA microarray analysis of vestibular schwannomas. *Otol Neurotol* 23: 736–748.
20. Cayé-Thomasen P, Borup R, Stangerup S-E, Thomsen J, Nielsen FC (2010) Deregulated genes in sporadic vestibular schwannomas. *Otol Neurotol* 31: 256–266. doi:10.1097/MAO.0b013e3181be6478.
21. Aarhus M, Bruland O, Sætran HA, Mork SJ, Lund-Johansen M, et al. (2010) Global gene expression profiling and tissue microarray reveal novel candidate genes and down-regulation of the tumor suppressor gene CAV1 in sporadic vestibular schwannomas. *Neurosurgery* 67: 998–1019; discussion 1019. doi:10.1227/NEU.0b013e3181ec7b71.
22. Torres-Martín M, Martínez-Glez V, Peña-Granero C, Lassaletta L, Isla A, et al. (2012) Expression analysis of tumor-related genes involved in critical regulatory pathways in schwannomas. *Clin Transl Oncol*. doi:10.1007/s12094-012-0937-5.
23. Torres-Martín M, Lassaletta L, San-Roman-Montero J, De Campos JM, Isla A, et al. (2013) Microarray analysis of gene expression in vestibular schwannomas reveals SPP1/MET signaling pathway and androgen receptor deregulation. *Int J Oncol* 42: 848–862. doi:10.3892/ijo.2013.1798.
24. Ambros V (2004) The functions of animal microRNAs. *Nature* 431: 350–355. doi:10.1038/nature02871.
25. Babak T, Zhang W, Morris Q, Blencowe BJ, Hughes TR (2004) Probing microRNAs with microarrays: Tissue specificity and functional inference. *RNA* 10: 1813–1819. doi:10.1261/rna.7119904.
26. Smith AL, Iwanaga R, Drasin DJ, Micalizzi DS, Vartuli RL, et al. (2012) The miR-106b-25 cluster targets Smad7, activates TGF- β signaling, and induces EMT and tumor initiating cell characteristics downstream of Six1 in human breast cancer. *Oncogene*. doi:10.1038/ncr.2012.11.
27. Wang Y, Toh HC, Chow P, Chung AYY, Meyers DJ, et al. (2012) MicroRNA-224 is up-regulated in hepatocellular carcinoma through epigenetic mechanisms. *FASEB J* 26: 3032–3041. doi:10.1096/fj.11-201855.
28. Zhang W, Qian J-X, Yi H-L, Yang Z-D, Wang C-F, et al. (2012) The microRNA-29 plays a central role in osteosarcoma pathogenesis and progression. *Mol Biol (Mosk)* 46: 622–627.
29. Iorio MV, Croce CM (2012) MicroRNA dysregulation in cancer: diagnostics, monitoring and therapeutics. A comprehensive review. *EMBO Mol Med* 4: 143–159. doi:10.1002/emmm.201100209.
30. Saydam O, Shen Y, Würdinger T, Senol O, Boke E, et al. (2009) Downregulated microRNA-200a in meningiomas promotes tumor growth by reducing E-cadherin and activating the Wnt/beta-catenin signaling pathway. *Mol Cell Biol* 29: 5923–5940. doi:10.1128/MCB.00332-09.
31. Papagiannakopoulos T, Friedmann-Morvinski D, Neveu P, Dugas JC, Gill RM, et al. (2012) Pro-neural miR-128 is a glioma tumor suppressor that targets mitogenic kinases. *Oncogene* 31: 1884–1895. doi:10.1038/ncr.2011.380.
32. Cioffi JA, Yue WY, Mendolia-Loffredo S, Hansen KR, Wackym PA, et al. (2010) MicroRNA-21 overexpression contributes to vestibular schwannoma cell proliferation and survival. *Otol Neurotol* 31: 1455–1462. doi:10.1097/MAO.0b013e3181f20655.
33. Saydam O, Senol O, Würdinger T, Mizrak A, Ozdener GB, et al. (2011) miRNA-7 attenuation in Schwannoma tumors stimulates growth by upregulating three oncogenic signaling pathways. *Cancer Res* 71: 852–861. doi:10.1158/0008-5472.CAN-10-1219.
34. Martínez-Glez V, Franco-Hernandez C, Alvarez L, De Campos JM, Isla A, et al. (2009) Meningiomas and schwannomas: molecular subgroup classification found by expression arrays. *Int J Oncol* 34: 493–504.
35. Kozomara A, Griffiths-Jones S (2011) miRBase: integrating microRNA annotation and deep-sequencing data. *Nucleic Acids Res* 39: D152–157. doi:10.1093/nar/gkq1027.
36. Irizarry RA, Bolstad BM, Collin F, Cope LM, Hobbs B, et al. (2003) Summaries of Affymetrix GeneChip probe level data. *Nucleic Acids Res* 31: e15.
37. Saeed AI, Sharov V, White J, Li J, Liang W, et al. (2003) TM4: a free, open-source system for microarray data management and analysis. *BioTechniques* 34: 374–378.
38. Dweep H, Sticht C, Pandey P, Gretz N (2011) miRWalk-database: prediction of possible miRNA binding sites by “walking” the genes of three genomes. *J Biomed Inform* 44: 839–847. doi:10.1016/j.jbi.2011.05.002.
39. Huang DW, Sherman BT, Lempicki RA (2009) Systematic and integrative analysis of large gene lists using DAVID bioinformatics resources. *Nat Protoc* 4: 44–57. doi:10.1038/nprot.2008.211.
40. Livak KJ, Schmittgen TD (2001) Analysis of relative gene expression data using real-time quantitative PCR and the 2(-Delta Delta C(T)) Method. *Methods* 25: 402–408. doi:10.1006/meth.2001.1262.
41. Oda Y, Okada Y, Katsuda S, Ikeda K, Nakanishi I (1989) A simple method for the Schwann cell preparation from newborn rat sciatic nerves. *J Neurosci Methods* 28: 163–169.
42. Jesuraj NJ, Nguyen PK, Wood MD, Moore AM, Borschel GH, et al. (2012) Differential gene expression in motor and sensory Schwann cells in the rat femoral nerve. *J Neurosci Res* 90: 96–104. doi:10.1002/jnr.22752.
43. Nohata N, Hanazawa T, Enokida H, Seki N (2012) microRNA-1/133a and microRNA-206/133b clusters: dysregulation and functional roles in human cancers. *Oncotarget* 3: 9–21.
44. Gabriely G, Yi M, Narayan RS, Niers JM, Wurdinger T, et al. (2011) Human glioma growth is controlled by microRNA-10b. *Cancer Res* 71: 3563–3572. doi:10.1158/0008-5472.CAN-10-3568.
45. Ma L, Teruya-Feldstein J, Weinberg RA (2007) Tumour invasion and metastasis initiated by microRNA-10b in breast cancer. *Nature* 449: 682–688. doi:10.1038/nature06174.
46. Nakata K, Ohuchida K, Mizumoto K, Kayashima T, Ikenaga N, et al. (2011) MicroRNA-10b is overexpressed in pancreatic cancer, promotes its invasiveness, and correlates with a poor prognosis. *Surgery* 150: 916–922. doi:10.1016/j.surg.2011.06.017.
47. Kim BS, Jung JS, Jang JH, Kang KS, Kang SK (2011) Nuclear Argonaute 2 regulates adipose tissue-derived stem cell survival through direct control of miR10b and selenoprotein N1 expression. *Aging Cell* 10: 277–291. doi:10.1111/j.1474-9726.2011.00670.x.
48. Bai AHC, Milde T, Remke M, Rolli CG, Hielscher T, et al. (2012) MicroRNA-182 promotes leptomeningeal spread of non-sonic hedgehog-medulloblastoma. *Acta Neuropathol* 123: 529–538. doi:10.1007/s00401-011-0924-x.
49. Mihelich BL, Khramtsova EA, Arva N, Vaishnav A, Johnson DN, et al. (2011) miR-183–96–182 cluster is overexpressed in prostate tissue and regulates zinc homeostasis in prostate cells. *J Biol Chem* 286: 44503–44511. doi:10.1074/jbc.M111.262915.
50. Yu B, Qian T, Wang Y, Zhou S, Ding G, et al. (2012) miR-182 inhibits Schwann cell proliferation and migration by targeting FGF9 and NTM, respectively at an early stage following sciatic nerve injury. *Nucleic Acids Res* 40: 10356–10365. doi:10.1093/nar/gks750.
51. Zhu J, Feng Y, Ke Z, Yang Z, Zhou J, et al. (2012) Down-regulation of miR-183 promotes migration and invasion of osteosarcoma by targeting Ezrin. *Am J Pathol* 180: 2440–2451. doi:10.1016/j.ajpath.2012.02.023.
52. Wang G, Mao W, Zheng S (2008) MicroRNA-183 regulates Ezrin expression in lung cancer cells. *FEBS Lett* 582: 3663–3668. doi:10.1016/j.febslet.2008.09.051.
53. Gong M, Ma J, Li M, Zhou M, Hock JM, et al. (2012) MicroRNA-204 critically regulates carcinogenesis in malignant peripheral nerve sheath tumors. *Neuro-oncology* 14: 1007–1017. doi:10.1093/neuonc/nos124.
54. Liu Z-L, Wang H, Liu J, Wang Z-X (2013) MicroRNA-21 (miR-21) expression promotes growth, metastasis, and chemo- or radioresistance in non-small cell lung cancer cells by targeting PTEN. *Mol Cell Biochem* 372: 35–45. doi:10.1007/s11010-012-1443-3.
55. Yu B, Zhou S, Wang Y, Qian T, Ding G, et al. (2012) miR-221 and miR-222 promote Schwann cell proliferation and migration by targeting LASS2 after sciatic nerve injury. *J Cell Sci* 125: 2675–2683. doi:10.1242/jcs.098996.
56. Yuan Q, Loya K, Rani B, Möbus S, Balakrishnan A, et al. (2012) MicroRNA-221 overexpression accelerates hepatocyte proliferation during liver regeneration. *Hepatology* (Baltimore, MD). doi:10.1002/hep.25984.
57. García-Ortí L, Cristóbal I, Cirauqui C, Guruceaga E, Marcoteví N, et al. (2012) Integration of SNP and mRNA Arrays with MicroRNA Profiling Reveals That MiR-370 Is Upregulated and Targets NF1 in Acute Myeloid Leukemia. *PLoS ONE* 7: e47717. doi:10.1371/journal.pone.0047717.
58. Wu Z, Sun H, Zeng W, He J, Mao X (2012) Upregulation of MicroRNA-370 Induces Proliferation in Human Prostate Cancer Cells by Downregulating the Transcription Factor FOXO1. *PLoS ONE* 7: e45825. doi:10.1371/journal.pone.0045825.
59. Ueno K, Hirata H, Majid S, Yamamura S, Shahryari V, et al. (2012) Tumor suppressor microRNA-493 decreases cell motility and migration ability in human bladder cancer cells by downregulating RhoC and FZD4. *Mol Cancer Ther* 11: 244–253. doi:10.1158/1535-7163.MCT-11-0592.
60. Benetatos L, Hatzimichael E, Londin E, Vartholomatos G, Lohrer P, et al. (2012) The microRNAs within the DLK1-DIO3 genomic region: involvement in disease pathogenesis. Cellular and molecular life sciences: CMLS. doi:10.1007/s00018-012-1080-8.
61. Altuvia Y, Landgraf P, Lithwick G, Elefant N, Pfeffer S, et al. (2005) Clustering and conservation patterns of human microRNAs. *Nucleic Acids Res* 33: 2697–2706. doi:10.1093/nar/gki567.
62. Lavon I, Zrihan D, Granit A, Einstein O, Fainstein N, et al. (2010) Gliomas display a microRNA expression profile reminiscent of neural precursor cells. *Neuro-oncology* 12: 422–433. doi:10.1093/neuonc/nop061.

63. Dixon-McIver A, East P, Mein CA, Cazier J-B, Molloy G, et al. (2008) Distinctive patterns of microRNA expression associated with karyotype in acute myeloid leukaemia. *PLoS ONE* 3: e2141. doi:10.1371/journal.pone.0002141.
64. Dong X-Y, Guo P, Boyd J, Sun X, Li Q, et al. (2009) Implication of snoRNA U50 in human breast cancer. *J Genet Genomics* 36: 447–454. doi:10.1016/S1673-8527(08)60134-4.
65. Valleron W, Laprevotte E, Gautier E-F, Quelen C, Demur C, et al. (2012) Specific small nucleolar RNA expression profiles in acute leukemia. *Leukemia* 26: 2052–2060. doi:10.1038/leu.2012.111.

3.5 ARTÍCULO 5 (En revisión)

TÍTULO: Genome-wide methylation analysis in vestibular schwannomas shows putative mechanisms of gene expression modulation and global hypomethylation at the HOX gene cluster

AUTORES: **Miguel Torres-Martín**, Luis Lassaletta, José María de Campos, Alberto Isla, Giovanni R. Pinto, Rommel R. Burbano, Bárbara Melendez, Javier S. Castresana y Juan A. Rey

RESUMEN: En este estudio comparamos el patrón de metilación del ADN de schwannomas vestibulares y controles sanos, así como una serie de schwannomas no-vestibulares. Nuestros resultados muestran una tendencia a la hipometilación en los tumores. Además, hallamos hipometilación en los 4 clústeres de genes HOX en numerosos sitios CpG en los schwannomas vestibulares, pero no en los no-vestibulares. Entre los genes y microRNAs hipometilados en la región promotora, encontramos casos con infraexpresión como el miRNA-21, *MET* y *PMEPA1*. También fueron establecidos patrones de metilación aberrante que podrían ser compatibles con splicing alternativo, como en los genes *NRXN1* y *MBP*. Este hecho incrementaría enormemente la complejidad de los patrones de expresión y metilación. Globalmente, nuestro estudio muestra patrones

de metilación que podrían originar desregulación en la expresión génica, y que por lo tanto podrían tener relevancia terapéutica.

METODOLOGÍA:

- Se estudiaron 36 schwannomas vestibulares (de los trabajos anteriores), 4 no vestibulares y 5 nervios no tumorales.
- La extracción del ADN, el análisis molecular del gen *NF2* y la LOH del cromosoma 22 fueron determinados de la misma manera que en el Artículo 1.
- Se trató el ADN con bisulfito con el kit EZ DNA methylation de Zymo Research. Después, este ADN fue hibridado en los microarrays Infinium Human Methylation 450K BeadChip de Illumina.
- Para el procesamiento y el análisis de los datos se utilizaron tres paquetes del programa estadístico R: Lumi, IMA y Methyanalysis. Al procesar los datos, se obtiene un número llamado valor Beta por cada CpG, que está comprendido entre 0 -nula probabilidad de que un sitio CpG esté metilado- y 1 -muy probable la metilación-. Este valor Beta es después transformado mediante una función logit al valor M, que mejora la validez estadística. Con la matriz de datos resultante y tras diversas normalizaciones, se comparan grupos mediante t-test. El umbral en este caso para considerar un sitio CpG como diferencialmente metilado o hipometilado en un grupo con respecto a otro, es de una diferencia de 1 en el valor M y un p-valor ajustado por Bonferroni de $p \leq 0.05$.

- Para la extracción de ARN de los schwannomas vestibulares, los controles sanos y de los 4 schwannomas no-vestibulares se utilizó el Rneasy® Mini Kit de Qiagen, que purifica los ARNs de más de 200 bases.
- El ARN fue hibridado en los microarrays de Affymetrix Human Gene 1.0 ST. La normalización y sumarización de los mismos se realizó mediante el algoritmo Robust Multichip Average (RMA). Los análisis fueron a nivel de exón. Se estudiaron las muestras del Artículo 3, otros 3 schwannomas vestibulares procedentes de pacientes de NF2 y 4 schwannomas no-vestibulares.

Genome-wide methylation analysis in vestibular schwannomas shows putative mechanisms of gene expression modulation and global hypomethylation at the HOX gene cluster

Miguel Torres-Martín¹, Luis Lassaletta², Jose M de Campos³, Alberto Isla⁴, Giovanni R. Pinto⁵, Rommel R. Burbano⁶, Bárbara Melendez⁷, Javier S. Castresana⁸, and Juan A. Rey¹

¹Molecular Neuro-oncogenetics Laboratory; Research Unit. Hospital Universitario La Paz; IdiPAZ; Madrid, Spain; ²Department of Otolaryngology; Hospital Universitario La Paz; IdiPAZ; Madrid, Spain; ³Neurosurgery Department; Fundacion Jimenez Diaz; Madrid, Spain; ⁴Neurosurgery Department; Hospital Universitario La Paz; IdiPAZ; Madrid, Spain; ⁵Genetics and Molecular Biology Laboratory; Federal University of Piau; Parnaiba, Brazil; ⁶Human Cytogenetics Laboratory; Institute of Biological Sciences, Federal University of Para; Belem, Brazil; ⁷Molecular Pathology Research Unit; Virgen de la Salud Hospital; Toledo, Spain; ⁸Department of Biochemistry and Genetics; University of Navarra School of Sciences; Pamplona, Spain.

Keywords: Tumor, DNA methylation, schwannomas, NF2, HOX, microarray, gene expression, Neurofibromatosis type 2.

Abbreviations: miRNA, microRNA; PCA, principal component analysis; LOH, Loss Of Heterozygosity; NF2, Neurofibromatosis type 2; Hox, Homeobox; CIMP, CpG island methylator phenotype; TSS, Transcriptional Start Site; GEO, Gene Expression Omnibus.

Disclosure of Potential Conflicts of Interest

The authors have no potential conflicts of interest.

Schwannomas are tumors that develop from Schwann cells in the peripheral nerves and commonly arise from the vestibular nerve. Vestibular schwannomas can present unilaterally and sporadically or bilaterally when the tumor is associated with neurofibromatosis type 2 syndrome. The hallmark of the disease is biallelic inactivation of *NF2* gene by mutation or loss of heterozygosity of chromosome 22q, where this gene is harbored. In this study, we employed Infinium Human Methylation 450K BeadChip microarrays in a series of 36 vestibular schwannomas, 4 nonvestibular schwannomas and 5 healthy nerves. Our results show a trend towards hypomethylation in schwannomas. Furthermore, HOX genes, located at 4 clusters in the genome, displayed hypomethylation in several CpG sites in the vestibular schwannomas but not in the nonvestibular schwannomas. Several microRNA and protein-coding genes were also found to be hypomethylated at promoter regions and were confirmed as upregulated by expression analysis; including miRNA-21, *MET* and *PMEPA1*. We also detected methylation patterns that might be involved in alternative transcripts of several genes such as *NRXN1* or *MBP*, which would increase the complexity of the methylation and expression pattern. Overall, our results show specific epigenetic signatures in several coding genes and microRNAs that could potentially be used as therapeutic targets.

Introduction

Schwannomas are low-grade tumors that arise from the Schwann cells of peripheral nerves. Although these tumors can originate from numerous locations, they usually develop from the vestibulocochlear nerve, accounting for up to 10% of intracranial tumors. Vestibular schwannomas can be sporadic and unilateral or bilateral when they are associated with the genetic disorder neurofibromatosis type 2 syndrome. Current treatment options for schwannomas include “wait and scan”, surgery and radiosurgery. Although recurrence is generally not expected, the consequences of treatment for patients can be devastating, especially for patients who have several tumors, such as NF2 patients. The most common molecular disorder of vestibular schwannomas is the mutation of the *NF2* tumor-suppressor gene and LOH in the locus of this gene at chromosome 22q, which at the cytogenetic level was observed as monosomy of chromosome 22.¹² *NF2* encodes for Merlin, a FERM domain protein that has 2 main isoforms and a wide variety of functions. Tumor mechanisms via the loss of Merlin function involve cytosol (via internalization of tyrosine kinase receptors, the hippo pathway or angiomotin³) and nuclear, which suppress tumorigenesis by inhibiting the ubiquitin ligase CRL4^{DCAF1}.⁴ Other molecular alterations include ErbB2-ErbB3/Nrg1 constitutional activation,⁵ caveolin-1 downregulation⁶ and *MET* and osteopontin upregulation, which has been suggested as an alternative to Merlin degradation in schwannomas.⁷ It has also been proposed that a YAP-driven signaling network induces tumor proliferation.⁸ Several clinical trials for treating schwannomas in NF2 patients have been conducted in recent years, a number of which have had promising outcomes,⁹ while others have shown no patient improvement.^{10,11}

Among epigenetic mechanisms, cytosine methylation at CpG dinucleotides is probably the most widely studied. The CpG sites are usually clustered within the DNA in enriched zones known as CpG islands, flanked by less enriched shores and then by shelves. Methylation has been studied in gene promoter at TSS and 5'UTR regions, normally in connection with mRNA transcriptional repression. Nevertheless, current research is increasing the attention on the lesser-known mechanisms of action of methylation within gene bodies and 3'UTR regions. Recent experiments have shown that intragenic DNA methylation might be related to the regulation of alternative promoters¹² or to controlling transcriptional noise.¹³ The methylation processes for diseases such as cancer have been widely reported.¹⁴ Tumor-suppressor gene silencing and oncogene hypomethylation are well known mechanisms of tumor development. The individual patient response to treatment can be predicted, such as the glioma response to alkylating agents based on *MGMT* methylation status.¹⁵ MiRNA also present aberrant epigenetic processes, in the same manner as protein-coding genes.¹⁶ DNA methylation also participates in embryogenesis and tissue development, with Hox cluster genes playing a pivotal role in this process.

In schwannomas, the aberrant methylation of genes (including *THBS1*, *MGMT*, *TP73* and *TIMP3*) has been identified by methylation-specific PCR.^{17,18} *NF2* methylation does not seem to be a mechanism of Merlin loss in schwannomas,^{19,20} although specific CpG sites might be involved.²¹ Thus, the epigenetic landscape of schwannomas remains poorly described and understood. Current wide epigenetic genomic profiling techniques include next generation sequencing and microarray technology. Using these techniques numerous prognostic factors have been identified, including the CIMP in various tumors such as oligodendrogliomas²² and ependymomas.²³ Using the Illumina 450k Infinium BeadChip kit, we tested 485 000 individual CpG sites to find aberrant

methylation in 36 vestibular and 4 nonvestibular schwannomas, with the aim of detecting aberrant methylation along tumors, differential methylation of CpG sites based on clinical characteristics and ultimately finding potential therapeutic targets. These findings were correlated with whole genome expression data from our previous analysis on the same cases, to determine whether there is any relationship between distinct epigenetic changes and gene expression variations.

Results

An overall view of vestibular schwannoma methylation patterns shows a trend to hypomethylation

A total of 6553 CpG sites were hypermethylated in vestibular schwannomas at autosomes when they were compared with control nerves (corrected p-value and M-value differences of at least 1). Hypomethylation occurred in 8307 CpG sites, suggesting that this alteration was more common in the tumors. Through chromosome shredding (**Table 1**), we observed that hypomethylation was more frequent in all autosomes except at chromosomes 16, 19 and 22, where hypermethylation involved more CpG sites. Chromosomes 2, 10, 12 and 21 had greater hypomethylation among its probes. Using genes as references for a given CpG, we established 6 categories for each mRNA transcript (TSS1500, TSS200, 5'UTR, 1st exon, gene body and 3'UTR). In all 6 regions, the hypomethylation was constant but was more frequent in the 3'UTR regions, followed by the 5'UTR and gene body regions (**Table 2**). The TSS regions and the 1st exon region were almost equal in the number of altered CpG sites. In terms of the location of a CpG site in an epigenetic context (in an island, shore or shelf), hypermethylation appeared more relevant on islands and slightly less so at the shores, while hypomethylation was greatly increased at island shelves and in open sea. By a significant margin, the open sea region had the most alterations in terms of total numbers. The north-south shores and shelves had similar levels in terms of the percentage of methylated and hypomethylated CpG sites. In relative numbers, the islands were less affected by epigenetic mechanisms.

Functional annotation tools for hypomethylated regulatory regions using DAVID (excluding those CpGs on gene bodies) showed enrichment in terms of axon projection, Semaphorin domains, homeobox sequence, apoptosis and Ras/rho signaling. Hypermethylated regulatory regions were enriched in cell motility, adhesion and cytoskeleton.

Gene methylation patterns

In order to compare the genes with altered methylated patterns in vestibular schwannoma and controls, we grouped the microarray probes into the 6 categories before used for each transcript (TSS1500, TSS200, 5'UTR, 1st exon, gene body and 3'UTR) with the *IMA regionswrapper* function. Hypomethylation was more frequent than hypermethylation (849 vs. 562 genes). By a significant margin, the region showing the largest number of altered genes in both hypomethylation and hypermethylation was 3'UTR. The 344 hypomethylated genes in this 3'UTR region included *MTOR*, *HOXD4*, *PAX8* and *SOX8*, while the 152 hypermethylated genes included *SOX1*, *ROBO4* and *NEU4*. The next region with the largest number of alterations was the gene body, with 127 hypomethylated genes including *EVI2A*, *HOXD4*, *CTNND1* and *PMP2* and 106 aberrant methylated genes including *VSTM1*, *NDEL1* and *ESM1*. *EVI2A* is located within an intron

of *NF1*, but this gene showed no epigenetic alteration. First exon hypomethylation was found in 75 genes (such as *PMP2*, *MBP* and *MOG*) and was similar to hypermethylation in 73 genes (including *S100P*, *SOX1* and *IGF1*). Region 5'UTR showed the lowest number of total altered genes with 127; 60 of them displayed hypermethylation (e.g., *HOXD3*, *S100B* and *HEPACAM*) and 67 presented hypomethylation (e.g., *APOL4* and *IGF1*). Finally, TSS regions had 407 altered genes, displaying 236 hypomethylated genes (such as *TP63*, *TNF*, *CTNND1* and *S100A2*) and 171 hypermethylated genes (including *ITGAE*, *FOXD2* and *TFAP2A*).

At the single CpG level, we also searched for genes showing several probes with aberrant methylation patterns. Since Schwann cells contribute to the insulation of axons by myelin (a lipid covering), we searched for genes involved in myelination and lipid processes. We found a set of these cells to be altered, including *MBP*, *PMP2*, *GOS2*, *FABP7*, *OSBPL5*, *CNP*, *APOB* and *MOG*. Numerous Hox genes, which participate in body plan development, showed a differential methylation pattern, in most cases hypomethylation. The *HOXD* cluster, located at chromosome 2q, showed *HOXD1*, *HOXD3*, *HOXD4*, *HOXD8* and *HOXD9* to be clearly hypomethylated in 35 probes (**Fig. 1**). The *HOXA* cluster, located at chromosome 7p, also had this pattern in a total of 27 probes in *HOXA3*, *HOXA4*, and *HOXA6*. In the *HOXB* cluster, at 17q, 15 CpG sites were hypomethylated (including *HOXB1* and *HOXB3*), and 3 were hypermethylated, 2 of them at the *HOXB2* gene. Finally, cluster *HOXC*, at chromosome 12q, had 16 hypomethylated probes, mainly at *HOXC4*. *MEIS1*, *MEIS2*, *PBX1* and *PBX2* (Hox gene cofactors) presented differential methylation patterns in 19, 10, 8 and 2 CpG sites, respectively, most located at the gene body. The *MEIS* cofactors showed hypermethylation while the *PBX* cofactors presented hypomethylation, except in 4 CpG sites of *PBX1*.

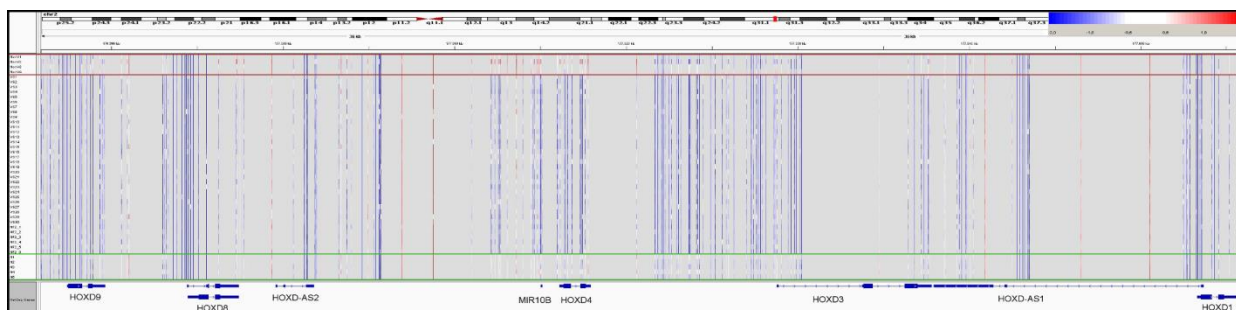


Figure 1. HoxD gene cluster at chromosome 2 shows hypomethylation processes. M-value graphical representation. Blue intensity reflects unmethylation, while red shows methylation. Control nerves are bounded by a green box, while nonvestibular schwannomas are above (red box). Vestibular samples are not highlighted. The miRNA-10b, present at the cluster, also had the same alteration.

A set of genes showed different methylation levels along CpG sites included within the gene, i.e., several CpGs were hypomethylated and others were hypermethylated. This might lead to alternative transcription. In the *MBP* gene, 3 CpG at 5'UTR and TSS sites of isoforms NM_001025100 and NM_001025101 were hypermethylated, while smaller isoforms (NM_001025090, NM_002385, NM_001025092 and NM_001025081) were clearly hypomethylated at 13 CpG sites within regulatory regions (**Fig. 2**). Thus, *MBP* might present

alternative isoform expression. Gene *ZNF238* (ZBTB18) showed hypermethylation in 4 probes in the NM_205768 isoform on the TSS region; while had hypomethylation in other 4 probes at the body gene of this isoform, which coincides with the first exon of isoform NM_006352. Therefore, if a canonical methylation mechanism operated on this gene, the last isoform would have a greater probability of being transcribed.

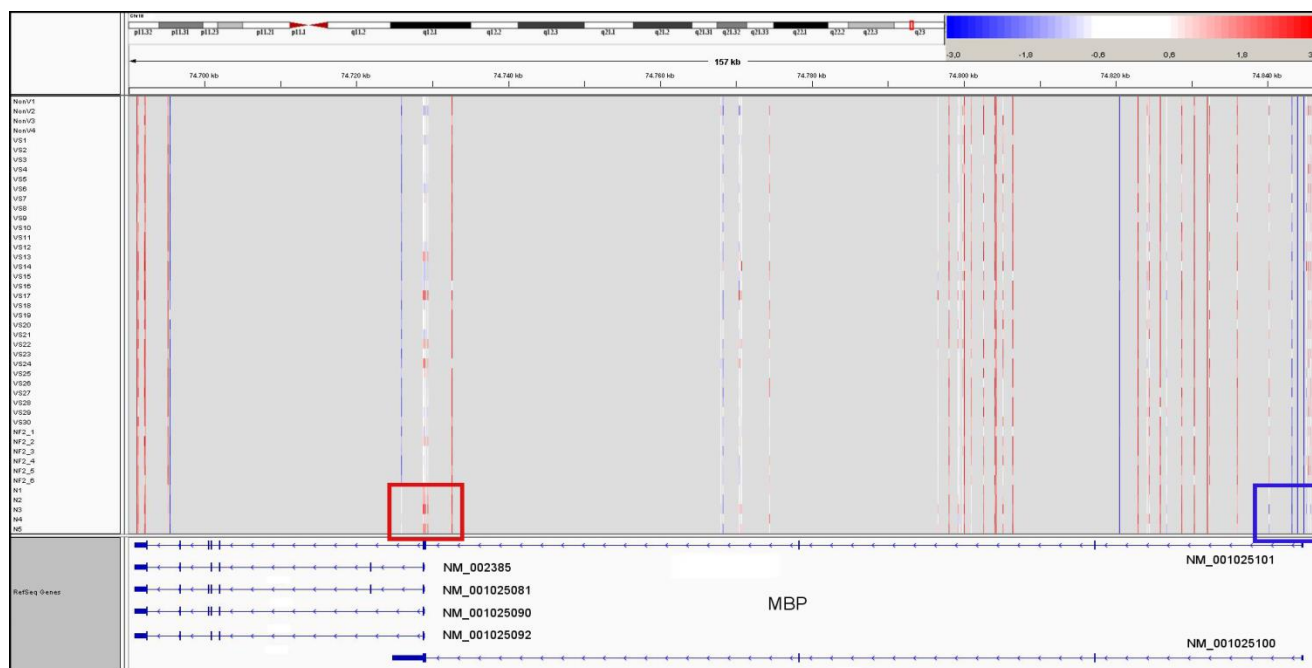


Figure 2. MBP gene methylation pattern. Long isoform promoter regions NM_001025100 and NM_001025101 were hypermethylated in schwannomas at CpG sites (blue box), while short isoforms NM_001025090, NM_002385, NM_001025092 and NM_001025081 were hypomethylated (red box).

The *NF2* gene did not present any differentially methylated probe in either the vestibular or nonvestibular tumors using this microarray.

Comparison of methylation with gene expression patterns

We used our previously published gene expression study of vestibular schwannomas to find altered methylation patterns that coincided with the expected deregulation observed in expression (hypomethylation underexpression or hypomethylation overexpression). In both altered epigenetic patterns, genes with these alterations were more extensive than those with a noncanonical epigenetic expression pattern. Given that the involvement of the gene body and 3'UTR methylation in gene expression is controversial, we only considered TSS1500, TSS200, 5'UTR and 1st exon regions for this purpose. The upregulated and hypomethylated genes included *MET*, *CX3CR1*, *HEPACAM*, *PMP2* and *MERTK*. The downregulated and hypermethylated genes included *CD177*, *MFAP5*, *GOS2*, *AQP9* and *VIT*.

The single CpG site-specific methylation suggested relevant changes related to DNA epigenetic differences within the gene and alternative isoform expression. An example of a gene that could be affected by this mechanism is *NRXN1*. A total of 17 CpGs were differentially methylated in this gene; 10 of them were hypomethylated and 7 were hypermethylated. Through the analysis of expression arrays at the exon level, we previously found an NM_138735 transcript of this gene with no level changes, while NM_004801 was overexpressed. Interestingly, hypomethylation was found in those CpG sites included in NM_004801 at the gene body and hypermethylation in probes also shared with NM_138735, mainly in the regulatory regions. A diagram of this process is shown in **Fig. 3**.

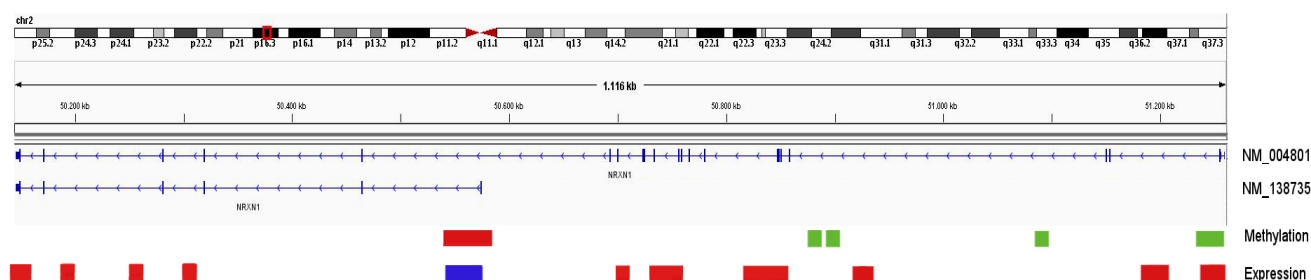


Figure 3. Neurexin-1 might present alternative splicing in schwannomas. Two isoforms of the *NRXN1* gene are shown. Long transcript NM_004801 shows overexpression (in red) and hypomethylation (in green). Transcript NM_138735 shows overexpression in probes shared with the long isoform and no changes in expression in those probes specifically for the short form. Additionally, the methylation pattern is increased in the region belonging to the promoter region of this isoform.

Methylation pattern in miRNAs

A total of 68 CpG sites located at miRNAs were hypomethylated in vestibular schwannomas, some of them with several affected CpG site probes, such as miR-10b and miR-1204. Hypermethylation in miRNAs occurred in 73 CpGs, including miR-596, miR-199a1 and miR-185. The miRNA-548 family was the most deregulated at the methylation level, with 19 probes altered. Of these probes, 11 were hypermethylated, 8 of which corresponded to miR-548f5 and 2 to miR-548n. The miR-548f5 gene also had 2 hypomethylated sites. The miRNA-548h4 displayed one CpG hypomethylated site and another one was hypermethylated. Using our previously published studies on miRNA expression profile in schwannomas, we found that methylation patterns generally corresponded to what was expected (hypermethylation as repressor). Examples of hypomethylation and upregulation include miR-21 (5 probes) and miR-145 (3 probes). Hypermethylation and repression was found in miR-199a1 at 5 probes and miR-185 at 2 probes.

Discrepancies with canonical expectations in methylation and expression

A set of genes presented an expression pattern that was not expected from the results obtained by methylation. An example of this was the *PDGFA* gene, which was hypermethylated in a single CpG at the TSS1500 promoter region and hypomethylated in the gene body, while it was upregulated in tumors. In the case of miR-10b (included in the HOXD cluster), the expected methylation and expression pattern was once again not found. MiRNA-10b presented hypomethylation of 10 CpGs sites, although in the expression study it was found to be clearly downregulated.

DNase hypersensitivity sites within transcriptional start sites and differentially methylated regions

DNase hypersensitivity sites (DHS) have been linked to cis-regulatory elements. We searched our data for DHS included in TSS with distinct methylation patterns between vestibular schwannomas and control nerves. We found 265 CpG sites matching this criterion, including several HOX genes (*HOXB8*, *HOXC8*, *HOXC4* and *HOXC5*), other protein-coding genes (*PDCD1*, *EYA4*, *CAV2*, *MEOX1* and *TFAP2A*) and miRNAs (miR-199a1, miR-196B, miR-219-1, miR-548F5, miR-1914 and miR-145). Differentially methylated regions (DMR), which are CpG sites identified as having distinct patterns among diverse tissues or conditions, were altered in 298 CpG sites, including *TFAP2* and *VAX1* in several probes. Cancer-specific DMRs were present in a total of 313 CpG sites and involved coding-genes such as *BCL2*, *SOX1*, *DLX5*, *EYA4* and a single site in *NOTCH1*. Reprogrammed progress DMRs were the most altered at 776 and included *TFAP2A*, *SOX9* and several HOX genes.

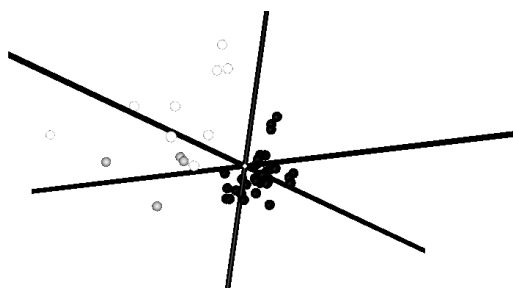


Figure 4. Hox gene expression represented by PCA. All probes available in Gene 1.0ST array at the exon level for Hox genes were used in this data-reduction approach. Control nerves (white dots) and nonvestibular schwannomas (grey) suggest a different pattern of expression than vestibular tumors (black).

Nonvestibular schwannomas

We tested 4 nonvestibular schwannoma cases with Infinium microarrays and established a list of 212 CpG sites that were differentially methylated with respect to the vestibular tumors. Of these 212 CpG sites, 88 corresponded to HOX clusters genes, which are usually hypermethylated in nonvestibular schwannomas. Additionally, *SOX1* was hypomethylated at 3

CpG sites in nonvestibular schwannomas, while *SOX2* (at 7 CpGs) appeared hypermethylated with respect to vestibular tumors. We wanted to know whether the expression patterns of HOX genes were also altered, so we performed an mRNA expression microarray assay for those 4 cases. We found that, in the exon-level expression analysis, PCA of all probes available for HOX genes separated vestibular and nonvestibular schwannomas (**Fig. 4**). Thus, the methylation and expression patterns of HOX and related genes seem to be similar in native nerves and nonvestibular schwannomas and are altered in vestibular tumors.

Clinical and molecular comparisons

We searched for CpG sites with differential methylation between schwannomas by using molecular and clinical data collected from patients at our institution. Sporadic vs. NF2-vestibular schwannomas showed 123 sites with differential methylation, including hypomethylation of *DIP2C*, while *WDR66* and *PTPRN2* were hypermethylated in 2 CpG sites each. By tumor location (side), 1 CpG was detected. By gender, 26 probes were found in autosomes, several of them with very low p-values and high fold-changes, such as gene *TLE1* at 3 CpG sites, which was hypermethylated in females. This suggests that, as previously reported,²⁴ this array might show some degree of gender bias. However, the low number of probes with this problem suggests that it was not an important issue in our data. Other clinical features tested without any probe with aberrant methylation included the schwannoma type (homogeneous, heterogeneous or cystic), tumor size (Koos 1 and 2 vs. Koos 3 and 4), smoking habits, presence of acufene prior to surgery, tumor pressure upon the pons, dizziness before surgery, whether the tumor reached CAI and whether facial conduction after surgery was less or equal at 0.05 mA. Moreover, PCA of all samples showed no apparent association among tumors based on their origin (**Fig. 5**).

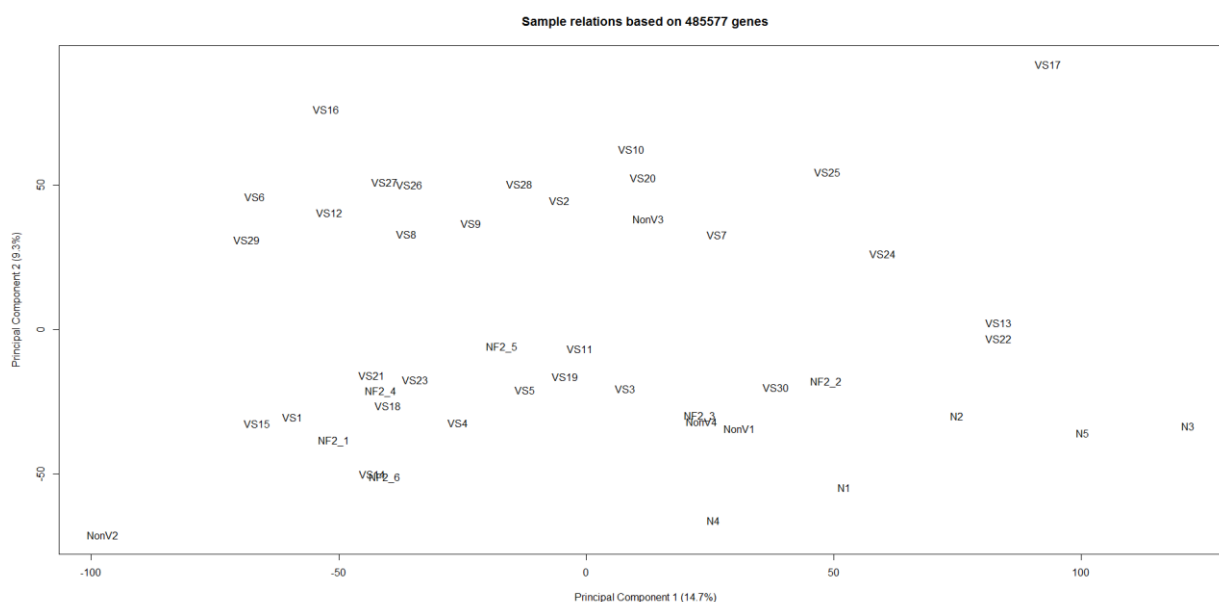


Figure 5. Principal component analysis of samples. Whole CpG sites were used to generate this graphical representation. Control nerves (N) were grouped outside tumors. Neither nonvestibular tumors nor NF2-vestibular schwannomas seemed to present differential behavior in overall CpG representation. Control nerves are grouped in the right corner.

A mutational analysis of *NF2* showed that 55% of samples had sequence alterations, whereas rearrangements detected by MLPA presented in 25% of cases, and LOH at 22q was identified in 62% of the tumors. Overall, 75% of the samples had at least 1 hit detected in the *NF2* gene. Every class was tested: sequence alteration vs. not found; MLPA normal vs. altered, normal constitution at 22q vs. LOH; and samples with no hits in *NF2* vs. at least 1 hit. When this last class comparison was performed, a subset of 32 CpGs displayed alterations. Of these, *MAFK* (at 7p) was hypermethylated at 2 CpG sites in those tumors with no *NF2* alterations. The other classes showed no differences.

Discussion

Schwannomas are benign neoplasms that arise from Schwann cells. Although genetic alterations have been investigated in this neoplasm, few studies are available on the epigenetic changes in schwannomas. In this study, we analyzed the epigenetic signature of individual CpG methylation among 36 vestibular schwannomas, 4 nonvestibular schwannomas and 5 healthy control samples of nerve tissue using microarray technology.

CpG islands, where cytosine is more abundant, showed a lower percentage of change via hypomethylation or aberrant methylation in schwannomas, not reaching 1%. In fact, flanking zones such as CpG shores, shelves and open sea presented increased numbers of changes (in relative levels). Thus, differential methylation levels between schwannomas and controls seem to increase as the distance from CpG islands increases. Non-CpG Island methylation, mainly at shores, has been identified as paramount in the regulation of numerous genes in cell reprogramming,²⁵ in the classification of various tissues²⁶ and in cancer.²⁷ Overall, hypomethylation and hypermethylation levels were similar, with a trend toward hypomethylation as previously described for colon cancer²⁸ but in contraposition for hepatocellular carcinoma, where methylation was clearly biased toward hypomethylation.²⁹ These differences among studies might be due to intrinsic tumor characteristics.

The epigenetics of vestibular schwannomas showed global hypomethylation (with few gene exceptions) of the 4 Hox gene clusters. These genes are involved in morphological changes and animal body plan evolution. Hox aberrant expression in tumoral tissue compared to control tissues³⁰ has been linked to multiples types of cancer such as pancreatic cancer,³¹ hepatocellular carcinoma³² and leukemia.³³ This alteration has also been identified as a prognostic factor in meningiomas³⁴ and thyroid cancer.³⁵ Moreover, the Hox cofactor proteins *MEIS* and *PBX* also experienced DNA methylation variations. Nonvestibular schwannomas displayed a different methylation profile in regard to Hox genes and cofactors, which was more similar to that found in nerves. The PCA of mRNA expression assay also distinguished between those tumors (**Fig. 4**). Nonvestibular schwannomas harbor *BRAF* mutations at a low rate, but this does not occur in vestibular schwannomas,³⁶ suggesting that there might be specific molecular signatures between the 2 neoplasms. Nonetheless, our results show that the methylation pattern of nonvestibular and vestibular schwannomas was very similar in the rest of CpG sites, given that no differences were found when the whole CpG probes were compared by PCA (**Fig. 5**). Overall, our results suggest that Hox genes could play an important role in vestibular schwannomas but do not seem to be involved in nonvestibular tumors, although the low number of cases presented here requires additional experiments in this regard.

Gene expression changes are one of the most studied consequences of CpG methylation. This relationship has been highlighted in tissue specificity,³⁷ differentiation,³⁸ cancer development³⁹ and recurrence.⁴⁰ In our study, the correlations between gene expression and DNA methylation were in general negative, i.e., hypomethylated and overexpressed, although there was a small fraction of genes that exhibited aberrant methylation overexpression or hypomethylation underexpression. This result has also been observed in other studies,⁴¹ suggesting that CpG sites methylation, even at promoter regions (at TSS, 5'UTR and first exon) is important but not decisive in gene expression. Although a single CpG has been shown to be able to produce gene silencing,⁴² we centered our wide-methylation analysis on those genes with more than 1 altered CpG.

PMEPA1 displayed 7 CpG sites to be hypomethylated, all corresponding to promoter regions. With mRNA overexpressed in schwannomas, this gene regulates androgen receptor (AR) levels, which is also downregulated in this neoplasm.⁷ Epigenetic processes in *PMEPA1* regulation have been described in prostate cancer.⁴³ Therefore, *PMEPA1* hypomethylation might lead to its overexpression and, as a consequence, to AR silencing. The effect of AR downregulation in schwannomas is not clear. A possibility might be linked to the interaction with caveolin-1, a gene that is also downregulated in this tumor. *CAV1* has been described as an AR coactivator in prostate cancer cell lines.^{44,45} The caveolin-2 gene, which is involved in caveolae formation with caveolin-1, was hypermethylated in 2 CpG-promoter sites and downregulated in schwannomas.

Another hypomethylated gene was *MET* oncogene, which presented 2 hypomethylated CpG sites at the promoter region and overexpressed mRNA. MET is a tyrosine kinase receptor that controls various functions including proliferation and migration. Phosphoprotein levels of MET have been reported in schwannomas, indicating that it is present in tumors.⁸ *MET* expression linked to promoter epigenetic regulation has been described in other oncogenic processes such as the metastasis of hepatocellular carcinoma.⁴⁶ Plexin B1, a tumor-suppressor protein that inhibits MET in melanoma⁴⁷ through direct association, was hypermethylated at the promoter region in 3 CpG sites.⁴⁸ Thus, *MET* gene mRNA overexpression might occur in schwannomas through epigenetic mechanisms.

Schwannomas showed a set of genes related to myelination processes with altered epigenetic signatures, including *MBP* and *PMP2*. Changes in these genes were also found in an immunohistochemistry study⁴⁹ and expression analysis.⁷ In the latter study, a developmental state between the neural crest and Schwann cell precursor was suggested. Thus, methylation seems to play an important role in processes related to myelin formation in schwannomas, possibly exhibiting epigenetic changes leading to dedifferentiation. Based on our data, the *NF2* gene does not seem to be affected by methylation processes in schwannomas, in agreement with refs. 19 and 20, although methylation in a small subset of samples should not be ruled out.^{17,50} Additionally, the *NF1* gene, which is involved in neurofibromatosis type 1 (NF1) syndrome, contains a small gene within an intron named *EVI2A*. In 2 *EVI2A* CpG sites, hypomethylation was detected. This finding agrees with the overexpression of *EVI2A* found in schwannomas⁷ and with that described in head and neck cancer.⁵¹ Thus, there might be a connection between both neurofibromatosis types (NF1 and NF2) via this gene; however, the mechanism remains elusive.

MiRNAs presented changes in DNA methylation pattern at the promoter and body regions. Numerous epigenetic mechanisms that modify the expression level of these small molecules have been found.¹⁶ Furthermore, miRNAs are epigenetically altered in tumors such as oral cancer,⁵² acute lymphoblastic leukemia,⁵³ colorectal carcinogenesis⁵⁴ and hepatocellular carcinoma.⁵⁵ In our tumor series, miR-21 was hypomethylated in 5 CpG sites, 3 of which corresponded to promoter region. As expected, miR-21 expression level was found to be clearly upregulated, in the same manner as other tumors, such as hepatocellular carcinoma⁵⁶ and gastric cancer.⁵⁷ Conversely, miRNA-199a1 was hypermethylated and downregulated. MiRNA-199a1 targets MET⁵⁸ and thus the downregulation of this miRNA could participate in *MET* overexpression. Additionally, despite having several hypomethylated CpG sites, several miRNAs exhibited downregulation. This process was very pronounced in miR-10b, with 10 CpG sites hypomethylated and with a clear downregulation in schwannomas. Given that 8 of these CpG are located within the *HOXD4* gene, there might be other mechanisms leading to this transcript downregulation. MiRNA hypomethylation and underexpression has also been previously reported,³⁸ suggesting that, although CpG methylation at miRNAs genes usually follows the expected pattern of action, this phenomenon is not completely able to predict the behavior of a particular miRNA.

Currently, body methylation does not have an obvious role in gene expression. Proposed models include a reduction of transcriptional noise,¹³ alternative splicing¹² and even transcription regulation but in a different manner than in promoters, with overexpressed and underexpressed genes having moderate methylation levels.⁵⁹ In our study, we detected various transcripts belonging to the same gene but not showing the same methylation pattern. Thus, we found neurexin-1 with hypomethylation and hypermethylation of distinct transcripts, as confirmed by mRNA expression. This gene, which is able to generate hundreds of alternative transcripts,⁶⁰ is involved in the formation of synapses and in the vascular system.⁶¹ Therefore, based on the specific methylation pattern of various isoforms, the picture of methylation expression in schwannomas significantly increases in complexity, because changes in methylation would not only be limited to changes in the expression of a specific gene but also in a subtle regulation of alternative transcripts.

In agreement with our previous expression analysis, we found no significant differences between vestibular schwannomas regarding clinical or molecular features in an epigenetic context. Nevertheless, a small subset of CpG sites were identified and could be a signature of certain subtypes, such as hypermethylated *MAFK* at 2 CpG sites in vestibular schwannomas with no detected *NF2* hits.

In conclusion, schwannoma CpG site-specific signatures compared to nontumor nerves show a trend toward hypomethylation. CpG islands seem to be less involved in epigenetic changes than shores, shelves and open sea. Furthermore, expression levels were altered in several genes where hypo or hypermethylation was present at the promoter region, including *MET* and *PMEPA1*. Moreover, we have identified a possible mechanism of expression in alternative transcripts in neurexin-1. We also report that *EVI2A* (located at the *NF1* gene intron) might be upregulated in tumors by hypomethylation. Finally, we detected Hox gene cluster global hypomethylation in vestibular schwannoma, but no changes in these genes were found in nonvestibular tumor cases.

Materials and Methods

Samples and DNA/RNA preparation

The study was performed on 40 tumors from 39 patients (16 men and 23 women) who underwent surgery in our institution. The local ethics review board of University Hospital La Paz approved the study protocol according to the principles of the Declaration of Helsinki. All patients received detailed information on the study and provided their written informed consent prior to their inclusion. The study population included 36 cases of vestibular schwannoma, 6 of which were related to NF2 syndrome. Four sporadic nonvestibular schwannomas were also added to the study (3 spinal and 1 cervical). For control purposes, 5 healthy nerves with exclusive axonal content were employed. DNA was isolated using the Wizard Genomic DNA purification kit (Promega). DNA from the corresponding patients' peripheral blood was also extracted. RNA from the 4 nonvestibular schwannomas was isolated using the RNeasy® Mini Kit (Qiagen).

Methylation microarray protocol

For the methylation analysis, 1 µg of DNA from the 40 tumors and 5 healthy nerves was treated with bisulfite using the EZ DNA methylation Kit (Zymo Research), according to the manufacturer's instructions. The converted DNA was then hybridized on the Infinium Human Methylation 450K BeadChip (Illumina), which examines 485 577 CpG sites across the whole genome. Arrays were processed at CEGEN, and the data can be accessed at the GEO database GSE56596.

Infinium Human Methylation 450K BeadChip analysis

The analysis was performed using R statistical software. To import iDAT files into the R environment for processing, a lumi package was used. After importing the iDAT files, we obtained a MethyLumiM class object. First, a background correction was performed with the bgAdjust method, and color bias was adjusted by the quantile method. Color bias adjustment was performed because the differences between the red and green channels were very pronounced (**Fig. S1**). Normalization was performed using simple scaling normalization. M-values were used instead of B-values due to the severe heteroscedasticity of the data when they are not in the middle of the methylation range;⁶² M-values are therefore more statistically valid. After processing the data, the methyAnalysis package was used for data visualization into the Integrative Genomics Viewer (IGV).^{63,64} This task was performed by converting the MethyLumiM class into the MethyGenoSet class. Next, the *export.methyGenoSet* function was used to create a .cgt file. M-values were exported to a text file, and the data was then analyzed with an IMA package.⁶⁵ The necessary p-values were obtained from GenomeStudio. With IMA functions, probes from X and Y chromosomes were removed due to the bias between male and female. In addition, low-quality CpG sites (p-value >.05 in 75% of the samples) were filtered, as were probes containing SNPs. Methylation index calculations were performed at gene-based (TSS, 5'-UTR, first exon, Gene Body and 3'-UTR region) and CpG location-based regions (CpG island, shores and shelves). This process was performed using the *regionswrapper* command, which is explained in ref.27. The specific methylation between groups for each CpG was analyzed using Student's t-test. Differential methylation among the groups was established at the Bonferroni-adjusted p-value <0.05 and an M-value cutoff of 1. This value is within the range recommended by Du et al.⁶² Four

groups of samples were created: sporadic vestibular schwannomas, NF2-related vestibular schwannomas, nonvestibular schwannomas and control nerves. Since both vestibular groups were homogeneous, we combined those 2 groups for comparison against healthy tissue and nonvestibular schwannomas. Additionally, vestibular samples were classified by clinical group. An enrichment analysis of hypermethylated and hypomethylated genes was performed using DAVID⁶⁶ with a single CpG list, removing duplicates and CpG sites with no associated name. In both lists, the total number of genes was below the limit supported by DAVID.

Expression microarrays

In order to investigate whether the methylation pattern had an impact on gene expression, we used our previously published and available gene expression microarray data on the same series of vestibular schwannoma⁷ and miRNAs⁶⁷ to compare with the methylation data. We defined a gene or miRNA as deregulated when we detected at least a 2-fold change in expression and a $p < .05$ cut-off by Student's t-test. For the *regionswrapper* analysis from the IMA package, the genes that met those criteria were selected. MultiExperiment Viewer (MeV) software^{68,69} was employed for the expression array analysis.

The 4 nonvestibular schwannomas that were not included in our previous analysis were tested with microarrays. Briefly, Human Gene 1.0 ST arrays were hybridized as previously described.⁷ Normalization and summarization were performed using the RMA (robust multichip average) algorithm and were batch corrected with the other vestibular tumors using ComBat.⁷⁰ An exon-level analysis, which allowed us to test several isoforms of a given gene, was employed. All statistical analyses were performed using MeV. The principal component analysis (PCA) was performed by eigenvalue decomposition of the 3 principal components for three-dimensional classification of the samples. The data can be accessed at GEO database GSE56597.

Clinical data

The tumor was on the left side in 50% of the cases. Tumor sizes were classified by the KOOS scale as stage 1 (intracanalicular) (1 case), stage 2 (where the largest diameter in the cerebellopontine angle [CPA] is 15 mm) (8 cases), stage 3 (16–30 mm in the CPA) (17 cases) or stage 4 (>30 mm in the CPA) (6 cases). The tumor appearance was homogeneous in 20 patients, heterogeneous in 8 and cystic in 4. The fundus of the IAC was involved in 22 cases but not in 10 cases. All tumor tissues obtained during surgery were fixed in 10% formalin and embedded in paraffin. Staining with hematoxylin-eosin was performed for routine microscopic diagnosis. Antoni type A regions consisted of interwoven bundles of long bipolar spindle cells, whereas Antoni type B regions showed a loose myxoid background containing more stellate tumor cells. The percentage of the different tissue types (A, B, mixed) in each tumor sample was assessed independently by 2 pathologists. The results were grouped into 2 types: type A, >70% of the tumor composed of type A tissue; and type B, <70% of the tumor composed of type A tissue. No clinical data were available from nonvestibular cases.

Mutational screening of NF2 and LOH of chromosome 22q analysis

The *NF2* gene was mutational tested by PCR/dHPLC, as previously reported.⁷ In brief, mutational screening was performed using dHPLC following the manufacturer's instructions

(Transgenomic WAVE® dHPLC Systems). Samples with different patterns by dHPLC were sequenced bidirectionally (ABI 3100-Avant, Applied Biosystems), using the BigDye sequencing kit (Applied Biosystems), to determine the position and nature of the alterations. We also conducted an MLPA analysis with SALSA P044 (MRC-Holland), which is able to detect large gene deletions or amplifications. The LOH analysis was performed using 5 microsatellite markers at 22q11-q12.3.

Acknowledgments

The authors would like to thank Carolina Peña-Granero for her excellent technical assistance. This work was supported by grants PI10/1972 and PI13/00055 from Fondo de Investigaciones Sanitarias, Ministerio de Ciencia e Innovación, Spain; and PI10-045, from the Fundación Sociosanitaria de Castilla-La Mancha, Spain.

References

1. Rey JA, Bello MJ, De Campos JM, Kusak ME, Moreno S. Cytogenetic analysis in human neurinomas. *Cancer Genet Cytogenet* 1987; 28:187–8.
2. Bello MJ, de Campos JM, Kusak ME, Vaquero J, Sarasa JL, Pestaña A, Rey JA. Clonal chromosome aberrations in neurinomas. *Genes Chromosomes Cancer* 1993; 6:206–11.
3. Yi C, Troutman S, Fera D, Stemmer-Rachamimov A, Avila JL, Christian N, Persson NL, Shimono A, Speicher DW, Marmorstein R, et al. A tight junction-associated Merlin-angiomotin complex mediates Merlin's regulation of mitogenic signaling and tumor suppressive functions. *Cancer Cell* 2011; 19:527–40.
4. Li W, You L, Cooper J, Schiavon G, Pepe-Caprio A, Zhou L, Ishii R, Giovannini M, Hanemann CO, Long SB, et al. Merlin/NF2 suppresses tumorigenesis by inhibiting the E3 ubiquitin ligase CRL4(DCAF1) in the nucleus. *Cell* 2010; 140:477–90.
5. Doherty JK, Ongkeko W, Crawley B, Andalibi A, Ryan AF. ErbB and Nrg: potential molecular targets for vestibular schwannoma pharmacotherapy. *Otol Neurotol Off Publ Am Otol Soc Am Neurotol Soc Eur Acad Otol Neurotol* 2008; 29:50–7.
6. Aarhus M, Bruland O, Sætran HA, Mork SJ, Lund-Johansen M, Knappskog PM. Global gene expression profiling and tissue microarray reveal novel candidate genes and down-regulation of the tumor suppressor gene CAV1 in sporadic vestibular schwannomas. *Neurosurgery* 2010; 67:998–1019; discussion 1019.
7. Torres-Martin M, Lassaletta L, San-Roman-Montero J, De Campos JM, Isla A, Gavilan J, Melendez B, Pinto GR, Burbano RR, Castresana JS, et al. Microarray analysis of gene expression in vestibular schwannomas reveals SPP1/MET signaling pathway and androgen receptor deregulation. *Int J Oncol* 2013; 42:848–62.
8. Boin A, Couvelard A, Couderc C, Brito I, Filipescu D, Kalamarides M, Bedossa P, De Koning L, Danelsky C, Dubois T, et al. Proteomic screening identifies a YAP-driven signaling network linked to tumor cell proliferation in human schwannomas. *Neuro-Oncol* 2014;
9. Plotkin SR, Stemmer-Rachamimov AO, Barker FG 2nd, Halpin C, Padera TP, Tyrrell A, Sorensen AG, Jain RK, di Tomaso E. Hearing improvement after bevacizumab in patients with neurofibromatosis type 2. *N Engl J Med* 2009; 361:358–67.
10. Plotkin SR, Halpin C, McKenna MJ, Loeffler JS, Batchelor TT, Barker FG 2nd. Erlotinib for progressive vestibular schwannoma in neurofibromatosis 2 patients. *Otol Neurotol Off Publ Am Otol Soc Am Neurotol Soc Eur Acad Otol Neurotol* 2010; 31:1135–43.

11. Karajannis MA, Legault G, Hagiwara M, Giancotti FG, Filatov A, Derman A, Hochman T, Goldberg JD, Vega E, Wisoff JH, et al. Phase II study of everolimus in children and adults with neurofibromatosis type 2 and progressive vestibular schwannomas. *Neuro-Oncol* 2014; 16:292–7.
12. Maunakea AK, Nagarajan RP, Bilenky M, Ballinger TJ, D'Souza C, Fouse SD, Johnson BE, Hong C, Nielsen C, Zhao Y, et al. Conserved role of intragenic DNA methylation in regulating alternative promoters. *Nature* 2010; 466:253–7.
13. Huh I, Zeng J, Park T, Yi SV. DNA methylation and transcriptional noise. *Epigenetics Chromatin* 2013; 6:9.
14. Portela A, Esteller M. Epigenetic modifications and human disease. *Nat Biotechnol* 2010; 28:1057–68.
15. Esteller M, Garcia-Foncillas J, Andion E, Goodman SN, Hidalgo OF, Vanaclocha V, Baylin SB, Herman JG. Inactivation of the DNA-repair gene MGMT and the clinical response of gliomas to alkylating agents. *N Engl J Med* 2000; 343:1350–4.
16. Lopez-Serra P, Esteller M. DNA methylation-associated silencing of tumor-suppressor microRNAs in cancer. *Oncogene* 2012; 31:1609–22.
17. Gonzalez-Gomez P, Bello MJ, Alonso ME, Lomas J, Arjona D, Campos JM de, Vaquero J, Isla A, Lassaletta L, Gutierrez M, et al. CpG island methylation in sporadic and neurofibromatosis type 2-associated schwannomas. *Clin Cancer Res Off J Am Assoc Cancer Res* 2003; 9:5601–6.
18. Bello MJ, Martinez-Glez V, Franco-Hernandez C, Pefla-Granero C, de Campos JM, Isla A, Lassaletta L, Vaquero J, Rey JA. DNA methylation pattern in 16 tumor-related genes in schwannomas. *Cancer Genet Cytogenet* 2007; 172:84–6.
19. Koutsimpelas D, Ruerup G, Mann WJ, Brieger J. Lack of neurofibromatosis type 2 gene promoter methylation in sporadic vestibular schwannomas. *ORL J Oto-Rhino-Laryngol Its Relat Spec* 2012; 74:33–7.
20. Lee JD, Kwon TJ, Kim U-K, Lee W-S. Genetic and epigenetic alterations of the NF2 gene in sporadic vestibular schwannomas. *PLoS One* 2012; 7:e30418.
21. Kino T, Takeshima H, Nakao M, Nishi T, Yamamoto K, Kimura T, Saito Y, Kochi M, Kuratsu J, Saya H, et al. Identification of the cis-acting region in the NF2 gene promoter as a potential target for mutation and methylation-dependent silencing in schwannoma. *Genes Cells Devoted Mol Cell Mech* 2001; 6:441–54.
22. Mur P, Mollejo M, Ruano Y, de Lope AR, Fiaño C, García JF, Castresana JS, Hernández-Laín A, Rey JA, Meléndez B. Codeletion of 1p and 19q determines distinct gene methylation and expression profiles in IDH-mutated oligodendroglial tumors. *Acta Neuropathol (Berl)* 2013; 126:277–89.
23. Mack SC, Witt H, Piro RM, Gu L, Zuyderduyn S, Stütz AM, Wang X, Gallo M, Garzia L, Zayne K, et al. Epigenomic alterations define lethal CIMP-positive ependymomas of infancy. *Nature* 2014; 506:445–50.
24. Chen Y, Lemire M, Choufani S, Butcher DT, Grafodatskaya D, Zanke BW, Gallinger S, Hudson TJ, Weksberg R. Discovery of cross-reactive probes and polymorphic CpGs in the Illumina Infinium HumanMethylation450 microarray. *Epigenetics Off J DNA Methylation Soc* 2013; 8:203–9.
25. Doi A, Park I-H, Wen B, Murakami P, Aryee MJ, Irizarry R, Herb B, Ladd-Acosta C, Rho J, Loewer S, et al. Differential methylation of tissue- and cancer-specific CpG island shores distinguishes human induced pluripotent stem cells, embryonic stem cells and fibroblasts. *Nat Genet* 2009; 41:1350–3.
26. Kozlenkov A, Roussos P, Timashpolsky A, Barbu M, Rudchenko S, Bibikova M, Klotzle B, Byne W, Lyddon R, Di Narzo AF, et al. Differences in DNA methylation between human neuronal and glial cells are concentrated in enhancers and non-CpG sites. *Nucleic Acids Res* 2014; 42:109–27.
27. Rao X, Evans J, Chae H, Pilrose J, Kim S, Yan P, Huang R-L, Lai H-C, Lin H, Liu Y, et al. CpG island shore methylation regulates caveolin-1 expression in breast cancer. *Oncogene* 2013; 32:4519–28.
28. Irizarry RA, Ladd-Acosta C, Wen B, Wu Z, Montano C, Onyango P, Cui H, Gabo K, Rongione M, Webster M, et al. The human colon cancer methylome shows similar hypo- and hypermethylation at conserved tissue-specific CpG island shores. *Nat Genet* 2009; 41:178–86.

29. Shen J, Wang S, Zhang Y-J, Wu H-C, Kibriya MG, Jasmine F, Ahsan H, Wu DPH, Siegel AB, Remotti H, et al. Exploring genome-wide DNA methylation profiles altered in hepatocellular carcinoma using Infinium HumanMethylation 450 BeadChips. *Epigenetics Off J DNA Methylation Soc* 2013; 8:34–43.
30. Abate-Shen C. Deregulated homeobox gene expression in cancer: cause or consequence? *Nat Rev Cancer* 2002; 2:777–85.
31. Cantile M, Franco R, Tschan A, Baumhoer D, Zlobec I, Schiavo G, Forte I, Bihl M, Liguori G, Botti G, et al. HOX D13 expression across 79 tumor tissue types. *Int J Cancer J Int Cancer* 2009; 125:1532–41.
32. Cillo C, Schiavo G, Cantile M, Bihl MP, Sorrentino P, Carafa V, D' Armiento M, Roncalli M, Sansano S, Vecchione R, et al. The HOX gene network in hepatocellular carcinoma. *Int J Cancer J Int Cancer* 2011; 129:2577–87.
33. Argiropoulos B, Humphries RK. Hox genes in hematopoiesis and leukemogenesis. *Oncogene* 2007; 26:6766–76.
34. Di Vinci A, Brigati C, Casciano I, Banelli B, Borzì L, Forlani A, Ravetti GL, Allemanni G, Melloni I, Zona G, et al. HOXA7, 9, and 10 are methylation targets associated with aggressive behavior in meningiomas. *Transl Res J Lab Clin Med* 2012; 160:355–62.
35. Cantile M, Scognamiglio G, La Sala L, La Mantia E, Scaramuzza V, Valentino E, Tatangelo F, Losito S, Pezzullo L, Chiofalo MG, et al. Aberrant expression of posterior HOX genes in well differentiated histotypes of thyroid cancers. *Int J Mol Sci* 2013; 14:21727–40.
36. De Vries M, Bruijn IB, Cleton-Jansen A-M, Malessy MJA, van der Mey AGL, Hogendoorn PCW. Mutations affecting BRAF, EGFR, PIK3CA, and KRAS are not associated with sporadic vestibular schwannomas. *Virchows Arch Int J Pathol* 2013; 462:211–7.
37. Lohk K, Modhukur V, Rajashekar B, Märtens K, Mägi R, Kolde R, Kolt Ina M, Nilsson TK, Vilo J, Salumets A, et al. DNA methylome profiling of human tissues identifies global and tissue-specific methylation patterns. *Genome Biol* 2014; 15:R54.
38. Liu Z, Jiang R, Yuan S, Wang N, Feng Y, Hu G, Zhu X, Huang K, Ma J, Xu G, et al. Integrated Analysis of DNA Methylation and RNA Transcriptome during In Vitro Differentiation of Human Pluripotent Stem Cells into Retinal Pigment Epithelial Cells. *PloS One* 2014; 9:e91416.
39. Dammann R, Li C, Yoon JH, Chin PL, Bates S, Pfeifer GP. Epigenetic inactivation of a RAS association domain family protein from the lung tumour suppressor locus 3p21.3. *Nat Genet* 2000; 25:315–9.
40. Tsunedomi R, Iizuka N, Yoshimura K, Iida M, Tsutsui M, Hashimoto N, Kanekiyo S, Sakamoto K, Tamesa T, Oka M. ABCB6 mRNA and DNA methylation levels serve as useful biomarkers for prediction of early intrahepatic recurrence of hepatitis C virus-related hepatocellular carcinoma. *Int J Oncol* 2013; 42:1551–9.
41. Dayeh T, Volkov P, Salö S, Hall E, Nilsson E, Olsson AH, Kirkpatrick CL, Wollheim CB, Eliasson L, Rönn T, et al. Genome-wide DNA methylation analysis of human pancreatic islets from type 2 diabetic and non-diabetic donors identifies candidate genes that influence insulin secretion. *PLoS Genet* 2014; 10:e1004160.
42. Zhang X, Wu M, Xiao H, Lee M-T, Levin L, Leung Y-K, Ho S-M. Methylation of a single intronic CpG mediates expression silencing of the PMP24 gene in prostate cancer. *The Prostate* 2010; 70:765–76.
43. Richter E, Masuda K, Cook C, Ehrich M, Tadese AY, Li H, Owusu A, Srivastava S, Dobi A. A role for DNA methylation in regulating the growth suppressor PMEPA1 gene in prostate cancer. *Epigenetics Off J DNA Methylation Soc* 2007; 2:100–9.
44. Bennett NC, Hooper JD, Johnson DW, Gobe GC. Expression profiles and functional associations of endogenous androgen receptor and caveolin-1 in prostate cancer cell lines. *The Prostate* 2014; 74:478–87.
45. Wu D, Terrian DM. Regulation of caveolin-1 expression and secretion by a protein kinase cepsilon signaling pathway in human prostate cancer cells. *J Biol Chem* 2002; 277:40449–55.

46. Ogunwobi OO, Puszyk W, Dong H-J, Liu C. Epigenetic upregulation of HGF and c-Met drives metastasis in hepatocellular carcinoma. *PLoS One* 2013; 8:e63765.
47. Stevens L, McClelland L, Fricke A, Williamson M, Kuo I, Scott G. Plexin B1 suppresses c-Met in melanoma: a role for plexin B1 as a tumor-suppressor protein through regulation of c-Met. *J Invest Dermatol* 2010; 130:1636–45.
48. Soong J, Scott G. Plexin B1 inhibits MET through direct association and regulates Shp2 expression in melanocytes. *J Cell Sci* 2013; 126:688–95.
49. Hung G, Colton J, Fisher L, Oppenheimer M, Faudoa R, Slattery W, Linthicum F. Immunohistochemistry study of human vestibular nerve schwannoma differentiation. *Glia* 2002; 38:363–70.
50. Kullar PJ, Pearson DM, Malley DS, Collins VP, Ichimura K. CpG island hypermethylation of the neurofibromatosis type 2 (NF2) gene is rare in sporadic vestibular schwannomas. *Neuropathol Appl Neurobiol* 2010; 36:505–14.
51. Poage GM, Houseman EA, Christensen BC, Butler RA, Avissar-Whiting M, McClean MD, Waterboer T, Pawlita M, Marsit CJ, Kelsey KT. Global hypomethylation identifies loci targeted for hypermethylation in head and neck cancer. *Clin Cancer Res Off J Am Assoc Cancer Res* 2011; 17:3579–89.
52. Kozaki K, Imoto I, Mogi S, Omura K, Inazawa J. Exploration of tumor-suppressive microRNAs silenced by DNA hypermethylation in oral cancer. *Cancer Res* 2008; 68:2094–105.
53. Agirre X, Vilas-Zornoza A, Jiménez-Velasco A, Martín-Subero JI, Cordeu L, Gárate L, San José-Eneriz E, Abizanda G, Rodríguez-Otero P, Fortes P, et al. Epigenetic silencing of the tumor suppressor microRNA Hsa-miR-124a regulates CDK6 expression and confers a poor prognosis in acute lymphoblastic leukemia. *Cancer Res* 2009; 69:4443–53.
54. Balaguer F, Link A, Lozano JJ, Cuatrecasas M, Nagasaka T, Boland CR, Goel A. Epigenetic silencing of miR-137 is an early event in colorectal carcinogenesis. *Cancer Res* 2010; 70:6609–18.
55. Furuta M, Kozaki K, Tanaka S, Arai S, Imoto I, Inazawa J. miR-124 and miR-203 are epigenetically silenced tumor-suppressive microRNAs in hepatocellular carcinoma. *Carcinogenesis* 2010; 31:766–76.
56. Xu G, Zhang Y, Wei J, Jia W, Ge Z, Zhang Z, Liu X. MicroRNA-21 promotes hepatocellular carcinoma HepG2 cell proliferation through repression of mitogen-activated protein kinase-kinase 3. *BMC Cancer* 2013; 13:469.
57. Zhang BG, Li JF, Yu BQ, Zhu ZG, Liu BY, Yan M. microRNA-21 promotes tumor proliferation and invasion in gastric cancer by targeting PTEN. *Oncol Rep* 2012; 27:1019–26.
58. Kim S, Lee UJ, Kim MN, Lee E-J, Kim JY, Lee MY, Choung S, Kim YJ, Choi Y-C. MicroRNA miR-199a* regulates the MET proto-oncogene and the downstream extracellular signal-regulated kinase 2 (ERK2). *J Biol Chem* 2008; 283:18158–66.
59. Su J, Wang Y, Xing X, Liu J, Zhang Y. Genome-wide analysis of DNA methylation in bovine placentas. *BMC Genomics* 2014; 15:12.
60. Ushkaryov YA, Petrenko AG, Geppert M, Südhof TC. Neurexins: synaptic cell surface proteins related to the alpha-latrotoxin receptor and laminin. *Science* 1992; 257:50–6.
61. Melani M, Weinstein BM. Common factors regulating patterning of the nervous and vascular systems. *Annu Rev Cell Dev Biol* 2010; 26:639–65.
62. Du P, Zhang X, Huang C-C, Jafari N, Kibbe WA, Hou L, Lin SM. Comparison of Beta-value and M-value methods for quantifying methylation levels by microarray analysis. *BMC Bioinformatics* 2010; 11:587.
63. Thorvaldsdóttir H, Robinson JT, Mesirov JP. Integrative Genomics Viewer (IGV): high-performance genomics data visualization and exploration. *Brief Bioinform* 2013; 14:178–92.
64. Robinson JT, Thorvaldsdóttir H, Winckler W, Guttman M, Lander ES, Getz G, Mesirov JP. Integrative genomics viewer. *Nat Biotechnol* 2011; 29:24–6.

65. Wang D, Yan L, Hu Q, Sucheston LE, Higgins MJ, Ambrosone CB, Johnson CS, Smiraglia DJ, Liu S. IMA: an R package for high-throughput analysis of Illumina's 450K Infinium methylation data. *Bioinforma Oxf Engl* 2012; 28:729–30.
66. Huang DW, Sherman BT, Lempicki RA. Systematic and integrative analysis of large gene lists using DAVID bioinformatics resources. *Nat Protoc* 2009; 4:44–57.
67. Torres-Martin M, Lassaletta L, de Campos JM, Isla A, Gavilan J, Pinto GR, Burbano RR, Latif F, Melendez B, Castresana JS, et al. Global profiling in vestibular schwannomas shows critical deregulation of microRNAs and upregulation in those included in chromosomal region 14q32. *PLoS One* 2013; 8:e65868.
68. Saeed AI, Sharov V, White J, Li J, Liang W, Bhagabati N, Braisted J, Klapa M, Currier T, Thiagarajan M, et al. TM4: a free, open-source system for microarray data management and analysis. *BioTechniques* 2003; 34:374–8.
69. Saeed AI, Bhagabati NK, Braisted JC, Liang W, Sharov V, Howe EA, Li J, Thiagarajan M, White JA, Quackenbush J. TM4 microarray software suite. *Methods Enzymol* 2006; 411:134–93.
70. Johnson WE, Li C, Rabinovic A. Adjusting batch effects in microarray expression data using empirical Bayes methods. *Biostat Oxf Engl* 2007; 8:118–27.

Supplementary Figure

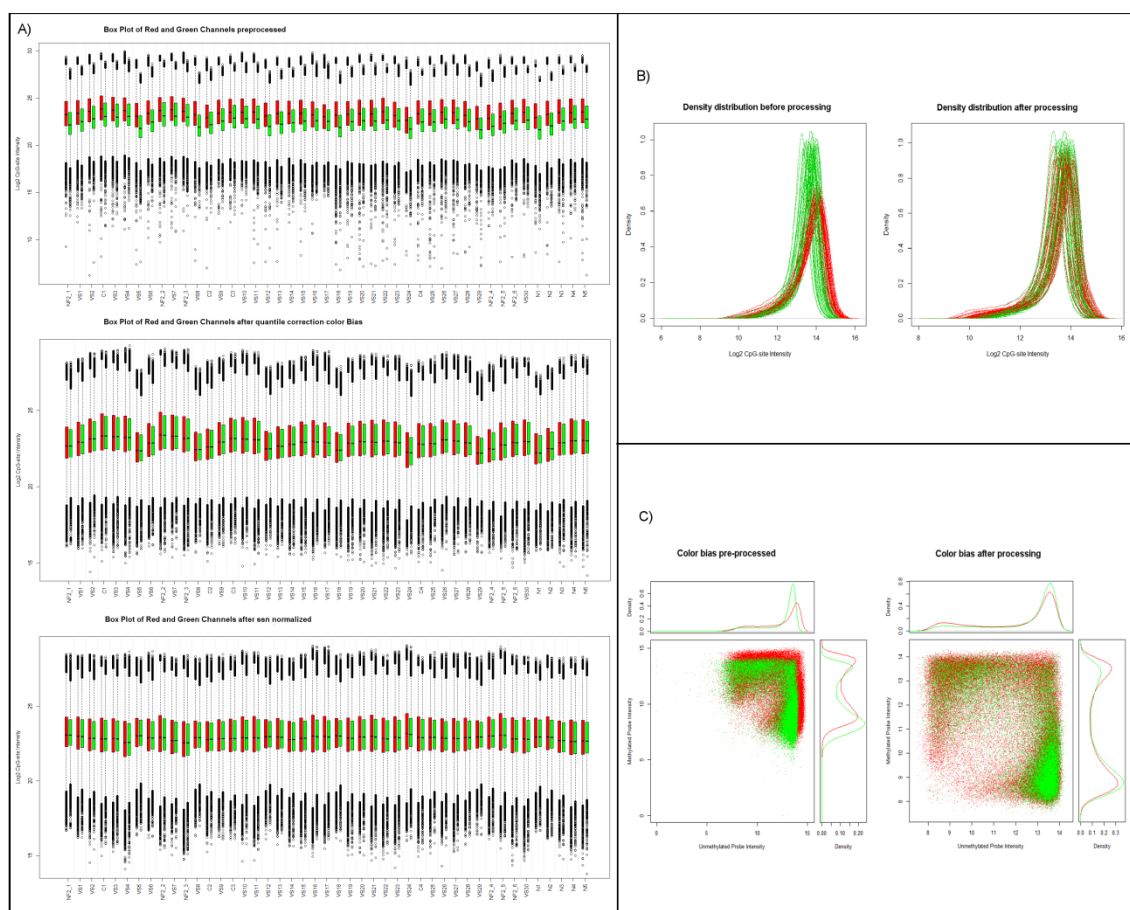


Figure S1. Color bias correction. A) Color bias was very pronounced in each probe. After quantile correction, this effect disappeared, but there were differences among samples. With ssn normalization, the samples shared similar intensities. B) Density distribution of the red channel was lower than that of the green channel, an effect that was corrected after color bias correction and normalization. C) Methylated and unmethylated probe intensities in sample NF2_1 show significant bias, corrected after color and ssn normalization.

Tables

Chromosome	Total Probes	Hypermethylation (%)	Hypomethylation (%)
1	35994	654 (1.82)	838 (2.33)
2	26725	546 (2.04)	764 (2.86)
3	19584	344 (1.76)	476 (2.43)
4	15512	238 (1.53)	336 (2.17)
5	18750	372 (1.98)	449 (2.39)
6	26873	527 (1.96)	596 (2.22)
7	22626	376 (1.66)	543 (2.40)
8	15890	358 (2.25)	388 (2.44)
9	7596	119 (1.57)	152 (2.00)
10	18503	358 (1.93)	509 (2.75)
11	22226	401 (1.80)	537 (2.42)
12	18943	284 (1.50)	484 (2.56)
13	9310	243 (2.61)	283 (3.04)
14	11453	171 (1.49)	251 (2.19)
15	11740	200 (1.70)	291 (2.48)
16	16691	353 (2.11)	327 (1.96)
17	21548	459 (2.13)	505 (2.34)
18	4531	64 (1.41)	95 (2.10)
19	19721	236 (1.20)	218 (1.11)
20	7811	105 (1.34)	114 (1.46)
21	3168	60 (1.89)	89 (2.81)
22	6579	85 (1.29)	62 (0.94)

Table 1. Chromosome Methylation Pattern in Vestibular Schwannomas. Hypermethylation and hypomethylation were calculated using the Bonferroni-adjusted p-value <.05 and an M-value cutoff of 1.

Region	CpG sites	Hypermethylation (%)	Hypomethylation (%)
TSS1500	63514	723 (1.14)	755 (1.19)
TSS200	45956	297 (0.65)	330 (0.72)
5'UTR	48878	606 (1.24)	935 (1.91)
First Exon	28955	207 (0.71)	232 (0.80)
Gene Body	131532	2948 (2.24)	3842 (2.92)
3'UTR	14438	294 (2.04)	508 (3.52)
Island	112398	788 (0.70)	665 (0.59)
N_Shore	47915	926 (1.93)	865 (1.81)
S_Shore	37332	651 (1.74)	656 (1.76)
N_Shelf	18342	409 (2.23)	539 (2.94)
S_Shelf	16357	338 (2.07)	474 (2.90)
Open sea	129495	3442 (2.66)	5109 (3.95)

Table 2. Probes organized by location of a particular CpG site. Hypermethylation and hypomethylation were calculated using a Bonferroni-adjusted p-value <0.05 and an M-value cutoff of 1.

3.6 ARTÍCULO 6 (En revisión)

TÍTULO: Global expression profile in low grade meningiomas and schwannomas shows up-regulation of PDGFD, CDH1 and SLIT2 in both tumors with respect to their healthy tissue.

AUTORES: **Miguel Torres-Martín**, Luis Lassaletta, Alberto Isla, Jose M de Campos, Giovanni R. Pinto, Rommel R. Burbano, Javier S. Castresana, Bárbara Meléndez y Juan A. Rey.

RESUMEN: Los schwannomas y los meningiomas comparten molecularmente la mutación del gen *NF2* y la LOH del cromosoma 22. Además, aparecen habitualmente en la *NF2*. Actualmente no hay medicación quimioterapéutica disponible para los pacientes que sufren de ambas neoplasias, cuya opción de tratamiento normalmente consiste en la resección quirúrgica. Por lo tanto, la búsqueda de elementos genéticos comunes en meningiomas y schwannomas resulta de vital interés con el objetivo de lograr un tratamiento común a ambas neoplasias. En este estudio, identificamos numerosos genes desregulados con el mismo patrón de expresión en schwannomas y meningiomas, es decir, con la misma desregulación entre cada tumor y su tejido control correspondiente, además de presentar un nivel similar entre los dos tipos tumorales. Entre los genes

sobreexpresados en ambos tumores, se incluyen *PDGFD*, *CDH1* y *SLIT2*. Estos y otros genes encontrados, podrían ser diana de tratamientos comunes para pacientes de NF2.

METODOLOGÍA

- Se estudiaron 22 meningiomas (20 de grado I y 2 de grado II), 3 muestras de meninge sana y los casos del Artículo 3 (31 schwannomas vestibulares y 9 muestras como control).
- Para la extracción de ARN se utilizó el Rneasy® Mini Kit de Qiagen, que purifica los ARNs de más de 200 bases.
- El ARN fue hibridado en los microarrays de Affymetrix Human Gene 1.0 ST. La normalización y sumarización de los mismos se realizó mediante el algoritmo Robust Multichip Average (RMA). Al permitir estos microarrays hacer análisis a nivel de gen y a nivel de exones, ambos fueron usados. La corrección de lote se hizo mediante el paquete ComBat del programa estadístico R. Los análisis estadísticos se realizaron con el programa MultiExperiment Viewer. El umbral para considerar un gen desregulado fue del doble o la mitad de cambio entre tumor y control, además de un p-valor ≤ 0.05 (t-test).
- Para verificar nuestros datos en meningiomas y sus correspondientes controles sanos, utilizamos otra serie de un estudio realizado por otro grupo (Tabernero *et al*, 2009) y libremente accesible en la base de datos del GEO: GSE43290.

Global expression profile in low grade meningiomas and schwannomas shows up-regulation of PDGFD, CDH1 and SLIT2 in both tumors with respect to their healthy tissue.

MIGUEL TORRES-MARTIN¹, LUIS LASSALETTA², ALBERTO ISLA³, JOSE M DE CAMPOS⁴, GIOVANNY R. PINTO⁵, ROMMEL R. BURBANO⁶, JAVIER S. CASTRESANA⁷, BARBARA MELENDEZ⁸ and JUAN A. REY¹

¹Molecular Neuro-oncogenetics Laboratory, Research Unit-Unidad de Investigación. IdiPAZ, Hospital Universitario La Paz. Madrid, Spain; ²Department of Otolaryngology, Hospital Universitario La Paz., IdiPAZ, Madrid, Spain; ³Neurosurgery Department. Hospital Universitario La Paz, IdiPAZ, Madrid, Spain; ⁴Neurosurgery Department. Fundacion Jimenez Diaz, Madrid, Spain; ⁵Genetics and Molecular Biology Laboratory, Federal University of Piau, Parnaiba, Brazil; ⁶Human Cytogenetics Laboratory. Institute of Biological Sciences, Federal University of Para, Belem, Brazil; ⁷Department of Biochemistry and Genetics, University of Navarra School of Sciences, Pamplona, Spain; ⁸Molecular Pathology Research Unit, Virgen de la Salud Hospital, Toledo, Spain

Correspondence to: Juan A. Rey, and Miguel Torres-Martin ¹Molecular Neuro-oncogenetics Laboratory, Research Unit-Unidad de Investigación. Hospital Universitario La Paz. Paseo de la Castellana 261, 28046, Madrid, IdiPAZ, Spain

E-mail: jreyh@salud.madrid.org

Email: migtorres.martin@gmail.com

Abstract. Schwannomas and grade I meningiomas are non-metastatic neoplasms that shares the common mutation of gene NF2. They usually appear in Neurofibromatosis type 2 patients. Currently, there is no drug treatment available for both tumors, so the use of wide expression technologies is crucial to find those therapeutic targets. Affymetrix Human Gene 1.0 ST was used to test global gene expression in 22 meningiomas, 31 schwannomas and, as non-tumoral controls, 3 healthy meningeal tissues, 8 non-tumoral nerves and 1 primary Schwann cells culture. A non-stringent p-cutoff and fold change were used to establish deregulated genes. We found a subset of genes that were upregulated in meningiomas and schwannomas when compared to their respectively healthy tissue, including *PDGFD*, *CDH1* and *SLIT2*. Thus, those genes could be more thoroughly studied as targets in a possible combined treatment.

Keywords: Schwannoma, meningioma, microarray, comparative gene expression, *NF2*, Neurofibromatosis 2.

Introduction

Schwannomas are benign tumors that arise from Schwann cells. They typically appear in the vestibulocochlear nerve and are considered to be grade I tumors; approximately 95% of them are unilateral and present sporadically, whereas 5% are associated with neurofibromatosis type 2 syndrome (NF2). Patients with NF2 present bilateral schwannomas and other tumors, frequently meningiomas, which originate from the arachnoid cells, and account for 20% of all primary intracranial tumors. The current classification of meningiomas by the World Health Organization (WHO) includes three grades: 90% are classified as grade I tumors; approximately 8%-9% are atypical grade II tumors; and 1%-2% are anaplastic/malignant grade III tumors (1). Meningiomas have a recurrence rate of 18%, 40% and 80% for grade I, II and III, respectively.

Preliminary cytogenetic studies demonstrated the absence of one chromosome 22 in both neoplasms (2,3), thus suggesting a common genetic origin for at least some subgroups of these neurogenic tumors. Subsequently, *NF2* gene (located at 22q12.2) inactivation was found to be due to several mechanisms, such as mutations or allelic loss due to monosomy or deletion of chromosome 22, accounting for up to 66% in schwannomas (4) and 18%-50% in sporadic meningiomas, depending on the histopathological subtypes (5).

In addition to the characteristic chromosome 22 loss, secondary alterations such as 1p deletions have been described in both tumor types, and these alterations appeared to be related to tumor progression in meningiomas (6-8). Although DNA methylation studies on these neurogenic tumors demonstrated the non-random involvement of this mechanism in the inactivation of some tumor-related genes (9-11), controversial data are available on the epigenetic (through CpG island aberrant methylation) *NF2* inactivation in both neoplasms (12-16). Indeed, recent studies on genome-wide methylation suggest that this mechanism is associated with malignant transformation in meningiomas, and allow for the epigenetic sub-classification of this tumor (17-18).

Global exome sequencing in meningiomas showed that, in grade I tumors, *NF2* gene alteration (by mutation and/or loss of chromosome 22) is mutually exclusive with other gene mutations such as *AKT1*, *TRAF7*, *KLF4* and *SMO* (19), but not with others such as *NF1* and *NEGR1* (20). In schwannomas no alternative to mutation has been found for those samples lacking hits over *NF2* and, however, Merlin (the *NF2* protein) does not seem to be present in the cases so far analyzed (21).

The expression analysis of tumor-related genes in meningiomas and schwannomas suggested a possible molecular subgroup classification in both tumors (22) with the involvement of differential regulatory pathways (23,24) related to the allelic losses at 1p and 14q in meningiomas (25). Whole genome expression analysis has been performed on schwannomas (26-28) and meningiomas (29-32). Whereas meningiomas have shown differential expression patterns based on progression and recurrence, but not strictly supported by grade (31), in schwannomas no distinctive pattern has been found using clinical correlations (28). However, a critical deregulation of microRNAs, including the up-regulation of those located at the 14q32 chromosomal region, was a characteristic feature of the vestibular tumors (33).

Intracranial non-recurrent WHO grade I meningiomas and schwannomas represent similar problems for patients, depending on the brain structures affected by their non-invasive growth. Currently, treatment options for patients with grade I meningiomas or schwannomas are surgery resection, radio-surgery and a "wait and see" strategy. Thus, there is no available chemotherapeutic treatment for these tumors besides surgery, a situation especially traumatic for patients suffering bilateral vestibular schwannomas and several meningiomas such as those affected by *NF2*. Due to the common genetic origin of these tumors (*NF2* inactivation), previous studies tried to find targets to inhibit both schwannoma and meningioma progression.

AR42, a histone deacetylase inhibitor, represses the proliferation of meningioma and schwannoma cell lines *in vitro* (34), and the same effect was shown by cucurbitacin D and goyazensolide in primary cultures (35).

In this study, we used microarray technology to compare gene expression patterns and identify genes and pathways of potential interest as key targets for the combined treatment of vestibular schwannomas and grade I meningiomas.

Materials and methods

Ethical statement and samples. The local Ethics Review Board of La Paz University Hospital approved the study protocol according to the principles of the Declaration of Helsinki. All patients received detailed information about the study and provided their written informed consent prior to their inclusion. In this study, we used RNA from 22 meningiomas, 31 schwannomas and, as non-tumoral controls, 3 healthy meningeal tissues, 8 non-tumoral nerves and 1 primary Schwann cell culture. The three control non-tumoral meningeal RNAs derived from two healthy males and one female and were purchased from BioChain® (Catalog No. R1234043-10-D03 Lot No. B108134, A602330 and B501146).

RNA extraction and microarray experiments. The RNA was extracted with the RNeasy® Mini Kit (Qiagen) as indicated previously (28). For global gene expression, the Affymetrix Human Gene 1.0 ST was used. The expression profile of the meningiomas and the meninges samples can be accessed at the Gene Expression Omnibus (GEO) database GSE54934. The arrays of schwannomas and control nerves were previously published (28) and are available at the GEO database GSE39645. The arrays were processed at IRB Barcelona.

Statistical analysis. The normalization and summarization were performed using the Robust Multichip Average (RMA). In order to reduce the batch effect among tumors (schwannomas and meningiomas) and controls (healthy nerves and meninges), a critical aspect for our analysis, we used ComBat (36). For data analysis, the genes were considered deregulated between groups when at least a 2-fold change of expression and a $p < 0.05$ cut-off (ANOVA) was identified, as previously recommended by the MAQC consortium (37). For the comparison between schwannomas and meningiomas in order to obtain a list of genes with no changes among both tumor types, we used a more restrictive fold (< 1.5) exclusively for this purpose, because the ComBat effect could have lowered these values and false positives could appear. For comparative

purposes, a list of differential expressed genes and fold-change was obtained with the GEO2R web tool (<http://www.ncbi.nlm.nih.gov/geo/geo2r/>) in the series GSE43290, which includes 4 meninges as controls and 47 tumors (29). As our meningioma series mainly included grade I tumors, only the 33 WHO grade I meningiomas and the four controls included in this report were used for comparison.

DNA extraction. The DNA was extracted by standard methods, as previously described (22). The data regarding the *NF2* status, including Loss of Heterozygosity of 22q (LOH), Multiplex Ligation-dependent Probe Amplification (MLPA) of *NF2* (SALSA P044) and sequence analysis by dHPLC have been reported previously in detail (22,28), and were performed as described (22). Clinical and *NF2* status data from the meningiomas correspond to cases M02, M04, M05, M07, M09, M10, M12, M14, M24, M25, M28, M29, M30, M31, M32, M33, M34, M38, M39, M40, M41 and M42, as previously reported (22). The complete case series of schwannomas from our previous report (28) was included.

Results and discussion

Comparison with respect to previous analyses of meningiomas and summary of results in schwannomas. Meningioma profiling has been analyzed extensively in previous studies, and up to five expression subgroups were characterized [31], although this classification did not represent actual WHO classification. Recurrence and progression seem to play a relevant role in the expression pattern of these tumors [32], and two meningioma groups were identified showing different clinical and pathological behaviors, more related to clinical outcome than to WHO grade *per se*. Furthermore, depending on the cytogenetic aberrations, differential expression patterns have been described [25,29]. Tumors that presented monosomy of chromosome 22 and cases with multiple karyotype alterations had a differential expression pattern, whereas those cases with the deletion of chromosome 1 alone showed a random behavior [29]. In summary, previous analyses of gene expression patterns in meningiomas do not seem to accurately represent the current WHO classification, although recurrence and progression status might be reflected in these studies.. We used 20 grade I meningiomas, 2 grade II meningiomas and 3 healthy meninges. Practically the same values were obtained when meningiomas grade II were removed from study (data not shown). When we compared our results in meningiomas with those obtained from the dataset GSE43290 [29], we found a high consistency in our results, such as the down-regulation of diverse genes like *SNAP25*, *MBP*, *TTR* and *VSNLI*, and the up-regulation of *FBN2*, *FGF9* and *SULF1* (full data available upon request). As in previous studies, our 2 cases

of meningioma grade II did not show a different trend. The schwannoma expression profile was previously explained [28]. In brief, the up-regulation of *SPPI1*, *MET* and associated genes or *LATS2* was reported, whereas the down-regulation of *CAVI*, *AR* and *PAWR* was found. In general, myelination genes were overexpressed, suggesting that schwannoma cells could resemble a previous state of mature Schwann cells.

Gene co-overexpression in meningiomas and schwannomas. Using the ANOVA test at $p < 0.05$ significance across the four groups (all meningiomas, schwannomas, control healthy meninges and control nerves), we obtained a list of 12395 genes with differential expression among these four groups. Of those, 346 (data not shown; available upon request) did not meet the criteria established for accepting deregulation differences between both tumor groups, which is equal or less than 1.5-fold of the differential expression between the schwannomas and the meningiomas, a limit value selected as deregulated between these two groups because the correction effect of Combat. Among those 346 genes with similar expression in tumors, 47 (Table 1) showed co-overexpression in schwannomas and meningiomas when compared with their respective controls at 2-fold (as Combat correction would only be based on batch effect). These genes included E-cadherin (*CDH1*), which is usually silenced by several mechanisms, such as the Wnt signaling pathway in human cancer, including meningiomas [38], and platelet derived growth factor D (*PDGFD*), an activator for PDGFR- β [39]. This pathway has been reported as overexpressed in multiple cancer types such as pancreatic cancer and brain tumors, including schwannomas [39]. Another gene reported as expressed (and protein present) in meningiomas and schwannomas is tyrosine kinase receptor *MET* [40], which is responsible for cell migration, anchorage-independent growth and many other functions. High levels of this receptor have been found in a wide variety of tumors, such as breast cancer, renal cell carcinoma and head and neck tumors [41]. Mechanisms such as point mutations, alternative splicing, genomic amplification and transcript amplification appear to participate in over-expression of *c-MET* (reviewed by Lai et al., [42]). Accordingly, we found *MET* up-regulation in both neoplasms compared with their respective control tissues, and again, a similar level of expression between both tumor types was detected. *SLIT2* is a member of the Slits family that modulates cell migration by binding with the Robo family. This gene has been found expressed in the development of several malignancies such as colorectal epithelial cell carcinogenesis [43]. The findings in this report [43], suggest that Slit2-Robo1 causes E-cadherin degradation, and although our results show an up-regulation of the E-cadherin gene, the former mechanism should not be ruled out in the tumors we studied. In other neoplasms, although expressed, *SLIT2* does not seem to play any role [44]. In agreement with the data from the study selected for validation [29], several genes, including *CDH1*, *PDGFD*, *CX3CR1*,

CCND1 and *SLIT2*, were also up-regulated, as shown in data obtained from meningioma dataset GSE43290 [29]; in contrast, *MET* showed a trend of up-regulation but did not reach 2-fold. Functional annotation using DAVID showed enrichment in inflammatory response, cell migration, defense response, etc. (data not shown; available upon request).

Gene co-infraexpression in meningiomas and schwannomas. A total of 35 genes (Table 2) with no differences in expression between schwannomas and meningiomas were underexpressed when compared with their respective controls in both neoplasms. Among them are selectin E (*SELE*) and Rho family GTPase 1 (*RND1*), which is linked to semaphorins [45][46] and cytoskeleton organization in axons. The chemokine (C-X-C motif) ligand 2 (*CXCL2*) was significantly down-regulated in schwannomas and meningiomas, whereas the opposite trend has been shown in malignant neoplasms such as ovarian and endometrial cancer and oral squamous cell carcinoma [47]. As schwannomas and meningiomas are usually non-invasive, this fact could explain the different trend in deregulation of *CXCL2*. Stathmin-like 2 (*STMN2*) showed the same pattern: up-regulation in hepatoma cells but down-regulation in schwannomas and meningiomas. Interestingly, *STMN2* interacts with Rho family GTPase 1 (*RND1*) in axon extension [48], another gene that is down-regulated in both tumors. Other down-regulated genes in both tumors are E-selectin (*SELE*) and vascular adhesion protein 1 (*AOC3*), related to the tethering and rolling of leukocytes [49]; thus, the non-invasive nature of grade I meningiomas and schwannomas could explain the down-regulation of these genes. Validation with the dataset GSE43290 was performed, and included, among others, down-regulation of *AOC3*, *STMN2*, *SELE*, *RGS4*, *THBS4* and *RND1*. Functional analysis with DAVID included leukocyte and cell migration, heparin binding or membrane fraction (data available upon request).

Gene expression differences between meningiomas and schwannomas. The main goal of our study was to test gene expression profiles common to schwannomas and meningiomas in regard to their respective controls, and having into account their relative expression. However, we also studied the gene expression differences between both neurogenic neoplasms. As samples were processed in various batches, we used a Bayesian method to reduce the batch effect. Because of this effect, the differential expression of certain genes in schwannomas and meningiomas could have decreased. This issue, although it limits our information, is vital to our study because the batch effect was very marked; 192 genes were up-regulated at 1.5-fold differences and $p < 0.05$ (data available upon request) in schwannomas as compared to meningioma

expression. Most of these genes are related to neuron migration and the myelin sheath, such as the following: Peripheral myelin protein 2 (*PMP2*), expressed in the cytoplasmic side of myelin in the peripheral nervous system [50]; Myelin protein zero (*MPZ*), representing 50% of the total myelin protein in the peripheral nervous system [51]; Neurexin 1 (*NRXN1*), which mediates formation and maintenance of synaptic junctions [52]; or Neural cell adhesion molecule 2 (*NCAM2*), which is involved axonal projection [53].

Up-regulation in meningiomas compared with schwannomas gave us 88 genes (data available upon request) and included either cellular retinoic acid binding protein 2 (*CRABP2*), a chaperon down-regulated in high-grade gliomas [54], or secreted frizzled-related protein 2 gene (*SFRP2*), a gene identified as a tumor suppressor in a renal cell carcinoma cell line [55].

Another comparison would be those genes that were up-regulated in schwannomas with respect to nerves, and down-regulated in meningiomas with respect to healthy meninges. These findings are summarized in supp Table 8, and include genes such as hepatocyte cell adhesion molecule (*HEPACAM*), neuritin 1 (*NRN1*) and kinesin family member 1A (*KIF1A*).

The *NF2* mutation rate (determined by sequencing, MLPA and chromosome 22q LOH analyses) in this series was 74% for schwannomas and 68% for meningiomas. We compared the expression patterns in samples from both tumor types, and with respect to the presence or lack of any alteration in the *NF2* gene (38 samples with alteration and 15 without any). Using these groups, we identified 2 genes with differential expression levels. The natriuretic peptide receptor C/guanylate cyclase C (atrionatriuretic peptide receptor C) (*NPR3*) was down-regulated in those samples without *NF2* alterations. This gene codes for a receptor coupled to various signaling transduction cascades in several tissues such as cardiac myocytes and fibroblasts [56]. On the other hand, the G antigen 12J (*GAGE12J*) gene, transcribed in human fetal and tumoral tissues [57], was also down-regulated, but on this occasion in tumors with *NF2* alteration. As only 2 genes were detected, based on our microarray results in both neoplasms, it would seem that there is no differentiated subset of expression profiles of genes between samples with or without alteration over *NF2* in grade I meningiomas and schwannomas (Figure 1). Nevertheless, single genes could be altered in tumors with or without *NF2* alteration, although such a reduced number could be due to outlier values.

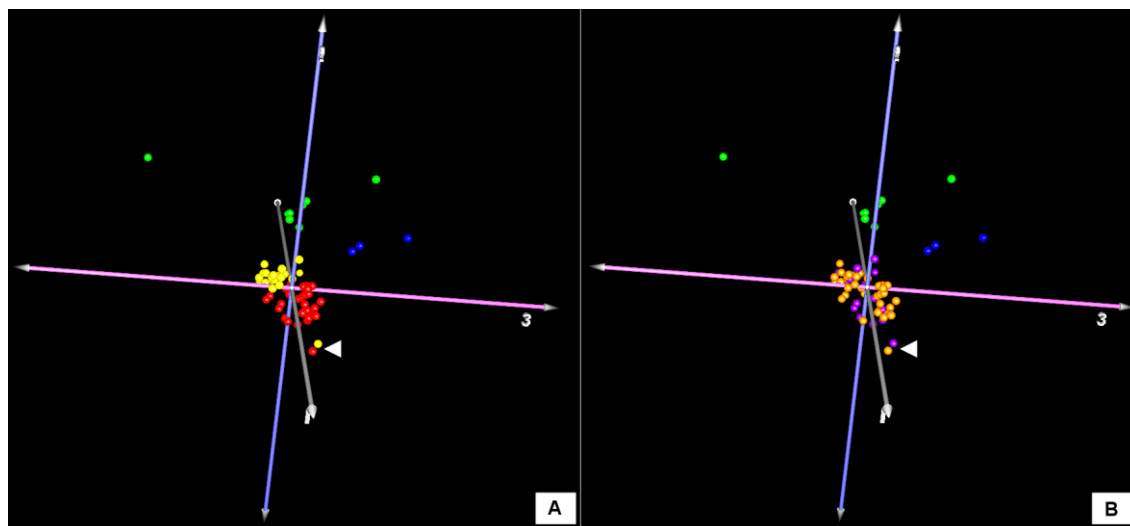


Figure 1. Principal component analysis (PCA) of all samples studied. Green dots represent non-tumoral healthy nerves and the blue dots non-tumoral meninges sample. A) Red dots are all schwannomas studied, while yellow are meningioma samples. Both entities are clearly separated, except for two samples (white arrow), one corresponding to a schwannoma from NF2 patient and the other to a grade I meningioma. The most remote green dot corresponds to the cultured schwann cells used as controls. In B), violet dots are samples without alteration in *NF2* gene, and gold dots are tumors carrying such alteration. The same point of view is shown in both images A and B, and no clear distinction between those two groups was found.

Currently, there is no chemotherapeutic treatment available for either meningiomas or schwannomas, so research for a combined solution could be of great value to those patients affected with both tumor types, primarily patients with neurofibromatosis type 2. In this study, we found a set of genes with aberrant expression in both entities compared with their respective control tissue, but with similar expression levels between these tumors, including PDGF, c-Met or Slit2 pathways. Thus, these and the other genes shown in this work, and their regulatory pathways, might be of interest for further experiments in the search for common solutions for patients affected by schwannomas and meningiomas.

Acknowledgments

The authors would like to thank Carolina Peña-Granero for her excellent technical assistance. Supported by grants PI10/1972 and PI13/00055 from Fondo de Investigaciones Sanitarias, Ministerio de Ciencia e Innovación, Spain; and PI10-045, from the Fundación Sociosanitaria de Castilla-La Mancha, Spain.

References

1. Louis DN, Ohgaki H, Wiestler OD and Cavenee WK: WHO classification of tumors of the central nervous system. IARC, Lyon 2007.
2. Zankl H and Zang KD: Cytological and cytogenetical studies on brain tumors. 4. Identification of the missing G chromosome in human meningiomas as no. 22 by fluorescence technique. *Humangenetik* 14: 167–169, 1972.
3. Rey JA, Bello MJ, De Campos JM, Kusak ME and Moreno S: Cytogenetic analysis in human neurinomas. *Cancer Genet Cytogenet* 28: 187–188, 1987.
4. Hadfield KD, Smith MJ, Urquhart JE, Wallace AJ, Bowers NL, King AT, Rutherford SA, Trump D, Newman WG and Evans DG: Rates of loss of heterozygosity and mitotic recombination in NF2 schwannomas, sporadic vestibular schwannomas and schwannomatosis schwannomas. *Oncogene* 29: 6216–6221, 2010.
5. Hansson CM, Buckley PG, Grigelioniene G, Piotrowski A, Hellström AR, Mantripragada K, Jarbo C, Mathiesen T and Dumanski JP: Comprehensive genetic and epigenetic analysis of sporadic meningioma for macro-mutations on 22q and micro-mutations within the NF2 locus. *BMC Genomics* 8: 16, 2007.
6. Leone PE, Bello MJ, de Campos JM, Vaquero J, Sarasa JL, Pestaña A and Rey JA: NF2 gene mutations and allelic status of 1p, 14q and 22q in sporadic meningiomas. *Oncogene* 18: 2231–2239, 1999.
7. Leone PE, Bello MJ, Mendiola M, Kusak ME, De Campos JM, Vaquero J, Sarasa JL, Pestana A and Rey JA: Allelic status of 1p, 14q, and 22q and NF2 gene mutations in sporadic schwannomas. *Int J Mol Med* 1: 889–892, 1998.
8. Bello MJ, de Campos JM, Kusak ME, Vaquero J, Sarasa JL, Pestaña A and Rey JA: Allelic loss at 1p is associated with tumor progression of meningiomas. *Genes Chromosomes Cancer* 9: 296–298, 1994.
9. Bello MJ, Martínez-Glez V, Franco-Hernández C, Pefla-Granero C, de Campos JM, Isla A, Lassaletta L, Vaquero J and Rey JA: DNA methylation pattern in 16 tumor-related genes in schwannomas. *Cancer Genet Cytogenet* 172: 84–86, 2007.
10. Bello MJ, Amiñoso C, López-Marín I, Arjona D, González-Gómez P, Alonso ME, Lomas J, de Campos JM, Kusak ME, Vaquero J, Isla A, Gutiérrez M, Sarasa JL and Rey JA: DNA methylation of multiple promoter-associated CpG islands in meningiomas: relationship with the allelic status at 1p and 22q. *Acta Neuropathol (Berl)* 108: 413–421, 2004.
11. Liu Y, Pang JC, Dong S, Mao B, Poon WS and Ng H: Aberrant CpG island hypermethylation profile is associated with atypical and anaplastic meningiomas. *Hum Pathol* 36: 416–425, 2005.
12. Kino T, Takeshima H, Nakao M, Nishi T, Yamamoto K, Kimura T, Saito Y, Kochi M, Kuratsu J, Saya H and Ushio Y: Identification of the cis-acting region in the NF2 gene promoter as a potential target for mutation and methylation-dependent silencing in schwannoma. *Genes Cell* 6: 441–454, 2001.
13. González-Gómez P, Bello MJ, Alonso ME, Lomas J, Arjona D, Campos JM de, Vaquero J, Isla A, Lassaletta L, Gutiérrez M, Sarasa JL and Rey JA: CpG island methylation in sporadic and neurofibromatosis type 2-associated schwannomas. *Clin Cancer Res* 9: 5601–5606, 2003.
14. Lomas J, Bello MJ, Arjona D, Alonso ME, Martínez-Glez V, López-Marín I, Amiñoso C, de Campos JM, Isla A, Vaquero J and Rey JA: Genetic and epigenetic alteration of the NF2 gene in sporadic meningiomas. *Genes Chromosomes Cancer* 42: 314–319, 2005.
15. Kullar PJ, Pearson DM, Malley DS, Collins VP and Ichimura K: CpG island hypermethylation of the neurofibromatosis type 2 (NF2) gene is rare in sporadic vestibular schwannomas. *Neuropathol Appl Neurobiol* 36: 505–514, 2010.
16. Koutsimpelas D, Ruerup G, Mann WJ and Brieger J: Lack of neurofibromatosis type 2 gene promoter methylation in sporadic vestibular schwannomas. *ORL J Oto-Rhino-Laryngol Its Relat Spec* 74: 33–37, 2012.
17. Kishida Y, Natsume A, Kondo Y, Takeuchi I, An B, Okamoto Y, Shinjo K, Saito K, Ando H, Ohka F, Sekido Y and Wakabayashi T: Epigenetic subclassification of meningiomas based on genome-wide DNA methylation analyses. *Carcinogenesis* 33: 436–441, 2012.
18. Gao F, Shi L, Russin J, Zeng L, Chang X, He S, Chen TC, Giannotta SL, Weisenberger DJ, Zada G, Mack WJ and Wang K: DNA methylation in the malignant transformation of meningiomas. *PLoS One* 8: e54114, 2013.
19. Clark VE, Erson-Omay EZ, Serin A, Yin J, Cotney J, Ozduman K, Avcı T, Li J, Murray PB, Henegariu O, Yilmaz S, Günel JM, Carrión-Grant G, Yilmaz B, Grady C, Tanrikulu B, Bakircioğlu M, Kaymakçalan H, Caglayan AO, Sencar L, Ceyhan E, Atik AF, Bayrı Y, Bai H, Kolb LE, Hebert RM, Omay SB, Mishra-Gorur K, Choi M, Overton JD, et al.: Genomic analysis of non-NF2 meningiomas reveals mutations in TRAF7, KLF4, AKT1, and SMO. *Science* 339: 1077–1080, 2013.
20. Brastianos PK, Horowitz PM, Santagata S, Jones RT, McKenna A, Getz G, Ligon KL, Palessandolo E, Van Hummelen P, Ducar MD, Raza A, Sunkavalli A, Macconail LE, Stemmer-Rachamimov AO, Louis DN, Hahn WC, Dunn IF and Beroukhim R: Genomic sequencing of meningiomas identifies oncogenic SMO and AKT1 mutations. *Nat Genet* 45: 285–289, 2013.
21. Stemmer-Rachamimov AO, Xu L, González-Agosti C, Burwick JA, Pinney D, Beauchamp R, Jacoby LB, Gusella JF, Ramesh V and Louis DN: Universal absence of merlin, but not other ERM family members, in schwannomas. *Am J Pathol* 151: 1649–1654, 1997.

22. Martínez-Glez V, Franco-Hernández C, Álvarez L, De Campos JM, Isla A, Vaquero J, Lassaletta L, Casartelli C and Rey JA: Meningiomas and schwannomas: molecular subgroup classification found by expression arrays. *Int J Oncol* 34: 493–504, 2009.
23. Torres-Martín M, Martínez-Glez V, Peña-Granero C, Isla A, Lassaletta L, DE Campos JM, Pinto GR, Burbano RR, Meléndez B, Castresana JS and Rey JA: Gene expression analysis of aberrant signaling pathways in meningiomas. *Oncol Lett* 6: 275–279, 2013.
24. Torres-Martín M, Martínez-Glez V, Peña-Granero C, Lassaletta L, Isla A, de Campos JM, Pinto GR, Burbano RR, Meléndez B, Castresana JS and Rey JA: Expression analysis of tumor-related genes involved in critical regulatory pathways in schwannomas. *Clin Transl Oncol* 15: 409–411, 2013.
25. Martínez-Glez V, Álvarez L, Franco-Hernández C, Torres-Martin M, de Campos JM, Isla A, Vaquero J, Lassaletta L, Castresana JS, Casartelli C and Rey JA: Genomic deletions at 1p and 14q are associated with an abnormal cDNA microarray gene expression pattern in meningiomas but not in schwannomas. *Cancer Genet Cytogenet* 196: 1–6, 2010.
26. Aarhus M, Bruland O, Sætran HA, Mork SJ, Lund-Johansen M and Knappskog PM: Global gene expression profiling and tissue microarray reveal novel candidate genes and down-regulation of the tumor suppressor gene CAV1 in sporadic vestibular schwannomas. *Neurosurgery* 67: 998–1019, 2010.
27. Cayé-Thomassen P, Borup R, Stangerup S-E, Thomsen J and Nielsen FC: Deregulated genes in sporadic vestibular schwannomas. *Otol Neurotol* 31: 256–266, 2010.
28. Torres-Martín M, Lassaletta L, San-Roman-Montero J, De Campos JM, Isla A, Gavilan J, Melendez B, Pinto GR, Burbano RR, Castresana JS and Rey JA: Microarray analysis of gene expression in vestibular schwannomas reveals SPP1/MET signaling pathway and androgen receptor deregulation. *Int J Oncol* 42: 848–86, 2013.
29. Tabernero MD, Maillo A, Gil-Bellosta CJ, Castrillo A, Sousa P, Merino M and Orfao A: Gene expression profiles of meningiomas are associated with tumor cytogenetics and patient outcome. *Brain Pathol* 19: 409–420, 2009.
30. Keller A, Ludwig N, Backes C, Romeike BFM, Comtesse N, Henn W, Steudel W-I, Mawrin C, Lenhof H-P and Meese E: Genome wide expression profiling identifies specific deregulated pathways in meningioma. *Int J Cancer* 124: 346–351, 2009.
31. Lee Y, Liu J, Patel S, Cloughesy T, Lai A, Farooqi H, Seligson D, Dong J, Liao L, Becker D, Mischel P, Shams S and Nelson S: Genomic landscape of meningiomas. *Brain Pathol* 20: 751–762, 2010.
32. Pérez-Magán E, Campos-Martín Y, Mur P, Fiaño C, Ribalta T, García JF, Rey JA, Rodríguez de Lope A, Mollejo M and Meléndez B: Genetic alterations associated with progression and recurrence in meningiomas. *J Neuropathol Exp Neurol* 71: 882–893, 2012.
33. Torres-Martín M, Lassaletta L, de Campos JM, Isla A, Gavilan J, Pinto GR, Burbano RR, Latif F, Melendez B, Castresana JS and Rey JA: Global profiling in vestibular schwannomas shows critical deregulation of microRNAs and upregulation in those included in chromosomal region 14q32. *PLoS One* 8: e65868, 2013.
34. Bush ML, Oblinger J, Brendel V, Santarelli G, Huang J, Akhrametyeva EM, Burns SS, Wheeler J, Davis J, Yates CW, Chaudhury AR, Kulp S, Chen C-S, Chang L-S, Welling DB and Jacob A: AR42, a novel histone deacetylase inhibitor, as a potential therapy for vestibular schwannomas and meningiomas. *Neuro-Oncol* 13: 983–999, 2011.
35. Spear SA, Burns SS, Oblinger JL, Ren Y, Pan L, Kinghorn AD, Welling DB and Chang L-S: Natural compounds as potential treatments of NF2-deficient schwannoma and meningioma: cucurbitacin D and goyazensolide. *Otol Neurotol* 34:1519–1527, 2013.
36. Johnson WE, Li C and Rabinovic A: Adjusting batch effects in microarray expression data using empirical Bayes methods. *Biostat* 2007, 8:118–127.
37. Shi L, Reid LH, Jones WD, Shippy R, Warrington JA, Baker SC, Collins PJ, de Longueville F, Kawasaki ES, Lee KY, Luo Y, Sun YA, Willey JC, Setterquist RA, Fischer GM, Tong W, Dragan YP, Dix DJ, Frueh FW, Goodsaid FM, Herman D, Jensen RV, Johnson CD, Lobenhofer EK, Puri RK, Schrf U, Thierry-Mieg J, Wang C, Wilson M, Wolber PK, et al.: The MicroArray Quality Control (MAQC) project shows inter- and intraplatform reproducibility of gene expression measurements. *Nat Biotechnol* 24: 1151–1161, 2006.
38. Zhou K, Wang G, Wang Y, Jin H, Yang S and Liu C: The potential involvement of E-cadherin and beta-catenins in meningioma. *PLoS One* 5: e11231, 2010.
39. Wang Z, Kong D, Li Y and Sarkar FH: PDGF-D signaling: a novel target in cancer therapy. *Curr Drug Targets* 10: 38–41, 2009.
40. Moriyama T, Kataoka H, Kawano H, Yokogami K, Nakano S, Goya T, Uchino H, Koono M and Wakisaka S: Comparative analysis of expression of hepatocyte growth factor and its receptor, c-met, in gliomas, meningiomas and schwannomas in humans. *Cancer Lett* 124: 149–155, 1998.
41. Cipriani NA, Abidoye OO, Vokes E and Salgia R: MET as a target for treatment of chest tumors. *Lung Cancer* 63: 169–179, 2009.
42. Lai AZ, Abella JV and Park M: Crosstalk in Met receptor oncogenesis. *Trends Cell Biol* 19: 542–551, 2009.
43. Zhou W-J, Geng ZH, Chi S, Zhang W, Niu X-F, Lan S-J, Ma L, Yang X, Wang L-J, Ding Y-Q and Geng J-G: Slit-Robo signaling induces malignant transformation through Hakai-mediated E-cadherin degradation during colorectal epithelial cell carcinogenesis. *Cell Res* 21: 609–626, 2011.

44. Dai CF, Jiang YZ, Li Y, Wang K, Liu PS, Patankar MS and Zheng J: Expression and roles of Slit/Robo in human ovarian cancer. *Histochem Cell Biol* 135: 475–485, 2011.
45. Zanata SM, Hovatta I, Rohm B and Püschel AW: Antagonistic effects of Rnd1 and RhoD GTPases regulate receptor activity in Semaphorin 3A-induced cytoskeletal collapse. *J Neurosci* 22: 471–477, 2002.
46. Hota PK and Buck M: Thermodynamic characterization of two homologous protein complexes: associations of the semaphorin receptor plexin-B1 RhoGTPase binding domain with Rnd1 and active Rac1. *Protein Sci* 18: 1060–1071, 2009.
47. Oue E, Lee J-W, Sakamoto K, Imura T, Aoki K, Kayamori K, Michi Y, Yamashiro M, Harada K, Amagasa T and Yamaguchi A: CXCL2 synthesized by oral squamous cell carcinoma is involved in cancer-associated bone destruction. *Biochem Biophys Res Commun* 424: 456–461, 2012.
48. Li Y-H, Ghavampur S, Bondallaz P, Will L, Grenningloh G and Püschel AW: Rnd1 regulates axon extension by enhancing the microtubule destabilizing activity of SCG10. *J Biol Chem* 284: 363–371, 2009.
49. Jalkanen S, Karikoski M, Mercier N, Koskinen K, Henttinen T, Elima K, Salmivirta K and Salmi M: The oxidase activity of vascular adhesion protein-1 (VAP-1) induces endothelial E- and P-selectins and leukocyte binding. *Blood* 110: 1864–1870, 2007.
50. Eylar EH, Szymanska I, Ishaque A, Ramwani J and Dubiski S: Localization of the P2 protein in peripheral nerve myelin. *J Immunol* 124: 1086–1092, 1980.
51. Everly JL, Brady RO and Quarles RH: Evidence that the major protein in rat sciatic nerve myelin is a glycoprotein. *J Neurochem* 21: 329–334, 1973.
52. Bottos A, Rissone A, Bussolino F and Arese M: Neurexins and neuroligins: synapses look out of the nervous system. *Cell Mol Life Sci CMLS* 68: 2655–2666, 2011.
53. Alenius M and Bohm S: Identification of a novel neural cell adhesion molecule-related gene with a potential role in selective axonal projection. *J Biol Chem* 272: 26083–26086, 1997.
54. Campos B, Warta R, Chaisaingmongkol J, Geiselhart L, Popanda O, Hartmann C, von Deimling A, Unterberg A, Plass C, Schmezer P and Herold-Mende C: Epigenetically mediated downregulation of the differentiation-promoting chaperon protein CRABP2 in astrocytic gliomas. *Int J Cancer J Int Cancer* 131:1963–1968, 2012.
55. Konac E, Varol N, Yilmaz A, Menevse S and Sozen S: DNA methyltransferase inhibitor-mediated apoptosis in the Wnt/ β -catenin signal pathway in a renal cell carcinoma cell line. *Exp Biol Med* 238: 1009–1016, 2013.
56. Rose RA and Giles WR: Natriuretic peptide C receptor signalling in the heart and vasculature. *J Physiol* 586: 353–366, 2008.
57. Gjerstorff MF and Ditzel HJ: An overview of the GAGE cancer/testis antigen family with the inclusion of newly identified members. *Tissue Antigens* 71: 187–192, 2008.

Table 1. Genes overexpressed in meningioma and schwannoma when compared with their respective control tissue.

Gene	Database	Chromosome	C-M	N-S	M-S	P-value
<i>CDH1</i>	NM_004360	16q22.1	5.4	5.8	-1.0	8.35E-09
<i>PDGFD</i>	NM_025208	11q22.3	4.4	6.2	-1.1	7.48E-13
<i>SLIT2</i>	NM_004787	4p15.2	3.6	5.8	-1.1	2.02E-13
<i>HLA-DPA1</i>	NM_033554	6p21.3	2.9	3.9	-1.1	5.24E-07
<i>PAPPA</i>	NM_002581	9q33.2	2.8	3.8	-1.1	3.68E-06
<i>TREM2</i>	NM_018965	6p21.1	2.7	5.5	-1.3	2.8E-12
<i>HLA-DPA1</i>	NM_033554	6p21.3	2.6	4.1	-1.2	5.24E-07
<i>HPGDS</i>	NM_014485	4q22.3	2.6	2.4	-1.1	3.83E-07
<i>GPR34</i>	NM_001097579	Xp11.4	2.6	12.0	-1.5	9.9E-11
<i>CX3CR1</i>	NM_001337	3p21 3p21.3	2.5	5.7	-1.2	2.15E-07
<i>ANKRD22</i>	NM_144590	10q23.31	2.5	7.3	-1.4	1.04E-06
<i>C3</i>	NM_000064	19p13.3-p13.2	2.4	2.6	-1.2	5.77E-05
<i>CYBB</i>	NM_000397	Xp21.1	2.4	4.1	-1.2	1.11E-07
<i>LGALS3BP</i>	NM_005567	17q25	2.4	2.9	-1.1	4.67E-13
<i>WIPI1</i>	NM_017983	17q24.2	2.4	2.0	-1.0	2.55E-12
<i>APOBEC3C</i>	NM_014508	22q13.1	2.4	2.5	-1.1	3.35E-08
<i>C3AR1</i>	NM_004054	12p13.31	2.4	4.8	-1.2	4.43E-09
<i>FCGBP</i>	NM_003890	19q13.1	2.3	9.7	-1.3	1.03E-11
<i>FRAS1</i>	NM_025074	4q21.21	2.3	3.2	-1.2	7.42E-08
<i>FLRT3</i>	NM_198391	20p11	2.3	3.8	-1.2	1.76E-05
<i>FCGRIA</i>	NM_000566	1q21.2-q21.3	2.3	4.3	-1.3	1.66E-08
<i>MET</i>	NM_001127500	7q31	2.3	4.9	-1.3	1.22E-08
<i>ITPR3</i>	NM_002224	6p21	2.3	3.7	-1.1	3.69E-12
<i>FCGR1B</i>	NM_001017986	1p11.2	2.3	2.9	-1.2	4.14E-08
<i>ALCAM</i>	NM_001627	3q13.1	2.2	2.5	-1.0	4.26E-09
<i>HLA-DPB1</i>	NM_002121	6p21.3	2.2	4.6	-1.3	1.75E-07
<i>LAMB1</i>	NM_002291	7q22	2.2	2.0	-1.2	4.57E-07
<i>C8orf84</i>	NM_153225	8q21.11	2.2	2.6	-1.2	8.11E-06
<i>SLFN12</i>	NM_018042	17q12	2.2	2.3	-1.2	4.14E-10
<i>FCGRIA</i>	NM_000566	1q21.2-q21.3	2.2	3.1	-1.2	1.66E-08
<i>LHFPL2</i>	NM_005779	5q14.1	2.1	2.3	-1.1	8.13E-09
<i>MS4A6A</i>	NM_152852	11q12.1	2.1	4.5	-1.3	4.8E-08
<i>CD84</i>	NM_001184879	1q24	2.1	2.7	-1.2	3.38E-09
<i>TRIM22</i>	NM_006074	11p15	2.1	2.2	-1.1	2.09E-09
<i>CD4</i>	NM_000616	12pter-p12	2.1	2.5	-1.1	1.69E-07
<i>CSF1R</i>	NM_005211	5q32	2.1	3.8	-1.2	5.21E-08
<i>GFRA1</i>	NM_005264	10q26.11	2.1	4.9	-1.4	1.34E-07
<i>HLA-DPB1</i>	NM_002121	6p21.3	2.1	4.5	-1.3	1.75E-07
<i>CD86</i>	NM_175862	3q21	2.1	2.9	-1.3	1.03E-06
<i>CIQA</i>	NM_015991	1p36.12	2.1	4.3	-1.2	1.24E-07
<i>TLR7</i>	NM_016562	Xp22.3	2.0	3.6	-1.3	7E-08
<i>CCND1</i>	NM_053056	11q13	2.0	2.7	-1.1	1.48E-11
<i>HLA-DQA1</i>	NM_002122	6p21.3	2.0	2.6	-1.2	4.19E-05
<i>FAM105A</i>	NM_019018	5p15.2	2.0	2.6	-1.1	9.2E-08
<i>C6orf138</i>	NM_001013732	6p12.3	2.0	3.4	-1.2	1.99E-10
<i>P2RY13</i>	NM_176894	3q24	2.0	2.4	-1.2	3.08E-06
<i>PROS1</i>	NM_000313	3q11.2	2.0	5.0	-1.4	9.1E-14

Official gene symbol is shown for every gene. C-M values correspond to the fold-change value of Control healthy meninges (C) minus meningioma (M). In the case of N-S, N is referred as Nerve healthy tissue minus schwannoma (S). In the column M-S, meningioma (M) minus schwannoma (S) is performed. Only those genes with less than 1.5 fold-change between both tumors were shown.

Table 2. Genes infraxpressed in meningioma and schwannoma when compared with their respective control tissue.

Gene	Database	Chromosome	C-M	N-S	M-S	P-value
<i>SAA1</i>	NM_000331	11p15.1	-2.0	-2.7	1.1	0.000414
<i>INHBA</i>	NM_002192	7p15-p13	-2.0	-4.1	1.2	2.42E-09
<i>PCDH18</i>	NM_019035	4q31	-2.0	-2.6	1.2	0.000183
<i>PTGIS</i>	NM_000961	20q13.13	-2.1	-3.4	1.3	1.72E-06
<i>HHIP</i>	NM_022475	4q28-q32	-2.1	-2.9	1.1	1.44E-06
<i>AQP9</i>	NM_020980	15q	-2.1	-4.5	1.0	2.78E-08
<i>TCEAL2</i>	NM_080390	Xq22.1-q22.3	-2.1	-2.4	1.4	0.000135
<i>S100A12</i>	NM_005621	1q21	-2.2	-5.6	1.1	9.51E-07
<i>PDE3A</i>	NM_000921	12p12	-2.2	-2.0	1.2	2.03E-08
<i>S100A9</i>	NM_002965	1q21	-2.2	-4.6	-1.0	2.63E-05
<i>PAK3</i>	NM_002578	Xq23	-2.3	-4.1	1.3	5.36E-11
<i>SLC16A7</i>	NM_004731	12q13	-2.3	-2.2	1.1	4.89E-12
<i>PII6</i>	NM_153370	6p21.2	-2.3	-5.1	1.2	1.76E-09
<i>MGST1</i>	NM_145792	12p12.3-p12.1	-2.3	-3.6	1.1	0.001079
<i>FGFR2</i>	NM_000141	10q26	-2.3	-2.6	1.3	1.69E-09
<i>TRPM3</i>	NM_206946	9q21.12	-2.4	-2.0	1.1	3.65E-11
<i>PDZRN4</i>	NM_013377	12q12	-2.5	-3.0	1.1	1.14E-08
<i>THBS4</i>	NM_003248	5q13	-2.5	-3.5	1.0	1.71E-09
<i>STEAP4</i>	NM_024636	7q21.12	-2.7	-4.2	1.1	1.38E-07
<i>DCLK1</i>	NM_004734	13q13	-2.8	-2.4	1.1	2.22E-07
<i>ZNF385D</i>	NM_024697	3p24.3	-3.0	-2.0	1.1	1.34E-05
<i>CXCL2</i>	NM_002089	4q21	-3.1	-3.3	-1.0	7.52E-09
<i>FABP4</i>	NM_001442	8q21	-3.1	-13.5	1.2	1.29E-12
<i>IL6</i>	NM_000600	7p21	-3.1	-4.6	-1.0	0.000397
<i>SELE</i>	NM_000450	1q22-q25	-3.3	-6.6	1.0	2.29E-09
<i>SLC14A1</i>	NM_001128588	18q11-q12	-4.0	-3.3	1.0	2.7E-09
<i>APLNR</i>	NM_005161	11q12	-4.8	-3.1	-1.0	8.05E-11
<i>ADH1B</i>	NM_000668	4q23	-4.9	-3.6	-1.1	6.95E-07
<i>ADCYAPIR1</i>	NM_001118	7p14	-5.1	-3.3	1.0	6.98E-11
<i>RND1</i>	NM_014470	12q12	-5.4	-3.1	-1.0	3.5E-09
<i>ADAMTS1</i>	NM_006988	21q21.2	-6.0	-2.4	-1.1	4.64E-11
<i>HSPB8</i>	NM_014365	12q24.23	-6.0	-3.5	1.0	5.3E-07
<i>AOC3</i>	NM_003734	17q21	-6.3	-2.5	-1.1	3.64E-11
<i>RGS4</i>	NM_001102445	1q23.3	-6.7	-2.1	-1.1	2.55E-10
<i>STMN2</i>	NM_007029	8q21.13	-9.2	-2.9	-1.1	4.92E-11

Official gene symbol is shown for every gene. C-M values correspond to the fold-change value of Control healthy meninges (C) minus meningioma (M). In the case of N-S, N is referred as Nerve healthy tissue minus schwannoma (S). In the column M-S, meningioma (M) minus schwannoma (S) is performed. Only those genes with less than 1.5 fold-change between both tumors were shown.

4. RESULTADOS GLOBALES

4. RESULTADOS GLOBALES

4.1 ANÁLISIS MUTACIONAL DE *NF2*

El total de las muestras utilizadas en estos trabajos asciende a 51 schwannomas vestibulares esporádicos, 6 schwannomas vestibulares procedentes de pacientes con *NF2* y 4 schwannomas no vestibulares -3 de columna y 1 cervical-. En el Artículo 1 se detallan los hallazgos de mutaciones de *NF2* y de la LOH del cromosoma 22 en schwannomas vestibulares esporádicos. En resumen, la LOH fue detectada en el 57% de los tumores, mutación por PCR/dHPLC en el 49% y alteraciones de MLPA se identificaron en el 13,7% de los casos. Un 45% de los schwannomas presentó al menos 2 eventos inactivadores sobre *NF2* y en el 27% de los tumores se identificó uno.

De los 4 casos de schwannomas no-vestibulares, 2 presentaron mutación y LOH del cromosoma 22, mientras que otros 2 -entre los que se incluye el cervical, NonV4- no mostraron alteraciones en el gen (Tabla 4).

Tabla 4. Mutaciones en los schwannomas no-vestibulares.

Muestra	LOH	MLPA	<i>NF2</i> NM_000268.3
NonV1	-	N/N	
NonV2	1	N/N	c.1735_1738del4 p.Lys579Stop
NonV3	1	N/14,16	c.535_540del6 p.Met179_Thr180del
NonV4	0	N/N	

Ninguno de ellos presentó alteración en sangre periférica. En la muestra NonV1 no se pudo determinar la LOH del cromosoma 22 debido a que no se dispuso de sangre periférica del paciente. Para nombrar la mutación, se utiliza como referencia el mensajero NM_000268.3 del gen *NF2*. En la LOH, 1 indica pérdida de heterocigosidad, mientras que 0 indica que no se detectaron alteraciones. En el MLPA, la N se refiere a un alelo sin alteraciones del gen *NF2*, los números indican el exón donde se detectaron pérdidas.

En las muestras de schwannomas provenientes de pacientes con NF2, se detectaron alteraciones sobre el gen *NF2* en 5 de los 6 casos -86%- (Tabla 5). No obstante, mutaciones en la sangre periférica pudieron ser halladas solamente en el caso NF2_2. En el caso NF2_3, a pesar de que los síntomas clínicos eran evidentes de NF2, no se pudo hallar ninguna alteración en el gen *NF2* tanto en el ADN de la sangre periférica como en el tumor mediante las técnicas utilizadas.

Tabla 5. Mutaciones en los schwannomas de pacientes con NF2.

MUESTRA	LOH	MLPA	NF2 NM_000268.3
NF2_1	1	N/2	c.169C>T p.Arg57Stop
NF2_2	1	N/2	c.169C>T p.Arg57Stop*
NF2_3	0	N/N	
NF2_4	1	4, 15, 16	
NF2_5	1	N	c.1033C>T p.Arg198Stop
NF2_6	1	N/2	c.169C>T p.Arg57Stop

Para nombrar la mutación, se utiliza como referencia el mensajero NM_000268.3 del gen *NF2*. En la LOH, 1 indica pérdida de heterocigosidad, mientras que 0 indica que no se detectaron alteraciones. En el MLPA, la N se refiere a un alelo sin alteraciones del gen *NF2*, los números indican el exón donde se detectaron pérdidas. * Paciente con mutación en sangre periférica. La muestra NF2_1 y la NF2_6 corresponden al mismo paciente.

De los 22 meningiomas del Artículo 6, 7 mostraron mutaciones en la secuencia de *NF2* -32%-, 2 alteraciones fueron encontradas por MLPA -9%- y 14 muestras con LOH del 22q -64%-. En total, un 73% de las muestras presentaron al menos un evento mutacional en el gen, 9 de ellas -41%- con un solo evento y 7 -32%- con dos. En 6 de los meningiomas -27%-, no se detectaron alteraciones de *NF2* mediante las técnicas usadas.

4.2 PATRONES GENERALES DE LOS MICROARRAYS

En los análisis de expresión, tanto de ARN mensajero como de miRNA, se observó una tendencia hacia la sobreexpresión génica. En el caso de los microarrays de ARN mensajero, usando los límites -para desregulación p-valor menor o igual a 0.05 y cambio de expresión de al menos el doble- expuestos en el Artículo 1, se encontraron 1105 genes sobreexpresados, mientras que menos de la mitad, un total de 411, estaban infraexpresados. En el volcano plot de la Figura 2 se aprecia cómo, independientemente del límite de p-valor como del cambio de expresión entre los schwannomas y los controles, el número de mediciones -genes- siempre será mayor para la sobreexpresión.

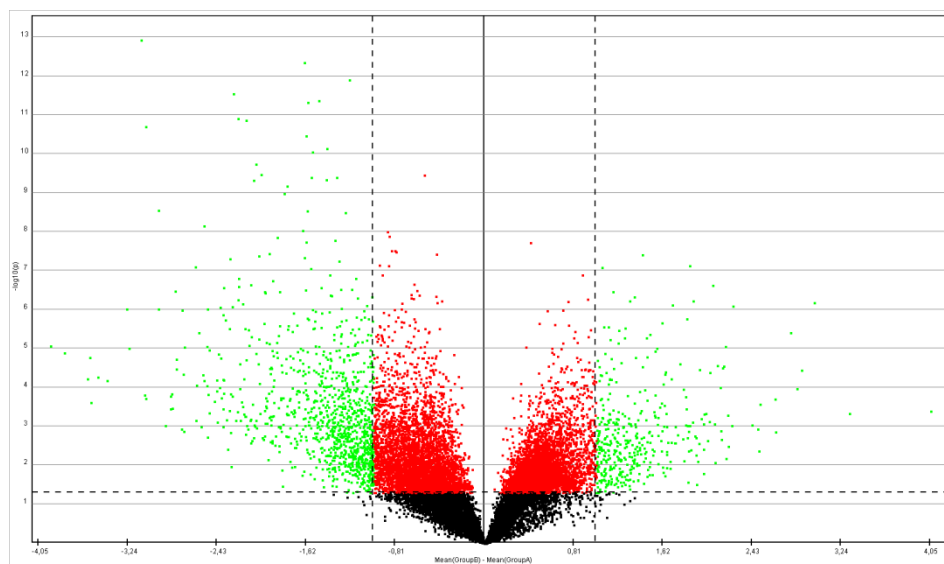


Figura 2. Volcano plot en color de la figura 3 del artículo 3. Los puntos verdes representan aquellos genes que cumplen el umbral para considerar desregulado. Los puntos negros son genes que no alcanzan nivel de significación suficiente. Los puntos rojos son los genes que, aunque significativos, el nivel de desregulación no llega a ser el doble o la mitad en los schwannomas en comparación con los controles no tumorales. Se observa cómo, incluso entre los que no llegan al umbral, el número de puntos en la zona de sobreexpresión (izquierda) es mayor.

El mismo fenómeno se observó para los microarrays de expresión de miRNA. Mientras que un 14% -119- de los miRNA se mostraron sobreexpresados, menos de la mitad, con el 6.7% -57- se consideraron infraexpresados. Como en el caso anterior, los valores límite para considerar desregulación fueron el p-valor menor o igual a 0.05 y cambio de expresión de al menos el doble. En la Figura 3, se muestra el volcano plot con este efecto. Por lo tanto, aunque numerosos genes y miRNA presentaron una menor expresión que los controles sanos, la mayor parte de la desregulación en los schwannomas se produjo por sobreexpresión.

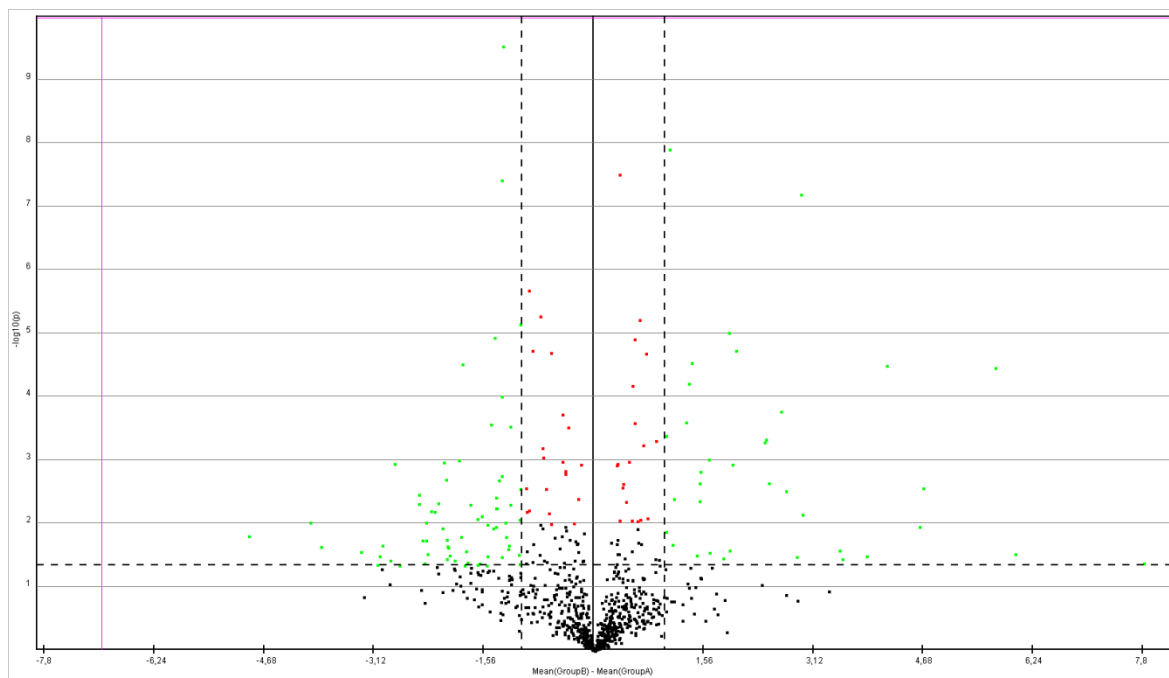


Figura 3. Volcano plot de los miRNAs 3. Como en la figura anterior, los puntos verdes representan aquellos genes que cumplen el umbral para considerar desregulado. Los puntos negros son genes que no alcanzan nivel de significación suficiente. Los puntos rojos son los genes que, aunque significativos, el nivel de desregulación no llega a ser el doble o la mitad en los schwannomas en comparación con los controles no tumorales. El número de puntos en la zona de sobreexpresión (izquierda) es mayor.

En el caso de la metilación en sitios CpG del ADN, lo que se observó fue una tendencia a la hipometilación, aunque numerosos sitios CpG sufrieron metilación aberrante. En concreto, usando los límites expuestos en el Artículo 5 -al menos diferencia

de 1 en el valor M y p-valor corregido por Bonferroni menor o igual a 0.05-, 8307 sitios CpG aparecieron hipometilados y 6553 hipermetilados. Reduciendo la astringencia de los límites de metilación, la proporción entre hipo e hipermetilación se mantenía estable a los valores anteriores, con mayor proporción de hipometilados. Por lo tanto, parece que en los schwannomas se tienden a expresar más genes -incluidos miRNA- que en tejido control, siendo este fenómeno apoyado por el patrón de metilación de los sitios CpG, cuya hipometilación más abundante que hipermetilación, sugiere mayor expresión génica que en los nervios no-tumorales.

4.3 AGRUPACIÓN DE LAS MUESTRAS

Los métodos estadísticos no supervisados usados en los artículos presentados, incluyendo el análisis de componentes principales -PCA- y el método de clúster de distancias de Pearson, mostraron una clara diferencia entre los schwannomas y los controles sanos. En los microarrays de expresión génica, el PCA separó de manera evidente los tumores y los controles. La distancia entre los propios controles fue mayor que la mostrada por los schwannomas, sugiriendo que la diversidad biológica entre los controles era relativamente alta en cuanto a los patrones de expresión de mensajeros. En el clúster de Pearson, además de la evidente separación schwannoma-control, las muestras tumorales se agruparon en lo que parecían dos o tres grupos (Figura 4). A pesar de este hecho, no se pudieron asignar estos grupos con ninguna característica molecular ni clínica recogida.

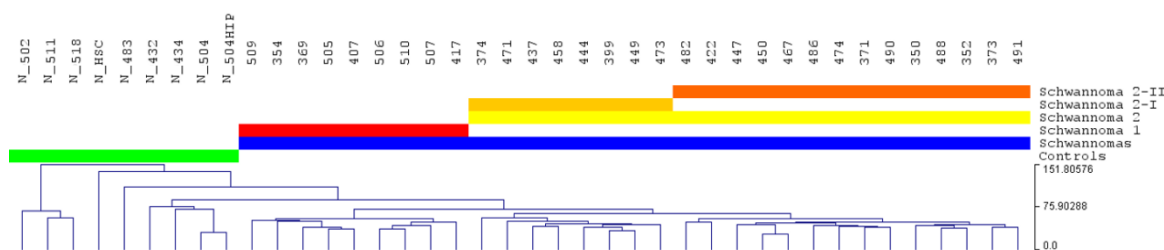


Figura 4. Clúster de distancias de Pearson de los 31 schwannomas vestibulares (línea azul) y 9 controles (línea verde). Los schwannomas se pueden separar en dos o tres grupos, aunque ninguno de ellos tiene características comunes moleculares ni clínicas.

En los microarrays de expresión de miRNAs, el PCA también mostró una clara separación entre los controles y los schwannomas (Figura 1 del Artículo 4). En este caso, los nervios se dispersaron menos que los tumores, que aún así mostraron una gran homogeneidad. En los microarrays de metilación, cuando todos los sitios CpG fueron testados, mostraron una pequeña tendencia a agruparse por el sexo del paciente. Los nervios sanos quedaron desplazados a la periferia, no habiendo ninguna característica clínica ni molecular que agrupara los schwannomas. No obstante, algunos genes aparecieron desregulados tanto en microarrays de expresión génica como de miRNAs, al usar métodos supervisados de análisis entre schwannomas con diferentes características clínicas y moleculares. Por ejemplo, el miR-125b-2* apareció infraexpresado en aquellos tumores con mutación de *NF2*. Por este motivo, no descartamos variaciones de expresión y metilación entre tumores con distinto tamaño, patrón de crecimiento, u otras características tumorales.

Al testar nuestra serie de 4 schwannomas no vestibulares, los métodos no supervisados como clústeres de Pearson o análisis de componentes principales, tampoco nos ofrecieron separación visible con los schwannomas vestibulares. Sin embargo,

contrariamente a lo que obtuvimos al comparar schwannomas vestibulares con distintas características clínicas y moleculares, en este caso los métodos supervisados (t-test), nos ofrecieron claras diferencias en varios genes entre los schwannomas vestibulares y los no vestibulares. Sin duda, los más llamativos fueron los genes HOX, que se distribuyen en cuatro clústeres; A, B, C y D, en diferentes cromosomas: 7p15, 17q21.2, 12q13 y 2q31 respectivamente. Las neoplasias no vestibulares presentaron un patrón más similar al de los controles no tumorales que al de los otros tumores en estos genes. Más aún, los resultados de microarrays de expresión de los genes HOX también confirmaron diferencias entre estos tipos tumorales (Figura 4 del Artículo 5). El reducido número de genes con este enorme grado de diferencias entre schwannomas vestibulares y no vestibulares hace suponer que, por norma general, los schwannomas de distintos orígenes tienen la mayor parte de su patrón epigenético muy similar, aunque en genes determinados se comportan de una manera más parecida al nervio de origen. Así mismo, conviene tener presente el reducido número de schwannomas no vestibulares empleados, por lo que se requieren estudios con mayor número de muestras.

4.4 VALIDACIÓN DE LOS ANÁLISIS DE EXPRESIÓN

Para comprobar la robustez de los resultados de los microarrays de expresión, se validaron 48 genes mediante PCR en tiempo real. En todos los genes seleccionados se mantuvo la tendencia de sobre, infraexpresión, o bien sin cambio entre tumores y nervios. En la Figura 5 se muestran estas tendencias. Como se hace evidente en esta figura, la valoración de un gen como sobre o infraexpresado por microarrays es muy fiable, al

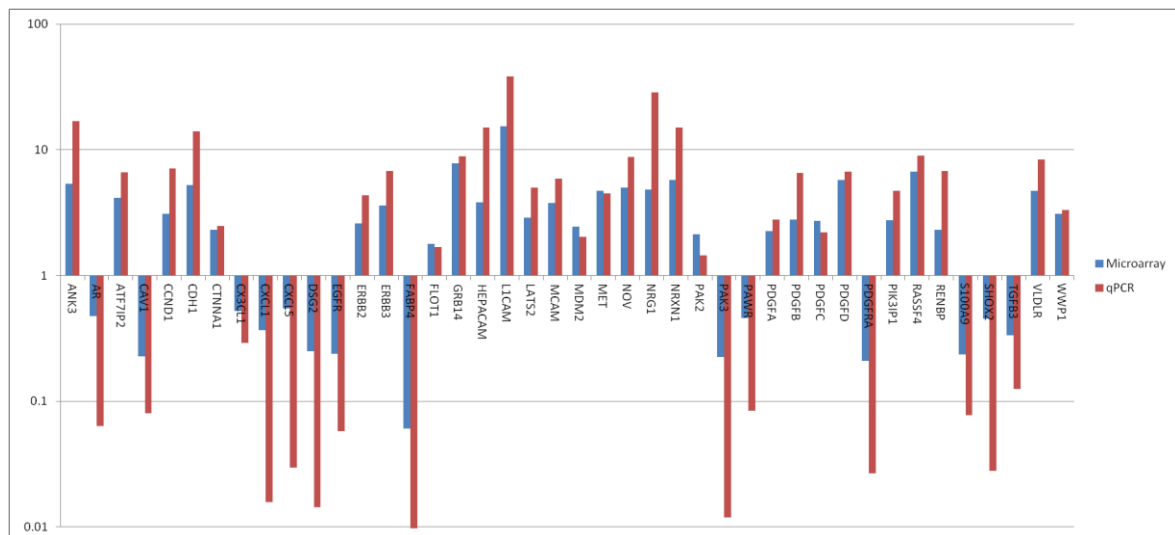


Figura 5. Gráfico que muestra los valores obtenidos en los genes validados por PCR en tiempo real (en rojo) y los hallazgos medidos mediante microarrays (en azul). En la mayoría de los casos, el valor obtenido mediante PCR en tiempo real es mayor al de los microarrays, aunque en todos los genes validados se conserva la tendencia.

No obstante, para cuantificar esa desregulación, los microarrays no son un método robusto, debido a la diferencia de rango dinámico con que cuentan ambas técnicas. Las mayores diferencias de variación en la expresión se encontraron en los genes *FABP4*, *AR*, *PAK3*, *CXCL1*, *CXCL5* y *SHOX2*, entre aquellos genes infraexpresados; y en *NRG1*, *NRXN1*, *HEPACAM* y *ANK3* entre los sobreexpresados. En el gen flotilina 1 -*FLOT1*-, había una tendencia a la sobreexpresión en los microarrays -incremento de 1.79 veces en schwannoma-. Cuando fue testado por PCR a tiempo real, se encontró un valor muy similar -1.67 veces-, por lo que, aunque se reflejó un ligero incremento en la expresión, no pudo ser identificado como desregulado debido al umbral usado. El gen *PAK2*, sobreexpresado por microarrays -2.1 incrementos en los schwannomas-, no se validó

mediante PCR en tiempo real -no se detectó diferencia suficiente entre las medias-, siendo el único gen desregulado que no pudo ser refrendado por esta técnica de todos los testados.

En la validación mediante PCR en tiempo real de miRNAs -que también cumplió lo identificado en los microarrays en todos los miRNAs analizados-, la variación de rango dinámico fue mucho más acentuada, sobre todo en los miRNAs infraexpresados (Figura 6). Por tanto, la validación en tiempo real indica que, en estos 6 miRNAs en concreto, más que fenómenos de modulación de la expresión, se dan mecanismos de desactivación total de la transcripción en los schwannomas.

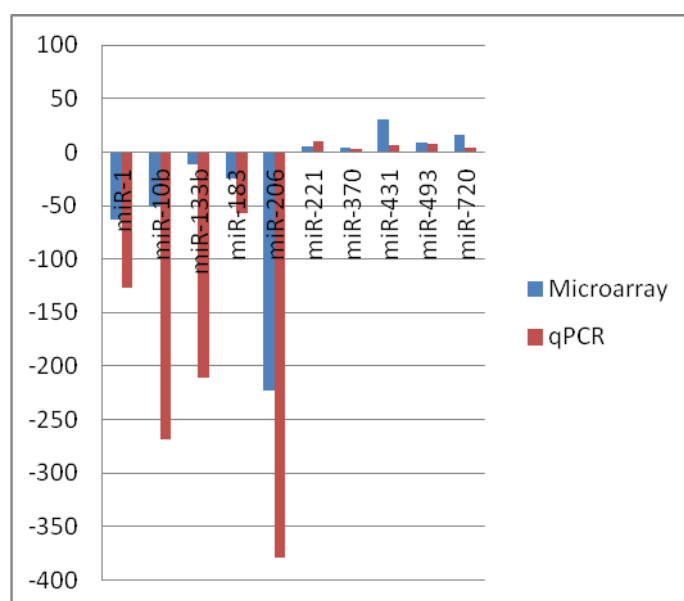


Figura 6. Validación de 10 miRNAs con expresión diferencial entre schwannomas y controles. El rango dinámico de los infraexpresados es mucho mayor que en los sobreexpresados.

4.5 GENES INVOLUCRADOS EN MIELINIZACIÓN

Tanto en los microarrays de expresión como en los de metilación, se encontraron alteraciones en numerosos genes descritos en procesos de mielinización, así como

específicos en la diferenciación de las células de Schwann (Mirsky *et al*, 2008). Desde las menos diferenciadas células de la cresta neural hasta las células de Schwann mielinizantes maduras, hay dos episodios intermedios: las células precursoras de las células de Schwann y las células de Schwann inmaduras. Cada una de estas etapas tiene características propias de expresión, por lo que su identificación en base a este parámetro es relativamente robusta. Los schwannomas comparten algún marcador de expresión con todas las etapas, por lo que encasillar este tumor con alguna en concreto no parece adecuado (Figura 7).

CDH19, que solo se da en la etapa de precursores de células de Schwann, mostró sobreexpresión en los schwannomas. Del grupo de las proteínas "S100 Calcium Binding Protein" -S100-, uno de los marcadores clásicos para reconocer schwannomas mediante inmunohistoquímica, el gen *S100B* fue encontrado sobreexpresado e hipometilado, mientras que 4 componentes de esta familia de genes -*S100A3*, *S100A9*, *S100A12* y *S100P*- aparecieron infraexpresados. En el caso del gen de la "S100 calcium binding protein P" -*S100P*-, además se encontró hipermetilación aberrante, lo que podría sugerir mecanismos epigenéticos participando en el silenciamiento del gen. Otros genes relacionados con procesos de mielinización aparecieron desregulados y con diferente patrón de metilación en los schwannomas. Por ejemplo, el gen "peripheral myelin protein 2" -*PMP2*-, se encontró sobreexpresado e hipometilado, mientras que el gen "myelin oligodendrocyte glycoprotein" -*MOG*- infraexpresado e hipometilado. El gen "myelin basic protein" -*MBP*- productor de una de las proteínas más abundantes de las vainas de mielina, presentó fenómenos de metilación compatibles con splicing alternativo (Figura 8); mientras que los promotores de las isoformas pequeñas del gen aparecieron hipometiladas, los promotores

de las isoformas más largas mostraron hipermetilación. Por tanto, parece que schwannomas y tejido control podrían expresar diferentes isoformas del gen. A nivel de expresión, *MBP* no presentó cambios entre los schwannomas y los controles no tumorales.

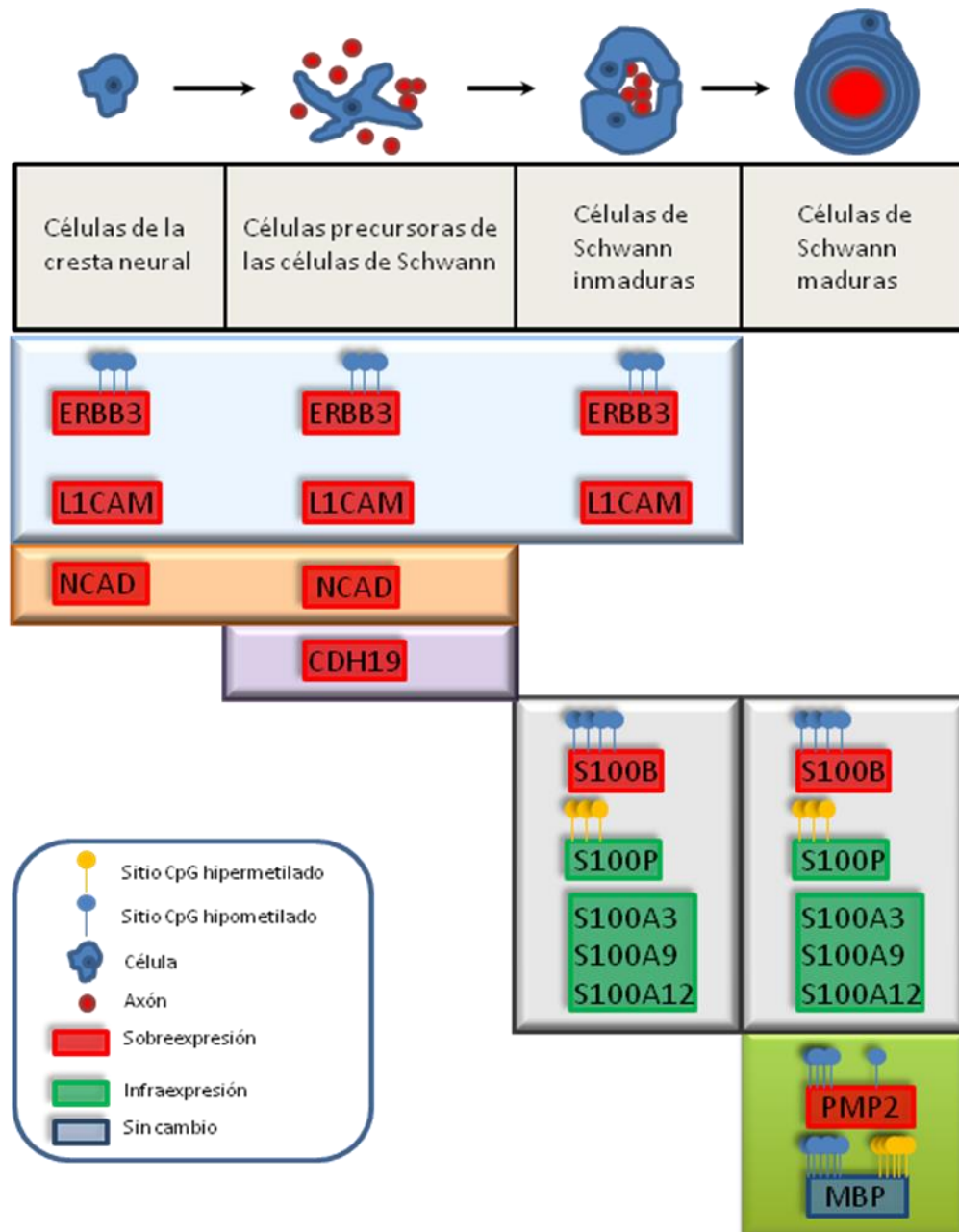


Figura 7. Etapas del desarrollo de las células de Schwann, desde las células de la cresta neural a las células de Schwann maduras. En cada etapa, se muestran genes que aparecieron desregulados en los microarrays de expresión, así como el patrón de metilación de los mismos. El gen *MBP*, sin cambios en expresión, presentó un patrón particular de metilación compatible con splicing alternativo.

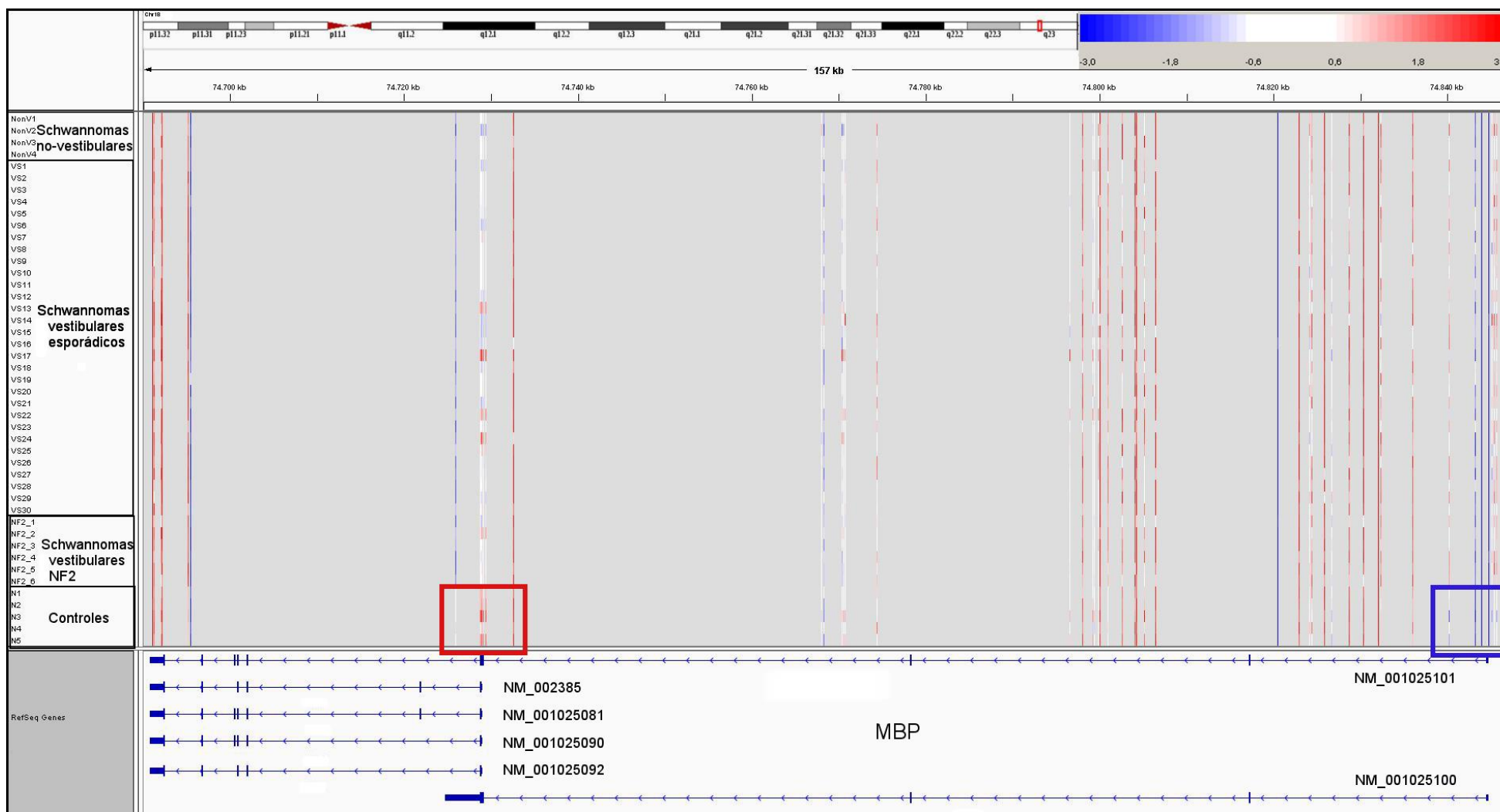


Figura 8. Patrón de metilación del gen *MBP*. La intensidad roja corresponde a hipermetilación, mientras que la azul a hipometilación (leyenda arriba a la derecha). Los sitios CpG de la región promotora de las isoformas cortas del gen (las cuatro centrales), aparecen hipometilados en los tumores (encima del recuadro rojo), mientras que las isoformas largas aparecen hipermetiladas en los tumores (encima del recuadro azul).

4.6 METILACIÓN Y EXPRESIÓN DEL GEN *NF2*

En cuanto al patrón de metilación y expresión en el gen *NF2*, no se encontró ningún tipo de alteración, presentando los schwannomas valores idénticos a los controles en ambos estudios (Figura 9).

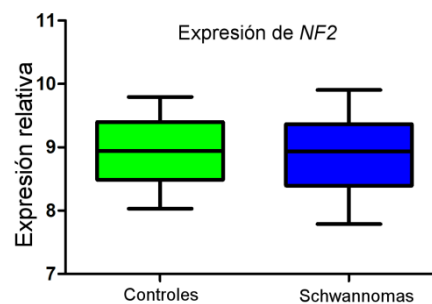


Figura 9. Diagrama de cajas que refleja la expresión del gen *NF2* en schwannomas y controles sanos. Como se aprecia, no hay diferencias estadísticas entre ellos. Datos obtenidos de los microarrays de expresión.

4.7 ALTERACIONES EN RECEPTORES TIROSINA QUINASA

Uno de los grupos de proteínas que más atención han recibido por sus aplicaciones clínicas son los receptores tirosina quinasa, ya que su activación aberrante o silenciamiento se asocia a numerosos tipos tumorales, como el receptor ErbB2 en cáncer de mama (Eccles, 2011) o MET en cáncer de pulmón y mesotelioma (Cipriani *et al*, 2009). La Tabla 6, recoge los datos de expresión de tirosina quinasa de interés en los schwannomas vestibulares, así como la metilación de sitios CpG de cada gen en los casos en los que hubiera. La mayoría de los receptores desregulados presentaron sobreexpresión, lo que las haría mejores dianas terapéuticas a través de tratamientos basados en su inhibición (Tsai & Nussinov, 2013; Fauvel & Yasri, 2014).

Tabla 6. Algunos de los receptores de tirosina quinasa desregulados en los schwannomas vestibulares.

Gen	Descripción	Cromosoma	P-valor	Diferencia	Metilación
MERTK	Tirosina quinasa c-mer	2	0.0005	3.48	
FER	Tirosina quinasa fer	5	0.0006	2.95	1 hipo
TYRO3	TYRO3 protein tyrosine kinase	15	0.0015	2.92	
NTRK2	Receptor neurotrófico tirosina quinasa tipo 2	9	0.0053	2.68	
BTK	Tirosina quinasa Bruton agammaglobulinemia	X	0.0000	2.59	
DDR1	Tirosina quinasa del dominio discoidina 1	6	0.0023	2.39	2 hipo
SYK	Tirosina quinasa del bazo	9	0.0032	2.14	
AATK	Tirosina quinasa asociada a apoptosis	17	0.0001	2.06	
AXL	Tirosina quinasa del receptor AXL	19	0.0021	2.02	1 hipo
ERBB3	Receptor del factor de crecimiento epidérmico humano tipo 3	12	0.0002	3.62	
ERBB2	Receptor del factor de crecimiento epidérmico humano tipo 2	17	0.0000	2.61	1 hipo
NTRK3	Receptor neurotrófico tirosina quinasa tipo 3	15	0.0038	-2.05	
EGFR	Receptor del factor de crecimiento epidérmico humano tipo 1	7	0.0000	-4.19	

La columna de metilación solamente incluye los sitios CpG de regiones promotoras, 5'UTR y primer exón.

4.8 ADHESIÓN EN SCHWANNOMAS VESTIBULARES

Una veintena de genes relacionados con funciones de adhesión se identificaron sobreexpresados en nuestros estudios (Tabla 7). Entre ellos se incluyen algunos de los genes codificantes de integrinas, cadherinas y genes de adhesión en procesos neuronales. En cambio, en los genes infraexpresados no se identificaron integrinas, así como solamente un gen de la familia de las cadherinas. En varios de los genes de adhesión alterados en schwannomas se encontraron procesos de regulación epigenética, aunque en algunos, como la integrina alfa E, la hipermetilación de la región promotora no se tradujo en infraexpresión. Los genes de las cadherinas no mostraron alteraciones epigenéticas que expliquen la sobreexpresión observada en varios de estos genes en schwannomas.

Tabla 7. Genes involucrados en adhesión desregulados en los schwannomas vestibulares.

Gen	Descripción	Cromosoma	P-valor	Diferencia	Metilación
ITGB8	Integrina beta 8	7	0.0010	5.19	
ITGB4	Integrina beta 4	17	0.0009	3.57	2 hipo 1 hiper
ITGA3	Integrina alfa 3	17	0.0009	2.88	
ITGA6	Integrina alfa 6	2	0.0005	2.64	
ITGAV	Integrina alfa V	2	0.0065	2.40	
ITGA2	Integrina alfa 2	5	0.0005	2.24	
ITGB1BP1	Proteína de unión 1 a la integrina beta 1	2	0.0043	2.09	1 hiper
CDH19	Cadherina 19	18	0.0001	10.77	
CDH1	E-cadherina	16	0.0002	5.25	
CDH2	N-cadherina	18	0.0005	4.50	
CDH6	K-cadherina	5	0.0003	2.67	
L1CAM	Molécula de adhesión celular L1	X	0.0000	15.39	
CHL1	Molécula de adhesión celular con homología a L1CAM	3	0.0002	8.52	4 hiper 1 hipo
NCAM2	neural cell adhesion molecule 2	21	0.0000	6.96	
NRCAM	neuronal cell adhesion molecule	7	0.0002	5.49	1 hipo 1 hiper
NCAM1	neural cell adhesion molecule 1	11	0.0004	5.00	
CADM4	Molécula de adhesión celular 4	19	0.0006	3.89	
HEPACAM	Molécula de adhesión de hepatocitos	11	0.0009	3.84	3 hipo
MCAM	Molécula de adhesión de melanoma	11	0.0002	3.77	
ALCAM	Molécula de adhesión de activación de leucocitos	3	0.0015	3.22	
CDH20	Cadherina 20	18	0.0174	-2.13	
ICAM1	Molécula de adhesión intercelular 1	19	0.0475	-2.04	
ASAM	Molécula de adhesión específica de adipocitos	11	0.0000	-3.70	
VCAM1	Molécula de adhesión vascular 1	1	0.0147	-2.34	

La columna de metilación solamente incluye los sitios CpG de regiones promotoras, 5'UTR y primer exón.

4.9 DESREGULACIONES POR CROMOSOMAS

Cada medición realizada en los microarrays de ARN mensajero, miRNA y metilación, se puede asignar a una localización concreta en los cromosomas. Debido a la naturaleza del cáncer y a las numerosas alteraciones cromosómicas que se pueden producir en el proceso neoplásico, se establecieron porcentajes de las mediciones

efectuadas, para buscar zonas en las que pudiera haber una especial predilección por el exceso o la carencia de alteraciones moleculares (Tabla 8).

Tabla 8. Porcentajes de desregulación por cromosomas.

CHR	Sobreexpresión			Infraexpresión			Porcentajes totales		
	Hipo-metilación	mRNA	miRNA	Hiper-metilación	mRNA	miRNA	Metilación total	mRNA	miRNAs
1	2,33	5,87	22,95	1,82	2,85	4,92	4,15	8,72	27,9
2	2,86	6,93	8,70	2,04	2,49	13,04	4,90	9,42	21,7
3	2,43	7,16	5,71	1,76	2,56	5,71	4,19	9,72	11,4
4	2,17	10,06	0,00	1,53	4,08	6,45	3,70	14,14	6,5
5	2,39	8,02	6,67	1,98	2,37	13,33	4,38	10,38	20
6	2,22	7,38	17,65	1,96	1,93	11,76	4,18	9,30	29,4
7	2,40	7,79	9,52	1,66	2,26	16,67	4,06	10,05	26,2
8	2,44	8,13	3,70	2,25	3,58	11,11	4,69	11,71	14,8
9	2,00	5,39	3,33	1,57	2,69	13,33	3,57	8,08	16,7
10	2,75	9,37	4,35	1,93	2,02	8,70	4,69	11,38	13
11	2,42	5,72	7,89	1,80	2,42	5,26	4,22	8,15	13,2
12	2,56	6,62	4,76	1,50	3,21	0,00	4,05	9,83	4,8
13	3,04	9,46	0,00	2,61	3,04	8,00	5,65	12,50	8
14	2,19	7,37	49,38	1,49	1,29	2,47	3,68	8,66	51,9
15	2,48	8,11	14,81	1,70	2,32	3,70	4,18	10,42	18,5
16	1,96	3,31	23,53	2,11	0,79	11,76	4,07	4,11	35,3
17	2,34	4,67	12,50	2,13	1,05	8,33	4,47	5,71	20,8
18	2,10	5,24	0,00	1,41	3,23	33,33	3,51	8,47	33,3
19	1,11	2,97	8,82	1,20	1,25	3,92	2,30	4,22	12,7
20	1,46	2,03	0,00	1,34	2,03	0,00	2,80	4,07	0
21	2,81	5,85	14,29	1,89	2,44	0,00	4,70	8,29	14,3
22	0,94	2,57	0,00	1,29	1,29	5,26	2,23	3,86	5,3
X	-	6,74	22,47	-	3,58	4,49	-	10,32	27

Los valores se desglosan por sobreexpresados, infraexpresados y porcentajes totales. Los sitios CpGs hipometilados se organizaron con los genes sobreexpresados, mientras que los hipermetilados con los infraexpresados. Los datos de metilación del cromosoma X no fueron tenidos en cuenta al no ser fiables debido a la hipermetilación en mujeres que distorsiona los resultados.

En la metilación diferencial entre schwannomas y controles, no hubo grandes variaciones entre los distintos cromosomas, fluctuando los rangos del 2.2% en el cromosoma 22 al 5.6% en el 13. En el caso de la expresión génica diferencial entre tumores y nervios sanos, la variación fue bastante mayor; desde el 2% en el cromosoma 20, al 10% en el 4 para los genes sobreexpresados; y del 0.8% en el autosoma 16 al 4% en el 4 entre los infraexpresados. Los miRNAs fueron, sin duda, los que presentaron una mayor diferencia de expresión entre cromosomas. Ningún miRNA fue encontrado sobreexpresado en los

cromosomas 4, 13, 18, 20 y 22; mientras que en otras localizaciones había numerosos como en el cromosoma 1 -23%-, 16 -23,5%- y especialmente en el 14 -49,4%-. Con la infraexpresión ocurrió un fenómeno similar, no habiendo ningún miRNA alterado en los cromosomas 12, 20 y 21; mientras que en el cromosoma 7 -16.7%- y el 18 -33.3%- se dieron porcentajes altos de desregulación.

El nivel de correlación entre metilación y expresión tanto de genes como de miRNAs, fue relativamente robusto -0.74, en una escala del 0 al 1- únicamente cuando se comparó el porcentaje de genes hipometilados y el número de genes sobreexpresados. En el resto de parámetros no hubo correlación. El cromosoma 22, que habitualmente sufre pérdida de heterocigosidad en el brazo largo en los schwannomas vestibulares, destacó por ser el autosoma con menor número de genes desregulados en nuestros estudios de expresión, y también el menor número de genes con distinto patrón de metilación entre schwannomas y controles. Las mayores variaciones moleculares ligadas a los cromosomas se dieron sin duda en los miRNAs. Casi un 50% de los miRNAs disponibles en los microarrays, sufrieron sobreexpresión en el cromosoma 14, la mayoría localizados en un conocido clúster de genes no codificantes de proteínas en el brazo largo de este autosoma.

4.10 ANÁLISIS DE ENRIQUECIMIENTO

En estos estudios, como es habitual en los trabajos de datos masivos con centenares o miles de datos que integrar, se realizaron los análisis de enriquecimiento. Los resultados de los análisis de enriquecimiento nos permitieron comparar grandes listas de genes y buscar rutas y términos de ontología génica especialmente afectadas en los genes

dados. Mediante el uso de la lista de genes obtenida al comparar schwannomas vestibulares y nervios periféricos en microarrays de expresión génica con la plataforma DAVID (Huang et al. 2009a; Huang et al. 2009b), identificamos numerosas rutas desreguladas. Los análisis de genes sobreexpresados e infraexpresados se realizaron independientemente (Tabla III del Artículo 3). La lista de genes sobreexpresados, tuvo como proceso más llamativo el desarrollo neuronal, la axonogénesis y la morfogénesis de proyecciones neuronales; así como procesos de lisosoma y vacuolas líticas. En la lista de genes infraexpresados, lo más llamativo fue el enriquecimiento de dominios EGF. Los datos proporcionados por el análisis de microarrays de metilación también fueron testados mediante análisis de enriquecimiento, aunque los genes que solo incluían sitios CpG diferencialmente metilados en el cuerpo génico fueron eliminados debido a la falta de consenso en la funcionalidad de la metilación de esta zona. Los genes hipometilados en schwannomas en regiones promotoras se mostraron enriquecidos en proyección axonal, dominios sema-plexina, secuencias homeobox y señalización Ras. Las funciones de los genes hipermetilados correspondían a motilidad celular, adhesión y citoesqueleto.

El análisis de los miRNAs, resulta más complejo y menos fiable mediante estos métodos de enriquecimiento. Previamente a insertar la lista de genes de interés para su análisis, hay que buscar qué genes son regulados por cada miRNA. Al ser cada miRNA potencialmente capaz de regular miles de mensajeros, la tarea de encontrar rutas comunes para las decenas de miRNAs desregulados se vuelve inabordable. Así, se consideraron en nuestro estudio solamente aquellos genes validados como dianas de miRNAs mediante experimentación. No obstante, este patrón puede inducir sesgos, ya que aquellas funciones más estudiadas como cáncer suelen tener mayor representación. Aún teniendo

en cuenta estas limitaciones, encontramos, de nuevo, enriquecimiento en genes implicados en el desarrollo del sistema nervioso como elementos desregulados.

4.11 CARACTERÍSTICAS CLÍNICAS Y MICROARRAYS

En los análisis mutacionales del gen *NF2*, así como en los microarrays, los datos obtenidos fueron comparados con las características clínicas de cada schwannoma. Los diferentes parámetros clínicos usados fueron: el sexo del paciente, origen del tumor -asociado a *NF2* o esporádico-, el lado afectado, la consistencia tumoral -sólido o quístico-, localización del tumor en la resonancia magnética -invasión del fundus del conducto auditivo interno, compresión del tronco cerebral, etc-. Las características moleculares comparadas entre los schwannomas fueron la presencia o no de mutaciones de *NF2* por dHPLC y/o MLPA, así como la pérdida de heterocigosidad del cromosoma 22.

Al comparar el lado de afectación, encontramos el gen *CST1* sobreexpresado en los schwannomas desarrollados en el lado izquierdo, así como hipermetilación del gen *PSAPL1* en aquellos del derecho. Los pacientes de schwannomas vestibulares que en la resonancia el tumor llegaba al fundus, presentaron 10 genes sobreexpresados - *CCDC80*, *CD3E*, *CLEC4E*, *EFEMP1*, *F13A1*, *GZMK*, *IGJ*, *KLRK1*, *ST8SIA6* y *ZBTB16*- y dos infraexpresados -*FREM2* y *MSTN*-.

Al comparar los tumores según el sexo del paciente, encontramos un miRNA sobreexpresado en hombres -miR-204- y otro en mujeres -miR-143*-. Los estudios de expresión génica mostraron 11 genes localizados en el cromosoma Y fuertemente sobreexpresados en hombres, lo que sirvió como control de la correcta clasificación en las

muestras. Asimismo, en los microarrays de metilación usamos la hipermetilación de uno de los cromosomas X en mujeres para comprobar el orden correcto. Aparte de los genes localizados en los cromosomas sexuales, encontramos hipometilación en hombres de 4 sitios CpG en el gen *TLE1*, e hipermetilación en dos CpG del gen *FOXP3*.

En los schwannomas quísticos, encontramos hipermetilación de un CpG del gen *SHOX2* y del *RMND5B*. También hallamos sobreexpresión de miR-195* y miR-885 en los schwannomas sólidos, e infraexpresión del miR-1274.

En los fumadores y exfumadores -en la mayoría de los casos eran hombres, por lo que no se tienen en cuenta cromosomas sexuales-, se identificó la sobreexpresión del gen *ZBTB16*, e infraexpresión de los genes *CNTN1*, *GPR83*, *KCNJ10*, *LRRN1* y *SLC24A2*.

En los schwannomas de pacientes de NF2, al compararlos con los esporádicos, los genes *PTPRN2* y *WDR66* mostraron hipermetilación en 2 sitios CpG cada uno.

En cuanto a alteraciones del gen NF2, los schwannomas con alguna alteración del gen presentaron hipometilación en un sitio CpG de los genes *NRXN2*, *PAX6* y *PAX9*, entre otros. El miR-195*, apareció infraexpresado en los pacientes con LOH del cromosoma 22.

Aunque no se han detallado todos los genes y miRNAs desregulados y sitios CpG con patrón de metilación alterado, lo anteriormente recogido da una idea de que entre los schwannomas con diferentes aspectos moleculares sobre NF2 y clínicos pueden existir distintas características genéticas intrínsecas. No obstante, lo sutil de la mayoría de estas asociaciones -salvo al comparar el sexo-, hacen necesarios estudios más en detalle sobre los patrones hallados en relación a la clínica.

4.12 SCHWANNOMAS Y MENINGIOMAS

La comparación de los schwannomas con los meningiomas en relación a su expresión con el tejido sano correspondiente, proporcionó una lista de genes cuyo patrón se compartía en ambas neoplasias. Estos rasgos comunes, se podrían aplicar en terapias dirigidas a pacientes de NF2 que sufren los dos tipos tumorales. Entre los genes infraexpresados en ambos tumores (Tabla 2 del Artículo 6) se incluyen el inhibidor de proteinasa 16 -*PI16*- o el receptor del factor de crecimiento de fibroblastos 2 -*FGFR2*-. Entre los sobreexpresados (Tabla 1 del Artículo 6), se incluyen genes como *PDGFD*, *CX3CR1* o *MET*. Aunque los genes desregulados en schwannomas y meningiomas con respecto a su tejido control no eran muy numerosos en términos totales -47 sobreexpresados y 35 infraexpresados-, encontramos varios como los arriba descritos, que podrían ser dianas para ensayos en ambos tipos tumorales.

5. DISCUSIÓN GENERAL

5. DISCUSIÓN GENERAL DE LOS TRABAJOS

Los microarrays han supuesto una revolución en el estudio de la biología y la medicina debido a la gran cantidad de datos que han sido capaces de ofrecer a los investigadores. Desde los primeros modelos de expresión génica en los que unas decenas o centenares de genes eran testados, se ha evolucionado hasta alcanzar centenares de miles de mediciones individuales. Además, se han desarrollado otros modelos para buscar diferentes alteraciones como los microarrays de metilación, de polimorfismo de nucleótido simple o los de hibridación genómica comparada. Éstos últimos microarrays son muy útiles para detectar aberraciones cromosómicas, y se han usado en pacientes con NF2 (Bruder *et al*, 2001), encontrando LOH del cromosoma 22 en igual proporción de pacientes con una forma suave, moderada o severa de la enfermedad.

La principal alteración molecular de los schwannomas vestibulares es la mutación del gen *NF2*, seguida de la pérdida de heterocigosidad del brazo largo del cromosoma 22, donde el locus de este gen se encuentra en 22q.12.2. Aparte de las múltiples funciones de *NF2*, la biología molecular de estos tumores permanece relativamente poco conocida, aunque gracias a las técnicas masivas, la información disponible se ha multiplicado durante los últimos años, a lo que han contribuido nuestros estudios.

Antes de establecer alteraciones de expresión y metilación mediante microarrays en nuestra serie de schwannomas vestibulares, realizamos una primera aproximación testando mutacionalmente el gen *NF2*. En la serie de 51 schwannomas vestibulares esporádicos, encontramos un 49% de las muestras con al menos 1 mutación de secuencia mediante PCR/dHPLC. En el estudio de Hadfield *et al*, (2010) sobre 104 pacientes,

encontraron un 66% de mutaciones, mientras que otros estudios el porcentaje baja al 34,8% (Martínez-Glez *et al*, 2009). Con otras técnicas, como por ejemplo secuenciación directa del transcrito de *NF2*, se han llegado a tasas del 76% (Aarhus *et al*, 2010). Así, los schwannomas utilizados estarían en un nivel de tasa de mutaciones intermedio. Al igual que en nuestros estudios, más de 2 eventos de desactivación sobre el gen *NF2* han sido descritos en pacientes con schwannomas vestibulares esporádicos (Aarhus *et al*, 2010). Este hecho puede sugerir una primera mutación en *NF2* común a todo el schwannoma en una célula de Schwann sana, seguido de alteraciones posteriores en dos células provenientes de la original. El mosaicismo para la mutación del gen *NF2* ocurre hasta en un 30% de los pacientes de *NF2*. En nuestro trabajo, encontramos 2 pacientes de schwannomas vestibulares esporádicos con la mutación también presente en la sangre periférica. Estos 2 sujetos podrían tener una forma suave de la enfermedad genética, ya que hasta ahora no presentaron otros síntomas que denoten la presencia de *NF2* aparte de sendos schwannomas vestibular. Aún así, no se descarta *NF2 de novo*.

La LOH del brazo largo del cromosoma 22 fue detectada en un 57% de los casos, prácticamente el mismo porcentaje que el hallado por Hadfield *et al*, (2010) que encontraron el 56%.

En aquellos tumores provenientes de pacientes con *NF2*, la práctica totalidad de ellos -86%- presentaban alguna alteración por mutación o LOH del cromosoma 22. En cambio, solamente un paciente fue hallado con la alteración en sangre periférica. En publicaciones previas con series de más de 700 pacientes de *NF2*, se ha detectado mutación en sangre periférica en el 26% de estos pacientes con schwannoma unilateral, mientras que el porcentaje se incrementa más -63%-, cuando es bilateral (Evans *et al*, 2007).

Por tanto, nuestra serie en estos pacientes confirma la dificultad que entraña en muchos casos localizar la alteración en tejido no tumoral.

Nuestros estudios mutacionales sobre *NF2* mediante PCR/dHPLC-MLPA y la pérdida de heterocigosidad del locus donde se aloja el gen, arrojan un patrón muy similar en porcentaje de alteraciones usando las mismas técnicas que otros estudios (Hadfield *et al*, 2010). Por lo tanto, podemos concluir que nuestra serie de schwannomas vestibulares esporádicos es representativa de lo ya descrito en la literatura en cuanto a alteraciones del gen *NF2*.

Conviene recalcar que, a pesar de los análisis llevados a cabo, una parte de los schwannomas vestibulares esporádicos no presentó ninguna alteración. Este hecho se hace patente en la totalidad de los estudios descritos previamente (Martinez-Glez *et al*, 2009; Hadfield *et al*, 2010; Aarhus *et al*, 2010). Está por verse si las nuevas técnicas de secuenciación masiva son capaces de detectar mutaciones en intrones u otras zonas adyacentes que afecten al gen, ya que parece evidente la falta de merlin funcional en la mayoría, si no todos, los schwannomas vestibulares (Stemmer-Rachamimov *et al*, 1997; Hitotsumatsu *et al*, 1997). A pesar de todo, otros mecanismos podrían intervenir en la desaparición del producto proteico de *NF2*, como veremos más adelante.

Aparte de las mutaciones encontradas, el gen *NF2* no presentó en las muestras estudiadas ninguna otra alteración tanto a nivel de expresión (Figura 9) como de metilación de sitios CpG. En estudios recientes (Koutsimpelas *et al*, 2012; Lee *et al*, 2012), tampoco se hallaron cambios que sugieran un patrón diferente de metilación. Por lo tanto, cambios epigenéticos ni de expresión parecen estar relacionados con la falta de proteína

merlin en los schwannomas vestibulares. No obstante, otros autores sí identificaron procesos epigenéticos en el gen *NF2* en más del 50% de las muestras (Kino *et al*, 2001).

Los umbrales usados para considerar un gen alterado o un CpG metilado, sin duda suponen uno de los puntos más controvertidos a la hora de interpretar los resultados en los microarrays. En nuestros estudios de expresión, tanto de genes codificantes como de miRNAs, hemos usado el umbral propuesto por el MAQC (Shi *et al*, 2006), esto es, al menos una diferencia del doble (o la mitad) entre grupos y un p-valor no astringente ≤ 0.05 . Con este umbral, según los estudios del MAQC, se consigue la mayor reproducibilidad de los resultados entre plataformas.

Para el procesamiento y análisis de los microarrays de metilación, utilizamos varios paquetes del programa estadístico R (<http://www.R-project.org>), detallados en el Artículo 5.

Para la correcta integración de los datos de estas técnicas, debemos tener presente la relación entre las moléculas que se estudian. Los miRNAs y el ARN mensajero, correlacionan por norma general de forma negativa, esto es, cuando un miRNA que participa en la regulación de un mensajero concreto y su expresión es elevada, la del mensajero en cuestión disminuiría. Este hecho es debido al mecanismo de acción del miRNA sobre el mensajero, uniéndose a la región 3'UTR de éste y provocando su degradación en el citoplasma. No obstante, hay que señalar que los miRNAs también se han descrito con funciones favorecedoras de la transcripción (Brevig & Esquela-Kerscher, 2010; Vasudevan, 2012). Así mismo, dentro del núcleo se han hallado miRNAs maduros y funcionales (Wei *et al*, 2014), cuyas funciones parecen estar relacionadas con la regulación de ARNs no codificantes (Liang *et al*, 2013). Teniendo esto presente, cada

pareja de miRNA y mensajero, debería ser testada empíricamente en cada tipo celular de interés antes de considerar que existe asociación entre ellas.

En el caso del vínculo entre la metilación de dinucleótidos de CpG del ADN y la expresión tanto de ARN mensajero como de miRNA, generalmente se considera que un gen con metilación en la región promotora, modularía su expresión reduciéndola. Los mecanismos sugeridos son que bien el complejo de transcripción no podría unirse con suficiente afinidad debido a la metilación de las citosinas o a la unión de proteínas específicas que dificultarían la transcripción (Lopez-Serra & Esteller, 2008). La metilación del ADN es ampliamente estudiada en cáncer, donde ha quedado patente su implicación en el desarrollo tumoral (Goelz *et al*, 1985) o en la respuesta terapéutica. Por ejemplo en glioblastoma multiforme se encontró una respuesta favorable a Temozolamida en aquellos pacientes con metilación de *MGMT* (Esteller *et al*, 2000). Sin embargo, los patrones de metilación aberrante del ADN no siempre suponen el silenciamiento del gen alojado en el locus. En ocasiones, especialmente en la zona codificante no promotora del gen, la metilación puede provocar un aumento de la expresión. Así mismo, diferentes isoformas de un mismo gen pueden expresarse o permanecer silenciadas mediante mecanismos epigenéticos (Maunakea *et al*, 2010). Este efecto se consigue mediante la metilación aberrante o bien la hipometilación del ADN en determinadas partes del locus de un mismo gen. Por lo tanto, conviene tener presente lo anteriormente expuesto a la hora de comparar los resultados de metilación y expresión, ya que datos aparentemente contradictorios podrían reflejar una relación biológica coherente. Por ejemplo, se podría dar hipometilación en un gen determinado y no producirse sobreexpresión, ya que ésta solo ocurriría si se activaran los factores de transcripción correspondientes.

En los estudios de expresión génica, miRNAs y metilación, coincidieron en el enriquecimiento de la axonogénesis y el desarrollo del sistema nervioso en genes hipometilados y en los genes sobreexpresados. Este hecho pone de relieve que tanto el transcriptoma como el patrón de metilación del ADN de los schwannomas están relacionado con formas celulares previas a las células de Schwann maduras. Esta hipótesis fue previamente propuesta por Hung *et al*, (2002) mediante técnicas inmunohistoquímicas. Así mismo, el gen “sex determining region Y box 2” -SOX2-, que actúa inhibiendo la mielinización y es un marcador de células de Schwann inmaduras (Le *et al*, 2005), presentó sobreexpresión en nuestra serie de schwannomas, resultado que concuerda con lo expuesto por Shivane *et al*, (2013) utilizando técnicas inmunohistoquímicas. Así, nuestros estudios genéticos concuerdan con lo previamente expuesto por otros autores mediante el estudio histológico de los schwannomas, con el hecho de que en estos tumores se dan procesos encaminados a inhibir genes relacionados con mielinización y maduración de células de Schwann.

Dentro de las numerosas vías moleculares que resultaron alteradas en los schwannomas vestibulares respecto al tejido control, destacamos varias en la presente discusión por la importancia de las mismas en este tumor, por su interés en el cáncer en general, o bien por lo marcado de estas perturbaciones. Las vías mostradas a continuación se basan en la descripción de las mismas obtenidas mediante recopilación bibliográfica. No obstante, la exactitud de estas vías en los schwannomas podría no ser completa, ya que en ciertos casos las interacciones entre proteínas, miRNAs y ARN mensajero, varían entre los distintos tipos celulares y también entre el tumor y su correspondiente tejido

sano. Por lo tanto, lo que se muestra a continuación es una simplificación de potenciales vías de señalización sobre las que se podrían aplicar tratamientos.

5.1 NEUREGULINA 1 Y LOS RECEPTORES ERBB2 Y ERBB3

El ligando Nrg1 y los receptores ErbB2 y ErbB3 (Figura 10), han sido descritos como activados en numerosos estudios de schwannomas, así como en otros tumores como en el cáncer de mama (Britsch, 2007). Estas tres proteínas son fundamentales para los procesos de mielinización de los axones periféricos, regulando entre otros parámetros el grosor axonal (Michailov *et al*, 2004).

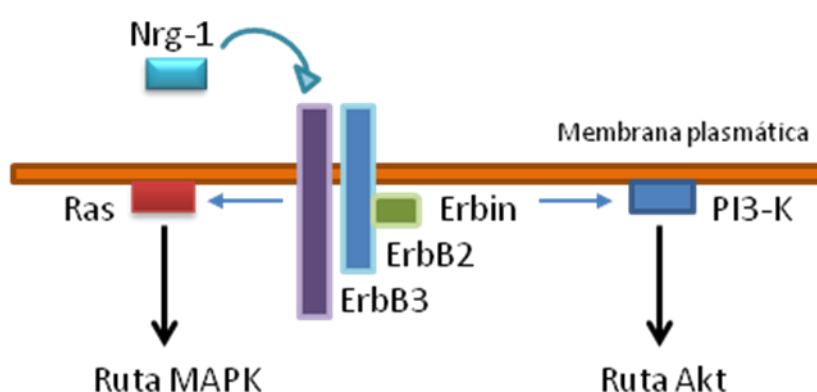


Figura 10. Mecanismo de acción en la ruta de la neuregulina 1 y sus receptores ErbB2 y ErbB3. El ligando neuregulina 1 se une a ErbB3, y éste dimeriza con ErbB2. Erbin regula la función y localización de ErbB2.

Se ha sugerido que la homocigosis en el polimorfismo Ile655Ile presente en *ERBB2* podría estar relacionado con el desarrollo de los schwannomas (Wang *et al*, 2011), aunque más estudios son necesarios debido al bajo número de casos de dicho trabajo. La activación de ErbB2, ErbB3 y Nrg1 en los schwannomas, parece producirse mediante sobreexpresión génica, algo que ha sido descrito en varios trabajos (Hansen *et al*, 2006; Doherty *et al*, 2008; Hansen & Linthicum, 2004). En nuestro estudio, comprobamos que estos tres genes presentan sobreexpresión, tanto por microarrays como por PCR en

tiempo real. El mecanismo subyacente de esta expresión aberrante, basado en nuestros hallazgos, parece estar más relacionado con la metilación que con la ganancia de copias o la amplificación génica. Los tres genes presentaron al menos 1 CpG hipometilado en la región promotora (Figura 11).

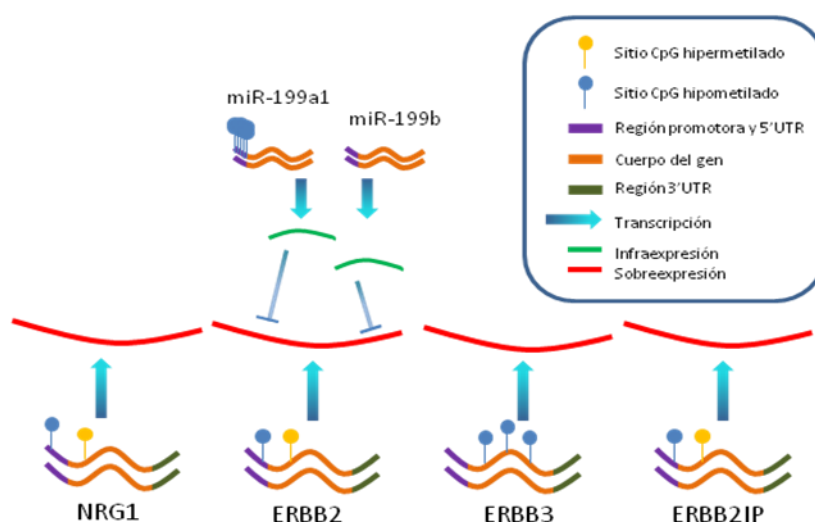


Figura 11. Patrón de expresión y metilación de los receptores ErbB. Se incluyen miRNAs relacionados con la abundancia del mensajero específico descrito en la literatura.

Además, los miRNAs miR-199a1 y miR-199b-5p, que han sido descritos como represores de ErbB2 en cáncer de ovario y en células de carcinoma de mama (He *et al*, 2013; Fang *et al*, 2013), se mostraron infraexpresados en nuestro estudio, lo que podría sugerir un mecanismo regulador análogo en los schwannomas para este receptor. La reducción de la expresión del el miR-199a1 pudo ser debida a factores epigenéticos, ya que mostró hasta 7 sitios CpG hipermetilados. Otra proteína involucrada en la señalización de Nrg1 y en la mielinización, llamada Erbin -ERBB2IP- (Tao *et al*, 2009), también mostró sobreexpresión en los schwannomas. Así, nuestros estudios, aparte de confirmar lo descrito en la literatura sobre la ruta de señalización que involucra a Nrg1,

ErbB2 y ErbB3, aporta mecanismos epigenéticos y miRNAs que podrían contribuir en la desregulación de esta ruta en los schwannomas.

5.2 RUTA DE LA AKT Y SU RELACIÓN CON MERLIN

Akt regula numerosos procesos en la célula, incluyendo la síntesis de proteínas, supervivencia, proliferación, metabolismo celular, angiogénesis y migración (revisado por (Manning & Cantley, 2007)). La activación por fosforilación de las diferentes isoformas de Akt se regula por varios mecanismos. Uno de los más comunes es el que induce la producción de fosfatidilinositol 3,4,5-trifosfato mediante la “phosphatidylinositol 3 kinase” -PI3K-, una quinasa que está anclada a la membrana. Un inhibidor de Akt, el “Phosphoinositide-3-Kinase-Interacting Protein 1” -*PIK3IP1*-, (Zhu *et al*, 2007) está sobreexpresado en nuestra serie. Una vez activada, Akt puede actuar sobre una amplia gama de proteínas, bloqueando la función de éstas o bien activándolas. La proteína merlin (Figura 12), que es fosforilada por Akt en la Treonina 230 y la Serina-315, se poliubiquitina y degrada mediante este mecanismo (Okada *et al*, 2009).

Merlin también es capaz de regular Akt a través de la inhibición de PIKE-L -*AGAP2*- (Okada *et al*, 2009) o del complejo mTORC1 (James *et al*, 2009). Por tanto, merlin y Akt se inhiben mutuamente. Al carecer de merlin funcional, parece evidente que la vía Akt presentará alteraciones en los schwannomas, como así describieron Hilton *et al*, (2009). Otras proteínas involucradas en esta ruta, mostraron desregulación de los niveles de expresión del mensajero en nuestros estudios (Figura 13).

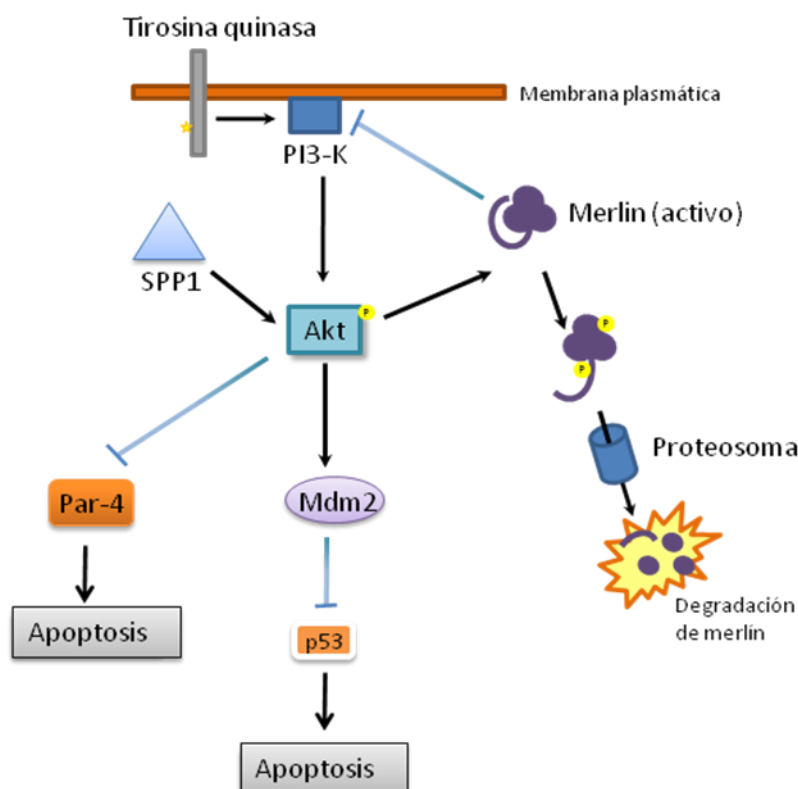


Figura 12. Ruta de Akt y su relación con merlin. Al ser merlin fosforilada por Akt, se degrada en el proteosoma. Así mismo, merlin activo (defosforilado) inhibe la señal de Akt mediante PIKE-L (no mostrado). La osteopontina (*SPP1*) es capaz de activar Akt, lo que podría provocar la degradación de merlin así como el bloqueo de la apoptosis mediante la inhibición de Par-4 y la activación de Mdm2.

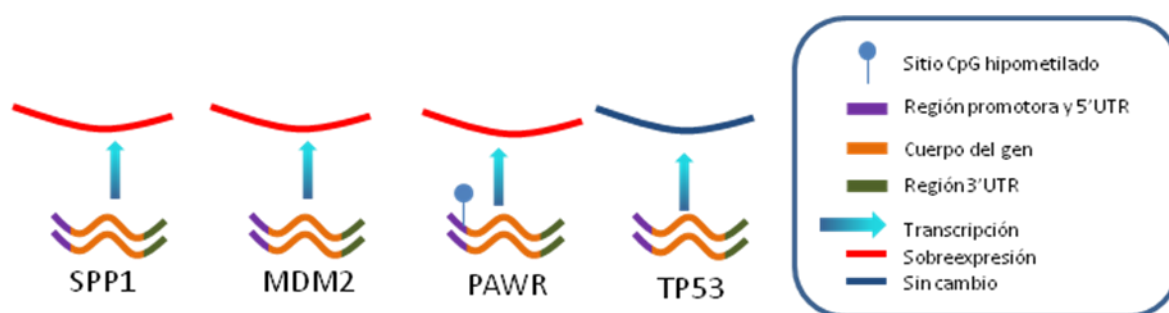


Figura 13. Patrones de expresión de los genes relacionados con la ruta de Akt.

El gen “mouse double minute 2 homolog” -*MDM2*-, que es fosforilado por Akt, presentó sobreexpresión, fenómeno común en procesos tumorales (Cahilly-Snyder *et al*, 1987; Fakharzadeh *et al*, 1991). Además, en nuestra serie tumoral hallamos al gen “Prostate Apoptosis Response-4” -*PAWR*- infraexpresado, algo que también ocurre con

frecuencia en neoplasias tanto a nivel de ARN mensajero como de proteína (Cook *et al*, 1999; Barradas *et al*, 1999; Moreno-Bueno *et al*, 2007; Zhang *et al*, 2011). La sobreexpresión de *MDM2* y la infraexpresión de *PAWR*, están asociadas al bloqueo de apoptosis. Al darse estos dos hechos en schwannomas, podríamos estar ante dos mecanismos que impidan la muerte programada en estos tumores. También hemos detectado diferencias en la metilación de los schwannomas comparados con los controles en el gen *PIK3R1*, cuyo patrón de metilación podría estar asociado a expresión diferencial de distintas isoformas por splicing alternativo.

5.3 OSTEOPONTINA

Como se ha detallado, a nivel de proteínas Akt es capaz de degradar en el proteosoma a merlin mediante su fosforilación, lo que conduce a la ubiquitinación. Un mecanismo alternativo para la activación de Akt fue recientemente descrito, a través de una fosfoglicoproteína llamada osteopontina, en cáncer de mama (Morrow *et al*, 2011). El locus de la osteopontina se localiza en el cromosoma 4, y el gen que la codifica es el *SPP1*. En nuestro estudio, *SPP1* fue hallado sobreexpresado en todas las muestras tumorales, siendo además esta expresión estable (Figura 14), con el mismo nivel en schwannomas con el gen *NF2* bialélicamente alterado o sin mutación.

Esto indica que, si bien la osteopontina podría eliminar merlin en aquellos schwannomas sin mutaciones de *NF2*, no parece que la sobreexpresión sea selectiva de aquellos tumores sin merlin alterado. Más bien parece que podría obedecer a la propia biología de los schwannomas.

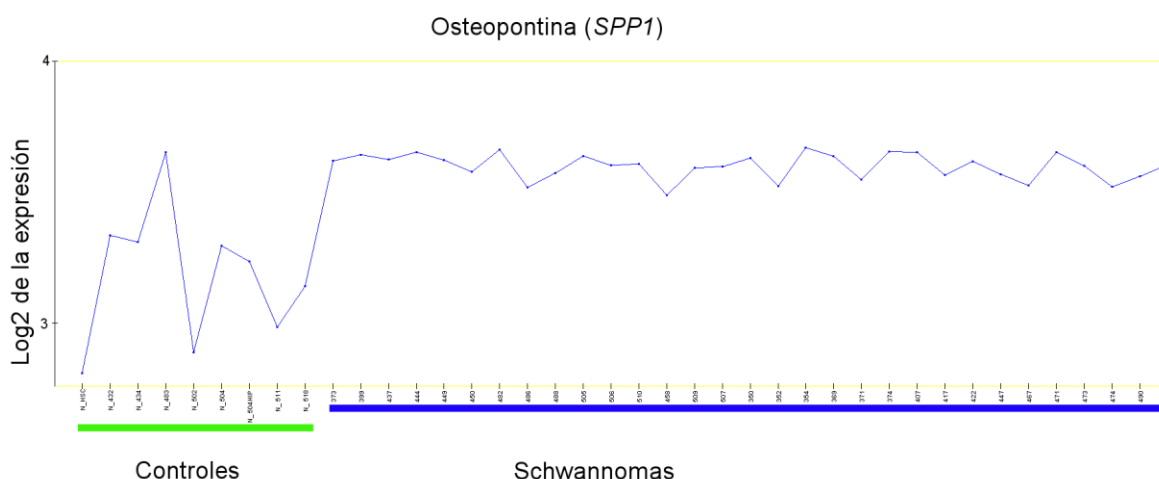


Figura 14. Niveles de expresión de osteopontina en los schwannomas vestibulares (azul) y los controles (verde). El valor de la expresión de cada muestra está obtenido directamente de los microarrays. Se aprecia cómo los tumores tienen prácticamente el mismo nivel de expresión entre ellos.

Por lo tanto, la sobreexpresión de osteopontina en schwannomas es un mecanismo que, de ser análogo a lo que ocurre en cáncer de mama (Morrow *et al*, 2011), eliminaría merlin en todos aquellos tumores en los que llega a producirse.

5.4 FACTORES DE CRECIMIENTO DERIVADOS DE PLAQUETAS (PDGF)

Un total de 6 genes codifican para las distintas isoformas de PDGF, en las que se incluyen 4 ligandos -A, B, C y D- codificados por los genes *PDGFA*, *PDGFB*, *PDGFC* y *PDGFD*; y dos receptores - α y β -, que provienen de los genes *PDGFRA* y *PDGFRB*. Los ligandos homodimerizan antes de unirse a los receptores, salvo las isoformas A y B que pueden heterodimerizar entre ellas. Así mismo, los receptores pueden formar homodímeros o heterodímeros. Las combinaciones de las uniones de los dímeros de ligando con los dímeros de receptores, están esquematizadas en la Figura 15. Las

principales vías de señalización activadas por la familia PDGF son las de Ras/MAPK y PI3K/Akt.

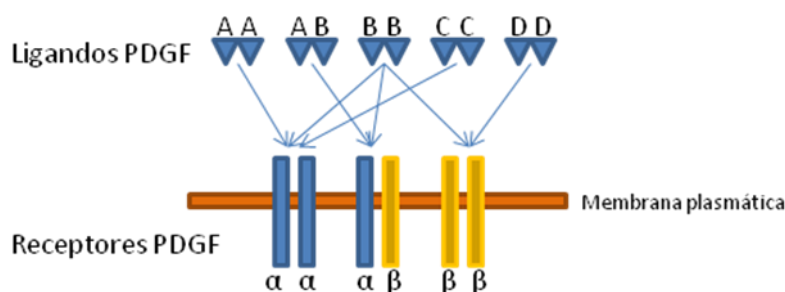


Figura 15. Combinaciones de homodimerización y heterodimerización entre los ligandos y receptores de la familia PDGF. Así mismo, se señalan los receptores que son capaces de activar los ligandos. A pesar de que algunos ligandos son capaces de activar varios receptores, no todos presentan la misma afinidad.

Nuestros datos de expresión en microarrays, validados por PCR en tiempo real, mostraron sobreexpresión en los 4 ligandos de la familia PDGF, muy marcada la alteración en los genes B y D -6.5 y 6.7 veces más expresados, respectivamente- que los controles no tumorales. En el caso de los receptores, mientras que el receptor PDGFR β no sufrió cambios de expresión, el receptor PDGFR α mostró una aguda infraexpresión (Figura 16).

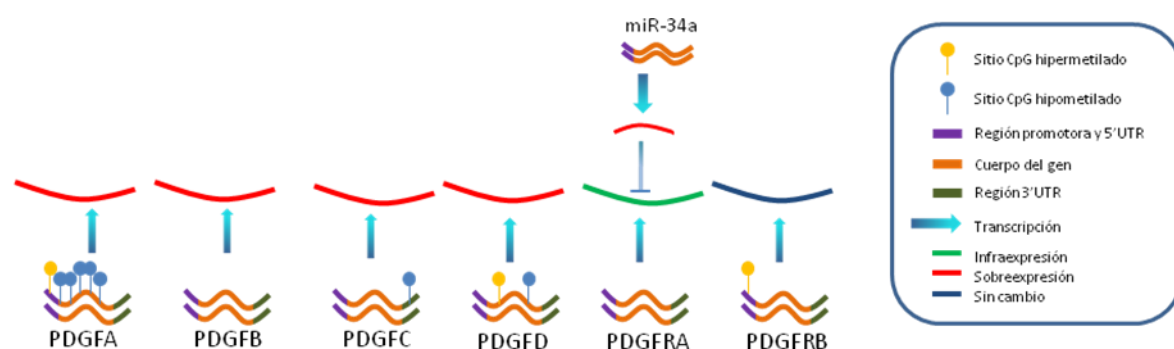


Figura 16. Patrones de expresión y metilación de la familia PDGF.

A pesar de que el patrón de metilación de *PDGFA* induciría a pensar en infraexpresión del mensajero -metilación en el promotor e hipometilación del cuerpo

génico-, este gen mostró sobreexpresión, aunque moderada en comparación con las isoformas B y D. Por otra parte, la infraexpresión de *PDGFRA* detectada en nuestros estudios, podría ser debida a la degradación del mensajero causada por la sobreexpresión de miRNA-34a en schwannomas. Esta relación entre el gen *PDGFRA* y el miRNA-34a se describió en el subtipo proneural del glioma (Silber *et al*, 2012), un tumor maligno del sistema nervioso y que podría ser equivalente en los schwannomas.

En trabajos previos sobre cultivos celulares, la adición del homodímeros del ligando B provoca la sobreexpresión de miR-9 (Yang *et al*, 2013), miR-221 (Davis *et al*, 2009) y miR-21 (Wei *et al*, 2013; Dey *et al*, 2012) (Figura 17). Estos tres miRNAs, sobreexpresados en nuestros estudios, podrían ser inducidos mediante la expresión aberrante del ligando PDGFB detectada también en nuestros trabajos.

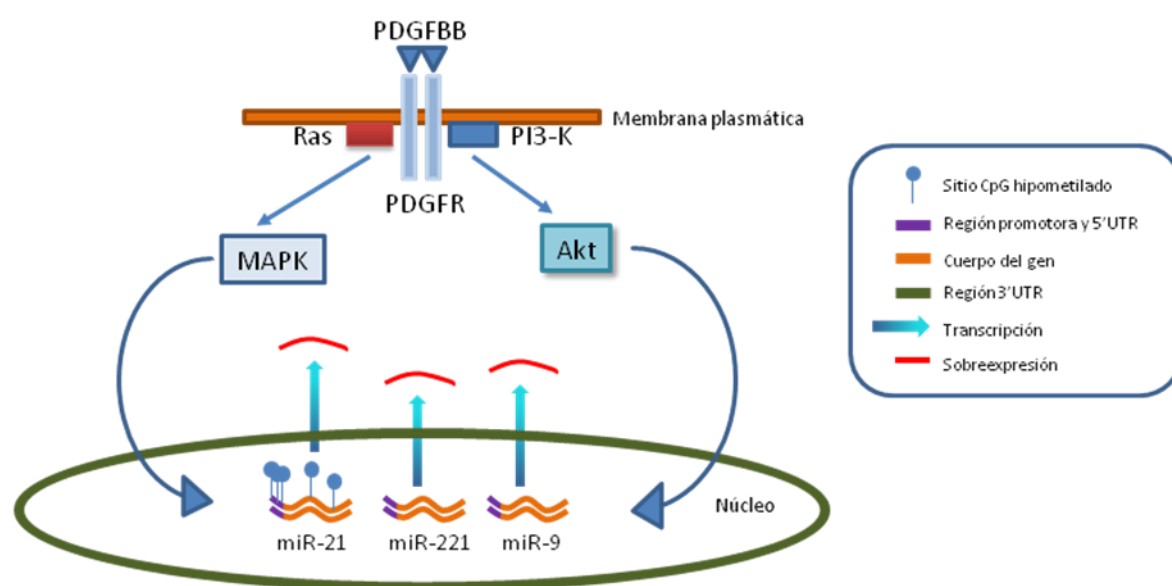


Figura 17. Mecanismo de acción general de la familia PDGF. El ligando PDGFB es capaz de provocar la expresión de varios miRNAs también encontrados sobreexpresados en nuestro trabajo.

El miR-21 presentó hipometilación en 6 sitios CpG -3 en la región promotora-, lo que podría incrementar su expresión mediante mecanismos epigenéticos. En conclusión,

nuestros datos de expresión indican que en schwannomas, la activación de los factores de crecimiento derivado de plaquetas mostrada en otros estudios, parece tener más relación con la forma β del receptor y ligandos que de la forma α , lo que habría que tener presente para un bloqueo terapéutico específico.

No obstante, una validación específica debería ser realizada en cada miRNA, ya que, por ejemplo, el miR-21 reduce su expresión en gliomas por el estímulo de PDGFB (Costa *et al*, 2012).

5.5 RUTA DEL RECEPTOR TIROSINA QUINASA C-MET

El gen del receptor del factor de crecimiento para hepatocitos -*MET*-, codifica un receptor de membrana con actividad proteína quinasa involucrado en numerosos procesos biológicos como morfogénesis, reparación de daños o metástasis en cáncer (Trusolino *et al*, 2010). En nuestros estudios, *MET* se halló sobreexpresado tanto por microarrays como por PCR en tiempo real en los schwannomas vestibulares. Además, 3 sitios CpG aparecieron hipometilados en este gen, según los datos de los microarrays de metilación, lo que podría explicar su expresión aberrante. La sobreexpresión en *MET* es, tras la amplificación, la forma más común de activación de este oncogén en tumores (Comoglio *et al*. 2008). Numerosas neoplasias presentan esta sobreexpresión, como por ejemplo cáncer de tiroides (Di Renzo *et al*, 1992), colorectal (Hiscox *et al*, 1997), de ovario (Di Renzo *et al*, 1994), de páncreas (Furukawa *et al*, 1995), o de mama (Lengyel *et al*, 2005). En schwannomas, mediante técnicas inmunohistoquímicas, la proteína MET fue hallada en los 8 tumores testados (Moriyama *et al*, 1998).

Por otra parte, existe una familia de miRNAs llamada myomiRs, que podrían tener un papel importante en la sobreexpresión de *MET*. Los myomiRs reciben este nombre porque se encuentran conservados en la musculatura de diversos animales, desde *Drosophila* a humanos. Están formados por 3 clústeres homólogos -miR-1-1/miR-133a-2, miR-1-2/miR-133a-1, y miR-206/miR-133b - y se localizan en tres regiones cromosómicas diferentes -20q13.33, 18q11.2 y 6p12.2 respectivamente-. En nuestros estudios de microarrays en schwannomas vestibulares, los myomiRs aparecieron infraexpresados, además de ser validados por PCR en tiempo real. Este grupo de miRNAs, aparece desregulado en numerosos tipos tumorales (Nohata *et al*, 2012; Yip *et al*, 2011; Datta *et al*, 2008; Nasser *et al*, 2008; Fleming *et al*, 2013), además de ser relacionado con el silenciamiento de *MET* (Yan *et al*, 2009; Hu *et al*, 2010; Taulli *et al*, 2009; Reid *et al*, 2012). Por lo tanto, la infraexpresión de los myomiRs -probablemente eliminación total de su expresión, debido a los valores de PCR en tiempo real-, podría tener relación con la sobreexpresión de *MET* en schwannomas vestibulares al no poder bloquearlo. Este silenciamiento no parece estar relacionado con procesos de metilación.

El factor de crecimiento para hepatocitos -HGF- es un ligando que, al unirse a *MET*, provoca la homodimerización y fosforilación de dos residuos de tirosina del receptor. Además, *MET* se puede unir a otros receptores de membrana que modulen esta activación (Figura 18), pudiendo incluso activarse de manera independiente a HGF.

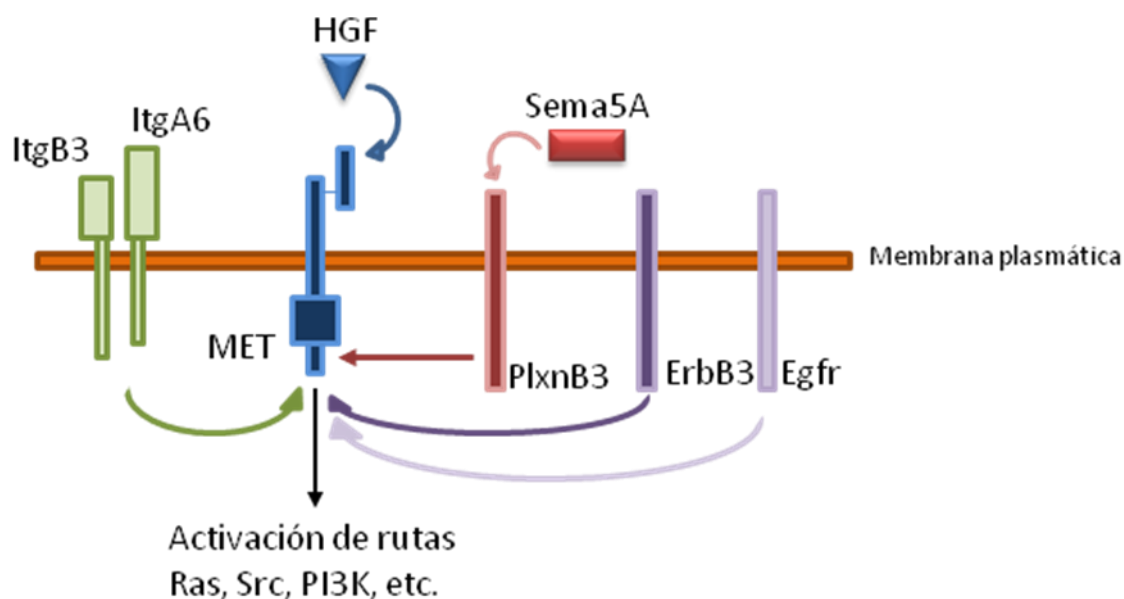


Figura 18. Diversos mecanismos de activación de MET. Aparte de la clásica unión con su ligando, MET puede activarse mediante un amplio abanico de receptores. Cada una de las formas de activación, implica diferencias con respecto a las demás, lo que confiere a MET gran versatilidad.

En nuestro estudio, encontramos varios de estos moduladores de MET desregulados en los schwannomas vestibulares (Figura 19). En uno de ellos, el gen codificador de la semaforina 5A -*SEMA5A*-, se encontró hipometilado en 3 sitios CpG, por lo que este ligando podría modular su expresión a través de mecanismos epigenéticos. En conclusión, tanto el oncogén MET como numerosos genes que codifican proteínas potencialmente activadoras de éste, presentaron sobreexpresión. Este hecho podría provocar la activación de rutas como Ras o PI3K, con la consiguiente inhibición de apoptosis o el aumento de la proliferación celular (Fresno Vara *et al*, 2004).

A día de hoy, existen numerosos ensayos clínicos dirigidos a bloquear la acción de HGF/MET en diversos tumores. Los mecanismos de esta inhibición son por anticuerpos monoclonales o bien pequeñas moléculas (Cañadas *et al*, 2010). Por tanto, MET es un firme

candidato como diana terapéutica en schwannomas, aunque ensayos funcionales previos son necesarios en este aspecto.

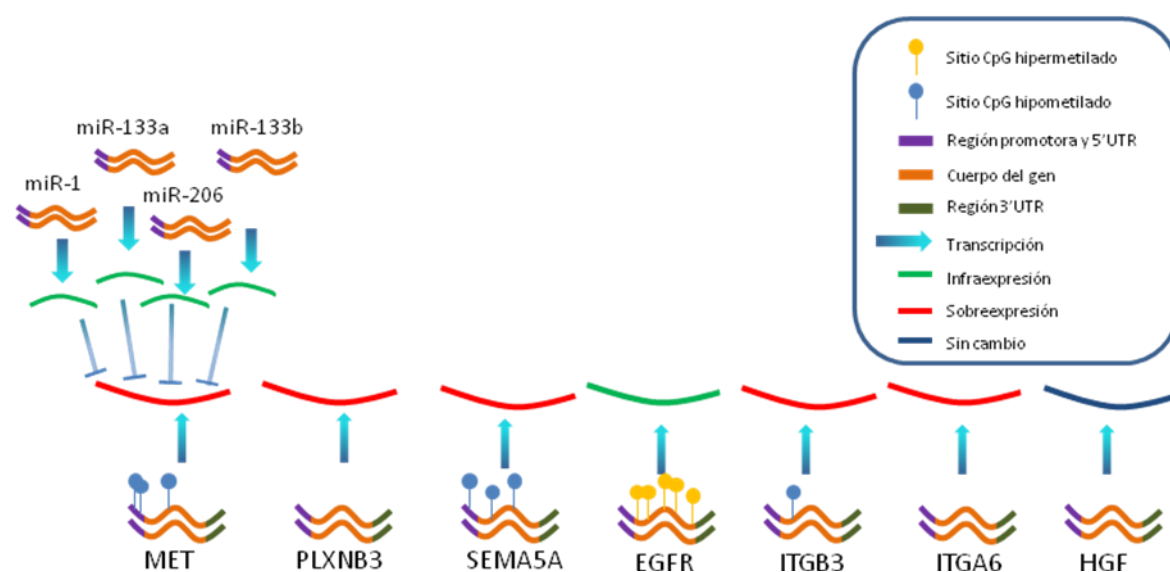


Figura 19. Patrones de expresión y metilación de genes relacionados con MET. Se incluyen también varios microRNAs implicados en el silenciamiento de MET según diferentes estudios.

5.6 EGFR

El gen *NF2* tiene capacidad de inhibir la señalización del receptor EGFR por contacto, el cual induce proliferación en las células de schwannoma (Curto *et al*, 2007). Sin embargo, diferentes trabajos mostraron resultados dispares en cuanto a su expresión, tanto a nivel de mensajero como de proteína en schwannomas. En nuestro estudio de microarrays mostró una clara infraexpresión, validado mediante PCR en tiempo real. Además, 5 sitios CpG estaban hipermetilados, sugiriendo un posible mecanismo epigenético en la regulación del mensajero de EGFR. En otros estudios, se encontró sobreexpresión del mensajero de *EGFR* (Doherty *et al*, 2008) o bien no se detectó expresión (Prayson *et al*, 2007; Wickremesekera *et al*, 2007). Un estudio reciente sobre el nivel de

proteína EGFR en schwannomas, mostró una falta total de expresión (Boin *et al*, 2014). Las consecuencias de una correcta medición de los niveles de EGFR en schwannomas son tremendamente importantes, ya que incluso se han llegado a realizar ensayos clínicos en 11 pacientes intentando bloquear EGFR con Erlotinib (Plotkin *et al*, 2010). La respuesta en la mejora radiológica -tamaño tumoral-, o de la audición en los pacientes testados fue nula, lo que podría explicarse por el hecho de que los niveles de EGFR en schwannomas son escasos, quizá nulos en base a recientes estudios proteicos.

5.7 RUTA DE LAS CAVEOLINAS

La familia de las caveolinas está formada por tres genes -*CAV1*, *CAV2* y *CAV3*-. Su función principal es la formación de caveolas, que son pequeñas invaginaciones de la membrana plasmática localizadas en balsas lipídicas de colesterol. El gen de la caveolina-1 fue encontrado infraexpresado en schwannomas vestibulares (Aarhus *et al*, 2010), dato refrendado por nuestros estudios. Así mismo, la caveolina-2 también apareció infraexpresada en nuestros estudios de expresión, además de hipermetilada en la región promotora (Figura 20), lo que podría explicar la desregulación.

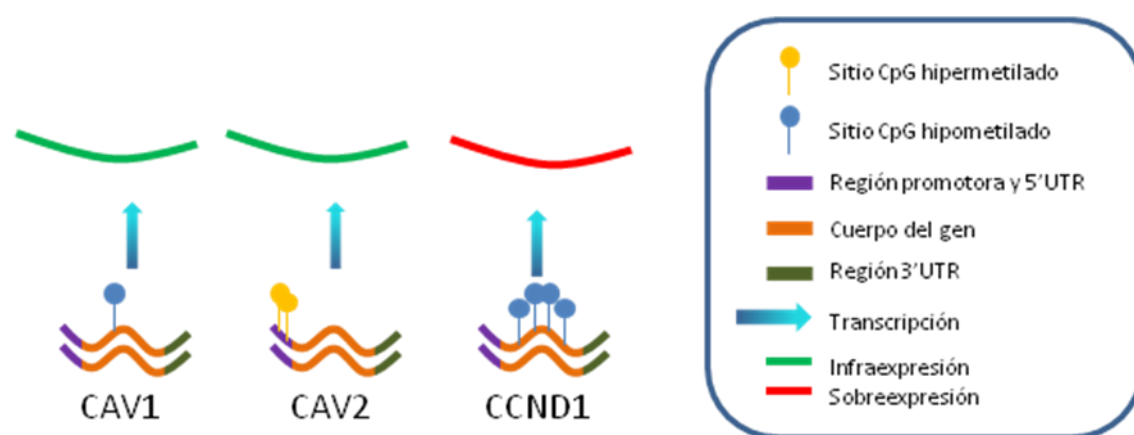


Figura 20. Expresión y metilación en las caveolinas 1 y 2 y en la ciclina D1.

La ausencia de caveolina-1 se ha descrito en procesos neoplásicos como el cáncer de mama (Lee *et al*, 1998) o en el de ovario (Bagnoli *et al*, 2000). Estudios in vitro de fibroblastos de embriones de ratón Cav1^{-/-}, es decir, sin copia alguna de este gen, encontraron un aumento de señal en las rutas Ras-MAPK, PI3K-Akt y PAK (del Pozo *et al*, 2005). No obstante, hay que señalar que en otros tumores, la sobreexpresión de caveolina-1 favorece la progresión tumoral como en el cáncer de próstata (Thompson *et al*, 1999; Yang *et al*, 2005; Tahir *et al*, 2008). Células deficientes en caveolina-1 han mostrado mayor acumulación de ciclina D1, una proteína necesaria para el progreso del ciclo celular y por lo tanto promotora de división (Cerezo *et al*, 2009). La ciclina D1 apareció sobreexpresada en nuestra serie, así como hipometilada en el cuerpo génico en 4 sitios CpG. En resumen, la infraexpresión de las caveolinas 1 y 2 descritas en nuestro trabajo, junto con la activación de la vía PI3K/Akt en schwannomas y la sobreexpresión de ciclina D1, podrían colaborar en la proliferación de estos tumores (Figura 21).

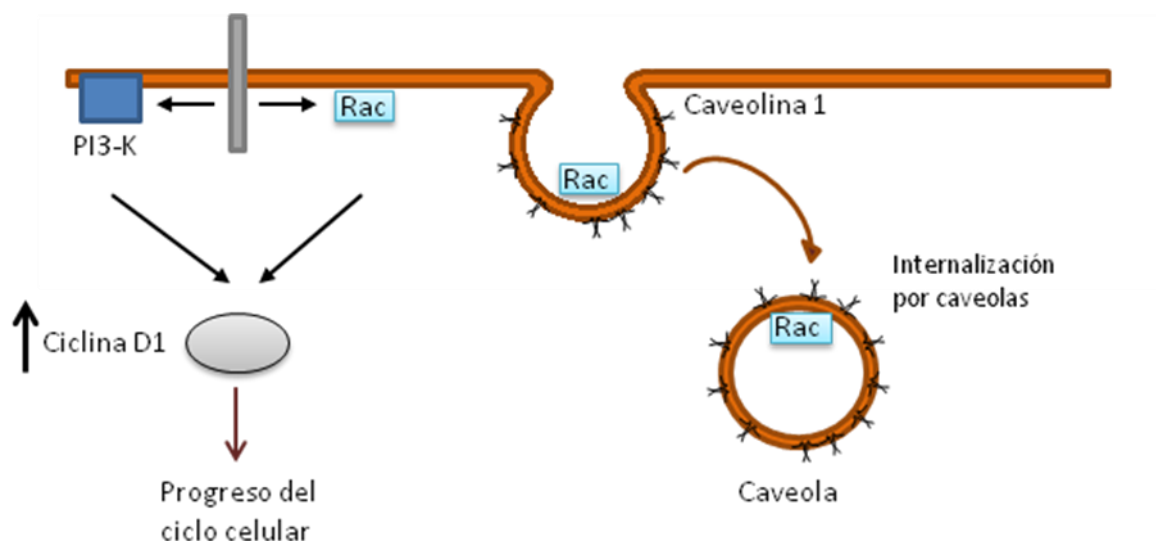


Figura 21. Esquema propuesto de uno de los posibles mecanismos de aumento de la proliferación en los schwannomas. En presencia de caveolina 1, Rac y otras proteínas señalizadoras son impedidas mediante su internalización. Sin caveolina 1, Rac aumenta los niveles de ciclina D1 en el núcleo, provocando un aumento de la proliferación.

5.8 RECEPTOR DE ANDRÓGENOS

La función biológica del receptor de andrógenos -AR- consiste en servir de receptor de hormonas androgénicas en el citosol celular, activándose y entrando en el núcleo como factor de transcripción (Mooradian *et al*, 1987). En cáncer de próstata, el AR juega un papel fundamental en la recidiva de estos tumores, que recaen tras bloquear los andrógenos en un primer paso del tratamiento (Yuan *et al*, 2013). Al contrario de la sobreexpresión y activación observada en las recidivas de cáncer de próstata (Shafi *et al*, 2013), en los schwannomas encontramos este receptor infraexpresado por microarrays y PCR en tiempo real. De la misma forma, encontramos patrón inverso -sobreexpresado en schwannomas e infraexpresado en cáncer de próstata- en el gen *HEPACAM*, que bloquea la translocación de AR al núcleo (Song *et al*, 2014) e impediría por tanto ejercer como factor de transcripción al receptor. Un gen cuya proteína está encargada de degradar el receptor de andrógenos (Li *et al*, 2008), *PMEPA1*, fue encontrado sobreexpresado en nuestros estudios, lo que podría provocar que en los schwannomas AR no sea solo infraexpresado a nivel de mensajero. Al igual que en cáncer de próstata, la sobreexpresión de *PMEPA1* en schwannomas podría ocurrir por mecanismos epigenéticos (Richter *et al*, 2007), ya que nuestros resultados mostraron 7 sitios CpG de la región promotora hipometilados, lo que podría facilitar su expresión. Por tanto, aunque resulta complejo establecer una vía clara de actuación, la alteración en la expresión en schwannomas puede reflejar un componente hormonal en estos tumores.

Como se describe en el Artículo 1, uno de los resultados más sorprendentes fue el hallazgo de que el hábito de fumar en los pacientes disminuía la probabilidad de

encontrar mutación en el gen *NF2*. En el estudio de Palmisano *et al*, (2012), identificaron que el hábito de fumar reducía la incidencia de schwannomas en hombres y algo menos en mujeres. En conjunto con los datos moleculares de los niveles del receptor de andrógenos, el hecho de que hombres y mujeres con los mismos hábitos de tabaquismo presenten diferencias en cuanto a la incidencia de schwannomas vestibulares, podría suponer algún tipo de relación hormonal con el fenómeno de la tumorigénesis, aunque los mecanismos concretos que expliquen la causa permanecen ocultos.

5.9 HOMOGENEIDAD EN LOS SCHWANNOMAS VESTIBULARES

Las asociaciones encontradas entre schwannomas vestibulares con distintos parámetros clínicos y moleculares, mostraron que a pesar de diferencias en los patrones de expresión génica, de miRNAs y de metilación del ADN, estos tumores se comportan de manera muy similar en los genes clave expuestos -*MET*, *ERBB2*, *ERBB3*, *NRG1*-, desregulados al compararlos con los controles no tumorales. No obstante, desde un punto de vista terapéutico, más estudios son necesarios con los schwannomas no vestibulares, ya que sí podrían requerir un tratamiento específico basado en nuestros hallazgos de expresión y metilación en los genes *HOX* y cofactores asociados.

5.10 SCHWANNOMAS Y MENINGIOMAS

Al ser uno de los principales objetivos la búsqueda de dianas terapéuticas para los pacientes de *NF2*, comparamos el patrón de expresión de los schwannomas con otro de los tumores que frecuentemente desarrollan los pacientes, los meningiomas.

Tanto schwannomas como meningiomas están relacionados por la frecuente inactivación del gen *NF2* -tanto por mutaciones como por LOH del cromosoma 22-, así

como de su aparición en pacientes con NF2. A pesar de que schwannomas y meningiomas provienen de distintos tejidos, como se indicó en la introducción, la frecuente presencia del mismo tipo de alteración molecular podría tener influencia en genes y rutas desreguladas en ambas neoplasias.

La comparación que más interés tiene con el objetivo de lograr dianas terapéuticas para ambos tumores, resulta de encontrar genes que compartan tendencia -sobrexpresión o infraexpresión- en cada tipo tumoral con respecto a su tejido control. Entre los genes sobreexpresados en los dos tumores, encontramos al ligando del factor derivado de plaquetas D -*PDGFD*-, que es capaz de activar *PDGFR-β*, como se ha descrito en otro apartado. Otro gen de interés para testar en ambos tumores, es el receptor *MET*, ya que tanto schwannomas y meningiomas lo sobreexpresan, algo demostrado también a nivel de proteínas (Moriyama *et al*, 1998).

Por lo tanto, nuestro trabajo combinando los niveles de expresión en schwannomas y meningiomas, muestran potenciales dianas para los pacientes con ambos tipos tumorales, aunque se requieren ensayos funcionales para comprobar si el bloqueo específico de genes como *MET* o *PDGFD* serían capaces de revertir los procesos de desarrollo y supervivencia neoplásica en cada tumor.

Las tres técnicas de alto rendimiento utilizadas en este trabajo -microarrays de expresión génica, de miRNA y de metilación-, han producido una ingente cantidad de datos que sin duda contribuirán a ampliar el conocimiento biológico del schwannoma vestibular. Las interrelaciones de los tres parámetros analizados, así mismo, reflejan la

extrema complejidad del proceso tumoral, donde incluso en una neoplasia de bajo grado como los schwannomas -en la que el único elemento molecular común es la inactivación del gen *NF2*-, se dan numerosos procesos de splicing alternativo, metilación diferencial o cambio en los niveles de expresión de miles de genes, incluyendo miRNAs.

6. CONCLUSIONES

6. CONCLUSIONES

1. El gen *NF2* sufre una alta tasa de mutaciones en los schwannomas vestibulares esporádicos, lo que unido a la frecuente pérdida de uno de los dos alelos del gen, hace suponer que una mayoría de los tumores presentan inactivación del producto proteico, merlin. En aquellos tumores sin alteración de *NF2*, la sobreexpresión del gen de la osteopontina -*SPP1*- en schwannomas podría ser otro mecanismo de eliminación de merlin.
2. Los schwannomas vestibulares presentan mecanismos de amplificación en los genes *ERBB2*, *ERBB3* y *MDM2*, a pesar de estar sobreexpresados en los tumores.
3. Los microarrays de expresión, constituyen una técnica fiable para determinar la desregulación génica, aunque para calcular el grado exacto la misma conviene realizar otras técnicas que nos ofrezcan mayor precisión como la PCR en tiempo real.
4. El gen *MET*, así como genes cuyas proteínas participan en su activación –incluyendo a *ERBB2*, *ERBB3* o *PLEXN3B*-, mostraron una clara sobreexpresión en los schwannomas, lo que sugiere que el oncogén *MET* podría ser una diana en los schwannomas. Además, los myomiRs, un grupo de miRNAs que se expresan en clústeres y que son capaces de reprimir el mensajero de *MET* en numerosos tumores, sufrieron infraexpresión.

5. La mayoría de los miRNAs alojados en la región 32q del cromosoma 14, presentaron sobreexpresión. Esta región, que contiene el mayor clúster de miRNAs del genoma, podría ser fundamental en el desarrollo de los schwannomas.
6. En los microarrays de expresión génica y de miRNAs, la tendencia fue a la sobreexpresión en los tumores, mientras que el patrón de metilación del ADN fue de menor número de sitios CpG metilados.
7. Los schwannomas vestibulares provenientes de pacientes de NF2 y los esporádicos, no presentaron grandes diferencias en cuanto a sus patrones de expresión y metilación.
8. En los schwannomas vestibulares, identificamos a los genes HOX con hipometilación general, hallada también en cofactores de estos genes. Los schwannomas no vestibulares presentaron un patrón de metilación y expresión distinto al de los schwannomas vestibulares, con mayor similitud a los nervios no tumorales.
9. Meningiomas y schwannomas, dos tumores que se desarrollan frecuentemente en pacientes con NF2, sobreexpresan *PDGFD* y *MET* con respecto a sus controles, por lo que estos genes podrían servir de diana en un tratamiento conjunto.

7. REFERENCIAS

1. Aarhus M, Bruland O, Sætran HA, Mork SJ, Lund-Johansen M & Knappskog PM (2010) Global gene expression profiling and tissue microarray reveal novel candidate genes and down-regulation of the tumor suppressor gene CAV1 in sporadic vestibular schwannomas. *Neurosurgery* **67**: 998–1019; discussion 1019
2. Abe M, Ohira M, Kaneda A, Yagi Y, Yamamoto S, Kitano Y, Takato T, Nakagawara A & Ushijima T (2005) CpG island methylator phenotype is a strong determinant of poor prognosis in neuroblastomas. *Cancer Res.* **65**: 828–834
3. Abruzzo LV, Lee KY, Fuller A, Silverman A, Keating MJ, Medeiros LJ & Coombes KR (2005) Validation of oligonucleotide microarray data using microfluidic low-density arrays: a new statistical method to normalize real-time RT-PCR data. *BioTechniques* **38**: 785–792
4. Adams MD, Kelley JM, Gocayne JD, Dubnick M, Polymeropoulos MH, Xiao H, Merril CR, Wu A, Olde B & Moreno RF (1991) Complementary DNA sequencing: expressed sequence tags and human genome project. *Science* **252**: 1651–1656
5. Alftan K, Heiska L, Grönholm M, Renkema GH & Carpén O (2004) Cyclic AMP-dependent protein kinase phosphorylates merlin at serine 518 independently of p21-activated kinase and promotes merlin-ezrin heterodimerization. *J. Biol. Chem.* **279**: 18559–18566
6. Anderson TD, Loevner LA, Bigelow DC & Mirza N (2000) Prevalence of unsuspected acoustic neuroma found by magnetic resonance imaging. *Otolaryngol.--Head Neck Surg. Off. J. Am. Acad. Otolaryngol.-Head Neck Surg.* **122**: 643–646
7. Antinheimo J, Sallinen SL, Sallinen P, Haapasalo H, Helin H, Horelli-Kuitunen N, Wessman M, Sainio M, Jääskeläinen J & Carpén O (2000a) Genetic aberrations in sporadic and neurofibromatosis 2 (NF2)-associated schwannomas studied by comparative genomic hybridization (CGH). *Acta Neurochir. (Wien)* **142**: 1099–1104; discussion 1104–1105
8. Antinheimo J, Sankila R, Carpén O, Pukkala E, Sainio M & Jääskeläinen J (2000b) Population-based analysis of sporadic and type 2 neurofibromatosis-associated meningiomas and schwannomas. *Neurology* **54**: 71–76
9. Antoni NR (1920) *Über Rückenmarksteumoren und Neurofibrome*. Munich: J. F. Bergmann
10. Arai E, Ikeuchi T, Karasawa S, Tamura A, Yamamoto K, Kida M, Ichimura K, Yuasa Y & Tonomura A (1992) Constitutional translocation t(4;22) (q12;q12.2) associated with neurofibromatosis type 2. *Am. J. Med. Genet.* **44**: 163–167
11. Asthagiri AR, Parry DM, Butman JA, Kim HJ, Tsilou ET, Zhuang Z & Lonser RR (2009) Neurofibromatosis type 2. *Lancet* **373**: 1974–1986
12. Babu R, Sharma R, Bagley JH, Hatef J, Friedman AH & Adamson C (2013) Vestibular schwannomas in the modern era: epidemiology, treatment trends, and disparities in management. *J. Neurosurg.* **119**: 121–130
13. Bagnoli M, Tomassetti A, Figini M, Flati S, Dolo V, Canevari S & Miotti S (2000) Downmodulation of caveolin-1 expression in human ovarian carcinoma is directly related to alpha-folate receptor overexpression. *Oncogene* **19**: 4754–4763
14. Bai Y, Liu Y-J, Wang H, Xu Y, Stamenkovic I & Yu Q (2007) Inhibition of the hyaluronan-CD44 interaction by merlin contributes to the tumor-suppressor activity of merlin. *Oncogene* **26**: 836–850

15. Ball CA, Brazma A, Causton H, Chervitz S, Edgar R, Hingamp P, Matese JC, Parkinson H, Quackenbush J, Ringwald M, Sansone S-A, Sherlock G, Spellman P, Stoeckert C, Tateno Y, Taylor R, White J & Winegarden N (2004) Submission of microarray data to public repositories. *PLoS Biol.* **2**: E317
16. Barradas M, Monjas A, Diaz-Meco MT, Serrano M & Moscat J (1999) The downregulation of the pro-apoptotic protein Par-4 is critical for Ras-induced survival and tumor progression. *EMBO J.* **18**: 6362–6369
17. Baur AM, Gamberger TI, Weerda HG, Gjuric M & Tamm ER (1995) Laminin promotes differentiation, adhesion and proliferation of cell cultures derived from human acoustic nerve schwannoma. *Acta Otolaryngol. (Stockh.)* **115**: 517–521
18. Bello MJ, de Campos JM, Kusak ME, Vaquero J, Sarasa JL, Pestaña A & Rey JA (1993) Clonal chromosome aberrations in neurinomas. *Genes. Chromosomes Cancer* **6**: 206–211
19. Bello MJ, Martinez-Glez V, Franco-Hernandez C, Pefla-Granero C, de Campos JM, Isla A, Lassaletta L, Vaquero J & Rey JA (2007) DNA methylation pattern in 16 tumor-related genes in schwannomas. *Cancer Genet. Cytogenet.* **172**: 84–86
20. Bianchi AB, Hara T, Ramesh V, Gao J, Klein-Szanto AJ, Morin F, Menon AG, Trofatter JA, Gusella JF & Seizinger BR (1994) Mutations in transcript isoforms of the neurofibromatosis 2 gene in multiple human tumour types. *Nat. Genet.* **6**: 185–192
21. Bianchi AB, Mitsunaga SI, Cheng JQ, Klein WM, Jhanwar SC, Seizinger B, Kley N, Klein-Szanto AJ & Testa JR (1995) High frequency of inactivating mutations in the neurofibromatosis type 2 gene (NF2) in primary malignant mesotheliomas. *Proc. Natl. Acad. Sci. U. S. A.* **92**: 10854–10858
22. Boin A, Couvelard A, Couderc C, Brito I, Filipescu D, Kalamarides M, Bedossa P, De Koning L, Danelsky C, Dubois T, Hupé P, Louvard D & Lallemand D (2014) Proteomic screening identifies a YAP-driven signaling network linked to tumor cell proliferation in human schwannomas. *Neuro-Oncol.*
23. Boyd C, Smith MJ, Kluwe L, Balogh A, Maccollin M & Plotkin SR (2008) Alterations in the SMARCB1 (INI1) tumor suppressor gene in familial schwannomatosis. *Clin. Genet.* **74**: 358–366
24. Brazma A, Hingamp P, Quackenbush J, Sherlock G, Spellman P, Stoeckert C, Aach J, Ansorge W, Ball CA, Causton HC, Gaasterland T, Glenisson P, Holstege FC, Kim IF, Markowitz V, Matese JC, Parkinson H, Robinson A, Sarkans U, Schulze-Kremer S, et al (2001) Minimum information about a microarray experiment (MIAME)-toward standards for microarray data. *Nat. Genet.* **29**: 365–371
25. Breving K & Esquela-Kerscher A (2010) The complexities of microRNA regulation: mirandering around the rules. *Int. J. Biochem. Cell Biol.* **42**: 1316–1329
26. Britsch S (2007) The neuregulin-I/ErbB signaling system in development and disease. *Adv. Anat. Embryol. Cell Biol.* **190**: 1–65
27. Bruder CE, Hirvelä C, Tapia-Paez I, Fransson I, Segraves R, Hamilton G, Zhang XX, Evans DG, Wallace AJ, Baser ME, Zucman-Rossi J, Hergersberg M, Boltshauser E, Papi L, Rouleau GA, Poptodorov G, Jordanova A, Rask-Andersen H, Kluwe L, Mautner V, et al (2001) High resolution deletion analysis of constitutional DNA from neurofibromatosis type 2 (NF2) patients using microarray-CGH. *Hum. Mol. Genet.* **10**: 271–282
28. Buckley PG, Mantripragada KK, Díaz de Ståhl T, Piotrowski A, Hansson CM, Kiss H, Vetrie D, Ernberg IT, Nordenskjöld M, Bolund L, Sainio M, Rouleau GA, Niimura M, Wallace AJ, Evans DGR, Grigellionis G, Menzel U & Dumanski JP (2005) Identification of genetic aberrations on chromosome 22 outside the NF2 locus in schwannomatosis and neurofibromatosis type 2. *Hum. Mutat.* **26**: 540–549

29. Cahilly-Snyder L, Yang-Feng T, Francke U & George DL (1987) Molecular analysis and chromosomal mapping of amplified genes isolated from a transformed mouse 3T3 cell line. *Somat. Cell Mol. Genet.* **13**: 235–244
30. Calin GA, Ferracin M, Cimmino A, Di Leva G, Shimizu M, Wojcik SE, Iorio MV, Visone R, Sever NI, Fabbri M, Iuliano R, Palumbo T, Pichiorri F, Roldo C, Garzon R, Sevignani C, Rassenti L, Alder H, Volinia S, Liu C, et al (2005) A MicroRNA signature associated with prognosis and progression in chronic lymphocytic leukemia. *N. Engl. J. Med.* **353**: 1793–1801
31. Callari M, Dugo M, Musella V, Marchesi E, Chiorino G, Grand MM, Pierotti MA, Daidone MG, Canevari S & De Cecco L (2012) Comparison of microarray platforms for measuring differential microRNA expression in paired normal/cancer colon tissues. *PloS One* **7**: e45105
32. Cañadas I, Rojo F, Arumí-Uría M, Rovira A, Albanell J & Arriola E (2010) C-MET as a new therapeutic target for the development of novel anticancer drugs. *Clin. Transl. Oncol. Off. Publ. Fed. Span. Oncol. Soc. Natl. Cancer Inst. Mex.* **12**: 253–260
33. Canales RD, Luo Y, Willey JC, Austermiller B, Barbacioru CC, Boysen C, Hunkapiller K, Jensen RV, Knight CR, Lee KY, Ma Y, Maqsoodi B, Papallo A, Peters EH, Poulter K, Ruppel PL, Samaha RR, Shi L, Yang W, Zhang L, et al (2006) Evaluation of DNA microarray results with quantitative gene expression platforms. *Nat. Biotechnol.* **24**: 1115–1122
34. Cayé-Thomasen P, Borup R, Stangerup S-E, Thomsen J & Nielsen FC (2010) Deregulated genes in sporadic vestibular schwannomas. *Otol. Neurotol. Off. Publ. Am. Otol. Soc. Am. Neurotol. Soc. Eur. Acad. Otol. Neurotol.* **31**: 256–266
35. Cerezo A, Guadamillas MC, Goetz JG, Sánchez-Perales S, Klein E, Assoian RK & del Pozo MA (2009) The absence of caveolin-1 increases proliferation and anchorage- independent growth by a Rac-dependent, Erk-independent mechanism. *Mol. Cell. Biol.* **29**: 5046–5059
36. Chen C, Grennan K, Badner J, Zhang D, Gershon E, Jin L & Liu C (2011) Removing batch effects in analysis of expression microarray data: an evaluation of six batch adjustment methods. *PloS One* **6**: e17238
37. Cioffi JA, Yue WY, Mendolia-Loffredo S, Hansen KR, Wackym PA & Hansen MR (2010) MicroRNA-21 overexpression contributes to vestibular schwannoma cell proliferation and survival. *Otol. Neurotol. Off. Publ. Am. Otol. Soc. Am. Neurotol. Soc. Eur. Acad. Otol. Neurotol.* **31**: 1455–1462
38. Cipriani NA, Abidoye OO, Vokes E & Salgia R (2009) MET as a target for treatment of chest tumors. *Lung Cancer Amst. Neth.* **63**: 169–179
39. Cook J, Krishnan S, Ananth S, Sells SF, Shi Y, Walther MM, Linehan WM, Sukhatme VP, Weinstein MH & Rangnekar VM (1999) Decreased expression of the pro-apoptotic protein Par-4 in renal cell carcinoma. *Oncogene* **18**: 1205–1208
40. Costa PM, Cardoso AL, Pereira de Almeida LF, Bruce JN, Canoll P & Pedroso de Lima MC (2012) PDGF-B-mediated downregulation of miR-21: new insights into PDGF signaling in glioblastoma. *Hum. Mol. Genet.* **21**: 5118–5130
41. Curto M, Cole BK, Lallemand D, Liu C-H & McClatchey AI (2007) Contact-dependent inhibition of EGFR signaling by Nf2/Merlin. *J. Cell Biol.* **177**: 893–903
42. Dallas PB, Gottardo NG, Firth MJ, Beesley AH, Hoffmann K, Terry PA, Freitas JR, Boag JM, Cummings AJ & Kees UR (2005) Gene expression levels assessed by oligonucleotide microarray analysis and quantitative real-time RT-PCR -- how well do they correlate? *BMC Genomics* **6**: 59

43. Datta J, Kutay H, Nasser MW, Nuovo GJ, Wang B, Majumder S, Liu C-G, Volinia S, Croce CM, Schmittgen TD, Ghoshal K & Jacob ST (2008) Methylation mediated silencing of MicroRNA-1 gene and its role in hepatocellular carcinogenesis. *Cancer Res.* **68**: 5049–5058
44. Davis BN, Hilyard AC, Nguyen PH, Lagna G & Hata A (2009) Induction of microRNA-221 by platelet-derived growth factor signaling is critical for modulation of vascular smooth muscle phenotype. *J. Biol. Chem.* **284**: 3728–3738
45. Dey N, Ghosh-Choudhury N, Kasinath BS & Choudhury GG (2012) TGF β -stimulated microRNA-21 utilizes PTEN to orchestrate AKT/mTORC1 signaling for mesangial cell hypertrophy and matrix expansion. *PLoS One* **7**: e42316
46. Diboun I, Wernisch L, Orengo CA & Koltzenburg M (2006) Microarray analysis after RNA amplification can detect pronounced differences in gene expression using limma. *BMC Genomics* **7**: 252
47. Doherty JK, Ongkeko W, Crawley B, Andalibi A & Ryan AF (2008) ErbB and Nrg: potential molecular targets for vestibular schwannoma pharmacotherapy. *Otol. Neurotol. Off. Publ. Am. Otol. Soc. Am. Neurotol. Soc. Eur. Acad. Otol. Neurotol.* **29**: 50–57
48. Eccles SA (2011) The epidermal growth factor receptor/Erb-B/HER family in normal and malignant breast biology. *Int. J. Dev. Biol.* **55**: 685–696
49. Esteller M, Garcia-Foncillas J, Andion E, Goodman SN, Hidalgo OF, Vanaclocha V, Baylin SB & Herman JG (2000) Inactivation of the DNA-repair gene MGMT and the clinical response of gliomas to alkylating agents. *N. Engl. J. Med.* **343**: 1350–1354
50. Evans DG, Howard E, Giblin C, Clancy T, Spencer H, Huson SM & Laloo F (2010) Birth incidence and prevalence of tumor-prone syndromes: estimates from a UK family genetic register service. *Am. J. Med. Genet. A.* **152A**: 327–332
51. Evans DGR, Ramsden RT, Shenton A, Gokhale C, Bowers NL, Huson SM, Pichert G & Wallace A (2007) Mosaicism in neurofibromatosis type 2: an update of risk based on uni/bilaterality of vestibular schwannoma at presentation and sensitive mutation analysis including multiple ligation-dependent probe amplification. *J. Med. Genet.* **44**: 424–428
52. Fakharzadeh SS, Trusko SP & George DL (1991) Tumorigenic potential associated with enhanced expression of a gene that is amplified in a mouse tumor cell line. *EMBO J.* **10**: 1565–1569
53. Fang C, Zhao Y & Guo B (2013) MiR-199b-5p targets HER2 in breast cancer cells. *J. Cell. Biochem.* **114**: 1457–1463
54. Fauvel B & Yasri A (2014) Antibodies directed against receptor tyrosine kinases: Current and future strategies to fight cancer. *mAbs* **6**:
55. Fernandez-Valle C, Tang Y, Ricard J, Rodenas-Ruano A, Taylor A, Hackler E, Biggerstaff J & Iacovelli J (2002) Paxillin binds schwannomin and regulates its density-dependent localization and effect on cell morphology. *Nat. Genet.* **31**: 354–362
56. Fleming JL, Gable DL, Samadzadeh-Tarighat S, Cheng L, Yu L, Gillespie JL & Toland AE (2013) Differential expression of miR-1, a putative tumor suppressing microRNA, in cancer resistant and cancer susceptible mice. *PeerJ* **1**: e68
57. Fouladi M, Helton K, Dalton J, Gilger E, Gajjar A, Merchant T, Kun L, Newsham I, Burger P & Fuller C (2003) Clear cell ependymoma: a clinicopathologic and radiographic analysis of 10 patients. *Cancer* **98**: 2232–2244

58. Fresno Vara JA, Casado E, de Castro J, Cejas P, Belda-Iniesta C & González-Barón M (2004) PI3K/Akt signalling pathway and cancer. *Cancer Treat. Rev.* **30**: 193–204
59. Frohnert PW, Stonecypher MS & Carroll SL (2003) Constitutive activation of the neuregulin-1/ErbB receptor signaling pathway is essential for the proliferation of a neoplastic Schwann cell line. *Glia* **43**: 104–118
60. Furukawa T, Duguid WP, Kobari M, Matsuno S & Tsao MS (1995) Hepatocyte growth factor and Met receptor expression in human pancreatic carcinogenesis. *Am. J. Pathol.* **147**: 889–895
61. Goelz SE, Vogelstein B, Hamilton SR & Feinberg AP (1985) Hypomethylation of DNA from benign and malignant human colon neoplasms. *Science* **228**: 187–190
62. Golub TR, Slonim DK, Tamayo P, Huard C, Gaasenbeek M, Mesirov JP, Coller H, Loh ML, Downing JR, Caligiuri MA, Bloomfield CD & Lander ES (1999) Molecular classification of cancer: class discovery and class prediction by gene expression monitoring. *Science* **286**: 531–537
63. Gonzalez-Agosti C, Wiederhold T, Herndon ME, Gusella J & Ramesh V (1999) Interdomain interaction of merlin isoforms and its influence on intermolecular binding to NHE-RF. *J. Biol. Chem.* **274**: 34438–34442
64. Gonzalez-Gomez P, Bello MJ, Alonso ME, Lomas J, Arjona D, Campos JM de, Vaquero J, Isla A, Lassaletta L, Gutierrez M, Sarasa JL & Rey JA (2003) CpG island methylation in sporadic and neurofibromatosis type 2-associated schwannomas. *Clin. Cancer Res. Off. J. Am. Assoc. Cancer Res.* **9**: 5601–5606
65. Guerra-Jiménez G, Camargo Camacho P, Ramos-Macías A & Morales Angulo C (2014) Neurofibromatosis type 2 and its head and neck manifestations: Literature review and population study in the Community of Cantabria and the province of Las Palmas. *Acta Otorrinolaringol. Esp.* **65**: 148–156
66. Gutmann DH, Aylsworth A, Carey JC, Korf B, Marks J, Pyeritz RE, Rubenstein A & Viskochil D (1997a) The diagnostic evaluation and multidisciplinary management of neurofibromatosis 1 and neurofibromatosis 2. *JAMA J. Am. Med. Assoc.* **278**: 51–57
67. Gutmann DH, Giordano MJ, Fishback AS & Guha A (1997b) Loss of merlin expression in sporadic meningiomas, ependymomas and schwannomas. *Neurology* **49**: 267–270
68. Hadfield KD, Smith MJ, Urquhart JE, Wallace AJ, Bowers NL, King AT, Rutherford SA, Trump D, Newman WG & Evans DG (2010) Rates of loss of heterozygosity and mitotic recombination in NF2 schwannomas, sporadic vestibular schwannomas and schwannomatosis schwannomas. *Oncogene* **29**: 6216–6221
69. Han SE, Park K-H, Lee G, Huh Y-J & Min B-M (2004) Mutation and aberrant expression of Caveolin-1 in human oral squamous cell carcinomas and oral cancer cell lines. *Int. J. Oncol.* **24**: 435–440
70. Hansen MR & Linthicum FH Jr (2004) Expression of neuregulin and activation of erbB receptors in vestibular schwannomas: possible autocrine loop stimulation. *Otol. Neurotol. Off. Publ. Am. Otol. Soc. Am. Neurotol. Soc. Eur. Acad. Otol. Neurotol.* **25**: 155–159
71. Hansen MR, Roehm PC, Chatterjee P & Green SH (2006) Constitutive neuregulin-1/ErbB signaling contributes to human vestibular schwannoma proliferation. *Glia* **53**: 593–600
72. He J, Jing Y, Li W, Qian X, Xu Q, Li F-S, Liu L-Z, Jiang B-H & Jiang Y (2013) Roles and mechanism of miR-199a and miR-125b in tumor angiogenesis. *PloS One* **8**: e56647
73. Hilton DA, Ristic N & Hanemann CO (2009) Activation of ERK, AKT and JNK signalling pathways in human schwannomas in situ. *Histopathology* **55**: 744–749

74. Hiscox SE, Hallett MB, Puntis MC, Nakamura T & Jiang WG (1997) Expression of the HGF/SF receptor, c-met, and its ligand in human colorectal cancers. *Cancer Invest.* **15**: 513–521
75. Hitotsumatsu T, Iwaki T, Kitamoto T, Mizoguchi M, Suzuki SO, Hamada Y, Fukui M & Tateishi J (1997) Expression of neurofibromatosis 2 protein in human brain tumors: an immunohistochemical study. *Acta Neuropathol. (Berl.)* **93**: 225–232
76. Hoa M & Slattery WH 3rd (2012) Neurofibromatosis 2. *Otolaryngol. Clin. North Am.* **45**: 315–332, viii
77. Hu G, Chen D, Li X, Yang K, Wang H & Wu W (2010) miR-133b regulates the MET proto-oncogene and inhibits the growth of colorectal cancer cells in vitro and in vivo. *Cancer Biol. Ther.* **10**: 190–197
78. Huang DW, Sherman BT & Lempicki RA (2009a) Systematic and integrative analysis of large gene lists using DAVID bioinformatics resources. *Nat. Protoc.* **4**: 44–57
79. Huang DW, Sherman BT & Lempicki RA (2009b) Bioinformatics enrichment tools: paths toward the comprehensive functional analysis of large gene lists. *Nucleic Acids Res.* **37**: 1–13
80. Hulsebos TJM, Plomp AS, Wolterman RA, Robanus-Maandag EC, Baas F & Wesseling P (2007) Germline mutation of INI1/SMARCB1 in familial schwannomatosis. *Am. J. Hum. Genet.* **80**: 805–810
81. Hung G, Colton J, Fisher L, Oppenheimer M, Faudoa R, Slattery W & Linthicum F (2002) Immunohistochemistry study of human vestibular nerve schwannoma differentiation. *Glia* **38**: 363–370
82. Iorio MV, Ferracin M, Liu C-G, Veronese A, Spizzo R, Sabbioni S, Magri E, Pedriali M, Fabbri M, Campiglio M, Ménard S, Palazzo JP, Rosenberg A, Musiani P, Volinia S, Nenci I, Calin GA, Querzoli P, Negrini M & Croce CM (2005) MicroRNA gene expression deregulation in human breast cancer. *Cancer Res.* **65**: 7065–7070
83. Jackler RK, Shapiro MS, Dillon WP, Pitts L & Lanser MJ (1990) Gadolinium-DTPA enhanced magnetic resonance imaging in acoustic neuroma diagnosis and management. *Otolaryngol.–Head Neck Surg. Off. J. Am. Acad. Otolaryngol.–Head Neck Surg.* **102**: 670–677
84. James MF, Han S, Polizzano C, Plotkin SR, Manning BD, Stemmer-Rachamimov AO, Gusella JF & Ramesh V (2009) NF2/merlin is a novel negative regulator of mTOR complex 1, and activation of mTORC1 is associated with meningioma and schwannoma growth. *Mol. Cell. Biol.* **29**: 4250–4261
85. Jang M, Rhee JE, Jang D-H & Kim SS (2011) Gene expression profiles are altered in human papillomavirus-16 E6 D25E-expressing cell lines. *Virol. J.* **8**: 453
86. Jannatipour M, Dion P, Khan S, Jindal H, Fan X, Laganière J, Chishti AH & Rouleau GA (2001) Schwannomin isoform-1 interacts with syntenin via PDZ domains. *J. Biol. Chem.* **276**: 33093–33100
87. Jia H, Marzin A, Dubreuil C & Tringali S (2008) Intralabyrinthine schwannomas: symptoms and managements. *Auris. Nasus. Larynx* **35**: 131–136
88. Jin H, Sperka T, Herrlich P & Morrison H (2006) Tumorigenic transformation by CPI-17 through inhibition of a merlin phosphatase. *Nature* **442**: 576–579
89. Johnson WE, Li C & Rabinovic A (2007) Adjusting batch effects in microarray expression data using empirical Bayes methods. *Biostat. Oxf. Engl.* **8**: 118–127
90. Kaempchen K, Mielke K, Utermark T, Langmesser S & Hanemann CO (2003) Upregulation of the Rac1/JNK signaling pathway in primary human schwannoma cells. *Hum. Mol. Genet.* **12**: 1211–1221
91. Karajannis MA, Legault G, Hagiwara M, Ballas MS, Brown K, Nusbaum AO, Hochman T, Goldberg JD, Koch KM, Golfinos JG, Roland JT & Allen JC (2012) Phase II trial of lapatinib in adult and pediatric

- patients with neurofibromatosis type 2 and progressive vestibular schwannomas. *Neuro-Oncol.* **14**: 1163–1170
92. Karajannis MA, Legault G, Hagiwara M, Giancotti FG, Filatov A, Derman A, Hochman T, Goldberg JD, Vega E, Wisoff JH, Golfinos JG, Merkelson A, Roland JT & Allen JC (2014) Phase II study of everolimus in children and adults with neurofibromatosis type 2 and progressive vestibular schwannomas. *Neuro-Oncol.* **16**: 292–297
 93. Karjalainen S, Nuutinen J, Neittaanmäki H, Naukkarinen A & Asikainen R (1984) The incidence of acoustic neuroma in autopsy material. *Arch. Otorhinolaryngol.* **240**: 91–93
 94. Kino T, Takeshima H, Nakao M, Nishi T, Yamamoto K, Kimura T, Saito Y, Kochi M, Kuratsu J, Saya H & Ushio Y (2001) Identification of the cis-acting region in the NF2 gene promoter as a potential target for mutation and methylation-dependent silencing in schwannoma. *Genes Cells Devoted Mol. Cell. Mech.* **6**: 441–454
 95. Kissil JL, Wilker EW, Johnson KC, Eckman MS, Yaffe MB & Jacks T (2003) Merlin, the product of the Nf2 tumor suppressor gene, is an inhibitor of the p21-activated kinase, Pak1. *Mol. Cell* **12**: 841–849
 96. Kogenaru S, Qing Y, Guo Y & Wang N (2012) RNA-seq and microarray complement each other in transcriptome profiling. *BMC Genomics* **13**: 629
 97. Koutsimpelas D, Felmeden U, Mann WJ & Brieger J (2011) Analysis of cytogenetic aberrations in sporadic vestibular schwannoma by comparative genomic hybridization. *J. Neurooncol.* **103**: 437–443
 98. Koutsimpelas D, Ruerup G, Mann WJ & Brieger J (2012) Lack of neurofibromatosis type 2 gene promoter methylation in sporadic vestibular schwannomas. *ORL J. Oto-Rhino-Laryngol. Its Relat. Spec.* **74**: 33–37
 99. Kullar PJ, Pearson DM, Malley DS, Collins VP & Ichimura K (2010) CpG island hypermethylation of the neurofibromatosis type 2 (NF2) gene is rare in sporadic vestibular schwannomas. *Neuropathol. Appl. Neurobiol.* **36**: 505–514
 100. Lallemand D, Manent J, Couvelard A, Watilliaux A, Siena M, Chareyre F, Lampin A, Niwa-Kawakita M, Kalamarides M & Giovannini M (2009) Merlin regulates transmembrane receptor accumulation and signaling at the plasma membrane in primary mouse Schwann cells and in human schwannomas. *Oncogene* **28**: 854–865
 101. Lamszus K, Lachenmayer L, Heinemann U, Kluwe L, Finckh U, Höppner W, Stavrou D, Fillbrandt R & Westphal M (2001) Molecular genetic alterations on chromosomes 11 and 22 in ependymomas. *Int. J. Cancer J. Int. Cancer* **91**: 803–808
 102. Lasak JM, Welling DB, Akhrametyeva EM, Salloum M & Chang L-S (2002) Retinoblastoma-cyclin-dependent kinase pathway deregulation in vestibular schwannomas. *The Laryngoscope* **112**: 1555–1561
 103. Lassaletta L, Patrón M, González T, Martínez-Glez V, Rey JA & Gavilan J (2007) RASSF1A methylation and cyclin D1 expression in vestibular schwannomas. *Acta Neuropathol. (Berl.)* **114**: 431–433
 104. Lau Y-KI, Murray LB, Houshmandi SS, Xu Y, Gutmann DH & Yu Q (2008) Merlin is a potent inhibitor of glioma growth. *Cancer Res.* **68**: 5733–5742
 105. Laulajainen M, Muranen T, Carpén O & Grönholm M (2008) Protein kinase A-mediated phosphorylation of the NF2 tumor suppressor protein merlin at serine 10 affects the actin cytoskeleton. *Oncogene* **27**: 3233–3243
 106. Le N, Nagarajan R, Wang JYT, Araki T, Schmidt RE & Milbrandt J (2005) Analysis of congenital hypomyelinating Egr2Lo/Lo nerves identifies Sox2 as an inhibitor of Schwann cell differentiation and myelination. *Proc. Natl. Acad. Sci. U. S. A.* **102**: 2596–2601

107. Lee H, Kim D, Dan HC, Wu EL, Gritsko TM, Cao C, Nicosia SV, Golemis EA, Liu W, Coppola D, Brem SS, Testa JR & Cheng JQ (2007) Identification and characterization of putative tumor suppressor NGB, a GTP-binding protein that interacts with the neurofibromatosis 2 protein. *Mol. Cell. Biol.* **27**: 2103–2119
108. Lee JD, Kwon TJ, Kim U-K & Lee W-S (2012) Genetic and epigenetic alterations of the NF2 gene in sporadic vestibular schwannomas. *PLoS One* **7**: e30418
109. Lee JY, Kim H, Ryu CH, Kim JY, Choi BH, Lim Y, Huh P-W, Kim Y-H, Lee K-H, Jun T-Y, Rha HK, Kang J-K & Choi CR (2004) Merlin, a tumor suppressor, interacts with transactivation-responsive RNA-binding protein and inhibits its oncogenic activity. *J. Biol. Chem.* **279**: 30265–30273
110. Lee JY, Moon HJ, Lee WK, Chun HJ, Han CW, Jeon Y-W, Lim Y, Kim YH, Yao T-P, Lee K-H, Jun T-Y, Rha HK & Kang J-K (2006) Merlin facilitates ubiquitination and degradation of transactivation-responsive RNA-binding protein. *Oncogene* **25**: 1143–1152
111. Lee SW, Reimer CL, Oh P, Campbell DB & Schnitzer JE (1998) Tumor cell growth inhibition by caveolin re-expression in human breast cancer cells. *Oncogene* **16**: 1391–1397
112. Lengyel E, Prechtel D, Resau JH, Gauger K, Welk A, Lindemann K, Salanti G, Richter T, Knudsen B, Vande Woude GF & Harbeck N (2005) C-Met overexpression in node-positive breast cancer identifies patients with poor clinical outcome independent of Her2/neu. *Int. J. Cancer J. Int. Cancer* **113**: 678–682
113. Li H, Xu LL, Masuda K, Raymundo E, McLeod DG, Dobi A & Srivastava S (2008) A feedback loop between the androgen receptor and a NEDD4-binding protein, PMEPA1, in prostate cancer cells. *J. Biol. Chem.* **283**: 28988–28995
114. Li L, Roden J, Shapiro BE, Wold BJ, Bhatia S, Forman SJ & Bhatia R (2005) Reproducibility, fidelity, and discriminant validity of mRNA amplification for microarray analysis from primary hematopoietic cells. *J. Mol. Diagn. JMD* **7**: 48–56
115. Li W, You L, Cooper J, Schiavon G, Pepe-Caprio A, Zhou L, Ishii R, Giovannini M, Hanemann CO, Long SB, Erdjument-Bromage H, Zhou P, Tempst P & Giancotti FG (2010) Merlin/NF2 suppresses tumorigenesis by inhibiting the E3 ubiquitin ligase CRL4(DCAF1) in the nucleus. *Cell* **140**: 477–490
116. Li Y, Wei Z, Zhang J, Yang Z & Zhang M (2014) Structural Basis of the Binding of Merlin FERM Domain to the E3 Ubiquitin Ligase Substrate Adaptor DCAF1. *J. Biol. Chem.*
117. Liang H, Zhang J, Zen K, Zhang C-Y & Chen X (2013) Nuclear microRNAs and their unconventional role in regulating non-coding RNAs. *Protein Cell* **4**: 325–330
118. Liu N, Chen N-Y, Cui R-X, Li W-F, Li Y, Wei R-R, Zhang M-Y, Sun Y, Huang B-J, Chen M, He Q-M, Jiang N, Chen L, Cho WCS, Yun J-P, Zeng J, Liu L-Z, Li L, Guo Y, Wang H-Y, et al (2012) Prognostic value of a microRNA signature in nasopharyngeal carcinoma: a microRNA expression analysis. *Lancet Oncol.* **13**: 633–641
119. Lockhart DJ, Dong H, Byrne MC, Follettie MT, Gallo MV, Chee MS, Mittmann M, Wang C, Kobayashi M, Horton H & Brown EL (1996) Expression monitoring by hybridization to high-density oligonucleotide arrays. *Nat. Biotechnol.* **14**: 1675–1680
120. Lopez-Serra L & Esteller M (2008) Proteins that bind methylated DNA and human cancer: reading the wrong words. *Br. J. Cancer* **98**: 1881–1885
121. Louis DN, Ohgaki H, Wiestler OD, Cavenee WK, Burger PC, Jouvet A, Scheithauer BW & Kleihues P (2007) The 2007 WHO classification of tumours of the central nervous system. *Acta Neuropathol. (Berl.)* **114**: 97–109

122. Lu J, Getz G, Miska EA, Alvarez-Saavedra E, Lamb J, Peck D, Sweet-Cordero A, Ebert BL, Mak RH, Ferrando AA, Downing JR, Jacks T, Horvitz HR & Golub TR (2005) MicroRNA expression profiles classify human cancers. *Nature* **435**: 834–838
123. MacCollin M, Chiocca EA, Evans DG, Friedman JM, Horvitz R, Jaramillo D, Lev M, Mautner VF, Niimura M, Plotkin SR, Sang CN, Stemmer-Rachamimov A & Roach ES (2005) Diagnostic criteria for schwannomatosis. *Neurology* **64**: 1838–1845
124. Manning BD & Cantley LC (2007) AKT/PKB signaling: navigating downstream. *Cell* **129**: 1261–1274
125. Martinez-Glez V, Franco-Hernandez C, Alvarez L, De Campos JM, Isla A, Vaquero J, Lassaletta L, Casartelli C & Rey JA (2009) Meningiomas and schwannomas: molecular subgroup classification found by expression arrays. *Int. J. Oncol.* **34**: 493–504
126. Maunakea AK, Nagarajan RP, Bilenky M, Ballinger TJ, D'Souza C, Fouse SD, Johnson BE, Hong C, Nielsen C, Zhao Y, Turecki G, Delaney A, Varhol R, Thiessen N, Shchors K, Heine VM, Rowitch DH, Xing X, Fiore C, Schillebeeckx M, et al (2010) Conserved role of intragenic DNA methylation in regulating alternative promoters. *Nature* **466**: 253–257
127. McClatchey AI & Giovannini M (2005) Membrane organization and tumorigenesis--the NF2 tumor suppressor, Merlin. *Genes Dev.* **19**: 2265–2277
128. McClintick JN, Jerome RE, Nicholson CR, Crabb DW & Edenberg HJ (2003) Reproducibility of oligonucleotide arrays using small samples. *BMC Genomics* **4**: 4
129. Michailov GV, Sereda MW, Brinkmann BG, Fischer TM, Haug B, Birchmeier C, Role L, Lai C, Schwab MH & Nave K-A (2004) Axonal neuregulin-1 regulates myelin sheath thickness. *Science* **304**: 700–703
130. Mirsky R, Woodhoo A, Parkinson DB, Arthur-Farraj P, Bhaskaran A & Jessen KR (2008) Novel signals controlling embryonic Schwann cell development, myelination and dedifferentiation. *J. Peripher. Nerv. Syst. JPNS* **13**: 122–135
131. Mooradian AD, Morley JE & Korenman SG (1987) Biological actions of androgens. *Endocr. Rev.* **8**: 1–28
132. Moreno-Bueno G, Fernandez-Marcos PJ, Collado M, Tendero MJ, Rodriguez-Pinilla SM, Garcia-Cao I, Hardisson D, Diaz-Meco MT, Moscat J, Serrano M & Palacios J (2007) Inactivation of the candidate tumor suppressor par-4 in endometrial cancer. *Cancer Res.* **67**: 1927–1934
133. Moriyama T, Kataoka H, Kawano H, Yokogami K, Nakano S, Goya T, Uchino H, Kono M & Wakisaka S (1998) Comparative analysis of expression of hepatocyte growth factor and its receptor, c-met, in gliomas, meningiomas and schwannomas in humans. *Cancer Lett.* **124**: 149–155
134. Morrison H, Sherman LS, Legg J, Banine F, Isacke C, Haipek CA, Gutmann DH, Ponta H & Herrlich P (2001) The NF2 tumor suppressor gene product, merlin, mediates contact inhibition of growth through interactions with CD44. *Genes Dev.* **15**: 968–980
135. Morrow KA, Das S, Metge BJ, Ye K, Mulekar MS, Tucker JA, Samant RS & Shevde LA (2011) Loss of tumor suppressor Merlin in advanced breast cancer is due to post-translational regulation. *J. Biol. Chem.* **286**: 40376–40385
136. Moyhuddin A, Baser ME, Watson C, Purcell S, Ramsden RT, Heiberg A, Wallace AJ & Evans DGR (2003) Somatic mosaicism in neurofibromatosis 2: prevalence and risk of disease transmission to offspring. *J. Med. Genet.* **40**: 459–463
137. Mur P, Mollejo M, Ruano Y, de Lope ÁR, Fiaño C, García JF, Castresana JS, Hernández-Laín A, Rey JA & Meléndez B (2013) Codeletion of 1p and 19q determines distinct gene methylation and expression profiles in IDH-mutated oligodendroglial tumors. *Acta Neuropathol. (Berl.)* **126**: 277–289

138. Muranen T, Grönholm M, Lampin A, Lallemand D, Zhao F, Giovannini M & Carpén O (2007) The tumor suppressor merlin interacts with microtubules and modulates Schwann cell microtubule cytoskeleton. *Hum. Mol. Genet.* **16**: 1742–1751
139. Murray LB, Lau Y-KI & Yu Q (2012) Merlin is a negative regulator of human melanoma growth. *PLoS One* **7**: e43295
140. Myrseth E, Pedersen P-H, Møller P & Lund-Johansen M (2007) Treatment of vestibular schwannomas. Why, when and how? *Acta Neurochir. (Wien)* **149**: 647–660; discussion 660
141. Nasser MW, Datta J, Nuovo G, Kutay H, Motiwala T, Majumder S, Wang B, Suster S, Jacob ST & Ghoshal K (2008) Down-regulation of micro-RNA-1 (miR-1) in lung cancer. Suppression of tumorigenic property of lung cancer cells and their sensitization to doxorubicin-induced apoptosis by miR-1. *J. Biol. Chem.* **283**: 33394–33405
142. Newbern J & Birchmeier C (2010) Nrg1/ErbB signaling networks in Schwann cell development and myelination. *Semin. Cell Dev. Biol.* **21**: 922–928
143. Nguyen R, Reczek D & Bretscher A (2001) Hierarchy of merlin and ezrin N- and C-terminal domain interactions in homo- and heterotypic associations and their relationship to binding of scaffolding proteins EBP50 and E3KARP. *J. Biol. Chem.* **276**: 7621–7629
144. Nikolopoulos TP & O'Donoghue GM (2002) Acoustic neuroma management: an evidence-based medicine approach. *Otol. Neurotol. Off. Publ. Am. Otol. Soc. Am. Neurotol. Soc. Eur. Acad. Otol. Neurotol.* **23**: 534–541
145. Nohata N, Hanazawa T, Enokida H & Seki N (2012) microRNA-1/133a and microRNA-206/133b clusters: dysregulation and functional roles in human cancers. *Oncotarget* **3**: 9–21
146. Okada M, Wang Y, Jang S-W, Tang X, Neri LM & Ye K (2009) Akt phosphorylation of merlin enhances its binding to phosphatidylinositols and inhibits the tumor-suppressive activities of merlin. *Cancer Res.* **69**: 4043–4051
147. Okada T, Lopez-Lago M & Giancotti FG (2005) Merlin/NF-2 mediates contact inhibition of growth by suppressing recruitment of Rac to the plasma membrane. *J. Cell Biol.* **171**: 361–371
148. Okoniewski MJ, Hey Y, Pepper SD & Miller CJ (2007) High correspondence between Affymetrix exon and standard expression arrays. *BioTechniques* **42**: 181–185
149. Palmisano S, Schwartzbaum J, Prochazka M, Pettersson D, Bergenheim T, Florentzson R, Harder H, Mathiesen T, Nyberg G, Siesjö P & Feychting M (2012) Role of tobacco use in the etiology of acoustic neuroma. *Am. J. Epidemiol.* **175**: 1243–1251
150. Plotkin SR, Halpin C, McKenna MJ, Loeffler JS, Batchelor TT & Barker FG 2nd (2010) Erlotinib for progressive vestibular schwannoma in neurofibromatosis 2 patients. *Otol. Neurotol. Off. Publ. Am. Otol. Soc. Am. Neurotol. Soc. Eur. Acad. Otol. Neurotol.* **31**: 1135–1143
151. Plotkin SR, Stemmer-Rachamimov AO, Barker FG 2nd, Halpin C, Padera TP, Tyrrell A, Sorensen AG, Jain RK & di Tomaso E (2009) Hearing improvement after bevacizumab in patients with neurofibromatosis type 2. *N. Engl. J. Med.* **361**: 358–367
152. Porkka KP, Pfeiffer MJ, Waltering KK, Vessella RL, Tammela TLJ & Visakorpi T (2007) MicroRNA expression profiling in prostate cancer. *Cancer Res.* **67**: 6130–6135
153. Del Pozo MA, Balasubramanian N, Alderson NB, Kiosses WB, Grande-García A, Anderson RGW & Schwartz MA (2005) Phospho-caveolin-1 mediates integrin-regulated membrane domain internalization. *Nat. Cell Biol.* **7**: 901–908

154. Pradervand S, Paillusson A, Thomas J, Weber J, Wirapati P, Hagenbüchle O & Harshman K (2008) Affymetrix Whole-Transcript Human Gene 1.0 ST array is highly concordant with standard 3' expression arrays. *BioTechniques* **44**: 759–762
155. Prayson RA, Yoder BJ & Barnett GH (2007) Epidermal growth factor receptor is not amplified in schwannomas. *Ann. Diagn. Pathol.* **11**: 326–329
156. Qi Q, Liu X, Brat DJ & Ye K (2013) Merlin sumoylation is required for its tumor suppressor activity. *Oncogene*
157. Rajaram V, Gutmann DH, Prasad SK, Mansur DB & Perry A (2005) Alterations of protein 4.1 family members in ependymomas: a study of 84 cases. *Mod. Pathol. Off. J. U. S. Can. Acad. Pathol. Inc* **18**: 991–997
158. Reid JF, Sokolova V, Zoni E, Lampis A, Pizzamiglio S, Bertan C, Zanutto S, Perrone F, Camerini T, Gallino G, Verderio P, Leo E, Pilotti S, Gariboldi M & Pierotti MA (2012) miRNA profiling in colorectal cancer highlights miR-1 involvement in MET-dependent proliferation. *Mol. Cancer Res. MCR* **10**: 504–515
159. Di Renzo MF, Olivero M, Ferro S, Prat M, Bongarzone I, Pilotti S, Belfiore A, Costantino A, Vigneri R & Pierotti MA (1992) Overexpression of the c-MET/HGF receptor gene in human thyroid carcinomas. *Oncogene* **7**: 2549–2553
160. Di Renzo MF, Olivero M, Katsaros D, Crepaldi T, Gaglia P, Zola P, Sismondi P & Comoglio PM (1994) Overexpression of the Met/HGF receptor in ovarian cancer. *Int. J. Cancer J. Int. Cancer* **58**: 658–662
161. Rey JA, Bello MJ, De Campos JM, Kusak ME & Moreno S (1987) Cytogenetic analysis in human neurinomas. *Cancer Genet. Cytogenet.* **28**: 187–188
162. Richter E, Masuda K, Cook C, Ehrich M, Tadese AY, Li H, Owusu A, Srivastava S & Dobi A (2007) A role for DNA methylation in regulating the growth suppressor PMEPA1 gene in prostate cancer. *Epigenetics Off. J. DNA Methylation Soc.* **2**: 100–109
163. Robinson MD & Speed TP (2007) A comparison of Affymetrix gene expression arrays. *BMC Bioinformatics* **8**: 449
164. Roldo C, Missiaglia E, Hagan JP, Falconi M, Capelli P, Bersani S, Calin GA, Volinia S, Liu C-G, Scarpa A & Croce CM (2006) MicroRNA expression abnormalities in pancreatic endocrine and acinar tumors are associated with distinctive pathologic features and clinical behavior. *J. Clin. Oncol. Off. J. Am. Soc. Clin. Oncol.* **24**: 4677–4684
165. Rong R, Tang X, Gutmann DH & Ye K (2004) Neurofibromatosis 2 (NF2) tumor suppressor merlin inhibits phosphatidylinositol 3-kinase through binding to PIKE-L. *Proc. Natl. Acad. Sci. U. S. A.* **101**: 18200–18205
166. Roosli C, Linthicum FH Jr, Cureoglu S & Merchant SN (2012) What is the site of origin of cochleovestibular schwannomas? *Audiol. Neurotol.* **17**: 121–125
167. Rosenfeld N, Aharonov R, Meiri E, Rosenwald S, Spector Y, Zepeniuk M, Benjamin H, Shabes N, Tabak S, Levy A, Lebanony D, Goren Y, Silberschein E, Targan N, Ben-Ari A, Gilad S, Sion-Vardy N, Tobar A, Feinmesser M, Kharenko O, et al (2008) MicroRNAs accurately identify cancer tissue origin. *Nat. Biotechnol.* **26**: 462–469
168. Rouleau GA, Merel P, Lutchman M, Sanson M, Zucman J, Marineau C, Hoang-Xuan K, Demczuk S, Desmaze C & Plougastel B (1993) Alteration in a new gene encoding a putative membrane-organizing protein causes neuro-fibromatosis type 2. *Nature* **363**: 515–521

169. Rouleau GA, Seizinger BR, Wertelecki W, Haines JL, Superneau DW, Martuza RL & Gusella JF (1990) Flanking markers bracket the neurofibromatosis type 2 (NF2) gene on chromosome 22. *Am. J. Hum. Genet.* **46**: 323–328
170. Rousseau G, Noguchi T, Bourdon V, Sobol H & Olschwang S (2011) SMARCB1/INI1 germline mutations contribute to 10% of sporadic schwannomatosis. *BMC Neurol.* **11**: 9
171. Sainio M, Zhao F, Heiska L, Turunen O, den Bakker M, Zwarthoff E, Lutchman M, Rouleau GA, Jääskeläinen J, Vaheri A & Carpén O (1997) Neurofibromatosis 2 tumor suppressor protein colocalizes with ezrin and CD44 and associates with actin-containing cytoskeleton. *J. Cell Sci.* **110 (Pt 18)**: 2249–2260
172. Saydam O, Senol O, Würdinger T, Mizrak A, Ozdener GB, Stemmer-Rachamimov AO, Yi M, Stephens RM, Krichevsky AM, Saydam N, Brenner GJ & Breakefield XO (2011) miRNA-7 attenuation in Schwannoma tumors stimulates growth by upregulating three oncogenic signaling pathways. *Cancer Res.* **71**: 852–861
173. Schena M, Shalon D, Davis RW & Brown PO (1995) Quantitative monitoring of gene expression patterns with a complementary DNA microarray. *Science* **270**: 467–470
174. Schneider J, Warzok R, Schreiber D & Güthert H (1983) [Tumors of the central nervous system in biopsy and autopsy material. 7th communication: neurinomas and neurofibromatoses with CNS involvement]. *Zentralblatt Für Allg. Pathol. Pathol. Anat.* **127**: 305–314
175. Schulz A, Baader SL, Niwa-Kawakita M, Jung MJ, Bauer R, Garcia C, Zoch A, Schacke S, Hagel C, Mautner V-F, Hanemann CO, Dun X-P, Parkinson DB, Weis J, Schröder JM, Gutmann DH, Giovannini M & Morrison H (2013) Merlin isoform 2 in neurofibromatosis type 2-associated polyneuropathy. *Nat. Neurosci.* **16**: 426–433
176. Schulz A, Kyselyova A, Baader SL, Jung MJ, Zoch A, Mautner V-F, Hagel C & Morrison H (2014) Neuronal merlin influences ERBB2 receptor expression on Schwann cells through neuregulin 1 type III signalling. *Brain J. Neurol.* **137**: 420–432
177. Scoles DR, Huynh DP, Morcos PA, Coulsell ER, Robinson NG, Tamanoi F & Pulst SM (1998) Neurofibromatosis 2 tumour suppressor schwannomin interacts with betaII-spectrin. *Nat. Genet.* **18**: 354–359
178. Scoles DR, Nguyen VD, Qin Y, Sun C-X, Morrison H, Gutmann DH & Pulst S-M (2002) Neurofibromatosis 2 (NF2) tumor suppressor schwannomin and its interacting protein HRS regulate STAT signaling. *Hum. Mol. Genet.* **11**: 3179–3189
179. Scoles DR, Qin Y, Nguyen V, Gutmann DH & Pulst S-M (2005) HRS inhibits EGF receptor signaling in the RT4 rat schwannoma cell line. *Biochem. Biophys. Res. Commun.* **335**: 385–392
180. Selesnick SH, Jackler RK & Pitts LW (1993) The changing clinical presentation of acoustic tumors in the MRI era. *The Laryngoscope* **103**: 431–436
181. Seo P-S, Quinn BJ, Khan AA, Zeng L, Takoudis CG, Hanada T, Bolis A, Bolino A & Chishti AH (2009) Identification of erythrocyte p55/MPP1 as a binding partner of NF2 tumor suppressor protein/Merlin. *Exp. Biol. Med. Maywood NJ* **234**: 255–262
182. Shafi AA, Yen AE & Weigel NL (2013) Androgen receptors in hormone-dependent and castration-resistant prostate cancer. *Pharmacol. Ther.* **140**: 223–238
183. Shi L, Reid LH, Jones WD, Shippy R, Warrington JA, Baker SC, Collins PJ, de Longueville F, Kawasaki ES, Lee KY, Luo Y, Sun YA, Willey JC, Setterquist RA, Fischer GM, Tong W, Dragan YP, Dix DJ, Frueh FW, Goodsaid FM, et al (2006) The MicroArray Quality Control (MAQC) project shows inter- and intraplatform reproducibility of gene expression measurements. *Nat. Biotechnol.* **24**: 1151–1161

184. Shivane A, Parkinson DB, Ammoun S & Hanemann CO (2013) Expression of c-Jun and Sox-2 in human schwannomas and traumatic neuromas. *Histopathology* **62**: 651–656
185. Sian CS & Ryan SF (1981) The ultrastructure of neurilemoma with emphasis on Antoni B tissue. *Hum. Pathol.* **12**: 145–160
186. Silber J, Jacobsen A, Ozawa T, Harinath G, Pedraza A, Sander C, Holland EC & Huse JT (2012) miR-34a repression in proneural malignant gliomas upregulates expression of its target PDGFRA and promotes tumorigenesis. *PLoS One* **7**: e33844
187. Song X, Wang Y, Du H, Fan Y, Yang X, Wang X, Wu X & Luo C (2014) Overexpression of HepaCAM inhibits cell viability and motility through suppressing nucleus translocation of androgen receptor and ERK signaling in prostate cancer. *The Prostate*
188. Sørlie T, Perou CM, Tibshirani R, Aas T, Geisler S, Johnsen H, Hastie T, Eisen MB, van de Rijn M, Jeffrey SS, Thorsen T, Quist H, Matese JC, Brown PO, Botstein D, Lønning PE & Børresen-Dale AL (2001) Gene expression patterns of breast carcinomas distinguish tumor subclasses with clinical implications. *Proc. Natl. Acad. Sci. U. S. A.* **98**: 10869–10874
189. Sottoriva A, Spiteri I, Piccirillo SGM, Touloumis A, Collins VP, Marioni JC, Curtis C, Watts C & Tavaré S (2013) Intratumor heterogeneity in human glioblastoma reflects cancer evolutionary dynamics. *Proc. Natl. Acad. Sci. U. S. A.* **110**: 4009–4014
190. Stemmer-Rachamimov AO, Xu L, Gonzalez-Agosti C, Burwick JA, Pinney D, Beauchamp R, Jacoby LB, Gusella JF, Ramesh V & Louis DN (1997) Universal absence of merlin, but not other ERM family members, in schwannomas. *Am. J. Pathol.* **151**: 1649–1654
191. Striedinger K, VandenBerg SR, Baia GS, McDermott MW, Gutmann DH & Lal A (2008) The neurofibromatosis 2 tumor suppressor gene product, merlin, regulates human meningioma cell growth by signaling through YAP. *Neoplasia N. Y. N* **10**: 1204–1212
192. Tabernero MD, Maillo A, Gil-Bellosta CJ, Castrillo A, Sousa P, Merino M & Orfao A (2009) Gene expression profiles of meningiomas are associated with tumor cytogenetics and patient outcome. *Brain Pathol. Zurich Switz.* **19**: 409–420
193. Tahir SA, Yang G, Goltsov AA, Watanabe M, Tabata K, Addai J, Fattah EMA, Kadmon D & Thompson TC (2008) Tumor cell-secreted caveolin-1 has proangiogenic activities in prostate cancer. *Cancer Res.* **68**: 731–739
194. Tang X, Jang S-W, Wang X, Liu Z, Bahr SM, Sun S-Y, Brat D, Gutmann DH & Ye K (2007) Akt phosphorylation regulates the tumour-suppressor merlin through ubiquitination and degradation. *Nat. Cell Biol.* **9**: 1199–1207
195. Tao Y, Dai P, Liu Y, Marchetto S, Xiong W-C, Borg J-P & Mei L (2009) Erbin regulates NRG1 signaling and myelination. *Proc. Natl. Acad. Sci. U. S. A.* **106**: 9477–9482
196. Taulli R, Bersani F, Foglizzo V, Linari A, Vigna E, Ladanyi M, Tuschl T & Ponzetto C (2009) The muscle-specific microRNA miR-206 blocks human rhabdomyosarcoma growth in xenotransplanted mice by promoting myogenic differentiation. *J. Clin. Invest.* **119**: 2366–2378
197. Thompson TC, Timme TL, Li L & Goltsov A (1999) Caveolin-1, a metastasis-related gene that promotes cell survival in prostate cancer. *Apoptosis Int. J. Program. Cell Death* **4**: 233–237
198. Tos M & Thomsen J (1984) Epidemiology of acoustic neuromas. *J. Laryngol. Otol.* **98**: 685–692

199. Trofatter JA, MacCollin MM, Rutter JL, Murrell JR, Duyao MP, Parry DM, Eldridge R, Kley N, Menon AG & Pulaski K (1993) A novel moesin-, ezrin-, radixin-like gene is a candidate for the neurofibromatosis 2 tumor suppressor. *Cell* **72**: 791–800
200. Trusolino L, Bertotti A & Comoglio PM (2010) MET signalling: principles and functions in development, organ regeneration and cancer. *Nat. Rev. Mol. Cell Biol.* **11**: 834–848
201. Tsai C-J & Nussinov R (2013) The molecular basis of targeting protein kinases in cancer therapeutics. *Semin. Cancer Biol.* **23**: 235–242
202. Twist EC, Ruttledge MH, Rousseau M, Sanson M, Papi L, Merel P, Delattre O, Thomas G & Rouleau GA (1994) The neurofibromatosis type 2 gene is inactivated in schwannomas. *Hum. Mol. Genet.* **3**: 147–151
203. Vasudevan S (2012) Posttranscriptional upregulation by microRNAs. *Wiley Interdiscip. Rev. RNA* **3**: 311–330
204. Verhaak RGW, Hoadley KA, Purdom E, Wang V, Qi Y, Wilkerson MD, Miller CR, Ding L, Golub T, Mesirov JP, Alexe G, Lawrence M, O'Kelly M, Tamayo P, Weir BA, Gabriel S, Winckler W, Gupta S, Jakkula L, Feiler HS, et al (2010) Integrated genomic analysis identifies clinically relevant subtypes of glioblastoma characterized by abnormalities in PDGFRA, IDH1, EGFR, and NF1. *Cancer Cell* **17**: 98–110
205. Verocay J (1910) Zur Kenntniss der 'neurofibrome'. *Beitr Pathol Anat* **48**: 1–69
206. Del Vescovo V, Meier T, Inga A, Denti MA & Borlak J (2013) A cross-platform comparison of affymetrix and Agilent microarrays reveals discordant miRNA expression in lung tumors of c-Raf transgenic mice. *PloS One* **8**: e78870
207. Wang V-C, Li J-W, Suen J-H, Chuang T-C & Kao M-C (2011) Ile/Ile homozygosity at codon 655 of HER2 in schwannoma. *Acta Neurol. Taiwanica* **20**: 243–248
208. Wang Y, Barbacioru C, Hyland F, Xiao W, Hunkapiller KL, Blake J, Chan F, Gonzalez C, Zhang L & Samaha RR (2006) Large scale real-time PCR validation on gene expression measurements from two commercial long-oligonucleotide microarrays. *BMC Genomics* **7**: 59
209. Wang Z, Gerstein M & Snyder M (2009) RNA-Seq: a revolutionary tool for transcriptomics. *Nat. Rev. Genet.* **10**: 57–63
210. Warren C, James LA, Ramsden RT, Wallace A, Baser ME, Varley JM & Evans DG (2003) Identification of recurrent regions of chromosome loss and gain in vestibular schwannomas using comparative genomic hybridisation. *J. Med. Genet.* **40**: 802–806
211. Wei J, Feng L, Li Z, Xu G & Fan X (2013) MicroRNA-21 activates hepatic stellate cells via PTEN/Akt signaling. *Biomed. Pharmacother. Bioméd. Pharmacothérapie* **67**: 387–392
212. Wei Y, Li L, Wang D, Zhang C-Y & Zen K (2014) Importin 8 regulates the transport of mature microRNAs into the cell nucleus. *J. Biol. Chem.* **289**: 10270–10275
213. Wellenreuther R, Kraus JA, Lenartz D, Menon AG, Schramm J, Louis DN, Ramesh V, Gusella JF, Wiestler OD & von Deimling A (1995) Analysis of the neurofibromatosis 2 gene reveals molecular variants of meningioma. *Am. J. Pathol.* **146**: 827–832
214. Welling DB, Lasak JM, Akhmametyeva E, Ghaheri B & Chang L-S (2002) cDNA microarray analysis of vestibular schwannomas. *Otol. Neurotol. Off. Publ. Am. Otol. Soc. Am. Neurotol. Soc. Eur. Acad. Otol. Neurotol.* **23**: 736–748
215. Wertenlecker W, Rouleau GA, Superneau DW, Forehand LW, Williams JP, Haines JL & Gusella JF (1988) Neurofibromatosis 2: clinical and DNA linkage studies of a large kindred. *N. Engl. J. Med.* **319**: 278–283

216. Wickremesekera A, Hovens CM & Kaye AH (2007) Expression of ErbB-1 and 2 in vestibular schwannomas. *J. Clin. Neurosci. Off. J. Neurosurg. Soc. Australas.* **14**: 1199–1206
217. Wilkes MC, Repellin CE, Hong M, Bracamonte M, Penheiter SG, Borg J-P & Leof EB (2009) Erbin and the NF2 tumor suppressor Merlin cooperatively regulate cell-type-specific activation of PAK2 by TGF-beta. *Dev. Cell* **16**: 433–444
218. Wippold FJ 2nd, Lubner M, Perrin RJ, Lämmle M & Perry A (2007) Neuropathology for the neuroradiologist: Antoni A and Antoni B tissue patterns. *AJNR Am. J. Neuroradiol.* **28**: 1633–1638
219. Wolff RK, Frazer KA, Jackler RK, Lanser MJ, Pitts LH & Cox DR (1992) Analysis of chromosome 22 deletions in neurofibromatosis type 2-related tumors. *Am. J. Hum. Genet.* **51**: 478–485
220. Yan D, Dong XDE, Chen X, Wang L, Lu C, Wang J, Qu J & Tu L (2009) MicroRNA-1/206 targets c-Met and inhibits rhabdomyosarcoma development. *J. Biol. Chem.* **284**: 29596–29604
221. Yang G, Timme TL, Frolov A, Wheeler TM & Thompson TC (2005) Combined c-Myc and caveolin-1 expression in human prostate carcinoma predicts prostate carcinoma progression. *Cancer* **103**: 1186–1194
222. Yang L, Chao J, Kook YH, Gao Y, Yao H & Buch SJ (2013) Involvement of miR-9/MCPIP1 axis in PDGF-BB-mediated neurogenesis in neuronal progenitor cells. *Cell Death Dis.* **4**: e960
223. Yi C, Troutman S, Fera D, Stemmer-Rachamimov A, Avila JL, Christian N, Persson NL, Shimono A, Speicher DW, Marmorstein R, Holmgren L & Kissil JL (2011) A tight junction-associated Merlin-angiomotin complex mediates Merlin's regulation of mitogenic signaling and tumor suppressive functions. *Cancer Cell* **19**: 527–540
224. Yi C, Wilker EW, Yaffe MB, Stemmer-Rachamimov A & Kissil JL (2008) Validation of the p21-activated kinases as targets for inhibition in neurofibromatosis type 2. *Cancer Res.* **68**: 7932–7937
225. Yip L, Kelly L, Shuai Y, Armstrong MJ, Nikiforov YE, Carty SE & Nikiforova MN (2011) MicroRNA signature distinguishes the degree of aggressiveness of papillary thyroid carcinoma. *Ann. Surg. Oncol.* **18**: 2035–2041
226. Yokoo H, Oishi T, Isoda K, Nakazato Y & Toyokuni S (2007) Oxidative stress is related to the formation of Antoni B patterns and eosinophilic hyaline droplets in schwannomas. *Neuropathol. Off. J. Jpn. Soc. Neuropathol.* **27**: 237–244
227. Yoo NJ, Park SW & Lee SH (2012) Mutational analysis of tumour suppressor gene NF2 in common solid cancers and acute leukaemias. *Pathology (Phila.)* **44**: 29–32
228. Yuan X, Cai C, Chen S, Chen S, Yu Z & Balk SP (2013) Androgen receptor functions in castration-resistant prostate cancer and mechanisms of resistance to new agents targeting the androgen axis. *Oncogene*
229. Zhang J-X, Song W, Chen Z-H, Wei J-H, Liao Y-J, Lei J, Hu M, Chen G-Z, Liao B, Lu J, Zhao H-W, Chen W, He Y-L, Wang H-Y, Xie D & Luo J-H (2013) Prognostic and predictive value of a microRNA signature in stage II colon cancer: a microRNA expression analysis. *Lancet Oncol.* **14**: 1295–1306
230. Zhang Y, Yu G, Jiang P, Xiang Y, Li W, Lee W & Zhang Y (2011) Decreased expression of protease-activated receptor 4 in human gastric cancer. *Int. J. Biochem. Cell Biol.* **43**: 1277–1283
231. Zhang Z, Wang Z, Sun L, Li X, Huang Q, Yang T & Wu H (2014) Mutation spectrum and differential gene expression in cystic and solid vestibular schwannoma. *Genet. Med. Off. J. Am. Coll. Med. Genet.* **16**: 264–270

232. Zhao S, Fung-Leung W-P, Bittner A, Ngo K & Liu X (2014) Comparison of RNA-Seq and microarray in transcriptome profiling of activated T cells. *PloS One* **9**: e78644
233. Zhu Z, He X, Johnson C, Stoops J, Eaker AE, Stoffer DS, Bell A, Zarnegar R & DeFrances MC (2007) PI3K is negatively regulated by PIK3IP1, a novel p110 interacting protein. *Biochem. Biophys. Res. Commun.* **358**: 66–72